IDŐJÁRÁS

AZ ORSZÁGOS METEOROLÓGIAI SZOLGÁLAT FOLYÓIRATA
86. ÉVF. ★ 2—4. SZÁM ★ 1982. MÁRCIUS—AUGUSZTUS

ÖSSZEVONT SZÁM

az 1981. augusztus 26—28. között
Hamburgban tartott

10. NEMZETKÖZI KONDENZÁCIÓS- ÉS JÉGMAG-KONFERENCIA

előadásaiból

SPECIAL ISSUE

TENTH INTERNATIONAL CONFERENCE ON CONDENSATION AND ICE NUCLEI

held at Hamburg Federal Republic of Germany

26—28. August, 1981

JOURNAL OF THE HUNGARIAN METEOROLOGICAL SERVICE

VOL. 86. ★ NO. 2—4. ★ MARCH—AUGUST ★ BUDAPEST

IDŐJÁRÁS

Az Országos Meteorológiai Szolgálat folyóirata
Journal of the Hungarian Meteorological Service

Szerkesztőség: Budapest, Postafiók 38. 1525
Előfizetés: 1 évre 228 Ft. Megrendelhető: Az Országos Meteorológiai Szolgálat Pénzügyi Osztályán Budapest, Kitaibel Pál utca 1. 1024. Levélcím: Budapest, Pf. 38. 1525 Megjelenik kéthavonként
Egyes szám ára 38 Ft

Editorial Office: H-1525 Budapest P. O. B. 38 — Hungary. This journal, published bimonthly, can be purchased from the distributor: KULTURA, H-1389 Budapest P.O.B. 149 — Hungary
The actual subscription rate is determined by the distributor

IDŐJÁRÁS

Az Országos Meteorológiai Szolgálat folyóirata. 86. évf. 2—4. szám. 1982, március – augusztus
Journal of the Hungarian Meteorological Service, Vol. 86. No 2—4. March – Aug. 1982. Budapest

TARTALOM—CONTENTS

IDŐJÁRÁS

Az Országos Meteorológiai Szolgálat folyóirata. 86. évf. 2—4. szám. 1982. Március—augusztus
Journal of the Hungarian Meteorological Service, Vol. 86. No 2—4. March—Aug 1982. Budapest

Editorial

This special issue contains a part of the material of the Tenth International Conference on Condensation and Ice Nuclei, held at Hamburg, F. R. G., 26—27 August 1981, on the occasion of the Third Scientific Assembly of the International Association of Meteorology and Atmospheric Physics (IAMAP). The conference was organized by the Nucleation Committee of the International Commission on Cloud Physics of IAMAP.

The speakers presenting materials which had not been published elsewhere were invited to submit their manuscripts to this journal. Of the manuscripts received, 26 have been accepted by the referees for publication. The papers are published in the order of presentation at the meeting. They give a good survey of our present knowledge of the physical and chemical properties of atmospheric particles and nuclei and their role in the formation of liquid water and ice in the clouds.

E. Mészáros
Chairman of the Editorial Board

Olvasóinkhoz!

Folyóiratunk 86. kötetének ez az összevont száma, a 10. Nemzetközi Kondenzációs- és Jégmag Konferencia anyagának egy részét tartalmazza. A konferenciát 1981. augusztus 26—28. között Hamburgban (NSZK) tartották a Nemzetközi Meteorológiai és Légkörfizikai Asszociáció Harmadik Tudományos Közgyűlése alkalmából. Szervezője az asszociáció Nemzetközi Felhőfizikai Bizottságának Nukleációs Albizottsága volt. Az előadók, a máshol még nem publikált eredményeket bemutató kéziratait — felhívásunkra — folyóiratunkhoz nyújtották be. A beérkezett kéziratokból huszonhatot fogadtak el a lektorok közlésre. Ezeket a konferencián való bemutatásuk sorrendjében publikáljuk. A cikkek jó áttekintést nyújtanak a légköri részecskék és magvak fizikai és kémiai tulajdonságaira, valamint felhőképződésben játszott szerepükre vonatkozó jelen ismereteinkről.

Mészáros Ernő
a szerkesztőbizottság elnöke

IDŐJÁRÁS

Az Országos Meteorológiai Szolgálat folyóirata, 86. évf. 2–4. szám, 1982. március–augusztus
Journal of the Hungarian Meteorological Service, Vol. 86. No. 2–4. March–August 1982, Budapest

The influence of aerosol particles on radiation parameters of clouds

H. GRASSL, *Max-Planck-Institut für Meteorologie*, Bundesstrasse 55, D—2000 Hamburg, Federal Republic of Germany*

Az aeroszol részecskék hatása a felhők sugárzási paramétereire. Az aeroszol részecskék a globális albedó kialakításában mind felhőtlen, mind felhős időben szerepet játszanak. A felhőkben ezek a részecskék optikai tulajdonságaik miatt közvetlenül meghatározzák a felhő optikai paramétereit, így a felhő-albedót és a sugárzási áram divergenciáját. Közvetett hatásuk is jelentős, mivel befolyásolják a felhők mikrostruktúráját. Koncentrációjuk és a törésmutatót befolyásoló kémiai összetételük megváltozása a rövid- és hosszúhullámú spektrumban az alábbi következményekkel jár: 1. Vékony felhők esetén a légszennyeződés növekedése növeli az albedót még akkor is, ha a részecskék egységnyi tömegére vonatkoztatott abszorpciós együttható nagyobb lesz. Vastag felhőknél az albedó csak akkor nő, ha az abszorpciós együttható változatlan marad vagy csökken. 2. Az aeroszol részecskék koncentrációjának emelkedése a felhő legfelső rétegében nagyobb hűlési sebességgel jár. 3. A rövidhullámú sugáráram egyenlege a vékony felhőket tartalmazó légréteg felső határán jelentősen csökken, ha a légszennyeződés erősödik. Hosszúhullámok esetén a változás kicsi. Kimutatható, hogy a koncentráció-növekedésnek a hatása ennél sokkal bonyolultabb, ha egyúttal a felületi feszültség, a részecskék nagyság szerinti eloszlása és a relatív nedvességgel való növekedés sebessége is megváltozik.

*

The influence of aerosol particles on radiation parameters of clouds. Aerosol particles contribute to the global albedo in both clear and cloudy areas. Inside clouds, these particles determine optical cloud parameters, such as cloud albedo and the radiative flux divergence, directly through their optical characteristics, and indirectly through their influence on the microphysics of the cloud. Calculated reactions to variations in the concentration and chemical composition (determining refractive index) of aerosol particles in the short- and longwave part of the spectrum are: 1. Increasing the atmospheric pollution increases the albedo of thin clouds, even though the mass absorption coefficient of the aerosol particles increases. Thick clouds will only have an increased albedo if there is no increase in the mass absorption coefficient of aerosol particles. 2. Increasing the aerosol particle concentration leads to larger cooling rates within the top layer of a cloud. 3. The net shortwave radiative flux at the top of an atmosphere containing thin cloud layers decreases substantially with increasing air pollution, while the net longwave radiative flux shows only small variations. It is also shown that the above mentioned results for particle increase are oversimplifications, if concurrent variations in surface tension, aerosol particle size distribution and growth rates with relative humidity are included.

*

Introduction. While the influence of aerosol particles on the clear sky radiation field and radiation balance is rather well known theoretically, recent work (*Twomey*, 1974, 1978 and *Grassl*, 1975, 1978, 1979) has now considered the role of particles in determining optical cloud parameters, such as the cloud

* Present affiliation: Institut für Meereskunde an der Universität Kiel, Düsternbrooker Weg 20, D-2300 Kiel 1, F. R. G.

albedo transmission, and absorption in the solar or shortwave (SW) interval from 0.3 to 4.0 μm. To the author's knowledge no work except a first estimate by *Twomey* (1978) has been reported on the effect of aerosol particles on radiative transfer in clouds in the longwawe (LW) domain, i.e. whether the LW emission of clouds depends on aerosol particle characteristics.

This paper tries to answer the following questions:

1. Are aerosol characteristics as important in changing the optical cloud parameters in the LW part of the spectrum as they are in the solar part?

2. Do more accurate calculations confirm previous (*Twomey*, 1978, *Grassl*, 1978, 1979) simple estimates based on crude approximations and on empirical relations between aerosol particle number and mean cloud droplet size?

3. Do LW radiation changes due to changes in aerosol characteristics enhance or counteract the changes in solar radiation?

To answer these questions, the first result section, after a short description of the radiative transfer model and input data, presents SW and LW parameters for different cloud droplet size spectra. The second section tries to confirm or abandon some simplifications already used for the SW region. The third section presents changes of net radiative flux values due to changes in aerosol particle concentration.

Radiative transfer model and cloud drop size spectra

The radiative transfer model adopted for both spectral regions ($SW \triangleq 0.3-3.7$ μm, $LW \triangleq 4-400$ μm) is the matrix operator theory, frequently called 'adding and doubling'-method, as summarized by *Plass* et al. (1973) together with the inhomogeneous source extension given by *Wiscombe* (1976a) for the LW part of the spectrum. The infinitesimal generator initialization (see *Wiscombe*, 1976b) is used to construct the starting matrices. Gaseous absorption is included via the fitting of the transmission function $\overline{T}_{\Delta\nu}$ averaged over a spectral interval $\Delta\nu$ by a sum of exponentials

$$\overline{T}(a) = \frac{1}{\Delta\nu} \int_{\Delta\nu} \exp(-k\nu \cdot a) d\nu = \sum_{n=1}^{M} w_n \exp(-k_n \cdot a)$$

where w_n and k_n are the weights and mass absorption coefficients derived by the fitting procedure and a is the absorber amount in g cm^{-2}. Results for 30 spectral intervals with M fixed to 6 have been reported elsewhere (*Grassl*, 1978). The extinction, scattering and absorption coefficient as well as the asymmetry factor g for each of the particle size distributions were calculated from the Mie theory. Since values of absorption of solar radiation calculated with the exact form of the phase function differ only slightly from those using the approximate Henyey–Greenstein-function, which uses the g factor (see *Hansen* and *Travis*, 1974), we have adopted only this latter approximation. One should be sceptic when using this approximation for the calculation of absolute values of cloud albedo; however the albedo changes are expected to agree with those obtained by applying the exact phase functions. As an example spectral albedo values $A\nu = 0.712$ at 0.35 μm wavelength for a plane-parallel cloud with the C1 size distribution using the exact phase function have to be compared to $A\nu = 0.706$ using the Henyey–Greenstein approximation. Within the SW region only absorbing gases considered are water vapour and ozone, in the LW region CO_2 is also introduced. The absorption

data for wavelength $\lambda \leq 10$ μm stem from *Moskalenko* (1969) and from *McClatchey* et al. (1972) for $\lambda \geq 10$ μm.

All the size distributions used are listed in *Table I*. The inclusion of some rather different measured size distributions in Table I might at a first glance cause some confusion, however, will be shown to lead to optical cloud parameters which are very close to the results for the analytical size distribution. This confirms the usefulness of the chosen analytical distributions. Some related parameters of these size distributions like peak or mode radius, r_c, mean square radius, r_{ms}, mean volume radius, r_v, are included in Table I.

Radiative transfer calculations were performed for all the cloud drop size distributions presented in Table I, integrating over 8 wavelength intervals in the *SW* and 16 wavelength intervals in the *LW* region for a cloud layer from 1,000 to 1,500 m above the surface and the atmospheric variables shown in *Table II*. The main features of the model atmosphere chosen are US-Standard-Atmosphere above 2,000 m, a temperature inversion of 3 *K* on top of the cloud, wet adiabatic lapse rate within the cloud and constant water vapour density below the cloud.

TABLE I

Cloud droplet size distributions and related parameters

Identification	$n(r)$ = size distribution, cm^{-3} μm^{-1}	r_c, μm	r_{ms}, μm	r_v, μm	Source
C1	$n(r) = 2.373\ r^6 \exp(-1.5\ r)$	4.00	4.98	5.30	*Deirmendjian* (1969)
C2	$n(r) = 1.0851\ 10^{-2}\ r^8 \exp(-1/24\ r^3)$	4.00	4.08	4.16	*Deirmendjian* (1969)
C3	$n(r) = 5.5556\ r^8 \exp(-0.3333\ r^3)$	2.00	2.04	2.15	*Deirmendjian* (1969)
C5	$n(r) = 0.5487\ r^4 \exp(-0.6667\ r)$	6.00	8.21	8.92	*Deirmendjian* (1969)
C6	$n(r) = 0.5\ 10^{-4}\ r^2 \exp(-0.1\ r)$	20.00	34.64	38.28	*Deirmendjian* (1969)
M (Stratus)	measured June 16, 1970		7.86	8.21	*Ryan* et al. (1972)
N (Stratus)	measured June 16, 1970		6.35	6.63	*Ryan* et al. (1972)
O (Cumulus Continental)	measured June 02, 1970		3.53	3.65	*Ryan* et al. (1972)
StI	measured		4.50	4.90	*Stephens* (1978) *Stephens* et al. (1978)
F1 a (fog)	measured Sept. 15, 1967		0.82	1.93	*Garland* (1971)
F1 b (fog)	measured Sept. 15, 1967 *		0.77	1.34	*Garland* (1971)
F2 (fog)	measured Nov. 22, 1967		0.76	1.24	*Garland* (1971)
F3 (fog)	measured Feb. 29, 1968		2.76	3.44	*Garland* (1971)
F4 (fog)	measured Oct. 21, 1968		1.61	2.95	*Garland* (1971)

* Neglecting the biggest droplets which were at clearly separated particle size in *Garland's* measurements

TABLE II

Height h, temperature T, pressure p, air density ϱ, water vapour density ϱ_{H_2O}, liquid water content LWC of the model atmosphere, and optical depth τ at 0.55 μm wavelength due to aerosol particles and cloud C1 *counted from the top of the atmosphere; total ozone and solar constant*

h, m	T, K	p, mbar	ϱ, kg m^{-3}	ϱ_{H_2O}, g m^{-3}	LWC, g m^{-3}	τ
10,000	223.25	265.00	0.4135	0.009	0.000	0.000
9,000	229.73	308.41	0.4671	0.020	0.000	0.002
8,000	236.21	356.52	0.5258	0.090	0.000	0.004
7,000	242.70	411.05	0.5900	0.190	0.000	0.006
6,000	249.19	472.18	0.6601	0.420	0.000	0.008
5,500	252.43	505.39	0.6975	0.580	0.000	0.010
5,000	255.68	540.48	0.7364	0.790	0.000	0.020
4,500	258.92	577.52	0.7770	1.020	0.000	0.030
4,000	262.17	616.60	0.8193	1.250	0.000	0.040
3,500	265.41	657.80	0.8634	1.580	0.000	0.050
3,000	268.66	701.27	0.9092	1.970	0.000	0.060
2,500	271.91	746.92	0.9562	2.480	0.000	0.070
2,000	275.15	795.01	1.0066	2.950	0.000	0.080
1,700	277.10	826.00	1.0379	3.315	0.000	0.085
1,600	277.71	835.20	1.0475	3.437	0.000	0.090
1,500	274.71	845.60	1.0581	5.316	0.000	0.100
1,475	274.86	847.00	1.0599	5.374	0.150	0.610
1,450	275.01	850.09	1.0625	5.425	0.300	2.140
1,400	275.30	855.70	1.0680	5.531	0.282	6.090
1,300	275.91	866.00	1.0790	5.767	0.243	13.190
1,200	276.52	877.90	1.0895	5.999	0.205	19.240
1,100	277.12	888.10	1.1010	6.249	0.165	24.230
1,000	277.71	898.76	1.1117	6.502	0.000	26.470
500	282 71	954.61	1.1673	6.502	0.000	26.520
0	287.71	1,013.25	1.2250	6.502	0.000	26.570

Total ozone = 0.3 atm cm, solar constant = 1353 Wm^{-2}

Optical characteristics of clouds with different drop size distributions

Since in this paper we want to determine cloud parameter changes caused solely by variations in aerosol particle number and absorption, calculations throughout the entire paper stick to a fixed mean liquid water content, thus implying no change in circulation pattern when changing aerosol characteristics. No feedbacks between changed cloud parameters and circulation are included in the main section. As a first impression of the possible feedbacks, some calculations using formulae given by *Hänel* (1981) are presented in the section on possible feedbacks.

At fixed liquid water content the integral *SW* parameters like total absorption within the cloud, albedo of the entire system, and net flux at the ground (shown in *Fig. 1* mainly for analytical distributions) differ strongly in their dependence on size distribution. The variable optical depth τ (at 0.55 μm wavelength), chosen for the abscissa in Fig. 1 and used without index throughout this paper, is a result of the changing radius r_{ms} of droplets, because τ is propotional to r_{ms} and the number of particles. At fixed liquid water content (LWC) small droplet radius r_{ms} is equivalent to high optical depth τ. Drawing smooth curves through five calculated points only—as done in Fig. 1—would be a risky procedure were it not justified by calculations at intermediate points even from different measured size distributions. The

agreement between the results of using real size distributions versus the analytical size distributions for radiative transfer calculations is demonstrated by comparing the *StI* (open circles) and (dots) results to the analytical size distribution results (smooth curves) shown in Fig. 1. While absorption is rather constant – if we neglect the size distribution C6 standing for an unrealistic distribution with an extremely low droplet concentration and a very big droplet

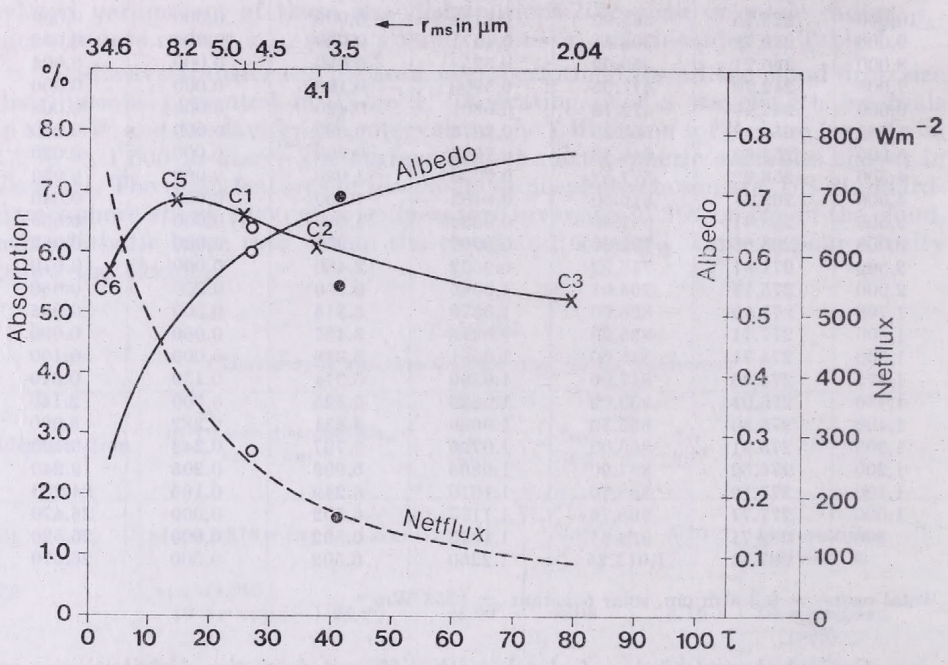

Fig. 1 : Some optical parameters, integrated over the solar spectrum (0.3 – 3.7 μm), for an atmosphere containing a vertically inhomogeneous stratus cloud between 1,000 and 1,500 m with a mean $LWC = 0.2$ gm^{-3}. The parameters: albedo of the atmosphere–cloud–ground system, fractional absorption within the cloud in % and net flux at the ground in W m^{-2} are shown for 4 analytical droplet size distributions as a function of the optical depth τ at 0.55 μm wavelength. The upper horizontal scale shows the corresponding r_{ms} values. The cosine of the sun's zenith angle is 0.9, surface albedo $A_s = 0.2$. The open circles stand for the measured distribution *StI*, the dots for distribution *O*, and crosses for *N*

size – system albedo and net flux at the ground change drastically with droplet size. Albedo is highest and net flux lowest with lowest droplet size. This result already shows the potential high influence of aerosol particles on cloud albedo, if we generally expect a dependence of mean radius r_{rms} of droplets on particle number.

Table III contains fractional absorption A^*, reflection or albedo A and downward flux $F\downarrow$ of the atmosphere-cloud-ground system together with these parameters for the stratus cloud only. The table shows the tremendous variation in cloud and system albedo at constant LWC (as given in Table II) caused only by variation in cloud droplet sizes. For the model cloud C1, the possible influence of absorbing aerosol particles is included, demonstrating their strong albedo-reducing effect and an enhancement of the cloud's fractional absorption

A^* roughly by a factor 2. The absorption coefficient of aerosol particles stems from measurements in a polluted industrial area at Mainz, F. R. Germany (*Fischer*, 1973), and possibly gives an upper limit on particle absorption. For details of the method of incorporating absorbing aerosol particles into clouds and the calculation of the resulting complex refractive index of the mixture of droplets and unactivated aerosol particles, see *Grassl* (1975, 1978).

TABLE III

System albedo A, SW downward flux $F_\downarrow$ at the ground and fractional absorption A^* given in % of the downward flux at the top of the atmosphere, for the model atmosphere containing a 500 m stratus cloud from 1.0 to 1.5 km with vertically inhomogeneous LWC. All values are given for 4 different cloud drop size distributions and 3 different zenith angles Θ of incoming solar radiation. Rows with label C pertain to the cloud only and percentage values are related to incoming flux at the cloud top. Surface albedo $A_S = 0.2$

Size distribution	C1 ($r_c = 4\mu m$)[b]			C3 ($r_c = 2\mu m$)[b]			C5 ($r_c = 6\mu m$)[b]			C6 ($r_c = 20\mu m$)[b]		
$\cos\Theta$	A	$F_\downarrow$	A*	A	$F_\downarrow$	A*	A	$F_\downarrow$	A*	A	$F_\downarrow$	A*
0.9	60.7	27.0	17.2	76.9	8.7	16.2	48.4	41.7	17.4	22.4	74.6	16.3
(a)	56.6	23.4	24.3									
0.9 C	68.6	29.3	6.6	86.9	9.3	5.2	54.5	45.4	6.8	25.1	81.9	5.4
(a)	64.0	25.8	14.4									
0.5	67.0	20.7	17.5	78.9	6.7	16.5	57.9	31.8	18.0	34.9	59.7	19.2
(a)	63.5	17.8	23.3									
0.5 C	76.6	23.0	5.0	90.2	7.3	3.9	66.1	35.5	5.5	39.6	66.9	6.3
(a)	72.7	19.8	11.4									
0.3	70.2	17.2	18.3	79.7	5.6	17.2	63.0	26.4	18.9	44.5	48.9	20.8
(a)	67.3	14.8	22.9									
0.3 C	81.0	19.8	4.1	92.1	6.3	3.1	72.4	30.4	4.6	50.5	56.8	6.0
(a)	77.6	17.0	9.5									

(a) Accounting for aerosol absorption using measured absorption coefficients from Mainz, F. R. Germany (*Fischer*, 1973); the optical depth τ_a of the dry aerosol particles from cloud top to the ground has been assumed to be 0.2. All other values assume pure water droplets using complex refractive index values given by *Irvine* and *Pollack* (1968).

(b) r_c = mode radius

While fractional absorption values for varying size distribution do not differ strongly, corresponding heating rates at distinct heights within the atmosphere differ considerably, since the vertical distribution of flux divergence is influenced by the changing phase function and the changing ratio of the coefficients of scattering k_{sc} to extinction k_{ext} (frequently called single scattering albedo ω_o). *Figure 2* first indicates strong heating of the top layers of a cloud by absorption of solar radiation and secondly shows an increasing maximum heating rate ($\simeq 40K/d$ for C1 and C3 cloud types) with decreasing droplet size, accompanied by a small upward shift of the maximum heating. Results for different zenith angles Θ are very similar to those shown for $\cos\Theta = 0.9$.

In the *LW* region the strong cloud top cooling rates show the same dependence on droplet size as solar heating rates; however the maxima within

the uppermost 50 m are higher by approximately a factor of 4. The magnitude of the cooling rates at cloud top by *LW* radiation will never be reached by heating rates in the solar spectral region, even with the strong aerosol particle absorption, as shown in Table III.

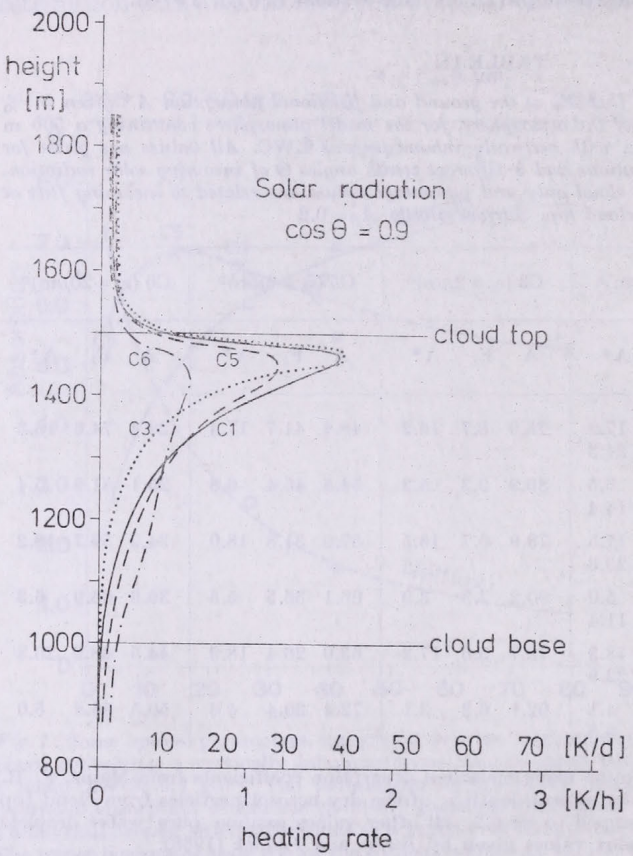

Fig. 2: Heating rates within the solar spectral region in a stratus cloud (details see Table II) with different droplet size distributions (see Table I) at small zenith distance of the sun ($\cos \Theta = 0.9$)

If we combine *SW* and *LW* radiation for noon conditions (when *SW* has the maximum possible influence), we still find a strong net cooling of the upper 80 m of a cloud, a moderate net heating within the cloud interior and an increased, but still moderate net heating of the lower parts of the cloud. The heating in the lower part of the cloud is mainly caused by the *LW* radiation and is proportional to the temperature difference between ground and cloud base.

Test of simplifications in the calculation of the optical depth of a cloud from basic microphysical parameters

This section tests the accuracy of simple formulae already used (*Twomey*, 1978; *Grassl*, 1978) for the calculation of the aerosol particle influence on cloud albedo. Since we postulate constant *LWC* (equivalent to constant volume *V*) for different size distributions

$$v_i = \frac{4n}{3} \int_{r_1}^{r_2} r^3 \cdot n_i(r)\, dr = \frac{4n}{3} N_i r_{vi}^3 \qquad (1)$$

with

$$r^3_v = \frac{\int_{r_1}^{r_2} r^3 n(r)\, dr}{\int_{r_1}^{r_2} n(r) \cdot dr = N},$$

we find the ratio of total droplet numbers N, for two size distributions i and j

$$\frac{N_i}{N_j} = \frac{r_{vj}^3}{r_{vi}^3}. \qquad (2)$$

The optical depth τ of a cloud is proportional to r_{ms}^2, where

$$r_{ms} = \frac{\int_{r_1}^{r_2} r^2 n(r)\, dr}{\int_{r_1}^{r_2} n(r)\, dr}$$

If we want to use equation (2) for the derivation of a simple formula for the optical depth ratio τ_i/τ_j of two clouds with the same vertical extent only

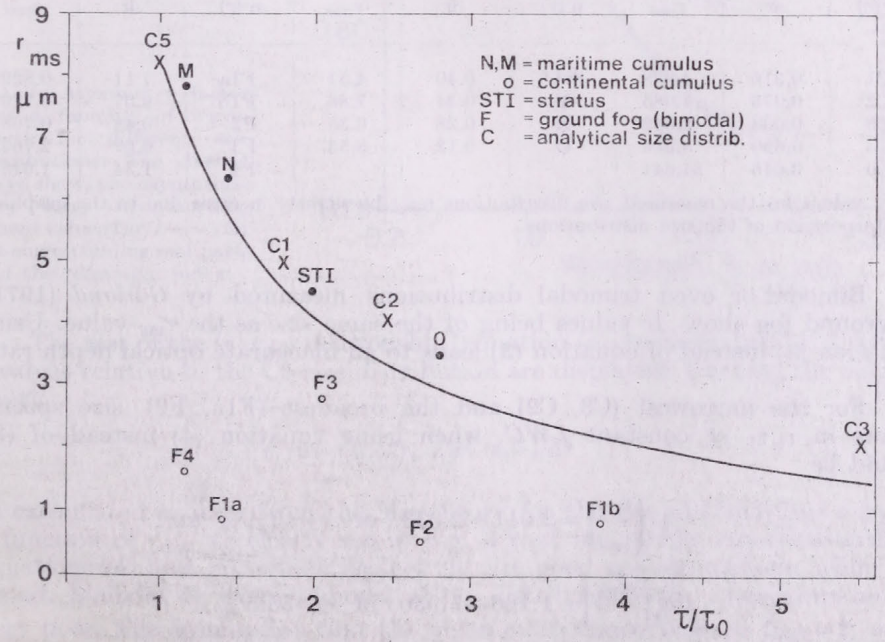

Fig. 3 : Mean square radius r_{ms} as a function of relative optical depth τ/τ_0, normalized with the C5 cloud droplet size distribution, for strongly different analytical and measured distributions as presented in Table I. The full curve follows equation (4) and therefore discards not only differences of extinction efficiency Q_{ext} to the value 2 adopted in equation (3), but also the differences Δr

knowing the number of droplets, we should account for the difference between the mean volume radius r_v and the mean square radius r_{ms}. This value, r_{ms}, is normally used for the approximation of the optical depth ratio.

$$\frac{\tau_i}{\tau_j} \simeq \frac{N_i}{N_j} \frac{r^2_{msi}}{r^2_{msj}} \tag{3}$$

Equation (3) implies a constant extinction efficiency Q_{ext} ($\simeq 2$), which is a justified approximation in the *SW* region for all droplet radii occuring. Within the *LW* region this assumption no longer holds for small droplets with $r = 10$ μm. Neglecting the difference $\Delta r = r_v - r_{ms}$ and combining equations (2) and (3) leads to

$$\frac{\tau_i}{\tau_j} = \left(\frac{N_i}{N_j}\right)^{1/3} \quad \text{or} \quad \frac{\tau_i}{\tau_j} = \frac{r_{msj}}{r_{msi}} \tag{4}$$

The first part of equation (4) has been proposed by *Twomey* (1978) and used by *Grassl* (1978, 1979). Δr depends strongly on size distribution (see *Table IV*) and the broader the distribution the larger the radius difference Δr.

TABLE IV

Radius differences Δr *in* μm *between mean volume radius* r_v *and the root-mean-square radius* r_{ms} *for all size distributions shown in Table I*

n (r)	Δr	r_{rms}	n (r)	Δr	r_{rms}	n (r)	Δr	r_{rms}
C1	0.316	4.988	StI*	0.40	4.51	F1a	1.11	0.829
C2	0.075	4.085	M	0.34	7.86	F1b	0.57	0.779
C3	0.038	2.042	N	0.28	6.35	F2	0.48	0.768
C5	0.690	8.215	O	0.12	3.53	F3	0.67	2.765
C6	3.646	34.641				F4	1.34	1.615

* All values for the measured size distributions may be slightly in error due to the graphical interpolation of the size distributions.

Bimodal or even trimodal distributions measured by *Garland* (1971), in ground fog show Δr values being of the same size as the r_{ms} value. Using equation (4) instead of equation (3) leads to an inaccurate optical depth ratio τ_i/τ_j.

For the narrowest (C3, C2) and the broadest (F1a, F2) size spectra errors in τ_i/τ_j at constant *LWC*, when using equation (4) instead of (3), would be

$$\Delta \left(\frac{\tau_{C3}}{\tau_{C2}}\right) = 2.011 - 2.033 \quad \text{or} \quad -1.1\% \text{ and}$$

$$\Delta \left(\frac{\tau_{F2}}{\tau_{F1a}}\right) = 1.186 - 1.930 \quad \text{or} \quad -38.5\%$$

respectively. For all the size distributions, expect the ground fog, with $\Delta r \simeq r_{ms}/10$, the error in τ_i/τ_j calculated with equation (4) instead of (3) is below 5% and thus tolerable. This allows us to proceed, as *Twomey* (1978), for many size distributions, from equation (4) to

$$\frac{\tau_i}{\tau_j} \simeq \left(\frac{N_{ai}}{N_{aj}}\right)^{0.267} \tag{5}$$

using an empirical relation between N and the number of the aerosol particles N_a

$$\frac{N_i}{N_j} \simeq \left(\frac{N_{ai}}{N_{aj}}\right)^{0.8} \tag{6}$$

derived from measurements reported by *Warner* and *Twomey* (1967). Equation (5) relates to the optical depth τ of a cloud directly to the number of aerosol particles N_a.

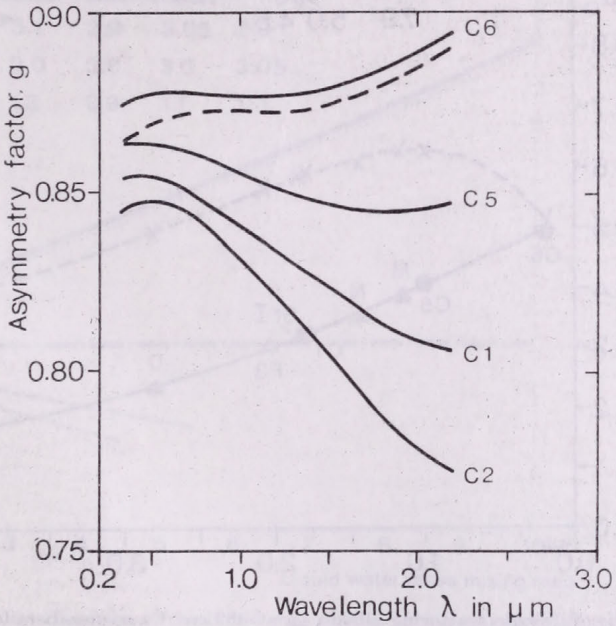

Fig. 4: Asymmetry factor g as a function of wavelength for different size distributions. The dashed curve shows the asymptotic very large nonabsorbing sphere value ($2\pi r/\lambda \to \infty$) for the corresponding real parts of the refractive index

The test of the (τ, r_{ms}) relationship [equation (4)] is shown in *Fig. 3*, where τ values relative to the C5-size distribution are displayed. Plotting the optical depth

$$\tau_i = \int_{r_{1i}}^{r_{2i}} Q_{ext}(r_i, \lambda) r^2 \cdot n_i(r)/dr \tag{7}$$

as caclculated exactly from the Mie-theory for the size distributions $n_i(r)$ as a function of r_{msi} we clearly see in Fig. 3 that for narrow size distributions equations (4) and (5), which neglect Δr, are good approximations, while for broad, bimodal or even trimodal (F1a) distributions the approximation is very poor. The assumption that the mean extinction efficiency $\bar{Q}_{ext} = 2$, used already for equation (3), shifts all exact results for small size distribution to the right and thus above the curve in *Fig. 6*, since $\bar{Q}_{ext} \geq 2$ and increases with decreasing radius for all distributions used. This explains the rather strong shift to the right for the narrow distribution C3 with small droplets.

Many measurements of droplet size distribution omit small droplets below approximately 1 μm radius, which in turn may have lead to the actual analytical distributions proposed by previous investigators. Therefore the poor approximations found in *Fig. 5* for ground fog (as measured by *Garland*, 1971) may apply to many cloud drop size distributions as well.

Up to now only two mechanisms for cloud albedo variations associated with changes in aerosol particle characteristics have been discussed; we found that increasing aerosol absorption reduces the cloud albedo and increasing

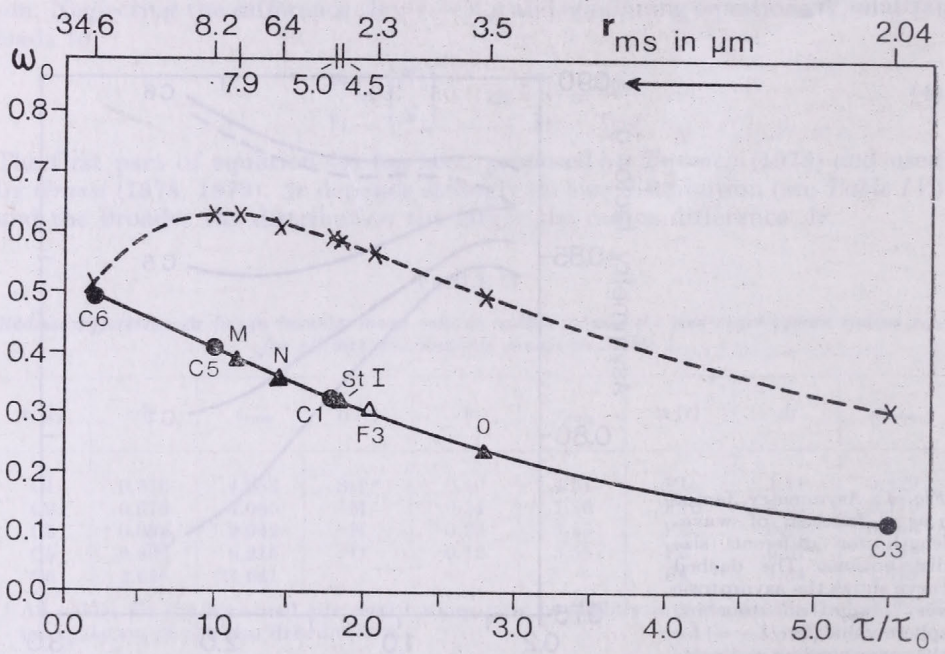

Fig. 5: Single scattering albedo ω_0 at 833 cm^{-1} wavenumbers for analytical (●) and measured drop size distributions as a function of τ/τ_0 (△ corresponds to bimodal ground fog and ▲ to monomodal stratus and cumulus drop size distributions). The upper horizontal scale shows the corresponding r_{ms} values, the dashed curve ω_0 values for 1,000 cm^{-1}

particle number may enhance cloud albedo. A third mechanism is albedo enhancement due to a flattening of the scattering or phase function with decreasing droplet size. This effect has already been shown by *Grassl* (1978, 1979), however it has been overestimated (see Fig. 5 in *Grassl*, 1979). *Fig. 4* displays the asymmetry factor g (the cosine of scattering angle weighted with the phase function – a measure for the steepness of the phase function within the forward peak) for several size distributions. This figure clearly indicates only small variations of g in the visible spectral region, where the cloud albedo values are mainly determined. An already asymptotic domain for g is reached by cloud droplets with several micrometers radius. For nonabsorbing spheres that are very large with respect to wavelength, the dashed curve in *Fig. 7* is valid. The numbers for this curve were taken from a table in *Van de Hulst* (1957, page 226). If there is absorption, the g-values for very large

spheres are increased and results should lie above the dashed curve in *Fig.* 4. This is true for size distribution C6 with the largest droplets of all distributions. The general strong increase in absorption by liquid water at wavelength $\lambda > 1$ μm, which should shift the C6 curve to still higher g-values, is compensated by the reduction of the size parameter $x = 2\pi r/\lambda$ governing the large sphere asymptotic region. Increasing optical depth alone, i.e. retaining g values for cloud C5, when calculating the albedo change due to a shift from a C5 to a C1 cloud, and comparing it to a calculation with changes in g, leaves a phase function influence on cloud albedo of 1.67, 1.45, 1.23, 0.99%

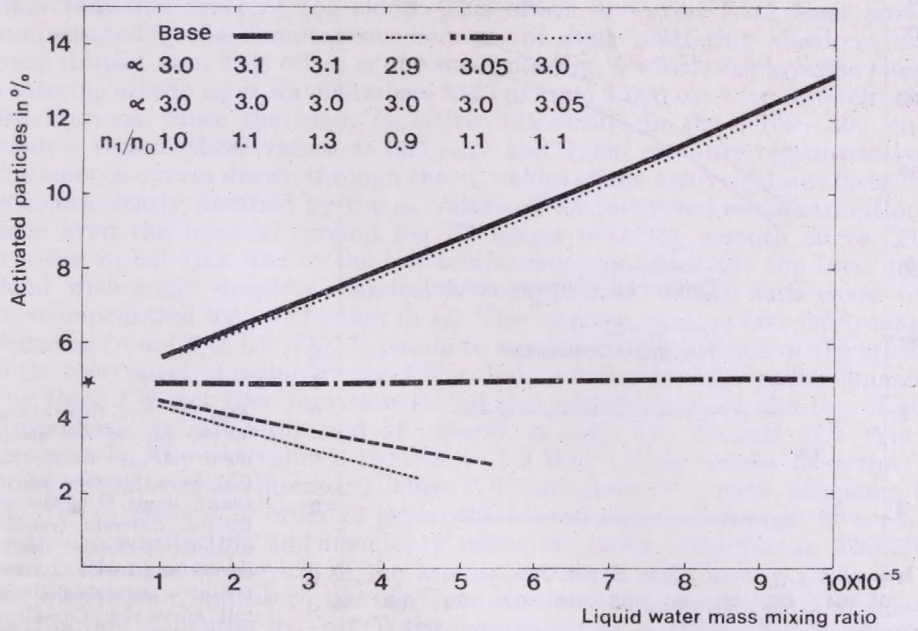

Fig. 6: Activated particles in % as a function of the liquid water mass mixing ratio for different aerosol particle size distribution and number concentration changes at a supersaturation (without feedback) of 5×10^{-3}

for the cos Θ values 0.9, 0.7, 0.5 and 0.3, respectively. Despite the reduction of the phase function influence on albedo enhancement, the already known general picture remains: Depending on the increase in the mass absorption coefficient of aerosol particles the crossover from albedo enhancement to albedo reduction for a pollution increase at constant liquid water content will occur at different optical depths of cloud (*Grassl*, 1979). However, rather thin clouds with $\tau \leq 25$ will always show an enhancement of albedo with increasing particle number.

Possible influence on the number of activated particles by other parameters

Up to now neither changed chemical composition, nor variations in the size distribution of aerosol particles have been considered. Also changes in

liquid water content and maximum supersaturation, which would change with aerosol particle characteristics, have been neglected. If variations of surface tension, the water uptake with relative humidity and particle size distribution, as well as the feedback on supersaturation and LWC are included, following formulae given by *Hänel* (1981), the simple approach in previous sections may be strongly modified. This is clearly demonsrated by Fig. 6, which compares different changes of the parameters mentioned. The

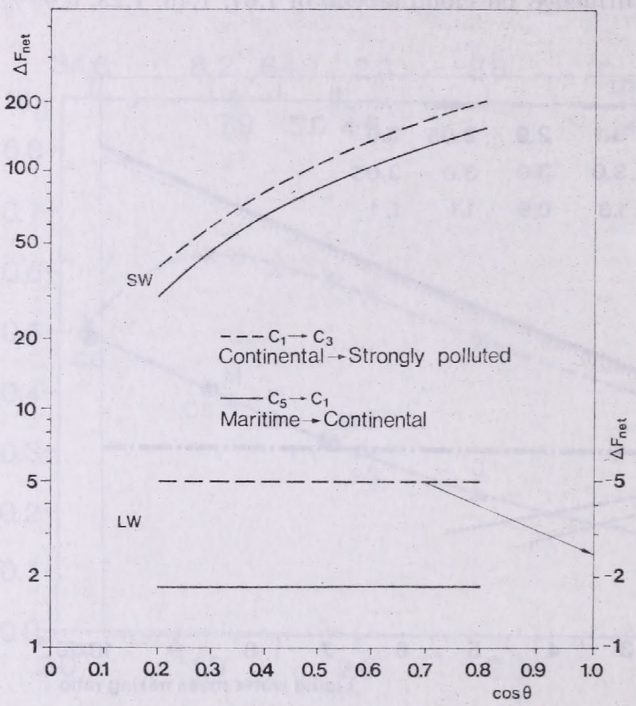

Fig. 7: Net flux change at the top of the atmosphere $\Delta F_{net} = F(C_i) - F_{net}(C_i)$ as a function of the zenith angle Θ of the sun for two different transformations of clouds: dashed curve for C1→C3 ≙ continental → strongly polluted, full curve for C5→C1 ≙ maritime → continental

percentage of activated particles, which up to now has been parameterized by the experimental result of *Warner* and *Twomey* (1967), changes drastically especially with variations in size distribution, α_1 and α_2 being the power law exponents of the $0.01-0.1$ and $0.1-10$ μm size range. Variatons of surface tension and the water uptake (expressed by the exponential mass increase coefficient η) are not shown directly, since, a 10% increase in the particle numbers (n_1, $n_0 = 1.1$) is equivalent to a lowering of surface tension by 6% and an increase of η by 6.6 %. Calculations for stronger parameter changes as those snown, have to be avoided, since the assumption of only minor changes in liquid water content for the basic and the changed state leading to *Hänel*'s formula would be stressed too much. In order to estimate the overall effect, the standarad relation $CCN_1/CCN_0 = (N_1/N_0)\gamma = (N_1/N_0)$ for sugar cane fires in Australia, which is the result of all influences of all parameters, has to be known for different areas and aerosol types.

Influence on radiation balance

All minor atmospheric constituents, as e.g. aerosol particles, influencing radiative transfer will change the radiation balance and thus the climate. The most interesting parameter in this context is the radiation balance at the top of the atmosphere. While this parameter is strongly dependent in the solar spectal region on the droplet size distribution for fixed liquid water content and cloud height (see albedo values at top of the atmosphere in Table III), the changes in the *LW* region are rather small and show no systematic behaviour. One might expect that clouds with smaller droplets will emit less radiation than those with bigger droplets because of an upward shift of the main radiation layer of the cloud. This effect, however, is at least partly compensated by the simultaneous decrease of single scattering albedo ω_0 and mean droplet size. This effect is obvious from Fig. 5 which displays the single scattering albedo ω_0 at wavenumbers 833 cm^{-1} and 1,000 cm^{-1} for different size distributions. Since the main radiative loss occurs in the 1,100 − 800 cm^{-1} window region, these values at 833 cm^{-1} and 1,000 cm^{-1} are representative. The smooth curves drawn through the ω_0 values of the analytical size distributions are clearly justified by the ω_0 values of the measured size distributions, since even the bimodal ground fog F3 agrees with the smooth curve. The decrease in net flux due to the low temperature at which the top layer of a cloud with small droplets radiates, is compensated, or (as with cloud C3) overcompensated by a reduction in ω_0. The increase in ω_0 (1,000 cm^{-1}) when changing from C6 to C5 (Fig. 5) points to a partial compensation of the effects in the solar spectral region by the *LW* radiative transfer in this radius domain. The total *LW* net flux variation for all size distributions at the top of the atmosphere, at cloud top and at ground, is only 7.7, 9.0 and 11.0 Wm^{-2}, respectively. The last value is reduced to 1.3 Wm^{-2}, if the results from the C6 cloud calculations are discarded. These *LW* variations have to be compared to the *SW* variations, in order to assess the overall effect of changes in aerosol particle concentration and imaginary refractive index (absorption). The *SW* netflux changes at the top of the atmosphere for a shift from a C5 to a C1 size distribution similar to the maritime-continental transformation of a size distribution, amounts to −62 Wm^{-2} (equivalent to a system albedo change from 57.9 to 67.0%) at $\cos \Theta = 0.5$ (Fig. 4). This number far outweighs the −2 Wm^{-2} for the corresponding *LW* net flux variation. The big difference between *LW* and *SW* effects generally holds for all zenith angles Θ (Table III) and a concomittant increase in the aerosol mass absorption coefficient, if $\tau = 25$. Thus the mean droplet size will, at least for clouds with $\tau = 25$, have a strong influence on the radiation balance ($SW + LW$) at the top of the atmosphere. A compensation of *SW* and *LW* effects may be possible for thick clouds with an increase in aerosol absorption coefficient simultaneously with an increase in particle number.

First estimate of a change of global albedo with pollution level

The aerosol particles' influence on the radiation balance and on albedo in clear areas shows the same broad features as those derived for cloudy areas. Depending on the amount of absorption of the particles, an increase in particle number may enhance or reduce albedo in both areas. The crossover in clear areas is a function of surface albedo and the absorption-to-backscattering ratio

of the particles (*Kellogg*, 1978), while in cloudy areas it is a function of the absorption coefficient and the optical depth of the clouds. These results disregard for the present, possible influences on cloud parameters due to changing solubility and surface tension (*Hänel*, 1976, 1981), which may well influence the cloud droplet size distribution. For the derivation for a possible upper limit of the global albedo change caused by variations of cloud parameters, let us assume a fixed aerosol particle absorption coefficient, leading to albedo enhancement only. With a cloud cover $N_c = 0.5$, a global albedo value $A_g = 0.3$, a mean albedo, $A_c = 0.45$ over cloudy areas and using $dA_c/d\tau = 0.2/\tau$, as given by *Twomey* (1978), A_c for a doubling of aerosol particle number will be 0.034 for rather thin clouds in the $10 \leq \tau = 30$ range. This leads to a global albedo change $\Delta A_g \simeq 1.7\%$. Since a doubling of aerosol particles over the entire globe is highly improbable, a reduction of this doubling to only 10 % of the cloudy areas leaves only +0.17% change in global elbedo.

Conclusion

Referring to the questions listed in the introduction, our results suggest a stronger influence of aerosol particles on optical cloud parameters for the solar region than the corresponding results for *LW* region. In the latter spectral region, increasing particle concentration steepens the gradient of the cloud top cooling rates. However, this has only a small influence on the total emitted radiation of an atmosphere containing a stratus cloud layer because of congruent relations between the optical depth and the single scattering albedo for changing particle concentrations. If we increase particle number while maintaining a constant *LWC* (thus fixing the circulation pattern), we increase optical depth. This will cause a shift of the layer with radiation losses upward to lower temperatures which (at constant single scattering albedo) would lead to a reduced emission. However, at the same time the single scattering albedo is lowered, causing a higher emissivity and thereby compensating for the lower temperatures.

Simplifications introduced for estimating cloud albedo changes for variations of the aerosol particle charecteristics will only hold, if the cloud drop size distributions are rather narrow. Since many drop size measurements omit droplets with $r \leq 3$ μm, bimodal or even trimodal distributions may be more probable than had been considered in previous cloud studies. This would raise doubts with regard to the applicability of the simplifications partly used in this study.

The changes in optical parameters of clouds in the *LW* spectral region caused by corresponding changes in aerosol characteristics may damp in parts of a layer cloud the strong changes in the *SW* region if looking at heating and cooling rates. However, these changes in particle number and thus mean droplet size may even modestly amplify the solar contributions to the net flux changes at the top of the atmosphere.

Since no data exist on the distribution of optical depth of clouds, a first estimate of the sign of a global albedo change for changing pollution levels can only be given for pollution changes that do not affect the mass absorption coefficient of the aerosol particles. In this case increasing turbidity or pollution will lead to an increase in the mean shortwave cloud albedo and this energy loss for the atmosphere-earth system is not compensated by a concomittant reduction of emission in the *LW* region. If the mass absorption coefficient

k in the *SW* region and the number of aerosol particles increase simultaneously – and this is confirmed by measurements (*Fischer*, 1973) from remote and industrialized areas – there may well be no effect at all, depending on the ratio $(\tau/\tau_0)/(k/k_0)$ which determines the crossover from an albedo increase to an albedo decrease.

The above results may be questionable if the relation between condensation nuclei and total particle concentration deviates strongly from $(CCN_{-1}/CCN_0) = (N_{-1}/N_0)^{0.8}$.

REFERENCES

Deirmendjian, D., 1969: Electromagnetic scattering by spherical polydispersions. American Elservier, New York.

Fischer, K., 1973: Mass absorption coefficient of natural aerosol particles in the 0.4 – 2.4 μm wavelength interval. *Contr. Atm. Phys. 46*, 89 – 100.

Garland, J. A., 1971: Some fog droplet size distributions obtained by an impaction method. *Quart. J. Roy. Met. Soc. 97*, 483 – 494.

Grassl, H., 1975: Albedo reduction and radiative heating of clouds by absorbing aerosol particles. *Contr. Atm. Phys. 48*, 199 – 210.

Grassl, H., 1978: Strahlung in getrübten Atmosphären und in Wolken. *Hamburger Geophysik.* Einzelschriften, Reihe A. Heft 37, 136 pages.

Grassl, H., 1979: *Possbile changes of planetary albedo due to aerosol particles*, in: *Man's Impact on Climate.* Editors: *Bach, Pankrath, Kellogg*, Elsevier, Amsterdam, 327.

Hansen, K. and *J. Travis*, 1974: Light scattering in planetary atmospheres. *Space Science Review 16*, 527 – 610.

Hänel, G., 1976: Extinction and absorption coefficients and liquid water content of fog depending on aerosol composition. *Proceeding of the Symposiun on Radiation in the Atmosphere;* Editor: *H.-J. Bolle*, Science Press, Princeton.

Hänel, G., 1981: Influences of physical and chemical properties of atmospheric particles on the activation process in fog and clouds. *Beitr. Phys. Atmosph. 54*, 159 – 171.

Irvine, W. M. and *Pollack, G. B.*, 1968: Infrared optical proporties of water and ice spheres. *Icarus 8*, 324 – 360.

Kellogg, W. W., 1978: *Global influences of mankind on the climate*, in: *Climate Change;* Editor: *I. Gribbin*, Cambridge University Press, London, 205 – 227.

McClatchey, R. A., Benedict, W. S., Clough, S. A., Burch, D. E., Calfee, R. F., Fox, K., Rothmann, L. S. and *Garing, J. S.*, 1973: AFCRL *Atmospheric absorption line parameters compilation.* AFORL – TR – 0016.

Moskalenko, N. I., 1969: The spectral transmission function in the bands of the water vapour, O_3, N_2O, and N_2 atmosheric comoponents. (in Russian) *Izv. Atmosph. and Oceanic Phys. 5.* 1179 – 1190.

Plass, G. N., Kattawar, G. E. and *Catchings, G. E.*, 1973: Matrix-operator-theory of radiative transfer. *Appl. Opt. 12*, 314 – 329.

Ryan, R. T., Blau, H. H., Jr. Von Thüna, P. C., Cohen, M. L., Roberts, and *G. D.*, 1972: Cloud microstructure as determined by an optical cloud particle spectrometer. *JAM. 11*, 149 – 156.

Stephens, G. L., 1978: Radiation profiles in extended water clouds. Parts I and II, *JAS, 35*, 2111 – 2132.

Stephens, G. L., Paltridge, G. W. and *Platt, C. M. R.*, 1978: Radiation profiles in extended water clouds. Part III: Observations, *JAS, 35*, 2133 – 2141.

Twomey, S., 1974: Pollution and the planetary albedo. *Atmos. Environment., 8*, 1251 – 1256.

Twomey, S., 1978: *Influence of the aerosol on optical properties of clouds*, GARP Climate Dynamics Sub-Programme, Report of IOC-Study Conference on parameterization of extended cloudines, Appendix E, WMO, Geneva, October 1978.

Van de Hulst, H. C., 1957: *Light scattering by small particles.* Wiley, New York, 1957, 470.

Warner, J. and *Twomey, S.*, 1967: The production of cloud nuclei by cane fires and the effect on cloud droplet concentration. *JAS, 24*, 704 – 706.

Wiscombe, W. J., 1976a: Extension of the doubling method to inhomogeneous sources. *J. Quant. Spectr. Rad. Transf., 16*, 477 – 489.

Wiscombe, W. J., 1976b: On intialisation, error and flux conservation in the doubling method. *J. Quant. Spectr. Rad. Transf., 16*, 637 – 658.

IDŐJÁRÁS

Az Országos Meteorológiai Szolgálat folyóirata, 86. évf. 2–4. szám, 1982, március–augusztus
Journal of the Hungarian Meteorological Service, Vol. 86. No. 2–4. March–August 1982. Budapest

An evaluation of the possible effect of anthropogenic sulfate particles on the precipitation ability of clouds over Europe

E. MÉSZÁROS and G. VÁRHELYI, *Institute for Atmospheric Physics, H—1675 Budapest, P.O.B. 39, Hungary*

Az antropogén szulfát részecskék hatása a csapadékképződésre Európa fölött. Európa fölött a kénvegyületek légköri körforgalmában a szulfát részecskék kb. 80%-a antropogén. Mivel ezek a részecskék aktív kondenzációs magvak, valószínű, hogy az ipari forradalom előtt a csapadékmennyiség különbözött a jelenlegi értéktől. Huszonkilenc európai állomás 1871–1970 közötti adatai szerint azonban a csapadékmennyiség időbeli változásai nem egyértelműek. Valószínű ezért, hogy a kondenzációs magvak számának ötszörös növekedése nem befolyásolja alapvetően a csapadékképződést.

⁎

An evaluation of the possible effect of anthropogenic sulfate particles on the precipitation ability of clouds over Europe. It is shown by atmospheric sulfur budget calculation that about 80% of sulfate particles are man-made over Europe. Considering that these particles are supposed to be effective cloud condensation nuclei, it is reasonable to suppose that before the industrial revolution the quantity of precipitation was different from the present value. However, no unambiguous trend is found in the amount of precipitation between 1871 and 1970 by using the data of 29 European stations. Hence, it is possible that a five-fold increase in the number of condensation nuclei does not influence essentially the precipitation formation.

⁎

Introduction. The study of the effects of air pollution on atmospheric phenomena is one of the most important tasks of atmospheric science at present. Such an effect can be caused by anthropogenic aerosol particles influencing the microphysical processes in clouds and subsequently the formation of precipitation which depends, among other parameters, on the initial cloud structure. Thus, a smaller number of cloud condensation nuclei (CCN) result in a lower droplet concentration and larger average droplet size and *vice versa* (see e.g. *Fletcher*, 1962). This means that, according to the coalescence theory of precipitation formation, an increase in the CCN concentration decreases the amount of precipitation.

Different measurements on the physical properties of CCN (e.g. *Twomey*, 1968 and 1971; *Dinger* et al., 1970) as well as on the chemical composition and size distribution of aerosol particles (e.g. *Mészáros*, 1968; *Mészáros* and *Vissy*, 1974) show that the majority of condensation nuclei consist mostly of fine sulfate particles formed in the air by gas-to-particle conversion.

It is reasonable to suppose that in industrialized areas, where sulfur dioxide emission is important, the precipitation regime has substantially been modified by sulfate particles attributable to human activity. The aim of this paper is to discuss this problem in the case of the European continent by

determining the anthropogenic fraction of sulfate particles on the basis of atmospheric sulfur budget calculations as well as by analyzing the trend of precipitation amount at different European stations between 1871 and 1970.

1. *The European sulfur budget*

The atmospheric sulfur budget presented is based on a previous paper dealing with the continental cycle of sulfur species (sulfur dioxide and sulfate) in oxidized form (*Mészáros* et al., 1978). The results of this previous work are completed now with estimates on the continental source strength of hydrogen sulfide, carbonyl sulfide, carbon disulfide and dimethyl sulfide emitted by the biosphere.

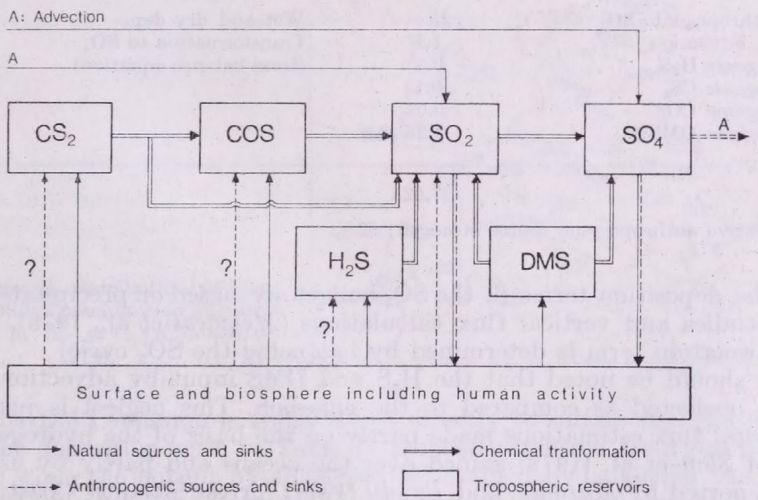

Fig. 1: Scheme of atmospheric sulfur budget (for further details see the text)

Briefly, it is assumed that over Europe there is a box, with an impermeable lid at the tropopause. The sulfur input into the box is due partly to advection and partly to surface emissions, while the output is determined by the wet and dry deposition and advection. In the box gaseous sulfur species transform chemically into a more oxidized state and the loss by advection is in sulfate form *(Fig. 1)*.

The source and sink terms in the budget of sulfur dioxide–sulfur over Europe are summarized in *Table I*. The anthropogenic source strength has been taken from Semb's paper (*Semb*, 1978), while SO_2 advection has been calculated from the results of atmospheric concentration measurements over the Atlantic by using a 25 km h^{-1} mean tropospheric wind speed (*Mészáros* et al., 1978). Further, the atmospheric H_2S burden has been determined from data published by *Jaeschke* et al. (1978). This burden was divided by a residence time of 12 hours to obtain the emission given in Table I. The emission of other biogenic gases, for lack of published observations made in the European air, has been estimated in the following manner. The natural emission rates

for these materials have been compiled by *Várhelyi* and *Gravenhorst* (1981). Their compilation gives the release of biogenic sulfur gases for different soils as well as for estuarine marshes. It should be noted that the area of estuarine marshes and intertidal flats around Europe (equal to 0.14×10^6 km^2) was considered to be within the box. By taking into account the extent of the source areas of different types and the emission rates given by the authors mentioned, the European biogenic source strengths of DMS, CS_2 and COS are calculated to be 0.56, 0.10 and 0.04 Tg S yr^{-1}, respectively.

TABLE I

The SO_2-S budget in the atmosphere over Europe. The values are expressed in Tg yr^{-1} sulfur

Source	Strength	Sink	Strength
Anthropogenic SO_2	25	Wet and dry dep.	17
SO_2 advection	1.1	Transformation to SO_4	10.3
Biogenic H_2S	0.8	(from balance equation)	
Biogenic CS_2	0.1		
Biogenic COS	0.04		
Biogenic DMS	0.28		
Σ	27.32		27.3

Relative anthropogenic source strength: 92%

The deposition terms in the SO_2 budget are based on precipitation chemistry studies and vertical flux calculations (*Mészáros* et al., 1978), while the transformation term is determined by balancing the SO_2 cycle.

It should be noted that the H_2S and DMS input by advection into the box is neglected as compared to the emission. This neglect is justified by horizontal flux estimations made partly on the basis of the hydrogen sulfide data of *Slatt* et al. (1978) gained over the oceans and partly by using DMS data reported by *Maroulis* and *Bandy* (1977) for the Atlantic Coast. In these estimations a scale height of 1 km was assumed for both species (see *Sze* and *Ko*, 1980). On the other hand, since, according to the results of atmospheric measurements reviewed by *Bandy* and *Maroulis* (1980), COS and CS_2 concentrations are practically the same over oceanic and continental locations (over continents they are a bit higher), we supposed that the input by advection

TABLE II

The SO_4-S budget in the atmosphere over Europe. The values are expressed in Tg yr^{-1} sulfur

Source	Strength	Sink	Strength
From anthropogenic SO_2	9.48	Wet and dry dep.	5.3
SO_4 advection	1.0	SO_4 advection	6.3
From biogenic SO_2	0.82	(from balance equation)	
From biogenic DMS	0.28		
Σ	11.58		11.6

Relative anthropogenic source strength: 82%

is at least equal to the output by advection. For this reason these terms were not taken into account in further considerations.

It follows from data given in Table I that 92% of the sulfur dioxide input into our box is due to anthropogenic emissions. Subsequently, the same fraction is man-made in the part of SO_2 transformed to sulfate particles.

Table II contains the European budget of sulfate–sulfur in the air. The SO_4–S advection is taken from our previous work (*Mészáros* et al., 1978), while the biogenic DMS source strength is based on the assumption that the

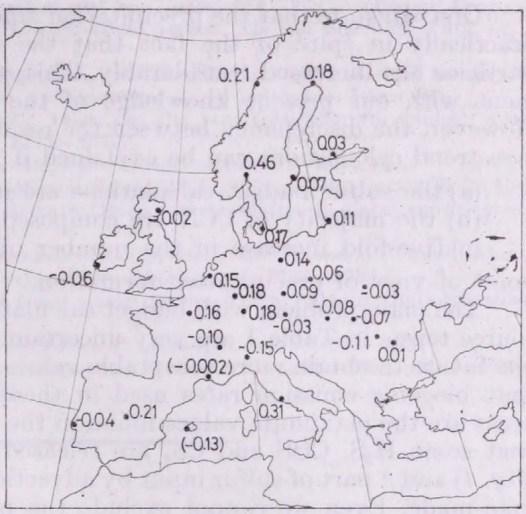

Fig. 2: Spatial distribution of the relative trend of precipitation amount expressed in % yr^{-1} (*Koflanovits*, 1974)

half of the DMS emission is transformed directly to sulfate (see *Sze* and *Ko*, 1980). The deposition term in Table II is mostly inferred from precipitation analyses, while the output by advection is obtained by balancing the atmospheric SO_4 budget over Europe. An important consequence of values in Table II is that 82% of sulfate particles come from sulfur gases emitted by anthropogenic sources. Thus, it is reasonable to suppose that before the industrial revolution the number of sulfate particles in the atmosphere over Europe was about five times less than at present provided that the size distribution of these particles was similar to the present average spectrum.

2. *The trend of precipitation amount over Europe*

It follows from the above discussion that theoretically there is a possibility that the precipitation formation ability of clouds over Europe has been modified due to the increase of the concentration of anthropogenic sulfate particles. To study this possibility the trend of the precipitation amount between 1871 and 1970 was calculated for 29 European meteorological stations (*Koflanovits*, 1974). The results of this calculation are plotted in *Fig. 2*. This figure shows the ratio expressed in % yr^{-1} of the absolute linear trend to the average precipitation amount. One can see from this figure that in NW Europe the precipitation amount slightly increased, while it decreased to a certain extent over the south-eastern part of the continent during the time interval consid-

ered. Except the rather high value for one station (Oslo) the increase of the amount of precipitation is maximum around 20% per 100 yr. The maximum decrease observed in Sibiu (Rumania) is only 11% per 100 yr. Thus we can conclude that, on the one hand, the variation in the amount of precipitation during the last hundred years over Europe is not consistent and, on the other hand, it can be neglected as compared to the change of the number of CCN from sulfate.

3. *Discussion*

One can state that the precipitation amount over Europe has not changed practically in spite of the fact that the number of anthropogenic sulfate particles has increased considerably. This statement seems to be in disagreement with our present knowledge of the cloud and precipitation physics. However, the discrepancy between the results of sulfur budget and precipitation trend calculations can be explained if

(a) the sulfur budget calculations are incorrect;

(b) the majority of CCN are composed of other than sulfate species;

(c) five-fold increase in the number of CCN is not important from the point of view of precipitation formation.

The main problem with budget calculations presented is that the biogenic source terms in Table I are very uncertain. Much more research is needed in the future to obtain more acceptable values. It should be noted in this respect that biogenic emission rates used in these calculations for different source areas are the maximum values found in the literature. Further, we can expect that some H_2S, COS and CS_2 are released from anthropogenic sources (see *Fig. 1*) and a part of sulfur input by advection into the box over Europe is also man-made. Even we cannot exclude the possibility that a part of biogenic carbonyl sulfide is transported into the stratosphere and lost for tropospheric sulfate particle formation. It follows from this discussion that the five-fold increase of sulfate burden calculated is likely a lower limit.

On the other hand it is probably also correct that CCN consist mostly of sulfate particles. First, one can demonstrate that the concentration of large particles, which can be activated at supersaturations occuring in the clouds, is much smaller than the concentration of cloud droplets (*Mészáros*, 1969). Moreover, it follows from thermodynamic calculations that Aitken-sized particles can be activated under atmospheric conditions only if they are composed of water soluble substances. According to chemical measurements made in different parts of the world, sulfate particles give the most important fraction of soluble materials in the atmospheric aerosol (for further details see *Mészáros*, 1981).

This discussion points into the direction that a five-fold increase in the quantity of CCN does not influence substantially the precipitation release from the clouds. In other words this means that changes in cloud-microphysics due to such a variation in nucleus population are not determinant concerning the formation of precipitation.

REFERENCES

Bandy, A. R. and *Maroulis, P. J.*, 1980: Impact of recent measurements of OCS, CS_2 and SO_2 in background air on the global sulfur cycles. In *Atmospheric sulfur deposition. Environmental impact and health effects*, 55–63, Ann Arbor Science Publ. Inc., Ann Arbor.

Dinger, J. E., Howell, H. B. and *Wojciechowski, T. A.*, 1970: On the source and composition of cloud nuclei in a subsident air mass over the North Atlantic. *J. Atmosph. Sci. 27*, 791–797.
Fletcher, N. H., 1962: *The physics of rainclouds.* University Press, Cambridge.
Jaeschke, W., Georgii, H. W., Claude, H. and *Malewski, H.*, 1978: Contributions of H_2S to the atmospheric sulfur cycle. *Pure and Appl. Geophysics 116*, 465–475.
Koflanovits, E., 1974: Hosszú csapadéksorok trendjének elemzése Európa területén. *Időjárás 78*, 88–96.
Maroulis, P. J. and *Bandy, A. R.*, 1977: Estimate of the contribution of biologically produced dimethyl sulfide to the global sulfur cycle. *Science 196*, 647–648.
Mészáros, E., 1968: On the size distribution of water soluble particles in the atmosphere. *Tellus 20*, 443–448.
Mészáros, A., 1969: Vertical profile of large and giant particles in the lower troposphere. *Proc. 7th International Conference of Condensation and Ice Nuclei*, 364–368, Academia, Prague.
Mészáros, E., 1981: *Atmospheric chemistry. Fundamental aspects.* Elsevier Scientific Publ. Co., Amsterdam.
Mészáros, A. and *Vissy, K.*, 1974: Concentration, size distribution and chemical nature of atmospheric aerosol particles in remote oceanic areas. *J. Aerosol Sci. 5*, 101–110.
Mészáros, E., Várhelyi, G. and *Haszpra, L.*, 1978: On the atmospheric sulfur budget over Europe. *Atmospheric Environment 12*, 2273–2277.
Semb, A., 1978: Sulfur emission in Europe. *Atmospheric Environment 12*, 455–460.
Slatt, B. J., Natusch, D. F. S., Prospero, J. M. and *Savoie, D. L.*, 1978: Hydrogen sulfide in the atmosphere in the northern equatorial Atlantic Ocean and its relation to global sulfur cycle. *Atmospheric Environment 12*, 981–991.
Sze, N. D. and *Ko, M. K. W.*, 1980: Photochemistry of COS, CS_2, CH_3SCH_3 and H_2S: implications for the atmospheric sulfur cycle. *Atmospheric Environment 14*, 1223–1239.
Twomey, S., 1968: On the composition of cloud nuclei in the North Eastern United States. *J. Rech. Atmosph. 4*, 281–285.
Twomey, S., 1971: The composition of cloud nuclei. *J. Atmosph. Sci. 28*, 377–381.
Várhelyi, G. and *Gravenhorst, G.*, 1981: An attempt to estimate biogenic sulfur emission into the atmosphere. *Időjárás 85*, 126–133.

IDŐJÁRÁS

Az Országos Meteorológiai Szolgálat folyóirata, 86. évf. 2–4. szám, 1982. március–augusztus
Journal of the Hungarian Meteorological Service, Vol. 86. No. 2–4 March–August 1982, Budapest

Heterogeneous SO_2-oxidation: Its contribution to the cloud condensation nuclei formation process

R. DLUGI and S. JORDAN, *Kernforschungszentrum Karlsruhe Gmbh, Laboratorium für Aerosolphysik und Filtertechnik I. D—7500 Karlsruhe 1, P.O.B. 3640* F. R. G.

A kén-dioxid heterogén oxidációjának szerepe a felhőmagvak keletkezésében. A légköri felhőmagvak keletkezésének egyik lehetséges mechanizmusa a gázok heterogén reakciója száraz vagy nedves aeroszol részecskék felületén. Jelen munkában a szerzők a kén-dioxid heterogén oxidációjának reakció-kamrában végzett vizsgálatáról számolnak be. A különböző aeroszolokra (pl. korom, pernye, vulkáni hamu, cement) vonatkozó eredményeik szerint a részecskék felületén képződő H_2SO_4 és szulfátok mennyisége erősen függ a relatív nedvességtől, a pH értékétől, a felületen lévő vegyületektől és a részecske formájától. Az ionok közötti vonzás elmélete alapján kiszámítható a különböző összetételű részecskék kritikus túltelítettsége. Az eredmények szerint a SO_2-vel reagált részecskékhez tartozó túltelítettség 2–50-szer kisebb, mint az oxidációban részt nem vevő részecskéké.

⁎

Heterogeneous SO_2-oxidation: Its contribution to the cloud condensation nuclei formation process. One of the possible mechanisms for the cloud nuclei formation in the atmosphere is the process of heterogeneous reactions on dry or wetted aerosol particles. Experiments to study the heterogeneous SO_2-oxidation were performed in a reaction chamber on airborne particles. The results for different aerosols (e. g. soots, fly ash, vulcanic ash, cement dust) show that the amount of H_2SO_4 and sulfates being formed on the particle surface is strongly dependent on relative humidity, pH-value, surface compounds and particle morphology. A theory based on the interionic attraction theory is used to calculate the critical supersaturation for the different particles from the knowledge of their chemical composition. The supersaturation for particles reacted with SO_2 is reduced by a factor of 2–50 compared with particles before the reaction with SO_2.

⁎

Introduction. Recently it was shown that heterogeneous reactions of SO_2 in the atmosphere can lead to considerable amounts of sulfuric acid and sulfate containing aerosol particles and droplets (ISSA, 1978). The heterogeneous oxidation on solid particles can be catalyzed by transition-metal compounds but also by acid or basic centers on their surfaces (e. g. *Britton* and *Clarke*, 1979; *Cofer III* et al., 1981; *Haury* et al., 1978; *Liberti* et al., 1978; *Judeikis* et al., 1978). As mentioned by some authors (*Britton* and *Clarke*, 1979; *Dlugi* et al., 1981) the results of these experiments may be influenced by the geometric arrangement of the different reactors used during these studies. The particle properties can vary remarkably and therefore have a large influence on the reaction rates and the total amount of sulfate or sulfuric acid being formed. The oxidation of SO_2 in aqueous solutions can be catalyzed by transition-metal compounds or take place by a reaction with oxidants as O_3 or H_2O_2 (e. g. *Barrie* and *Georgii*, 1976; *Beilke* and *Gravenhorst*, 1978; *Hegg* and *Hobbs*, 1978; *Penkett* et al., 1979). Also for these reactions a large scatter

of experimental data was found, which can be possibly explained by different mass transfer conditions during these experiments. On the other hand ionic strength effects were neglected when the reaction constants were calculated from experimental data as discussed by *Clarke* (1980). Hence an estimation: which reaction pathway will be more important in the atmosphere, can give only qualitative results at present. As aerosol particles take up water with increasing relative humidity (e. g. *Winkler* and *Junge*, 1972; *Hänel*, 1976), the two types of reactions on particles and inside droplets are only different by the amount of water in an activated particle – being a droplet – or a non activated particle being a particle with concentrated electrolyte solution possibly containing insoluble nuclei. It was discussed, for example by *Kortüm* (1972) and *Clarke* (1980) that ionic parameters can remarkably enhance or reduce the reaction velocity in those electrolyte solutions. So the water uptake of salt containing particles and their chemical reactivity should be controlled by the same physical and chemical quantities.

When aerosol particles are released into the atmosphere, they usually contain different amounts of soluble compounds. If mainly insoluble particles are present, they act as condensation nuclei if the actual supersaturation is larger than for a soluble particle of the same size (*Pruppacher* and *Klett*, 1978). Heterogeneous reactions can produce soluble compounds on insoluble particles. Hence these particles can act as condensation nuclei at lower supersaturations than before the reaction with trace gases.

Some results are presented of an experimental study on the heterogeneous SO_2-oxidation on the surface of coal fly ash particles, cement dusts, vulcanic fly ash and soots. From these experiments and the chemical analysis of reaction products the critical supersaturation is calculated by a theory which is based on the interionic attraction theory (e. g. *Hänel*, 1976; *Thudium*, 1978).

1. *The SO_2-oxidation on solid particles*

The SO_2-oxidation on the surface of different types of airborne aerosol particles was studied in a temperature and humidity controlled reaction chamber (*Dlugi* et al., 1981; *Haury* et al., 1978). A description of the other experimental techniques used for these examinations can be found in a preceding article (*Dlugi* et al., 1981). So only the theoretical approximation used to calculate a reaction velocity $a_0[\mathrm{in}(g_{SO_4^{2-}})\,(g^{-1}_{\mathrm{aerosol}})\,(\mathrm{min})^{-1}]$ should be shortly discussed again. Equation (1) is used which describes the increasing surface coverage by the formation of a reaction product (see *Britton* and *Clarke*, 1979; *Dlugi* et al., 1981).

$$\frac{1}{m_{\mathrm{aerosol}}}\,\frac{d}{dt}\,m_{SO_{4p}^{2-}}(t) = a_0\left(1-\frac{m_{SO_4^{2-}}(t)}{m^{\infty}_{SO_4^{2-}}}\right)^2, \qquad a_0 = k[SO_2]_0^m \qquad (1)$$

with the mass of aerosol m_{aerosol}, the mass of sulfate produced as a function of time $m_{SO_{4p}^{2-}}(t)$, the mass of sulfate being produced at time t $m_{SO_4^{2-}}(t)$ and the mass of sulfate at the end of the reaction $m^{\infty}_{SO_4^{2-}}(t)$. For low relative humidities m is about $0.5-0.8$, while for $r.h.>0.75$ $m\cong 1$. In this notation a_0 is a function of all parameters which effect a gas-solid reaction, e. g. the mass transfer conditions the chemical (surface-) properties of the particles and the influence of ionic strength effects on the reaction velocity.

To characterize the acid or basic properties of the different types of aerosol particles, the pH-value of a suspension of 1 g aerosol substance in 30 ml H_2O_{bidest} (pH = 7) was used. As the amount of acids like H_2SO_4 on these particles was very small or neglible before the reaction with SO_2 the change of the pH-value is mainly due to the adsorption of H_3O^+ or HO^- on the dust

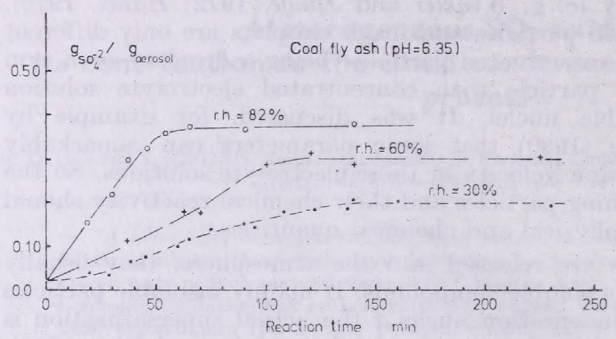

Fig. 1: The sulfate formation for coal fly ash particle as a function of time and relative humidity

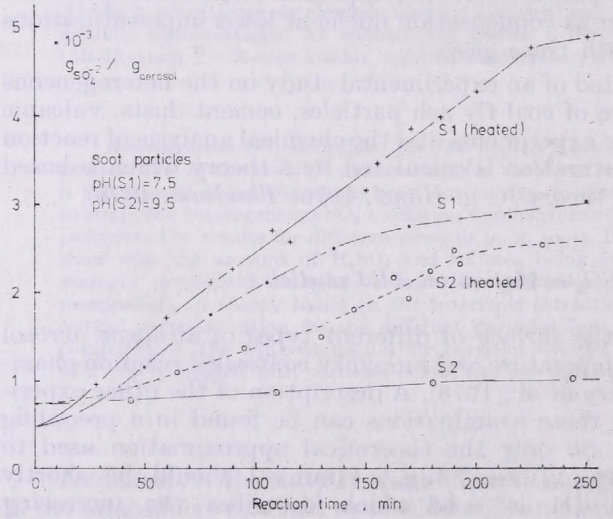

Fig. 2: The sulfate formation as a function of time for basic soot particles. The particles were heated for 1 h by 20 °C and 250 °C

surfaces. So these measurements give a classification of the aerosol properties as a function of pH-value without a detailed analysis of possible mechanisms.

All the experiments on the sulfate formation as a function of time were performed for SO_2 concentrations between 0.05 – 5 mg m^{-3}, temperatures of 8 °C to 35 °C, and relative humidities of 25% to 92% for coal fly ash, cement dust, vulcanic ash and soots. Typical results are presented in *Figs. 1–2*. In both cases the sulfate mass per mass of aerosol substance increases until a saturation value (the capacity) for these special thermodynamic conditions is reached. For fly ash the capacity increases remarkably with increasing relative humidity. For soot particles this is not observed, but a heating of particles before the reaction with SO_2 causes an increase of the capacity. The sulfate formation for cement dusts and vulcanic ash from St.

Helens shows a behaviour comparable to this of coal fly ash particles. Some results of the capacities per m² of specific surface area for these aerosol particles are shown in *Fig. 3*. While for airborne basic soots the results from different experiments agree well, the capacities per m² for the other types of particles are larger by a factor of about $10^2 - 10^3$ than values published by *Liberti* et al.

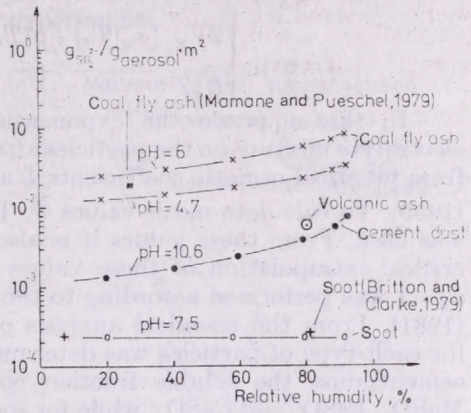

Fig. 3: The reaction capacity per m² for some types of aerosol particles

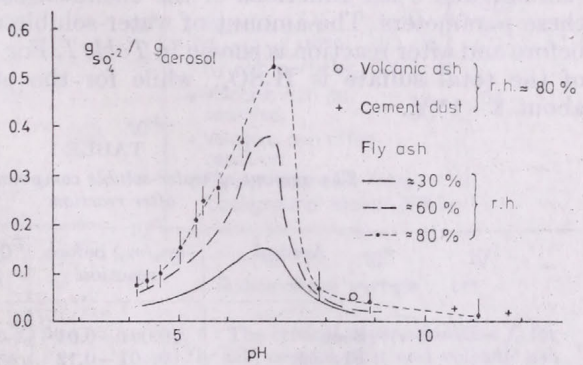

Fig. 4: The dependence of capacity on the pH-value and relative humidity for different types of aerosols

(1978) and *Judeikis* et al. (1978). This can be caused as well by the type of chemical reactor used for these measurements as by the different properties of aerosol particles studied (*Britton* and *Clarke*, 1979; *Dlugi* et al., 1981). But in all cases for fly ash and cement dusts the capacity increases with increasing relative humidity. The "influence of the pH-value" on the capacity is shown in *Fig. 4*. For neutral or slightly acid particles the capacity is maximal, but the reaction proceeds somewhat differently compared with the results from Fig. 1. For the experimental conditions ($pH \cong 7$, $r.\,h. \cong 80\,\%$ or $60\,\%$, $[SO_2]_0 \cong 4$ mg m^{-3}) the sulfate production is small for about 60 minutes, and only a value of 0.1 $g_{SO_4^{2-}}$ g^{-1} aerosol is measured. Then – on the more acid particles – the rate increases and the maximum capacity is reached for a reaction time of about 3 h. So the maximum of the reaction velocity is calculated for $pH \cong 5.5$ and not for $pH \cong 7$ (*Dlugi* et al., 1981). The a_0 values also increase with increasing relative humidity for all particles without soots.

2. *The calculation of the equilibrium water uptake of aerosol particles*

The water uptake of aerosol particles which had reacted with SO_2 was calculated following the theoretical way proposed by *Hänel* (1976), *Thudium* (1978) and *Hänel* and *Lehmann* (1981). The relative humidity f over a particle surface and therefore also the critical supersaturation f_c are calculated according to equation (6.4) from *Hänel* (1976)

$$f = \exp.\left(\frac{2V_w}{R_w T}\,\frac{[\sigma_w(T_0)+a(T_0-T)+b\,\dfrac{m_s}{m_0}\dfrac{m_0}{m_w}]}{r} - \eta\,\frac{m_0}{m_w}\right) \qquad (2)$$

In this equation the exponential mass increase coefficient η for the electrolyte mixture on the particles after the chemical reaction can be computed from practical osmotic coefficients Φ as tabulated e. g. by *Robinson* and *Stokes* (1959). To calculate mean values $\bar{\Phi}$, Thudium's mixing rule *(Thudium*, 1978) was used. From these values it is also possible to calculate η. The somewhat critical extrapolation of these values from water activities $a_w \leq 0.965$ up to $a_w = 1$ was performed according to the way described by *Hänel* and *Lehmann* (1981). From the chemical analysis of particle samples a mean composition for each type of particles was determined. For coal, fly ash, vulcanic ash and cement dust the soluble fraction contains mainly H_2SO_4, K_2SO_4, Na_2SO_4, $MgSO_4$, $FeSO_4$ and $CaSO_4$, while for soots only H_2SO_4 should control the water uptake. Since the exponential mass increase coefficient, the term m_w/m_0, the radius r and σ are functions of the chemical composition, also f_c depends on these parameters. The amount of water-soluble mass for the different aerosols before and after reaction is shown in *Table I*. For soot particles about 25 – 80% of the total sulfate is H_2SO_4, while for the other particles this amount is about 8 – 15%.

TABLE I

The amount of water-soluble compounds before and after reaction

Aerosol	(m_s/m_0) before reaction	(m_s/m_0) after reaction
Soot	0.001 – 0.01	0.01 – 0.06
Fly ash	0. 01 – 0.12	0.05 – 0.55
Cement	0. 02 – 0.06	0.04 – 0.13
Volcanic ash	0. 02 – 0.03	0.05 – 0.08

The critical supersaturation is calculated for soots and for fly ash, cements and volcanic ash. Including the experimental errors, one can estimate a statistical error of about ± 20 % for the values of critical supersaturation. The maximum value is presented. For basic soots, from our experiments only a reduction of the critical supersaturation is obtained by a factor of 2 – 10 *(Fig. 5)*. A value for soot particles before reaction with SO_4 with about 0.5% of soluble mass was deduced from microbalance measurements (*Hänel* and *Zankl*, 1980). This value agrees with data calculated only from chemical analysis to about 30%. The critical supersaturation for acid soots (*Cofer III* et al., 1981) is sometimes lower. So – as a function of soot formation processes – these particles, which are often found in the accumulation mode of the size distribution, need a supersaturation of about 0.05 % or more to be activated.

Other particles (fly ash, cement, volcanic ash) react with SO_2 to a larger extent. So the range of the critical supersaturation shows a reduction by a factor of 10 – 50 compared with insoluble particles and about a factor of 7 – 25 (sometimes 40) compared with particles before the reaction *(Fig. 6)*. The larger the capacity, the larger the reduction of supersaturation. For different single fly ash particle samples in plumes (*Mamane* and *Pueschel*, 1979) and near the ground (*Andre* et al., 1981) a reduction of f_c was calculated comparable to aerosols from laboratory experiments.

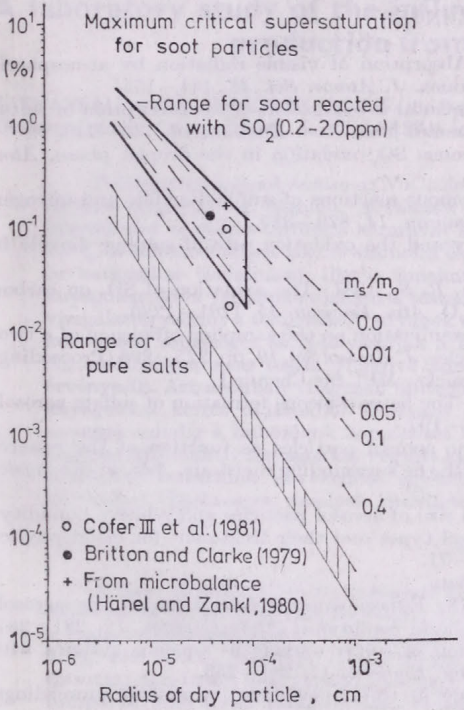

Fig. 5: The critical supersaturation f_c for different types of soot particles

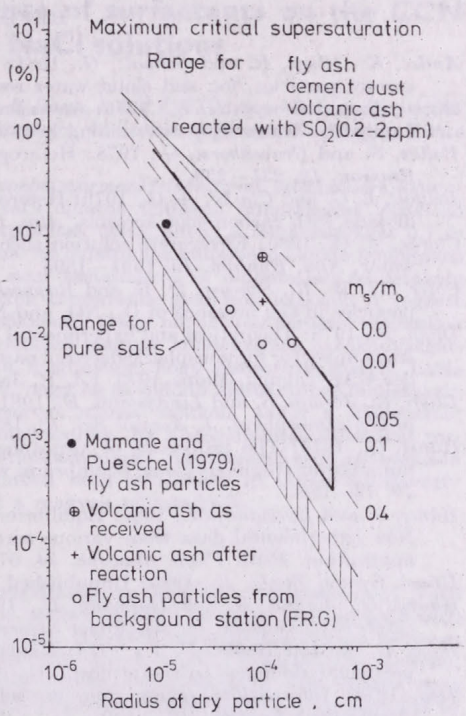

Fig. 6: The critical supersaturation f_c for coal fly ash, cement dust and volcanic ash

3. *Conclusions*

It is shown that SO_2 is oxidized on different aerosol particles to sulfuric acid and sulfates. The amount of sulfate and H_2SO_4 is dependent on relative humidity, amount of basic and acid compounds, amount of water-soluble compounds and solar radiation (*Dlugi* et al., 1981). Additionally, the reaction velocity is dependent on the SO_2 concentration. So – as a consequence – the critical supersaturation being necessary to activate a particle, is reduced by a factor of about 2 – 50 during a chemical reaction with SO_2.

Soots are very important for the light absorption of aerosols in the free atmosphere and inside clouds. As they are not so reactive, they need a larger supersaturation than particles of the same size to grow to a droplet. This explains the results found by *Andre* et al. (1981) that the light absorption of visible radiation for non-activited particles is larger compared with large

particles due to the large soot content of these samples. Additionally, *Puxbaum* (1979) and *Dlugi* (1978) found that soot particles in wet air are collected by impactors in the same manner as in dry air, while sulfate particles show a water uptake with increasing relative humidity.

Further on, it can be concluded that for some types of aerosols the reaction rate with SO_2 may be largest in non-activated particles and not in droplets. This may be due to the limited solubility of catalysts and also an increasing reaction velocity with increasing water activity (*Clarke*, 1980).

REFERENCES

Andre, K., Dlugi, R. and *Schnatz, G.*, 1981: Absorption of visible radiation by atmospheric aerosol particles, fog and cloud water residues. *J. Atmos. Sci. 38*, 141–155.

Barrie, L. and *Georgii, H.-W.*, 1976: An experimental investigation of the absorption of sulfur dioxide by water drops containing heavy metal ions. *Atm. Environ. 10*, 743–749.

Beilke, S. and *Gravenhorst, G.*, 1978: Heterogenous SO_2-oxidation in the droplet phase. *Atm. Environ. 12*, 231–239.

Britton, L. G. and *Clarke, A. G.*, 1979: Heterogenous reactions of sulfur dixodide and nitrogen dioxide with carbon soot aerosols, *Atm. Environ. 14*, 829–839.

Clarke, A. G., 1980: Electrolyte solution theory and the oxidation rate of sulphur dioxide in water. *Atm. Environ. 15*, 1591–1595.

Cofer III, W. R., Schryer, D. R. and *Rogowski, R. S.*, 1981: The oxidation of SO_2 on carbon particles in the presence of O_3, NO_2 and N_2O. *Atm. Environ. 15*, 1281–1286.

Dlugi, R., 1978: Theoretical and experimental examination on the sampling efficiency of a two-stage impactor for nonsphericalaerosol particles. *J. Aerosol Sci. 10*, pp. 225–226 (Proceedings der GAF-Tagung, Mainz 1979, Ed. R. Jaenicke, MPI für Chemie.)

Dlugi, R., Jordan, S. and *Lindemann, E.*, 1981: The heterogeneous formation of sulfate aerosols in the atmosphere. *J. Aerosol Sci. 12*, 185–197.

Hänel, G., 1976: The properties of atmospheric aerosol particles as function of the relative humidity at thermodynamic equilibrium with the surrounding moist air. *Adv. in Geophysics 19*, 73–188.

Hänel, G. and *Lehmann, M.*, 1981: Equilibrium size of aerosol particles and relative humidity: New experimental data from various aerosol types and their treatment for cloud physics application. *Beitr. Phys. Atmosph. 54*, 57–71.

Hänel, G. and *Zankl, B.*, 1980: Unpublished data.

Haury, G., Jordan, S. and *Hofmann, C.*, 1978: Experimental investigation of the aerosol-catalyzed oxidation of SO_2 under atmospheric conditions. *Atm. Environ. 12*, 281–287.

Hegg, D. A. and *Hobbs, P. V.*, 1978: Oxidation of sulfur dioxide in aqueous systems with particular reference to the atmosphere. *Atm. Environ. 12*, 241–253.

Issa, 1978: International symposium on sulfur in the atmosphere; workshop proceedings. *Atmospheric Environ. 12*, 7–23.

Judeikis, H. S., Stewart, T. B. and *Wren, A. G.*, 1978: Laboratory studies of heterogenous reactions of SO_2. *Atm. Environ. 12*, 1633–1641.

Kortüm, G., 1972: *Lehrbuch der Elektrochemie.* Verlag Chemie, Weinheim.

Liberti, A., Brocco, D. and *Possanzini, M.*, 1978: Adsorption and oxidation of sulfur dioxide on particles. *Atm. Environ. 12*, 255–261.

Mamane, Y. and *Pueschel, R. F.*, 1979: Oxidation of SO_2 on the surface of fly ash particles under low relative humidity conditions. *Geophys. Research Lett. 6*, 109–112.

Penkett, S. S., Jones, B. M. R., Brice, K. A. and *Eggleton A. E. J.*, 1979: The importance of ozone and hydrogen peroxide in oxidizing sulfur dioxide in cloud and rainwater. *Atm. Environ. 13*, 123–137.

Pruppacher, H. R. and *Klett, J. D.*, 1978: *Microphysics of clouds and precipitation.* D. Reidel, Dordrecht, Holland.

Puxbaum, H., 1979: Thermo-Gasanalysator zur Charakterisierung von Kohlenstoff- und Schwefelverbindungen in luftgetragenen Stäuben. *Fresenius Z. Anal. Chem. 298*, 250–259.

Robinson, R. A. and *Stokes, R. H.*, 1959: *Electrolyte Solutions*, Butterworth, London.

Thudium, J., 1978: Water uptake and equilibrium sizes of aerosol particles at high relative humidities: Their dependence on the composition of the water-soluble material. *Pageoph. 116*, 130–148.

Winkler, P. and *Junge, C.*, 1972: The growth of atmospheric aerosol particles as a function of relative humidity. Part I: Method and measurements at different locations. *J. Rech. Atmos.* (Mémorial Henri Dessens), 617–638.

IDŐJÁRÁS

Az Országos Meteorológiai Szolgálat folyóirata, 86. évf. 2–4. szám, 1982. március–augusztus
Journal of the Hungarian Meteorological Service, Vol. 86. No. 2–4. March–August 1982, Budapest

A laboratory study of the influence of surfactants on the CCN production from NaCl solutions

B. THAVEAU and R. SERPOLAY, *I.O.P.G. du Puy de Dome, L.A.M.P. 12, avenue des Landais, 63001 Clermont-Ferrand Cedex, France*, S. PIEKARSKI, *Laboratoire de Chimie Organique B. Limoges, France*

Felületaktív anyagok hatása az NaCl oldatokból származó felhőmagvak keletkezésére, laboratóriumi megfigyelések alapján. A szerzők NaCl oldatok felületén buborékokat létrehozó berendezést termikus diffúziós kamrával kapcsoltak össze, amely a felhőmagvakat 0,1 és 1,0%-os túltelítettségek között számolta össze. Az oldatokhoz különböző oldódó (anionokat és kationokat tartalmazó, illetve ionokat nem tartalmazó) és oldhatatlan felületaktív anyagokat adva tanulmányozható a részecskék képződésére gyakorolt hatásuk. A végzett vizsgálatok szerint a felületaktív anyagok csökkentik (vagy növelik) az aeroszol részecskék keletkezési sebességét és befolyásolják a keletkező magvak kondenzációs hatékonyságát. Az eredmények nem teszik lehetővé annak megítélését, hogy elsősorban melyik hatás érvényesül. Azt azonban világosan mutatják, hogy ha az oldódó higroszkópos felületaktív anyagokkal kezelt oldatokból származó magvak száma csökken, akkor a felületaktív anyagok mindig a buborékok képződését befolyásolják. Ez a megállapítás anionokat tartalmazó felületaktív anyagokkal végzett kísérleteken alapul. Az ellenkező eset, nevezetesen a magvak számának növekedése egyértelműen nem mutatható ki olyan felületaktív anyagokat alkalmazva, amelyek késleltetik a magvak növekedését.

⁎

A laboratory study of the influence of surfactants on the CCN production from NaCl solutions. A device producing bubbles at the surface of NaCl solutions was coupled with a static thermal diffusion chamber for counting the CCN at supersaturations between 0.1% and 1.0%. Different types of surfactants—among them water-soluble (anionic, cationic, non-ionic) and -insoluble ones—were added to the solutions. The results were compared with those obtained when a superficially clean saline solution was supplied to the bubbling device. It appears that the surfactants decrease or increase the rate of production of aerosol particles and affect the ability of these particles to act as CCN. The present experiments cannot usually determine which of these effects predominates. However, when a decrease of the CCN count is noticed in an aerosol generated by a solution in the presence of a soluble hygroscopic surfactant, it seems obvious that this effect must occur at the bubble formation level. This results from the use of anionic surfactants such as sodium dodecyl sulfate or sodium dodecylbenzenesulfonate. The opposite case, an increase of CCN count for an aerosol originating in the presence of a surfactant which retards the growth of nuclei has never been clearly observed in these experiments.

⁎

Introduction. The influence of surfactants on the growth rate of isolated NaCl crystals under conditions very close to saturation with respect to water vapour was presented last year in a paper during the International Conference on Cloud Physics in Clermont-Ferrand (*Thaveau* et al., 1980).

In an attempt to clarify the behaviour of the tested surfactants, the latter have been classified into water-insolube and -solube ones and, within the second class, into anionic, cationic and non-ionic surfactants (*Table I*, 1st column).

The main results may be summarized as follows (*Table I*, 2nd column):

– insoluble surfactants generally reduce the growth rate of the crystal, essentially during the first stage of the growth – that is to say until the crystal has completely disappeared into the growning droplet of salt solution.
– some soluble surfactants of the anionic and the cationic type unexpectedly increase the crystal growth rate. These surfactants have been found to assume a hygroscopic feature and to act as condensation nuclei just beneath the saturation.

TABLE I

Influence of various surfactants (1st column) on (a) *the growth rate of a NaCl crystal (2nd column),* (b) *the CCN number produced by bubbling from a NaCl solution (3rd column). The behaviour of a polluted crystal (or a polluted solution) is compared with a pure one (or a superficially clean one*

SOLUBLE SURFACTANTS		Growth rate	Effect on CCN number N produced by bubbling
Non-ionic:	Tween 20	Decrease	Decrease
	Cemulsol NP 23	Not very sensible	Not very sensible
	Tertiary amine	Decrease	Not very sensible
Anionic:	Sodium dodecyl sulfate	Increase	Decrease
	Sodium dodecylbenzenesulfonate	Increase	Decrease
Cationic:	Quaternary ammonium compound	Not very sensible	Increase
	Dodecylpiperazione hydrochloride	Increase	Increase
INSOLUBLE SURFACTANTS			
	Glycerol monostearate	Decrease	Decrease
	Octadecanol	Decrease	Decrease
	Oleic acid	Not very sensible	Increase

The present study is based upon the consideration that bubbling at the sea surface is one of the major processes in bubbling at the sea surface is one the major processes in producing natural hygroscopic aerosols and that this is responsible for a not negligible part of the enrichment of the atmosphere in surfactants resulting from biological mechanisms or human activities (*Blanchard*, 1964; *Barger* and *Garrett*, 1970). That is why the bubbling process has been reproduced in the laboratory with superficially clean NaCl solutions gradually polluted by the same surfactants as those used during the above mentioned work and classified in the same way. Immediately after generation, the aerosols were tested inside a thermal diffusion chamber for CCN counting.

In the recent past, some authors have used such an experimental method consisting in coupling a bubbling device with a condensation nuclei counter (CNC) operating at high supersaturation (*Day* and *Lease*, 1968; *Paterson* and *Spillane*, 1969). Our experimentation is somewhat different from theirs in the type of the bubbling device – which includes a teflon membrane instead of a filter plate (*Guichard* and *Lamauve*, 1980) – and in the type of the counter chosen. In fact, our interest does not lie in the whole amount of the nuclei produced by bubbling, but only in those which can be activated as cloud condensation nuclei (CCN), i.e. at a supersaturation beneath 1.0%.

Description of the bubbling device

The bubbling device is composed of three parts *(Fig. 1)*. The lower one is a first chamber into which filtered air is introduced under a slight overpressure and passes through a teflon membrane supporting a layer of saline solution. The bubbling process is achieved at that level. The aerosol so produced

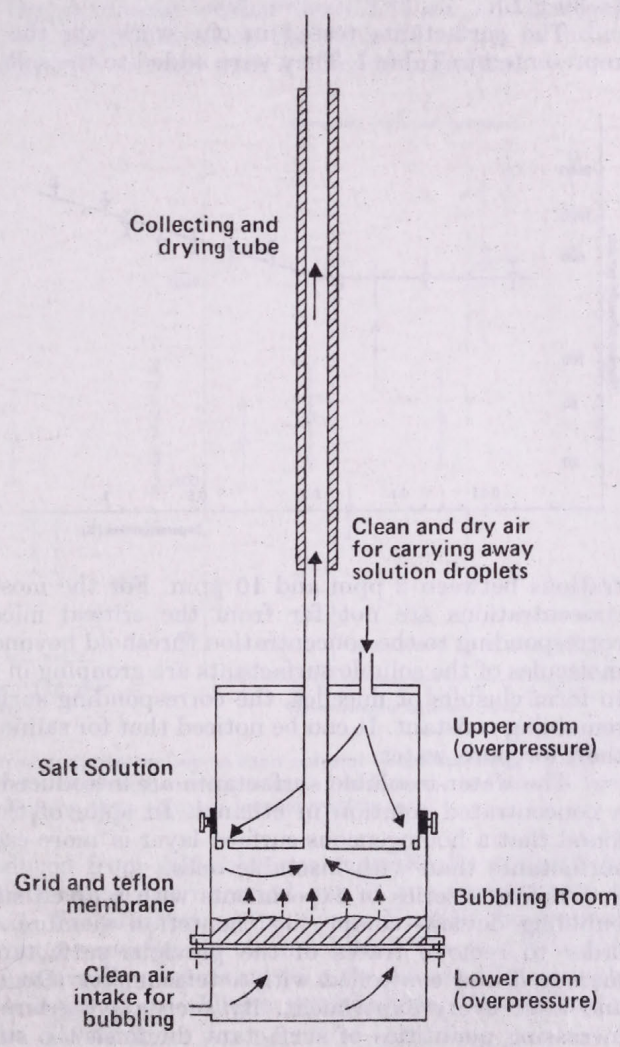

Fig. 1 : Scheme of the bubbling device

fills a second chamber into which filtered air is admitted to carry away the aerosol into the drying tube which completes the device. The simulation of bubbling made in such a way has been found closer to the natural process than when the air is passed through a fritted glass filter plate.

The air intake of the CCN counter is directly connected to the drying tube of the bubbling device.

The thermal diffusion chamber (CCN counter) is of the static type. The same model has been used during the International Workshop on CCN in Reno (1980) (*Serpolay*, 1981).

Experimental procedure

The concentration of the NaCl solutions used equals that of the sea-water ($\simeq 30$ g/L).

The surfactants tested in our work are the same as those previously represented in Table I. They were added to the salt solutions to obtain concentrations between 2 ppm and 10 ppm. For the most soluble surfactants these concentrations are not far from the critical micellar concentration (CMC) corresponding to the concentration threshold beyond which the supplementary molecules of the soluble surfactants are grouping in the aqueous phase in order to form clusters or micelles, the corresponding surface tension of the solution remaining constant. It can be noticed that for saline solutions the CMC is lower than for pure water.

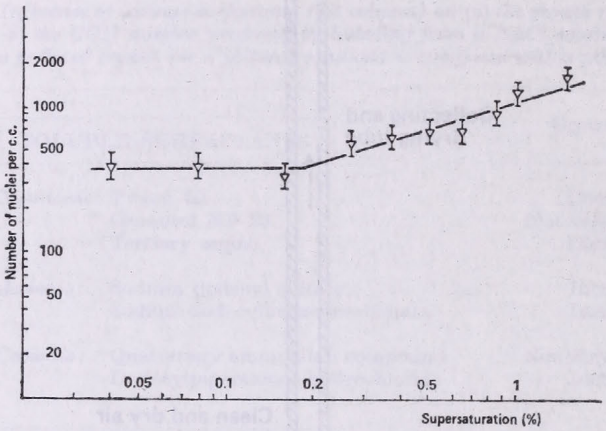

Fig. 2: $N = f(S)$ diagram for a superficially clean NaCl solution

The water-insoluble surfactants are introduced in the NaCl solution from a concentrated solution in ethanol. In spite of this precaution, it has been found that a homogeneous surface layer is more easily obtained with soluble surfactants than with insoluble ones.

Before a series of experiments with a given surfactant, the whole of the bubbling device – comprising the teflon membrane – is carefully cleaned in order to remove traces of the previous surfactant. The surface tension is measured and controlled with a tensiometer (Dognon – Abribat type) before and after every experiment. By such a procedure it has been verified that increasing quantities of surfactant diminish the surface tension, and that at the end of the experiment the surface tension is very sligthly higher than at the beginning.

Results

(1) For a superficially clean NaCl solution, the curve represented in *Fig. 2* as a log S *vs.* log N diagram, where S = supersaturation and N = number of activated nuclei, has been obtained.

For S values between 0.04% and 0.2%, N remains constant. This may mean that no more CCN are activated between 0.04% and 0.2% than at 0.04% or beneath this value, for which the calculated critical radius (dry salt particles) is about 0.33 μm.

Above an S value of 0.2% – 0.3%, corresponding to a critical nuclei radius of 0.1 μm, the number N is increasing with the degree of supersaturation. So it appears that the size distribution spectrum of the aerosol produced by bubbling is bimodal with a first maximum located above 0.33 μm, and a second one beneath 0.1 μm. In fact, a peak centred on the value of 0.5 μm in radius has been detected by sampling the aerosol with a cascade impactor.

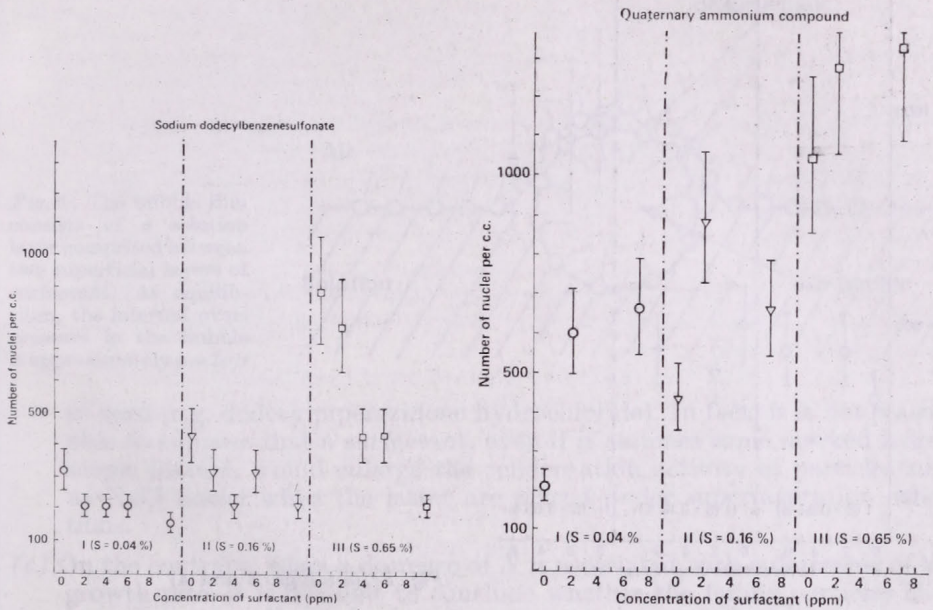

Fig. 3–4: On the graphs here presented, one can see in each column – corresponding to a given supersaturation – the results of N for increasing concentrations of surfactant, the first one being for the superficially clean solution (concentration zero)

(2) With aerosols produced from salt solutions superficially polluted by surfactants, the measurements have been carried out at supersaturations of $S = 0.04\%$, 0.16% and 0.65%. The supersaturation curves $N = f(S)$ obtained are similar to that resulting from a superficially clean solution, the two first dots (for $S = 0.04\%$ and 0.16%) generally pertaining to a first horizontal straight line, while the third dot belongs to an oblique straight line. The difference lies only at the level of the N values.

Three kinds of results may be distinguished:

(a) The N values are lower than for a superficially clean solution with Tween 20 (non-ionic), sodium dodecyl sulfate and sodium dodecylbenzenesulfonate (anionic), glycerol monostearate and octadecanol (insoluble). The decreasing of N appears more important at the highest supersaturation, that is to say for the smallest sizes of CCN, as it can be seen in *Fig. 3*.

(b) The N values are higher than for a superficially clean solution with solutions of quaternary ammonium compound *(Fig. 4)*, dodecylpiperazinone hydrochloride (cationic) and oleic acid (insoluble).

(c) No sensible modification with respect to the superficially clean solution is observed with non-ionic surfactants such as Cemulsol NP 23 *(Fig. 5)* and tertiary amine.

The complete results of this study are summarized in the 3rd column of Table I.

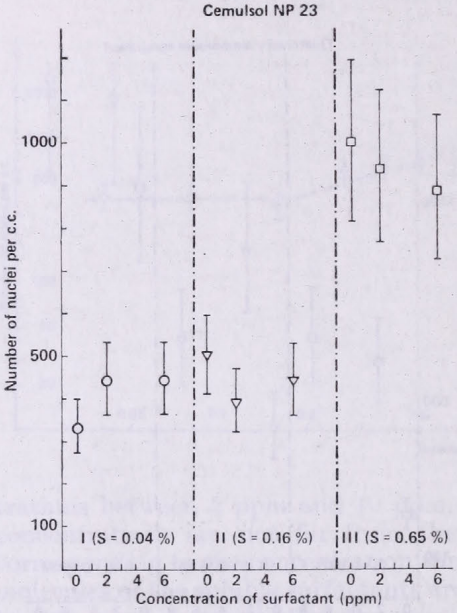

Fig. 5 : (see Figs. 3 and 4)

Discussion of the results

As the experimental method has combined two main phenomena, the results have to be analyzed according to the following aspects:

Particle production. The surface state of the solution is modified by the surfactant. This modification is causing a change in the size spectrum of the nuclei produced by bubbling.

Particle activation in the CCN counter. Traces of surfactant are carried away upon the aerosol particles when the bubbles burst, and may change the growth rate of the resulting nuclei, as it has been said before. For the insoluble surfactants this behaviour is well explained by a change of the value of the condensation coefficient in the theoretical growth equation (*Thaveau*, 1981).

By confronting the results in columns 2 and 3 of Table I, an attempt at their interpretation can be made:

(a) When a decrease of the N values and an increase of the growth rate – or no sensible effect on this growth rate – are simultaneously observed for a given surfactant (e.g. sodium dodecylbenzenesulfonate), the lowering

of N has likely to be located at the level of the nuclei production by bubbling because of a larger proportion of small nuclei, or because of an actual reduction of N. This consideration seems to be quite well supported by the conclusions of *Garrett*'s studies (1967, 1968) and a number of Russian works based upon laboratory experiments (*Bakhanova* et al., 1974).

(b) A similar conclusion can be drawn when an increase of N and an increase of the growth rate – or no detectable effect on this growth rate – occur

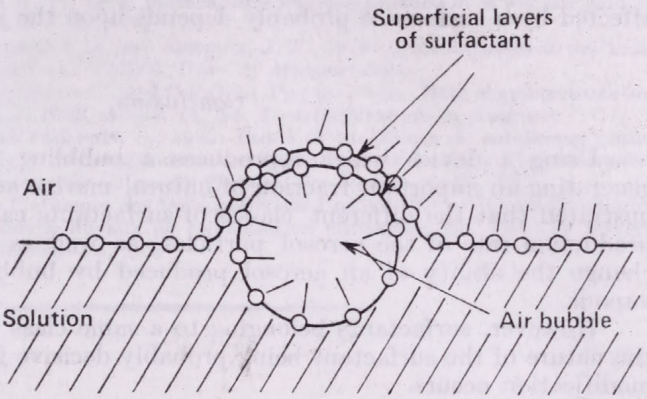

Fig. 6 : The bubble film consists of a solution layer comprised between two superficial layers of surfactant. At equilibrium, the internal overpressure in the bubble is approximately $p = 3\sigma/r$

at once (e.g. dodecylpiperazinone hydrochloride). In fact, it is not reasonable to suppose that a surfactant, even if it assumes some marked hygroscopic feature, would enlarge the condensation activity of particles such as NaCl nuclei when the latter are placed under supersaturation conditions.

(c) On the contrary, when a decrease of N is associated with a descrease of the growth rate, it is difficult to conclude whether the failing particles have been deactivated or have not been produced at all. Such a case occurs with Tween 20, glycerol monostearate and octadecanol.

Whatever is the class of the surfactant, it is verified that the surface tension of the polluted salt solution is lowered with respect to that of a superficially clean one. For the same excess of pressure P inside the bubble, this lowering of the surface tension σ results in diminishing the bubble radius r – according to the formula: $P = 3\sigma/r$ – as well as its life-time. Consequently, the reduction of the area of the film producing the film-drops ought to lead to a modification of the number and size of CCN. Such a remark is likewise derived from the laboratory works of *Garrett* (1967, 1968) and *Blanchard* and *Syzdek* (1972).

In order to arrive at a better understanding of the initimate process, it should be very helpful to determine the rate of bubble production and the size distribution for each surfactant and for a given bubbling device. With a high rate of bubble production for instance, the clustering of several bubbles is frequently observed, which enlarges the bubble size before bursting.

However, it seems that the mechanism responsible for the change of N at the bubbling level is more complicated, and closely related to the structure of the surfactant.

In fact, it must be emphasized that the film producing the film-drops consists of a thin film of salt solution, comprised between two layers of surfactant *(Fig. 6)*. Consequently it seems obvious that the ratio of the mass of surfactant to the mass of salt must be higher for the smallest particles. This opinion proceeds also from a lot of works (*Blanchard*, 1971; *Podzimek* et al., 1978; *Jaenicke*, 1978) and the hypothesis of a more important deactivation of the smallest particles by the surfactant is consistent whith it.

It is probable that the bubble film assumes a structure – i.e. physical properties and behaviour – differing according to the surfactant used. Our results indicate that the way by which the number of CCN produced by bubbling is affected by a surfactant probably depends upon the nature of the latter.

Conclusion

Using a device which reproduces a bubbling process similar to that generating an important fraction of natural marine aerosol, it has been demonstrated that the different classes of surfactants can probably modify the production rate of the aerosol particles, as well as the particle sizes, and change the ability of an aerosol produced by bubbling to condense water vapour.

However, surfactants belonging to a same class may behave differently, the nature of the surfactant being probably decisive for the way in which the modification occurs.

An extension of the results to natural conditions seems difficult because the chemicals capable of modifying the surface tension of the sea surface probably consist of mixtures of different natural and industrial surfactants. Nevertheless one has to keep in mind the possibility that the spectrum of the cloud droplets produced from marine aerosol can be changed by the effect of admixed surfactants on the CCN. The influence of such a change on the cloud and fog development and the precipitation inducement have been clearly expressed in previous papers (*Morachevsky* and *Kiriukhin*, 1968; *Garrett*, 1978).

Acknowledgements. We are very grateful to Dr. J. C. *Guichard*, from Institut National de Recherche Chimique Appliquée (IRCHA), France, for having kindly provided the design of the bubbling device, as well as some helpful comments for building it. This research was supported by the Délégation Générale á la Recherche Scientifique et Technique, under the grant No. 78 – 7 – 0093.

REFERENCES

Bakhanova, R. A., Deryaguin, B. V., Kurgin, Yu S., Leonov, L. F., Prokhorov, P. S., Rosentsvayg, L. A., Silaiev A. V., Storozhilova, A. I. and *Fedoseyev, V. A.*, 1974: Research on conditions which determine the passivating action of surface-active substances on hygroscopic condensation nuclei. *IFCh. AN USSR, Ukr. NIGMI, KGU, OGMI, FTD – MT – 24*, 224.

Barger, W. R. and *Garrett, W. D.*, 1970: Surface-active organic material in the marine atmosphere. *J. Geophys. Res. 75*, 4561 – 4566.

Blanchard, D. C., 1964: Sea-to-air transport of surface-active material. *Science 146*, 396 – 397.

Blanchard, D. C., 1971: The oceanic production of volatile cloud nuclei. *J. Atmos. Sci. 28*, 811 – 812.

Blanchard, D. C. and *Syzdek, L. D.*, 1971: Concentration of bacteria in jet drop from bursting. *J. Geophys. Res. 77*, 5087 – 5099.

Day, J. A. and *Lease, J. C.*, 1968: Cloud nuclei generated by bursting air bubbles at the air-sea interface. *Proc. Int. Conf. on Cloud Physics, Toronto*, 20 – 24.

Garrett, W. D., 1967: Stabilization of air bubbles at the air–sea interface by surface-active material. *Deep Sea Res. 14*, 661–672.

Garrett, W. D., 1968: The influence of monomolecular surface films on the production of condensation nuclei from bubbled sea water. *J. Geophys. Res. 73*, 5145–5150.

Garrett, W. D., 1978: The impact of organic material on cloud and fog processes. *Pageoph. 116*, 316–334.

Guichard, J. C. and *Lamauve, M.*, 1980: Conséquences éventuelles pour les noyaux de condensation d'origine marine de la pollution des mers par les produits organiques. *Rapport final, D. G. R. S. T., n° 78–7–0090.*

Jaenicke, R., 1978: The role of organic material in atmospheric aerosol. *Pageoph. 116*, 283–292.

Morachevsky, V. G. and *Kiriukhin, B. V.*, 1968: On the artificial control of the chain process of raindrop growth in clouds. *Proc. Int. Conf. on Cloud Physics, Toronto*, 683–687.

Paterson, M. P. and *Spillane, K. T.*, 1969: Surface films and the production of sea salt aerosol. *Q.J.R.M.S. 95*, 526–534.

Podzimek, J., Preining, O., Russell, C. A. and *Stampfer, J. F.*, 1978: Aerosol studies at the Texas Seashore. *Tech. Rep. NoAG–8, GCCPR, Univ. of Missouri-Rolla.*

Serpolay, R., 1981: The CCN counter of the I.O.P.G. of Puy de Dôme: Main characteristics and results of measurements. *J. Rech. Atmos. 15*, No. 3–4 (publication in progress).

Thaveau, B., Serpolay, R. and *Piekarski, S.*, 1980: Étude de l'influence de substances tensioactives sur la cinétique de la condensation sur des noyaux géants de NaCl. *Communications á la VIIIe Conférence Internationale sur la Physique des Nuages, 1*, 25–28.

Thaveau, B., 1981: Etude de l'influence des tensioactifs sur l'activité de particules de chlorure de sodium considérées comme noyaux de condensation atmosphérique. *Thése de Doctorat 3e cycle, Université de Clermont-Fd*, 132.

IDŐJÁRÁS

Az Országos Meteorológiai Szolgálat folyóirata, 86. évf. 2—4. szám, 1982. március—augusztus
Journal of the Hungarian Meteorological Service, Vol. 86. No. 2—4. March—August 1982, Budapest

Ice nucleation mechanisms and ice nucleus measurements

N. FUKUTA, *Department of Meteorology, University of Utah, Salt Lake City, Utah 84112, U. S. A.*

Jégkeletkezési folyamatok és a jégmagvak mérése. A tanulmány a jégképződés mechanizmusaira vonatkozó újabb ismeretek fényében áttekinti a jégmagvak mérésére jelenleg használatos módszereket és analizálja a felmerülő problémákat. Szerző véleménye szerint értékesebb és használhatóbb adatok eléréséhez a meglévő eljárások kombinációja és egymás közötti hitelesítése szükséges. Azt javasolja, hogy definiáljuk a jég keletkezésének három alapvető módját, és a nukleációs elméleteket használjuk fel a legfontosabb paraméterek meghatározására. Végül olyan módszert mutat be, amelynek segítségével a környezeti feltételekre vonatkozó nukleációs adatok nyerhetők.

*

Ice nucleation mechanisms and ice nucleus measurements. The current methods of ice nucleus measurement are reviewed with the help of the knowledge gained recently for the mechanisms of ice nucleation on aerosol particles and the problems are analyzed. To obtain more meaningful and useful data, combination and calibration among existing methods are suggested. The suggested method involves separation and identification of three basic mechanisms of ice nucleation and their analysis for key parameter determination using the corresponding nucleation theories. A method of reconstructing the nucleation data under the environmental conditions of the natural clouds is described.

*

Introduction. Ice nuclei are particles that assist formation of ice crystals in the atmosphere. Due to this ability, they are considered to be important in understanding as well as in controlling the ice phase cloud processes. In order to determine the activity of ice nuclei, a great deal of effort has been expended in design and development of the nucleus counters and in their operations, i.e., ice nucleus measurements. Recent studies of ice nucleation have revealed, however, that there exist at least three basic mechanisms of atmospheric ice nucleus activation, viz., the deposition, the condensation- (or immersion-) freezing, and the contact-freezing nucleations, and their relationships under different combinations of environmental variables and nucleus parameters (*Schaller* and *Fukuta*, 1979; *Tomlinson*, 1980). The existence of three different mechanisms has casted a serious doubt on the past approaches of merely comparing data of ice nucleus counters based on different operation principles in the workshops. It is therefore the purpose of this paper to re-examine the problems of ice nucleus measurement in the light of basic ice nucleation mechanisms and subsequently to suggest its future possible direction, as well as to show a method of applying such data to the natural clouds.

1. *Activation mechanisms of ice nuclei*

Since all the present ice nucleus measuring methods deliberately let the ice nucleation take place in their own environments, it is important to understand the nucleations mechanisms. Heterogeneous ice nucleation requires interaction between an ice nucleus particle and the surrounding environment, as shown in *Fig. 1.* Although two modes of ice nucleation, i.e., deposition and freezing, are thermodynamically possible, recent studies suggest that there are two distinctly different modes of freezing nucleation, viz., condensation- (or immersion-) freezing and contact-freezing.

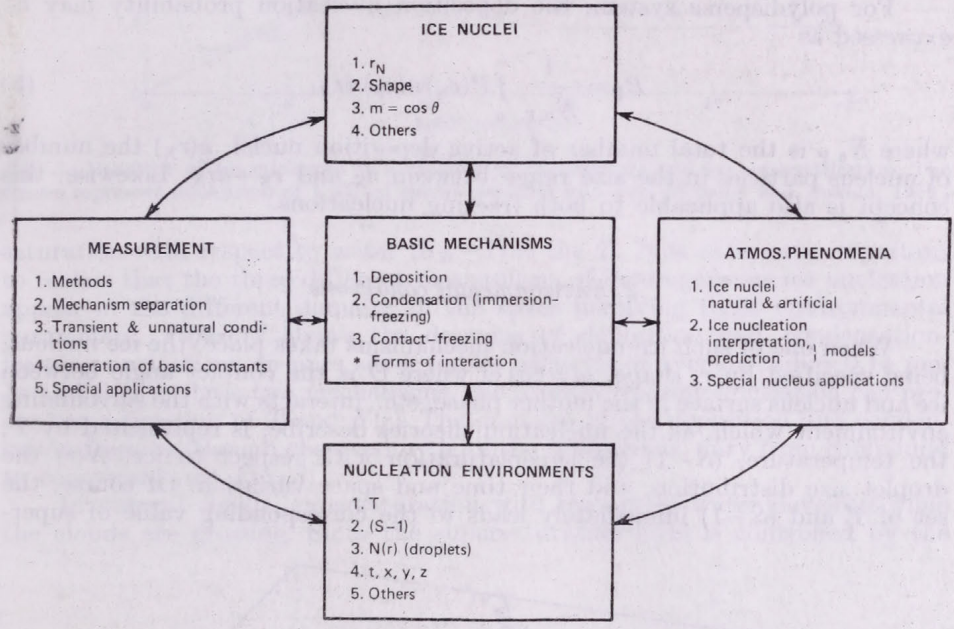

Fig. 1: The relationship among factors involved in ice nucleus measurements

The deposition nucleation is a single process where the probability of nucleation for monodisperse particles P is shown as

$$P = \frac{N}{N_0} = 1 - e^{-J_D t}, \tag{1}$$

where N is the number of particles nucleated, N_0 that of total *active* particles, J_D the deposition nucleation rate and t the time.

The probabilities of freezing nucleations P_{AB} are, on the other hand, always expressed by the product of the probability of bringing the required liquid water to the nucleus surface P_A, and that of the particular freezing nucleation P_B, either ordinary freezing or contact-freezing:

$$P_{AB} = P_A \cdot P_B. \tag{2}$$

For condensation-freezing nucleation of a monodisperse aerosol, the probability of the nucleation is given as *(Fukuta* and *Schaller,* to be published)

$$P_{CF}=1+\frac{1}{J_C-J_F}\left[J_F\cdot e^{-J_C t}-J_C\cdot e^{-J_F t}\right] \tag{3}$$

where J_C is the rate of condensation nucleation, and J_F that of freezing nucleation. When t is small, Eq. (3) becomes

$$P_{CF}=\tfrac{1}{2}J_C J_F t^2. \tag{4}$$

For contact-freezing nucleation, P_A becomes the probability of an ice nucleus particle to collide with a supercooled cloud droplet, and P_B that of contact-freezing which involves the rate of contact-freezing instead of that of ordinary freezing.

For polydisperse system, the deposition nucleation probability may be expressed as

$$P_P=\frac{1}{N_{0,P}}\int_0^\infty P(r_N)\,n(r_N)\,dr_N, \tag{5}$$

where $N_{0,P}$ is the total number of active deposition nuclei, $n(r_N)$ the number of nucleus particles in the size range between r_N and r_N+dr_N. Likewise, this concept is also applicable to both freezing nucleations.

2. *Environmental conditions*

When one of such ice nucleation mechanisms takes place, the ice nucleus, being specified by r, shape, $m=\cos\Theta$ where Θ is the contact angle between ice and nucleus surface in the mother phase, etc., interacts with the surrounding environment which, as the nucleation theories describe, is represented by T, the temperature, $(S-1)$ the supersaturation with respect to ice, $N(r)$ the droplet size distribution, and their time and space variation. Of course, the set of T and $(S-1)$ immediately leads to the corresponding value of super-

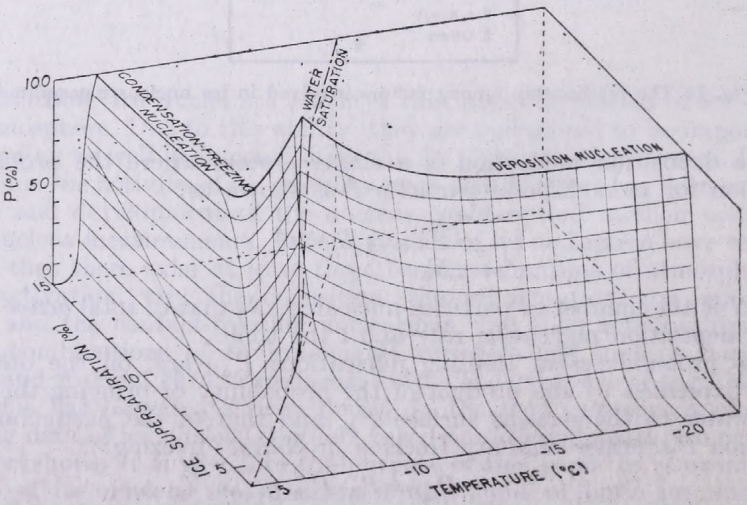

Fig. 2: Computed ice nucleation isopleths for silver iodide particles with average radius 0.14 μm (based on data reported by *Schaller* and *Fukuta*, 1979)

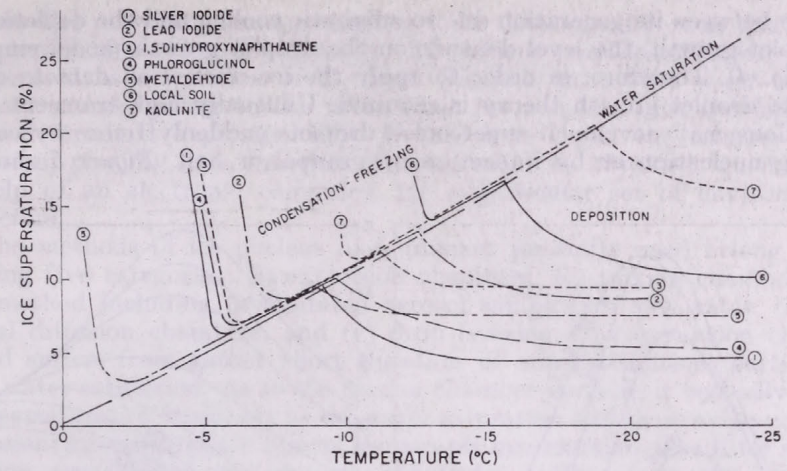

Fig. 3: Behavior of ice nucleants as a function of temperature and ice supersaturation. The curves represent nucleation of 1.3% of smoke particles in 1 min *(Schaller* and *Fukuta,* 1979)

saturation with respect to water $(S_W - 1)$ at the T. It is extremely important to realize that the three different mechanisms of heterogeneous ice nucleation appear in the different domains of the space involving these environmental parameters. *Figure 2* shows the domains of deposition and condensation-freezing nucleations on pure silver iodide particles of average radius 0.14 μm. In addition to these two mechanisms, the contact-freezing nucleation can proceed as a function of T and $N(r)$. The domains of the deposition and condensation-freezing, though observed with all the compounds, vary from compound to compound (see *Fig. 3*).

In natural clouds, supersaturation with respect to water develops while the clouds are growing. Since the supersaturation level is controlled by the

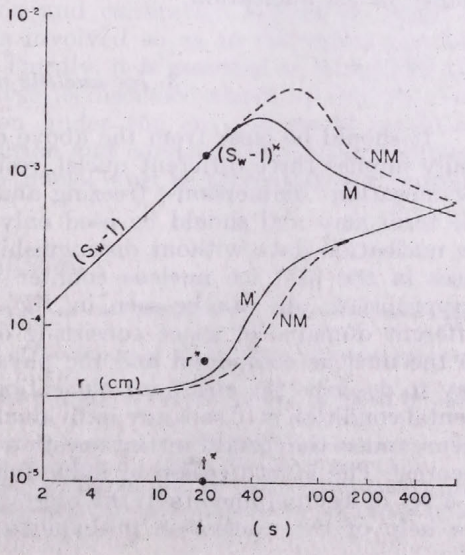

Fig. 4: Comparison of Maxwellian (M) and non-Maxwellian (NM) competitive droplet growth theories *(cf. Fukuta* and *Walter,* 1970). Initial conditions: 100 CCN/cm³, each containing 10^{-15} g NaCl, growing in a 10 cm/s updraft. The critical supersaturation for these nuclei, $(S_w\text{-}1)^*$, is reached in time t^* as shown; r^* is the critical radius for continued droplet growth. The non-Maxwellian theory (dashed curves) predicts a retardation of droplet growth (lower curves) and a greater maximum supersaturation (upper curves)

balance between its generation due to adiabatic cooling and the depletion due to droplet growth, the level depends on the droplet growth model employed (see *Fig. 4*). Therefore, in order to apply the ice nucleation data to clouds, accurate droplet growth theory is required. Unusually high transient supersaturations may develop if supercooled droplets suddenly freeze by contact-freezing nucleation or by impaction on graupel or hail. *Figure 5* shows an

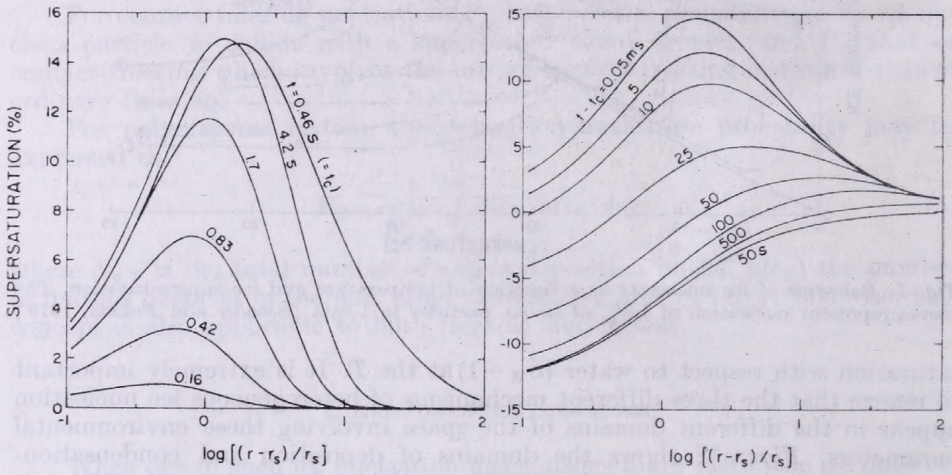

Fig. 5: Development of transient water-supersaturations in the vicinity of a freezing droplet in a water-saturated environment. $r = 50$ μm and $T = -15$°C *(Nix* and *Fukuta,* 1974)

example of water-supersaturation as high as 15% spreading into a considerable volume surrounding the droplet. However, as this transient effect disappears, the ice supersaturation gradually decreases. The system of growing ice crystals, once developed, thus reduces the supersaturation and therefore the subsequent chance of ice nucleation.

3. *Ice nucleus measurements*

It should be clear from the above discussions that the term "ice nuclei" really implies three different nuclei, respectively corresponding to deposition, condensation- (immersion-) freezing and contact-freezing mechanisms. Hence the term may and should be used only in the general sense. Comparison of ice nucleation data without distinguishing the mechanisms involved, as were cases in the past ice nucleus counter workshops, is for this reason clearly inappropriate. As can be seen in *Fig. 3*, these three mechanisms occur in different domains of space consisting of environmental variables depending on the nucleus compound and the physical conditions. So, the only possible way to describe the entire ice nucleation process under an arbitrary environmental condition is to separate individual mechanisms, identify and reconstruct them under the condition in question with the help of proper nucleation theories. The identification of individual mechanisms requires determination of a set of key parameters in the corresponding basic nucleation theories with the help of the nucleation probability expressions (1) through (5) in data

analysis. The most important parameter to be determined is m in this regard. The activity of a given population of ice nucleus particles therefore cannot be expressed as a function of T alone. Instead, it requires a set of three equations corresponding to the three basic mechanisms with the key parameters determined experimentally. If this were done, the number of ice nucleation, possibly as a function of time, could be obtained, quickly with the help of an electronic computer, for a particular set of environmental parameters.

The methods of ice nucleus measurement presently used belong to the following five categories: (i) expansion chambers, (ii) mixing chambers, (iii) filter method including precipitated aerosol samples on substrates, (iv) ice-thermal diffusion chambers, and (v) drop freezing. The expansion chamber method suffers from rather short duration of supersaturation, particularly above water saturation. As to the mixing chamber method, it basically allows the supersaturation level only at the water saturation and there exists a danger of transient supersaturation during the sample introduction. The filter method including precipitated particles on substrates suffers from the substrate effect. The thermal diffusion chamber method, although the ice crystal detection is the main problem, does provide a good control of $(S-1)$ and T. The drop freezing method requires an independent estimation of P_A as described above. Although every one of these methods has its own problems, the thermal diffusion chamber method gives a stable $(S-1)$ and T fields and therefore is suitable for mechanism identifiaction and calibration without substrate and other effects. However, other methods may find specific uses if properly calibrated against a *reliable* method, such as the ice-thermal diffusion chamber. For example, if the filter method with the possible substrate effect were checked against a thermal diffusion chamber, not against a mixing chamber, it could be utilized with its specific advantages, such as portability and ability to sample a large volume.

In measuring ice nuclei, it is important first to understand the features and limitations of the method used with respect to the three nucleation mechanisms. Secondly, considering the difficulties and advantages of different methods available, proper combination and calibration should be made to identify and separate the mechanisms involved so as to determine the key parameters of ice nucleation in them. Thirdly, it is essential to reconsider the method of data presentation after analysis as discussed above, so that the data can lead to the number of nucleation under the environmental condition predicted in natural clouds. For deposition and condensation-freezing nucleations, the data for a given population of nuclei must be presented as a function of $(S-1)$ and T.

REFERENCES

Fukuta, N. and *Schaller, R. C.*: Ice nucleation by aerosol particles: Theory of condensation-freezing nucleation (to be published).

Fukuta, N. and *Walter, L. A.*, 1970: Kinetics of hydrometeor growth from a vapor-spherical model. *J. Atmos. Sci. 27*, 1160–1172.

Nix, N. and *Fukuta, N.*, 1974: Nonsteady-state kinetics of droplet growth in cloud physics. *J. Atmos. Sci. 31*, 1334–1343.

Schaller, R. C. and *Fukuta, N.*, 1979: Ice nucleation by aerosol particles; Experimental studies using a wedge-shaped ice thermal diffusion chamber. *J. Atmos. Sci. 36*, 1788–1802.

Tomlinson, E. M., 1980: *A new horizontal gradient, continuous flow, ice thermal diffusion chamber and detailed observation of condensation-freezing and deposition nucleations.* Ph. D. Dissertation, Meteorology Department, University of Utah.

IDŐJÁRÁS

Az Országos Meteorológiai Szolgálat folyóirata, 86. évf. 2—4. szám, 1982. március—augusztus
Journal of the Hungarian Meteorological Service, Vol. 86. No. 2—4. March—August 1982, Budapest

Aerosols, description and descriptors

O. PREINING and G. REISCHL, *Institut für Experimentalphysik, University of Vienna, Strudlhofgasse 4, A—1090 Wien, Austria*

Aeroszolok, leírások és leírók. Az aeroszolok gázközegben szuszpendált részecskék komplex rendszerei. A leírások rendszerint figyelmen kívül hagyják a komplexitás aspektusait, egyszerűen megadva a számszerű vagy tömegkoncentrációt, vagy legfeljebb a nagyság szerinti eloszlást. A részecskefelhők inhomogenitásait, valamint a szabálytalan alakú részecskék komplex geometriáját vagy kémiáját ezidáig alig vették figyelembe. A nemlineáris folyamatok azonban, mint pl. a koaguláció vagy a részecskék felületén végbemenő kémiai reakciók igen nagy mértékben függnek ezektől az inhomogenitásoktól. Ezért az aeroszol felhő térbeli inhomogenitásait, valamint a részecskefelszín és a kémiai összetétel részletes szerkezetét feltétlenül le kell írni. Az ilyen jellegű leíráshoz igen jól felhasználható a „fractal"-ok fogalma, melyet *Mandelbrot* vezetett be a tudományba 1977-ben. Ennél egyszerű számok — *fractal dimenziók* — írják le a komplex struktúrát, amelyek csupán szükségesek, de nem elégségesek az adott szerkezet minden részletének leírására. A koncepciót jelen munkában szél adatokra alkalmazva mutatjuk be.

*

Aerosols, description and descriptors. Aerosols are inherently complex systems of particles suspended in gases. Descriptions usually neglect some aspects of the complexity, merely giving mass or number concentrations or, at the most, size distributions. The inhomogeneities of particulate clouds as well as the complex geometry and chemistry of irregularly shaped particles have so far been hardly discussed. However, essentially nonlinear processes like coagulation and chemical reactions on particle surfaces are highly dependent on these inhomogeneities. Hence it is necessary to describe spatial inhomogeneities of aerosol clouds, as well as the detailed structure of particle surfaces and chemical composition. An appropriate tool for such a description is the concept of fractals as introduced by *B. B. Mandelbrot* into science in 1977. Simple numbers — fractal dimensions —, are used to describe complex structures; they are only necessary but not sufficient to describe all the details of a given structure. The concept is applied to describe wind data.

*

Aerosols are inherently complex systems of particles suspended in gases. Descriptions usually neglect some aspects of the complexity, merely giving mass or number concentrations or distributions. The inhomogeneities of particulate clouds as well as the complex geometry and chemistry of irregularly shaped particles have so far been hardly discussed. However, essentially nonlinear processes like coagulation and chemical reactions on particle surfaces are highly dependent on these inhomogeneities. Hence it is essential to describe spatial inhomogeneities of aerosol clouds. An appropriate tool for such a description is the concept of fractals as introduced by *Mandelbrot* (1977) into science. Simple numbers—fractal dimensions—are used as descriptors of complex sutructures. They are only necessary but never sufficient to describe all the details of a given structure, yet they are more efficient than any other method used so far.

The here used inherent property of a complex system is to reveal the structures in greater detail, with increasing resolution of the observations. The fluctuating wind speed in the lower troposphere is an obvious example of the internal structures of a large system. The fluctuations indicated by the measuring device depend strongly on the time averaging process. If the momentary wind speed is registered for a certain length of time, the total length of the registration curve for a given period increases with decreasing averaging time. This is a simple example of a method of determining fractal dimensions (actually: relative similarity dimensions: *Mandelbrot*, 1977). Generally, if a parameter of a system increases with increasing resolution, a corresponding plot of the logarithm of the parameter *vs.* the logarithm of the resolution is called a "Richardson plot" (e.g., *Kaye*, 1978). The slope of the usually linear plot yields directly the fractal dimension by adding 1 to its absolute value.

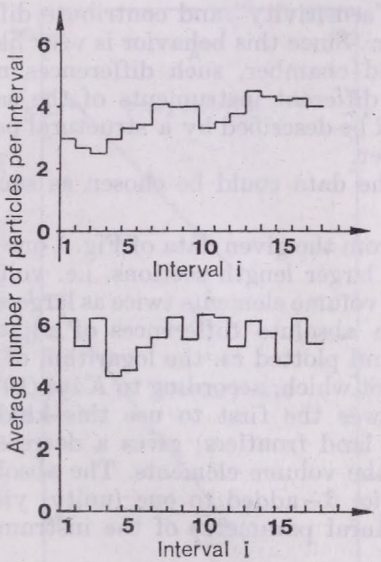

Fig. 1: The distribution of particles in a cloud chamber at two different particle concentrations, averaged over 30 individual experiments. Upper curve: approx. 1,800 particles/cm³, lower curve: approx. 3,000 particles/cm³

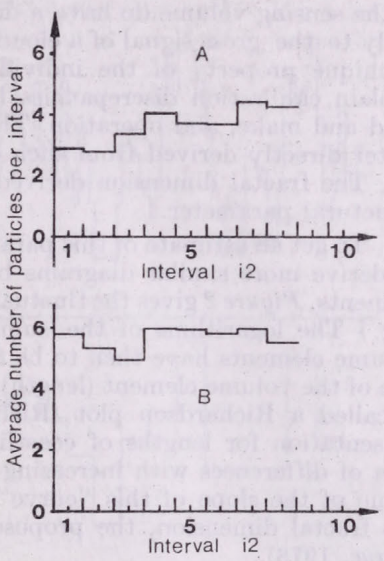

Fig. 2: The distribution of particles in a cloud chamber: Derived from the same data set, sensing volume (internal length) twice as large as in Fig. 1. A. upper curve: approx. 1,800 particles/cm³; B. lower curve: approx. 3,000 particles/cm³

An example is the distribution of particles in a cloud chamber shortly after an expansion. Particles in an expansion cloud chamber grow as a monodisperse system, i.e. all particles have at any given time the same size (within a rather narrow size interval) (*Preining* et. al., 1981). To obtain an answer to the question how homogeneously the monodispersed particles – droplets in an expansion cloud chamber are distributed within the chamber, photographs of the particles were taken approx. 100 ms after expansion. The cylindrical volume lit by the laser beam contained a small number of particles (50 – 100), so that the probability of two particles being aligned in the direction to the camera was negligible. Therefore the particle number concentration could be obtained simply by counting the number of spots on the photograph

within a given length interval representing the cylindrical volume element defined by a section of a certain length of the laser beam. The sensing volume was divided into 18 sections of equal length. *Figure 1* shows the number of counted particles within such volume elements averaged over 30 individual experiments (i.e. expansion of the cloud chamber) for two different concentrations. One would expect a horizontal line and only minor fluctuations caused by the statistical concentration fluctuations. But Fig. 1 shows a different behavior; the variation in concentration is systematic indicating that different sections within the sensing volume, i.e. the laser beam, have different efficiencies in activating or collecting nuclei. This indicates that different elements of the sensing volume do have a different "sensitivity" and contribute differently to the gross signal of a cloud chamber. Since this behavior is very likely a unique property of the individual cloud chamber, such differences may explain calibration discrepancies between different instruments of the same kind and make, and operation. They could be described by a structural parameter directly derived from such a data set.

The fractal dimension derived from the data could be chosen as such a structural parameter.

To get an estimate of this parameter, from the given data of Fig. 1 one has to derive more similar diagrams based on larger length sections, i.e. volume elements. *Figure 2* gives the fluctuations for volume elements twice as large as in Fig. 1 The logarithms of the sums of the absolute differences of adjacent volume elements have then to be formed and plotted *vs.* the logarithm of the size of the volume element (length). This plot which, according to *Kaye* (1978), is called a Richardson plot (Richardson was the first to use this kind of presentation for lengths of coastlines and land frontiers) gives a decreasing sum of differences with increasing size of the volume elements. The absolute value of the slope of this "curve" – see *Fig. 3* – added to one (unity) yields the fractal dimension, the proposed structural parameter of the instrument (*Kaye*, 1978).

Another example is the wind speed measured on top of the physics building of the University of Vienna, demonstrated in *Fig. 4*. In the upper part of the graph the one-minute average of the wind speed is plotted *versus* the time. The lower part shows 5-minute averages calculated from the same data set. As one can easily understand, the curve becomes less structured with increasing averaging time. The second of these qualitative examples was selected to be the subject of more detailed studies and an attempt was made to derive the fractal dimension of parameters of the wind field using measurements of wind direction and wind velocities.

The wind data were obtained on the top of a 5-m tower mounted on the roof of a 6-story building approx. 45 m above street level. The building is located close to the center of Vienna city on a little elevation, the measuring site being some 15 m above the average height of the roof tops of the surrounding buildings.

The signals from the wind speed sensor (a current generator type anemometer sensor, Nr. 1467 Wilhelm Lambrecht KG, Göttingen) and the wind direction sensor (a ring potentiometer type sensor, Nr. 1456, Wilhelm Lambrecht KG, Göttingen) are decoded, amplified and finally encoded into a pulse train suitable to be fed directly into a 1024-channel pulse-height analyzer (TN 1705 Traicor Northern Inc., Wisconsin). The coding was performed in the following way: each revolution of the anemometer wheel produces a certain

number of pulses, the pulse frequency is, in good approximation, proportional to the wind speed. Therefore the number of pulses within a time interval corresponds to a wind path. With the anemometer used, the smallest detectable wind path (equivalent to 1 pulse) is about 8.5 cm. The wind direction signal is encoded into the pulse height so that finally one single pulse is equivalent to a wind path of 8.5 cm in the direction given by the pulse height, hence it yields the dimension of an elementary vector. In the pulse-height analyzer these pulses are sampled in 40 channels, each channel containing the sum of

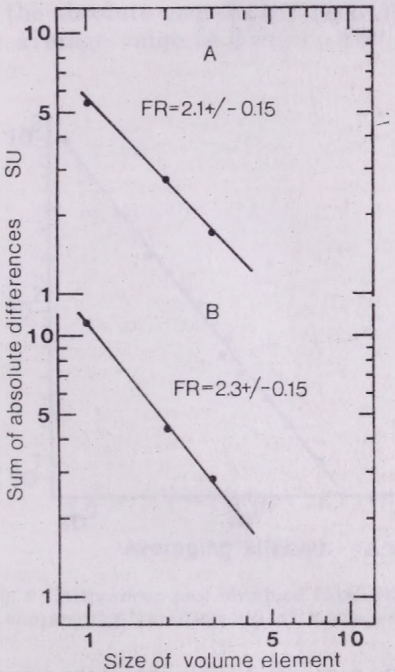

Fig. 3: Richardson plots obtained from the distribution of particles in a cloud chamber at different particle concentrations. A. upper curve: approx. 1,800 particles/cm³, B. lower curve: approx. 3,000 particles/cm³

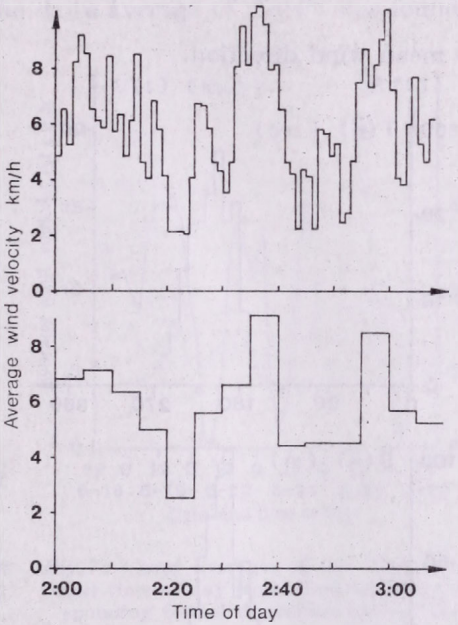

Fig. 4: Wind velocity *versus* time. Upper curve: 1-minute averaging time interval, lower curve: 5-minute averaging time interval, both curves calculated from the same data set

the wind paths in a certain wind direction interval with the width of nine degrees.

Furthermore, pulses with a constant frequency of 1 kHz, coded with the voltage level proportional to the wind direction are sampled in 40 adjacent channels of the PHA. Each channel contains the time when the wind was blowing in the wind direction interval represented by the channel number. *Figure 5* shows a three-minute sample of the primary wind data obtained by this method, $T(\alpha)$ denotes the total time the wind was blowing in the wind direction interval α, and $S(\alpha)$ is the total wind path in the wind direction interval α. From this set of data various parameters can be derived, like the average wind velocity, given by

$$V(t) = A \cdot \sum_{\alpha} S(\alpha)/\Delta t$$

A being a constant factor, proportional to the resolution of the wind-speed sensor, and Δt is the sampling time interval; the angular variation ε is defined by

$$\varepsilon(t) = 2 \cdot \arctan\left(\sum_{\alpha^*} |S(\alpha^*) \cdot \sin \alpha^*| / 2 \cdot \sum_{\alpha^*} S(\alpha^*) \cdot \cos \alpha^*\right)$$

with

$$\alpha^* = \alpha - \bar{\alpha}$$

and

$$\bar{\alpha} = \arctan\left[\sum_{\alpha} S(\alpha) \cdot \sin \alpha / \sum_{\alpha} S(\alpha) \cdot \cos \alpha\right]$$

the mean wind direction.

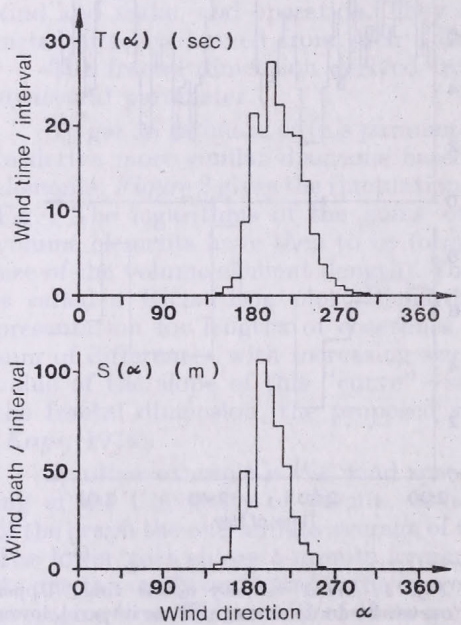

Fig. 5: Three-minute sample of the primary data of a wind field, obtained by the method of sampling coded pulses in a pulse height analyzer

The concept of fractal dimensions can be applied to these parameters to obtain a simple number describing the complex structure of the data. Let us select ε for analysis. The specific procedure is as follows: first the values ε_k, i.e. the angular variation for $\Delta t = 3$-minute samples, are arranged consecutively, $k = 1, 2 \ldots m$ denoting the specific time interval. Then the values ε_{ij} are defined by averaging ε_k over i time intervals Δt:

$$\varepsilon_{ij} = \frac{1}{i} \sum_{l=1}^{i} \varepsilon_k = \varepsilon_{i \cdot (j-1)+1} \qquad j = 1 \ldots \text{integer}\,(m/i)$$

Then the sum $SU(\Delta\tau)$ of all absolute differences of adjacent ε_{ij} is calculated for the averaging interval $\Delta\tau = i \cdot \Delta t$

$$SU(i \cdot \Delta t) = \sum_{j=1}^{(m/i)} |\varepsilon_{ij+1} - \varepsilon_{ij}|$$

The fractal dimension is approximately given by

$$FR(\varepsilon) = 1 + |d[\log(SU(\Delta\tau))]/d[\log(\Delta\tau))]|$$

Figure 6 shows an example of the Richardson plot log $[SU(\Delta\tau)]$ *versus* log $(\Delta\tau)$ for the angular variation $\varepsilon(t)$ for $i = 1, 2, 3, 4, 6, 7, 8, 9, 10, 15, 20, 30$. The data points almost perfectly fit a straight line with the slope of -1.35, representing the relative fractal dimension $FR(\varepsilon) = 2.35$.

Figure 7 shows 3-hour averages of the wind velocity *versus* time of day. The average fractal dimension (calculated as discribed above) is plotted as a dotted line. The average wind velocity shows great variation over the period of one day; the corresponding fractal dimensions do not seem to be correlated to the absolute magnitude of the wind velocity and vary between 2 and 3 with an average value of $FR(V) = 2.38$. The daily average of $FR(V)$ was found to

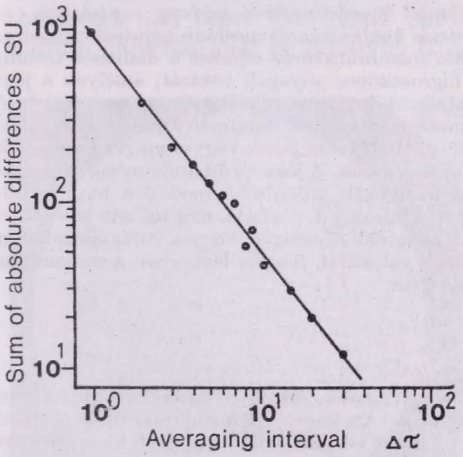

Fig. 6: Richardson plot obtained from values of the angular variation $\varepsilon(t)$ of a wind field

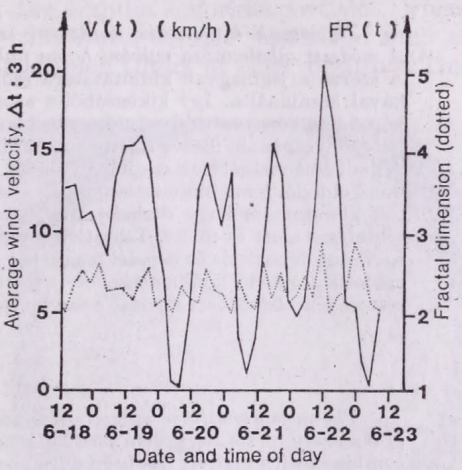

Fig. 7: 3-hour averages of the wind velocity *versus* time of day (solid line) and the corresponding fractal dimension (dotted line)

vary only very little around the same value. The fractal dimensions of all the parameters obtained from the wind speed and wind velocity were found to be 2.4 ± 0.1.

The fractal dimension derived seems to be a convenient measure of the local structure of the atmosphere in the vinicity of a measuring station. One may speculate that this parameter correlates with the Turner classes and would give an experimentally derived measure of the structure of turbulences of the local atmosphere, but this could be proved only by further investigations.

REFERENCES

Kaye, B. H., 1978: Specification of the ruggedness and/or texture of a fine particle profile by its fractal dimension. *Powder Technology 21*, 1.

Mandelbrot, B. B., 1977: *Fractals: Form, chance and dimension.* W. H. Freemand and Company, San Francisco.

Preining, O., Wagner, P. E., Pohl, F. G. and *Syzamsnki, W.*, 1981: in *Aerosol research at the Institute for Experimental Physics of the University of Vienna*, (O. *Preining*, ed.) Vol. III, University of Vienna.

IDŐJÁRÁS

Az Országos Meteorológiai Szolgálat folyóirata, 86. évf. 2–4. szám, 1982. március–augusztus
Journal of the Hungarian Meteorological Service, Vol. 86. No. 2–4. March–August 1982, Budapest

The membrane filter method combined with dialysis to detect ice nuclei; an application to the study of ice nucleation mode of volcanic ash

T. TANAKA, *Meteorological Research Institute, Tsukuba 305, Japan*

Jégmagvak kimutatása dializissel kombinált membránszűrős módszer segítségével. – A módszer alkalmazása vulkáni hamu nukleációs hatásmechanizmusának tanulmányozására. A szerző a jégmagvak kimutatására szolgáló membránszűrős eljárást a dializises technikával kombinálta. Így kiküszöbölte azon higroszkópos anyagok hatását, amelyek a jégképződést környezetükben erősen befolyásolják. A módszert a vulkanikus hamu jégképző hatékonyságának, illetve a hatásmechanizmus természetének tanulmányozására használta. A dializises vizsgálatok szerint a vulkáni hamuból álló részecskék vegyes magvak, amelyek mind oldódó, mind oldhatatlan anyagokat tartalmaznak. A jégképző-hatékonyság vizsgálatok kimutatták, hogy dialízis után ezek a részecskék különböző módokon hatnak túltelítettség alatt és fölött. Telítetlen levegőben kizárólag depozíciós, míg telített levegőben egyaránt depozíciós és fagyási magvakat szolgáltatnak. Tekintve, hogy a vulkanikus hamu eredetileg oldódó komponenseket is tartalmaz, valószínű, hogy a légkörben a vulkanikus részecskék elsősorban fagyási magvakat alkotnak.

*

The membrane filter method combined with dialysis to detect ice nuclei; an application to the study of ice nucleation mode of volcanic ash. An improved membrane filter method combined with dialysis has been developed to detect ice nuclei on a specimen filter without being affected by hygroscopic materials, which act as a strong vapour sink and supress the ice nucleation of neighboring particles. The method was applied to the study of the nature and the mode of action of volcanic ash as ice nuclei. Dialysis of the specimen filter loaded with volcanic ash revealed ash particles to be mixed nuclei which consist of solid particles and water-soluble components. The temperature and humidity dependence of the ice nucleating activity also revealed a difference in activation mode between below and above water saturation; below water saturation, the volcanic ash particles act as ice nuclei in the deposition mode, whereas above water saturation they act in both the modes of deposition and condensation-freezing. Taking into account the nature of mixed nuclei of volcanic ash, the mode of action is presumed to be primarily a condensation-freezing mechanism in the atmosphere.

*

Introduction. The membrane filter method for detecting ice nuclei has been widely used because of simplicity of the sampling technique of specimen filters (*Bigg*, et al., 1963; *Gagin* and *Aroyo*, 1963; *Stevenson*, 1968). However, when specimen filters are processed in a diffusion chamber, a couple of problems arise concerning the humidity in the diffusion chamber: *(a)* 'Volume effect', caused by hygroscopic materials on the specimen filter (*Mossop* and *Thorndike*, 1966; *Huffman* and *Vali*, 1973), *(b)* 'Degree of Supersaturation' achieved in a diffusion chamber (*Lala* and *Jiusto*, 1972). In this study, these problems have been solved by the membrane filter method combined with

dialysis. The method was applied to the specimen filter loaded with volcanic ash from Mt. Usu in Hokkaido, and the mode of action as ice nuclei was examined.

1. Dialysis-technique of removal of water-soluble components

To observe the removing process of hygroscopic materials from the filter, a test filter was prepared by loading it with sodium chloride particles as hygroscopic material and floated on the surface of a 2% solution of silver nitrate as shown in *Fig. 1a* and *b*. The removal takes place by the precipitation of silver chloride *(Fig. 1c)*. After a few precipitates of AgCl were found, the filter was carefully picked up and dried in a dark room. Silver chloride particles formed on the filter were detected under irradiation of light *(Fig. 1d)*. Their positions coincided with that of the sodium chloride particles, where the latter had been. The result shows that water-soluble materials, such as sodium chloride, can be removed from specimen filters at their position. This

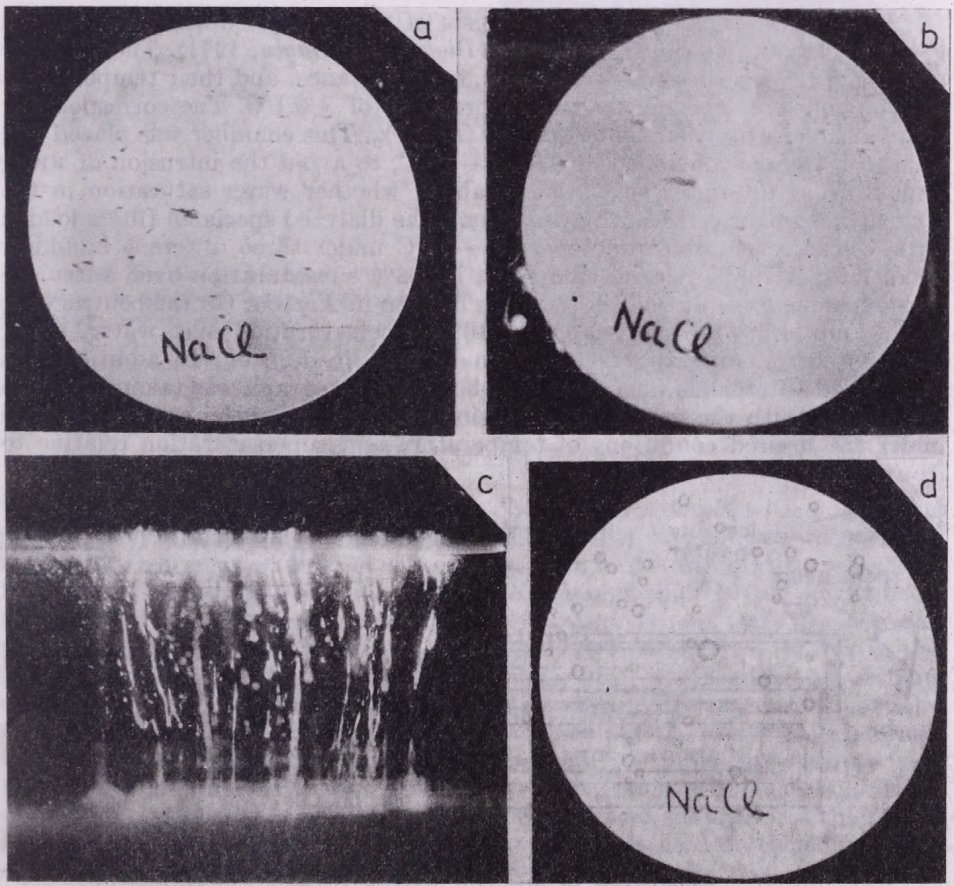

Fig. 1: Removal of sodium chloride particles as a water-soluble component from the surface of a Millipore filter floated on the surface of a 2% solution of silver nitrate

technique of removal was applied to the specimen filter of volcanic ash. In this case distilled water was used in place of the silver nitrate solution, and the filter was floated for 12 hours.

2. *Volcanic ash as mixed nuclei*

After dialysis, no morphological variation of volcanic ash was observed by electron microscopy, and a lot of chemical components were detected in the solution used for dialysis. The total quantity of water-soluble components was calculated as amounting to 1,250 mg per kg of ash. This amount of soluble components corresponds to 1.6×10^{-15} gram per ash particle of 1 μm in diameter, assuming a particle density of 2.5 g cm^{-3}. From these results, volcanic ash was presumed to be mixed nuclei which consist of solid particles and water-soluble components.

3. Supersaturation relative to water in the diffusion chamber

The diffusion chamber used consists of two parallel brass plates spaced apart by 15 mm, as shown in *Fig. 2* (*Bigg*, 1971; *Gagin*, 1971). The ice plate and the specimen filters are spaced at 5 mm distance, and their temperatures are controlled independently with a precision of ± 0.1°C. The corresponding error in supersaturation is not more than $\pm 2\%$. This chamber was placed and used in a freezer controlled at about -15°C, to avoid the intrusion of water vapour from the outer space. To establish whether water saturation in the diffusion chamber can be achieved or not, the dialyzed specimen filters loaded with volcanic ash were processed at -15°C under three different humidity conditions. At 98% relative humidity, i.e., 2% subsaturation over water, ice crystals alone grew on the filter as can be seen in *Fig. 3a*. On the contrary, at 102% and 110% RH, i.e., 2% and 10% supersaturation over water, water droplets surrounding the crystals can be seen in *Fig. 3b*. In addition, the freezing of water films was observed when the photograph was taken as shown in *Fig. 3c*. With the use of this diffusion chamber ice nuclei can be detected under the desired conditions of temperature and supersaturation relative to ice or water.

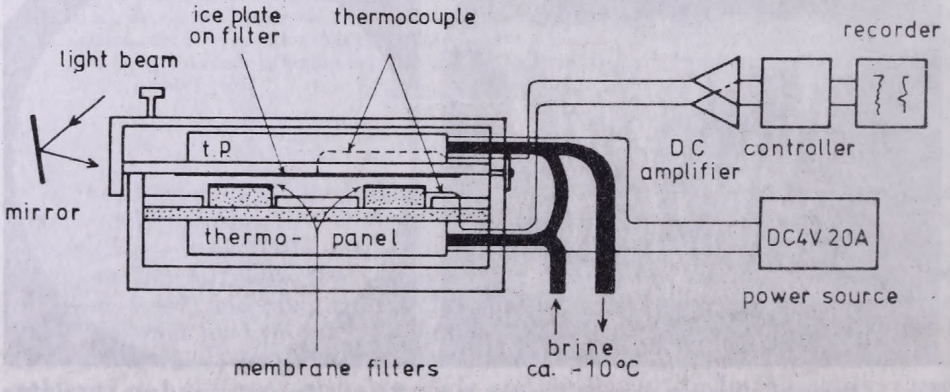

Fig. 2: Thermal diffusion chamber used for the processing of specimen filters

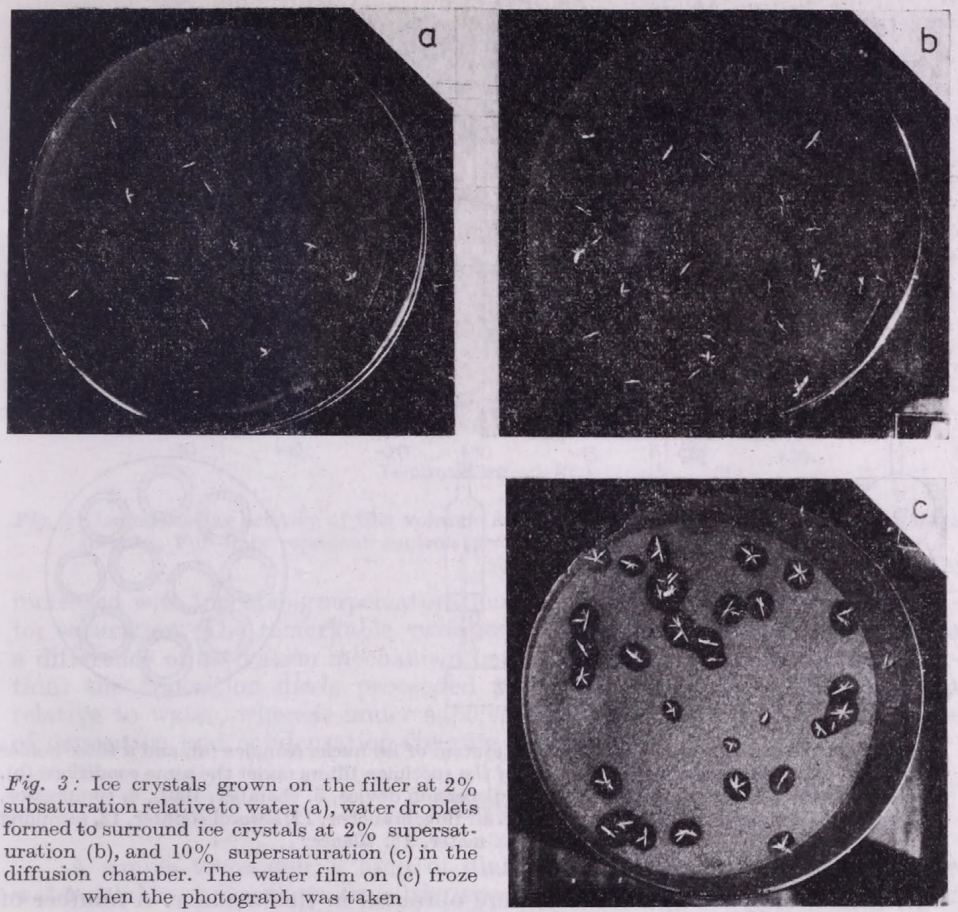

Fig. 3: Ice crystals grown on the filter at 2% subsaturation relative to water (a), water droplets formed to surround ice crystals at 2% supersaturation (b), and 10% supersaturation (c) in the diffusion chamber. The water film on (c) froze when the photograph was taken

4. Preparation of specimen filters

Specimen filters of volcanic ash were obtained by a device with a dispersion system as shown in *Fig. 4a* and *b*. A few milligrams of volcanic ash was weighed and put into a sample holder (1). The ash sample was blown off into a flask (4) by compressed aerosol-free air. Ash particles larger than 10 μm in diameter collided to the inner wall of the flask and were trapped there. Only fine particles passed on into a chamber (5), well-dispersed by dry and aerosol-free air driven from a compressor (6). They were finally captured by filters in a sampling device (13) which is shown in Fig. 4b in more detail. The number of particles captured was estimated from the result of measurement by an optical aerosol counter (11 – 12) set in the outlet of the chamber. Ten specimen filters were prepared simultaneously under the same conditions. To check the same number of particles on each filter, the ten filters were subjected to the test of activation of ice nuclei. The numbers of ice nuclei detected on each filter were equal within an accuracy of 7%.

Of the ten filters sampled for each dispersion of volcanic ash, five filters were dialyzed and the others were used as controls. A set of five pairs of speci-

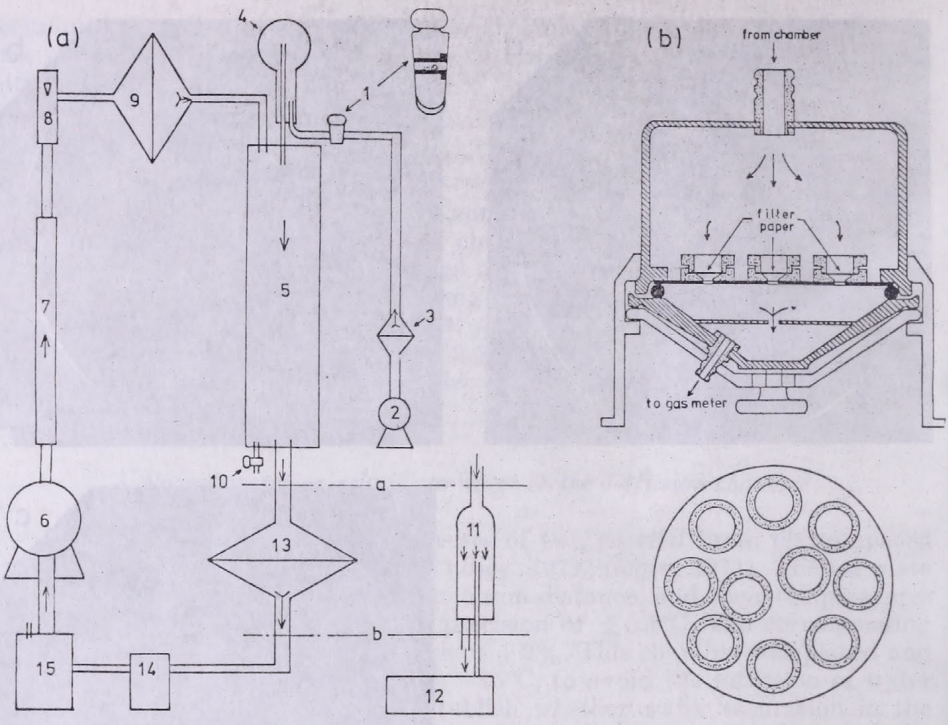

Fig. 4: Schematic diagram of the dispersion system of ice nuclei samples (a), and a filter holder capable of taking simultaneously ten sheets of the specimen filters under the same conditions (b). 1. Sample holder, 2. compressor, 3. filter, 4. dispersion device, 5. chamber, 100L, 6. compressor, 7. silicagel, 8. flow meter, 9. filter, 10. cock, 11. air flow brancher, 12. aerosol counter, 13. sampling device, 14. gas meter, 15. silencer

men filters, dialyzed and control, were obtained in this manner. A number of sets of the specimen filters were used in the experiment.

5. Modes of action of volcanic ash

Both the control and dialyzed specimen filters loaded with volcanic ash were subjected to the test of temperature- and humidity-dependence of ice nucleating activity. The results are shown in *Fig. 5a, b,* and *Fig. 6.* The numbers of ice nuclei detected on the dialyzed specimen filters are larger than those on the control filters, in both temperature and humidity spectra. No difference in the morphology between the control and dialyzed specimens leads us to the conclusion that water-soluble components decrease the ice nucleating ability. Two mechanisms are proposed to account for the causes: the clogging of active sites and the lowering of the freezing point. These figures, especially Fig. 6, also show the humidity dependence of ice nucleating ability. In the figure, full lines represent the case of the processing temperature $-20\,°C$, and dashed lines represent $-15\,°C$; D and C stand for dialyzed and control specimens, respectively, and two shaded columns are inserted in each place relating to the water saturation. One of the pronounced features of the humidity spectra is that the number of ice nuclei detected on each spectrum

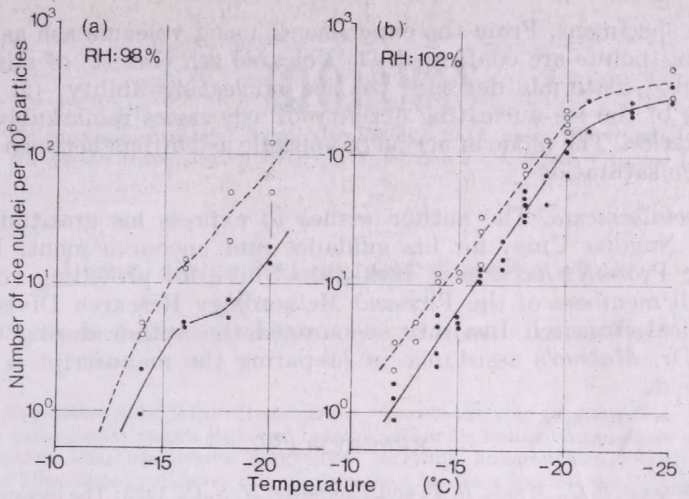

Fig. 5: Ice nucleating activity of Usu volcanic ash as a function of temperature (temperature spectra). Full lines represent control specimens, dashed lines the dialyzed ones

increased with increasing supersaturation and varied remarkably at about water saturation. The remarkable variation at about water saturation suggests a difference of activation mechanism between below and above water saturation: the deposition mode proceeded under the condition of subsaturation relative to water, whereas under supersaturation conditions, both the modes of deposition and condensation-freezing proceeded.

6. Conclusions

A simple technique, a kind of dialysis, has been developed to remove water-soluble components from the specimen filter, and the achievement of supersaturation in the diffusion chamber was also confirmed by the processing

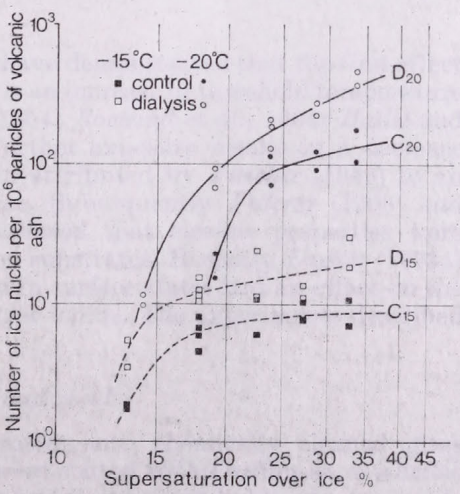

Fig. 6: Ice nucleating ability of volcanic ash of Mt. Usu as a function of degree of supersaturation over ice (humidity spectra). Full lines represent the case of processing temperature −20°C, and dashed lines represent −15°C

of dialyzed specimens. From the experiments using volcanic ash as specimen, the following points are confirmed. (1) Volcanic ash consists of mixed nuclei. Water soluble materials decrease the ice nucleating ability. (2) Humidity dependence of the ice-nucleating activity of ash varies remarkably at about water saturation. The mode of action of volcanic ash differs between below and above water saturation.

Acknowledgements. The author wishes to express his gratitude to Prof. *A. Ono* of Nagoya Univ. for his guidance and encouragement. He is also indebted to Prof. *K. Kikuchi* of Hokkaido Univ., for providing volcanic ash samples. All members of the Physical Meteorology Research Division of the Meteorological Research Institute encouraged the author during this work; especially Dr. *Matsuo*'s assistance in preparing the manuscript is gratefully acknowledged.

REFERENCES

Bigg, E. K., Mossop, S. C., Meade, R. T. and *Thorndike, N. S. C.*, 1963: The measurement of ice nucleus concentrations by means of Millipore filters. *J. Appl. Meteor. 2*, 266–269.

Bigg, E. K., 1971: Apparatus for detection of ice nuclei on filters. The Second International Workshop on Condensation and Ice Nuclei. *Dept. Atmos. Sci.*, Colorado State Univ., 52–53.

Gagin, A. and *Aroyo, M.*, 1969: A thermal diffusion chamber for the measurement of ice nuclei concentrations. *J. Rech. Atmos., 4*, 115–122.

Gagin, A., 1971: A thermal diffusion chamber for ice nuclei measurements. The Second International Workshop on Condensation and Ice Nuclei. *Dept. Atmos. Sci.*, Colorado State Univ., 52–53.

Huffman, P. J. and *Vali, G.*, 1973: The effect of vapor depletion on ice nucleus measurements with membrane filters. *J. Appl. Meteor., 12*, 1018–1024.

Lala, G. G. and *Jiusto, J. E.*, 1972: Numerical estimates of humidity in a membrane filter ice nucleus chamber. *J. Appl. Meteor., 11*, 674–683.

Mossop, S. C. and *Thorndike, N. S. C.*, 1966: The use of membrane filters in measurements of ice nucleus concentration. 1. Effect of sampled air volume. *J. Appl. Meteor., 5*, 474–480.

Stevenson, C. M., 1968: An improved Millipore filter technique for measuring the concentrations of freezing nuclei in the atmosphere. *Quart. J. R. Met., 94*, 35–43.

IDŐJÁRÁS

Az Országos Meteorológiai Szolgálat folyóirata, 86. évf. 2–4. szám, 1982. március–augusztus
Journal of the Hungarian Meteorological Service, Vol. 86. No. 2–4. March–August 1982, Budapest

Light, silver iodide, and the size effect

R. G. LAYTON, *Physics Department, Northern Arizona University, P.O.B. 6010 Flagstaff, AZ 86011, U.S.A.*

A fény hatása ezüst-jodid részecskékre a részecske-nagyság függvényében. A fény hatása vékony ezüst-jodid rétegek jégképző hatékonyságára a hullámhosszúság és a réteg eredeti hőmérsékleti küszöbértékének függvénye. Nagyobb hullámhosszú ibolyántúli sugárzás növeli a küszöbhőmérsékletet, míg a vörös fény hatása a kezdeti feltételektől függ. Ezek az eredmények a réteg felületén, illetve ennek közelében kialakuló hosszú élettartamú töltéscsapdák és a vízmolekulák kölcsönhatásával magyarázhatók. A töltéscsapdák ugyanis befolyásolják a felületi energiát, amelytől a jég nukleációja függ. Az eredmények továbbá megerősítik a részecskenagyság hatását, amelyet előzetesen ezüst-jodiddal figyeltek meg. Az elmélet valószínűvé teszi, hogy vannak olyan anyagok, amelyeknél a részecskenagyság hatása a jégképző hatékonyság növekedését eredményezi. Ez a hatás szerves jégképző anyagok esetén jelentéktelen.

*

Light, silver iodide, and the size effect. The effect of light on the ice nucleating ability of thin films of silver iodide is a function of both the wavelength of the light and the initial threshold temperature of the film. Long-wavelength ultraviolet light has a tendency to increase the threshold temperature, but red light will lower or raise the threshold temperature depending on the initial conditions. These results can be explained theoretically in terms of increases and decreases in the population of long-lived charge traps near or on the surface of the films. The interaction between the trapped charge and the water molecules varies the interfacial energy which affects the ice nucleation characteristics. These results further confirm the cause of the previously observed size effect in silver iodide. Although this particular effect has only been demonstrared in silver iodide, the theory suggests that substances may exist for which the size effect would result in an enhancement rather than a degradation of ice nucleating ability. It is also evident that this size effect should not be significant in most organic nucleators.

*

Introduction. Several experimenters have demonstrated that the first effect of light on ice nucleation by silver iodide is an increase in threshold temperature (*Bryant* and *Mason* 1960; *Papee* et al., 1964; *Rowland* et al., 1964; *Hallet* and *Shrivastava*, 1972 and *Gravey*, 1973). Further exposure results in a decrease of ice nucleation ability, which has been attributed by *Fletcher* (1959) to an increase in metallic silver at the surface. Subsequently *Federer* (1968) and *Pruppacher* and *Pflaum* (1975) demonstrated that electric properties were important in the case of ice nucleation on substrates. Recently *Layton* (1973a) found that the amount of charge trapped in surface states had an effect on the ice nucleating ability of thin films of silver iodide. The experiments described in this paper extend these studies.

1. Procedure and results

Silver iodide was vacuum evaporated onto chemically cleaned glass microscope slides which for some tests were coated with Drifilm-88, a silicone varnish. Direct illumination of the films by incandescant light, and any expo-

sure to sun or flouorescent light was avoided. Crystal structure analysis by X-ray powder pattern techniques of material scraped from a slide showed that these films were predominately in a wurtzite structure, βAgI, with a small amount in zincblende structure, γAgI.

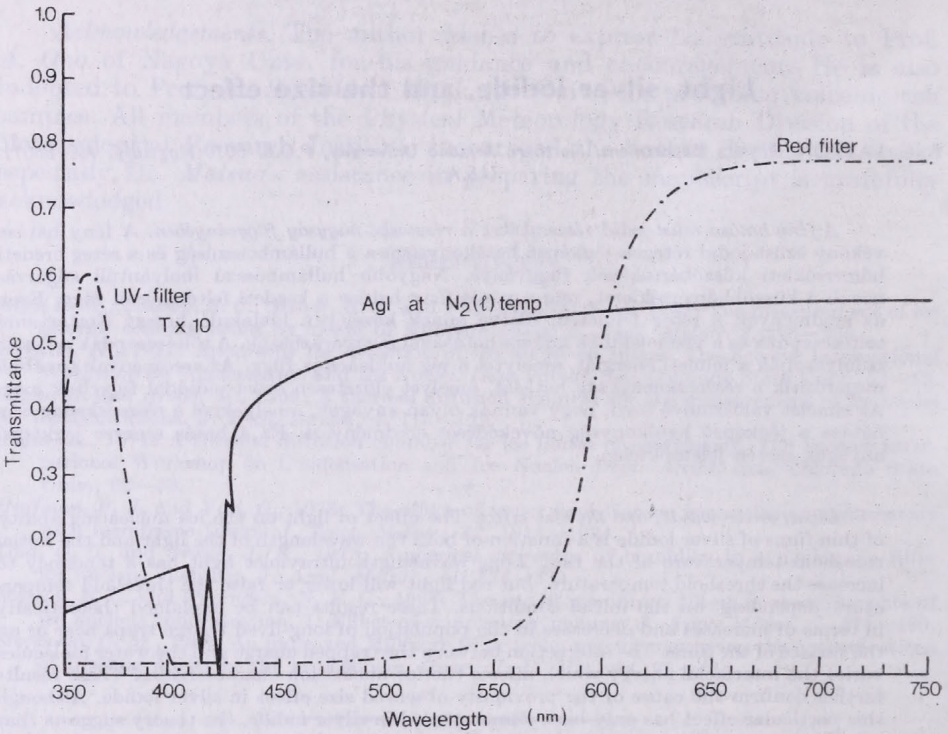

Fig. 1: The transmittance of a AgI thin film at liquid nitrogen temperature, of the red filter and transmittance times ten of the UV filter

The optical transmittance of some of the evaporated films at liquid nitrogen temperature was measured using a Cary 15 spectrophotometer for wavelengths between 350 nm and 500 nm. The films, which were deposited on unheated substrates, had large absorption peaks at 421.0 nm and 415.5 nm plus an additional small peak or shoulder at 425.0 nm *(Fig. 1)*. *Cardona* (1963) has shown that the two main peaks at 421.0 and 415.5 nm are exction peaks associated with the wurtzite structure and the small peak or shoulder at 425.0 nm corresponds to the exction peak in the zincblende structure, thus confirming the X-ray data. The thickness of the films, around 300 nm, was measured using an interference microscope.

The experiments were done using two light sources: A high pressure mercury lamp (hereafter designated "UV") with a filter whose transmission centered around the 366 nm line with a half-width of 30 nm and a quartz–iodine incandescent lamp with a red plastic broadband filter. The red filter freely transmitted yellow, red and infrared, but absorbed strongly in the blue and green regions of the spectrum (Fig. 1). At the slide's surface the irradiance

as measured by a thermopile was, for the UV and red sources, 4.9 mW/cm² and 52 mW/cm², respectively. The exposure times were determined experimentally to give approximately the same effect and were 9 minutes for UV light and 2.5 minutes for red light.

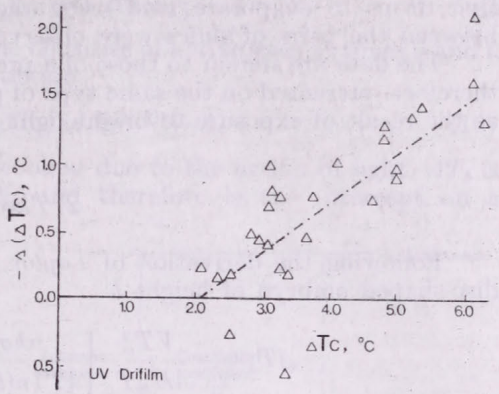

Fig. 2: The change in supercooling *vs.* the original supercooling for AgI films deposited on a silicone varnish substrate and exposed UV light; the line shown is the least squares fit

Millimeter-sized drops of distilled water (30/run), which had been passed through activated carbon, deionized and filtered (pleated membrane 0.2 μm pore size), were placed on the silver iodide-coated slides, which were in thermal contact with a thermoelectric cooler. The slide was then covered with a box made of polarizing material and the drops were observed using light from a microscope illuminator on its lowest range. The light was directed from the side to the water drops with only scattered light striking the silver iodide film. The cooling rate did not exceed 1°C/min. Temperature was measured to the nearest 0.1°C using a thermocouple in good contact with the upper surface of the slide and the temperature at which each drop froze was noted. A typical standard deviation of the temperature spread about the mean freezing temperature was 0.2°C. The slide was then warmed and exposed to UV or red

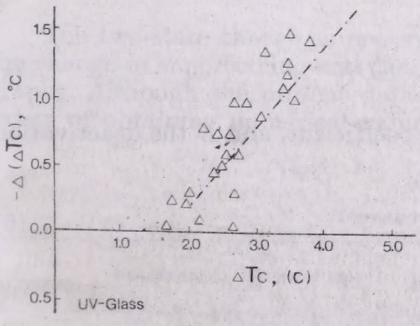

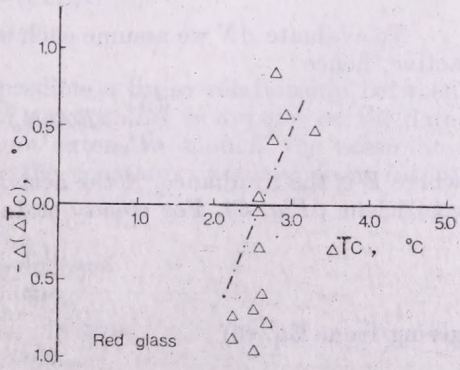

Fig. 3–4: The change in supercooling *vs.* the original supercooling for AgI films deposited on a glass substrate and exposed to UV light (Fig. 3) and to red light (Fig. 4); the line shown is the least squares fit

light with the cover removed. Additional drops were placed on the slide in positions adjacent to the original drops and the initial procedure was repeated. A typical standard deviation of the freezing temperature was 0.6°C for these cases. Experiments were also run using pairs of slides, one exposed and one not exposed, or by exposing the slide to light while taking care not to allow the first drops to evaporate, and using them again. No significant differences between the pairs of slides were observed.

The data are similar to those of a previous report (*Layton*, 1973a) and are, therefore, presented on the same type of plot, i.e., $\Delta(\Delta T_c)$ is the change in ΔT_c as the result of exposure to bright light *(Figs. 2, 3, 4)*.

2. Theory

Following the derivation of *Layton* (1973a) it can be shown that for a disc-shaped embryo of height h

$$\Delta T_c = -\frac{\bar{V} T_m^2}{\Delta H_m T_c}\left[\frac{\pi h \sigma_e}{kT \ln(\Omega/J)} + \frac{2\sigma_{iw} - U}{h}\right] \tag{1}$$

where $\bar{V}$ is the molecular volume, ΔH_m, the heat of fusion, k, Boltzman's constant, σ_e, the interfacial energy for the cylindrical face, σ_{iw}, the plane ice-water interfacial energy, and U is the free energy of interaction across the ice-silver iodide interface.

Let us assume a surface which has N active sites per unit area such that U is linearly dependent on N plus other constant surface characteristics.

$$U = CN + M \tag{2}$$

where C and M are constants. For small temperature changes we will assume all quantities are constant except ΔT_c and U; we can then group constant and approximately constant quantities and name them A_o and B.

$$\Delta T_c = A_o + BCN \tag{3}$$

A change in N of ΔN changes ΔT_c by

$$\Delta(\Delta T_c) = BC\Delta N \tag{4}$$

To evaluate ΔN we assume each unit area contains N_0 sites N of which are active, hence

$$\frac{dN}{dt} = EA(N_o - N) - EDN \tag{5}$$

where E is the irradiance, A the activation coefficient, and D the deactivation coefficient *(Fig. 5)*. For steady state

$$\frac{dN}{dt} = 0 \tag{6}$$

giving from Eq. (5)

$$N_s = N_o \frac{A}{A + D} \tag{7}$$

where N_s is the steady state site density.

Rewriting Eq. (5) in terms of N_s gives

$$\frac{dN}{dt} = E(A+D)\,(N_s - N) \tag{8}$$

which can be integrated to obtain

$$\Delta N = (N_s - N_1)\,(e^{-E(A+D)t} - 1) \tag{9}$$

where ΔN is the difference between the densities of active sites at times 0 and t. Combining Eqs. (3), (4) and (9) we obtain

$$\Delta(\Delta T_c) = (\Delta T_i - \Delta T_o)\,(e^{-E(A+D)t} - 1) \tag{10}$$

where $\Delta(\Delta T_c)$ is the change in supercooling due to the action of light, ΔT_i is the supercooling obtained at $N = N_s$ and therefore is the intercept on a

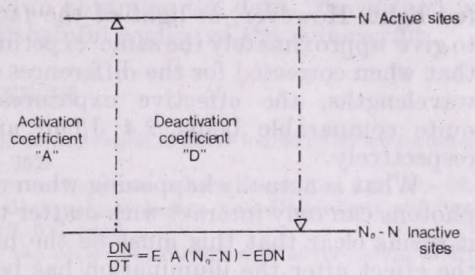

Fig. 5: Two-state site model

$\Delta(\Delta T_c)$ *vs.* ΔT_o curve, and ΔT_o is the initial supercooling before the silver iodide slide is exposed to bright light.

Consideration of Eqs. (1) and (3) shows that ΔT_i depends only on the steady state density of active sites which from Eq. (7) is

$$N_s = N_o \frac{A}{A+D}$$

while the slope depends on E, A, D, and t. The slopes, intercepts, standard deviations, and multiple correlation coefficients (r^2) for the data are given in *Table I*.

3. Discussion

The two-state theory as presented predicts a linear relationship between the change in supercooling and the initial supercooling as appears on the data graphs. Although the present data are not extensive enough, the possibility exists of obtaining numerical values for the constants involved from future

TABLE I

Regression analysis of data

Illumination	Substrate	ΔT intercept	σ_i	Slope	σ_s	r^2
UV	Drifilm	−2.10°C	0.2°C	0.39°C	0.05°C	66.5%
UV	Glass	−1.62°C	0.2°C	0.63°C	0.15°C	47.0%
Red	Glass	−2.68°C	0.06°C	−1.27°C	0.52°C	29.4%

experiments. Comparison of Eqs. (7) and (10) reveal that the intercept depends on N_0, A, and D, but not on the time or exposure; the slope depends on exposure, A, and D, but not on N_0 or N_s. Thus, when comparing the two UV tests where the substrate changed but the exposure and wavelength were the same, if we compare the slope it is evident that the change in substrate resulted in a change in A or D, since they are the only terms in the exponential that were not held constant. The change in the coefficients could be due to the change in internal electric field due to the change in boundary conditions or to a change in energy states at the AgI–slide interface.

For the case involving the UV and red light and the glass substrate, the structure and the interface did not change implying a constant N_0 Eq. (7) implies a clear wavelength dependence for the term involving the activation and deactivation coefficients due to the change in intercept. The change in slope is less useful for this case, as the exposures differed for the UV and the red light. However, in light of the fact that the exposures were determined to give approximately the same experimenteal effect, it is interesting to note that when corrected for the differences in absorptance of light for the different wavelengths, the effective exposures (irradiance $\times$ time $\times$ absorptance) are quite comparable being 2.4 J/cm^2 and 3.3 J/cm^2 for UV and red light, respectively.

What is actually happening when a site is activated or deactivated? Since photons can only interact with matter through the changing energy of charges, it seems clear that this must be the mechanism involved. The persistence of the effect after the illumination has been removed implies that the charge is trapped in long-lived states which may persist for extended periods of time – hours to months – depending on the ambient conditions. This change in charge distribution results in a change of the surface electrostatic field which in turn changes the free energy of interaction, U, which results in the change of nucleation characteristics. The redistribution of charge also results in changes in the optical constants of the silver iodide surface which have been measured by ellipsometry (*Layton*, 1977). The preceding theory also more fully explains our previous results regarding the effect of electric fields on ice nucleation by silver iodide (*Layton*, 1973a).

4. Significance for atmospheric nucleation

The preceding data and theory provide an increased insight into the nature of the interactions which affect nucleation. A specific application can be made regarding the effect of particle size on nucleation. The data and theory reported in this paper reinforce those presented in a previous report which demonstrated the existence of a size effect for thin films of silver iodide, predicted to occur due to change in the ratio of surface states to the total volume as film thickness (or particle radius) decreased (*Layton*, 1973b).

This size does not depend on the specific geometry of the particle, but does depend on the effect of trapped charge such as that demonstrated in silver iodide. Some organic nucleators interact through hydrogen bonding and should not exhibit this particular effect.

The present experiment also reminds us that there may be enchancement as well as degradation of the nucleation process through changes in the free energy of interaction. Most experimental and theoretical treatments have a built-in bias toward negative effects since it is common to consider how

a good nucleator behaves as the particle size decreases. The fact that a substance is a good nucleator indicates that the free energy of interaction is near optimum and any change in either direction will degrade its performance. If, however, the interaction energy is not optimum for good nucleation, then a good possibility exists that any changes in U which occur as the radius of the particle becomes smaller will result in a value which is closer to the optimum, hence resulting in a better nucleator. The work reported here combined with previous work on the size effect implies that it would be quite surprising if this did not happen in the atmosphere.

Acknowledgement. This research was supported partly under Grant GA – 19074 as a part of the research sponsored by the Weather Modification Program, National Science Foundation, and partly by the Natural Resources Institute of Northern Arizona University. The absorption spectra were obtained by Dr. *Ken O'Dell; G. D. Owens* assisted in obtaining the data. The author is indebted to Dr. *Don Gilbert* for his most helpful review of the manuscript.

REFERENCES

Bryant, G. W. and *Mason, B. J.*, 1960: Photolytic de-activation of silver iodide as an ice-forming nucleus. *Quart. J. Roy. Met. Soc. 86*, 354 – 357.

Cardona, M., 1963: Optical properties of the silver and cuprous halides. *Phys. Rev. 129*, 69 – 78.

Federer, R., 1968: Über den Eifluss der Oberflächeneigenschaften von Halbleitern auf ihre Eiskeimfähigkeit. *Z. Angew. Math. Phys. 19*, 637 – 655.

Fletscher, N. H., 1959: A descriptive theory of the photo de-activation of silver iodide as an ice-crystal nucleus. *J. Met. 16*, 249 – 255.

Garvey, D. M., 1973: Photolytic activation of the ice-nucleating properties of silver iodide hydrosols. *J. Atmos. Sci. 30*, 165 – 167.

Hallet, J. and *Shrivastava, S. K.*, 1972: Nucleation of supercooled water by large single crystals of silver iodide. *J. Rech. Atmos. 6*, 223 – 236.

Layton, R. G., 1973a: Ice nucleation by silver iodide: Influence of an electric field. *J. Coll. Interface Sci. 42*, 214 – 217.

Layton, R. G., 1973b: Ice nucleation by silver iodide: A new size effect. *J. Coll. Interface Sci. 45*, 215 – 216.

Layton, R. G., 1977: Ellipsometric study of light-induced changes in silver iodide thin films. *Society of Photo-Optical Instrumentation Engineers Seminar Proceedings 112*, 88 – 91.

Papée, H. M., Montefinale, A. C. and *Zawidzki, T. W.*, 1964: Ice nucleation and growth in supercooled water films condensed on a hydrophobic surface. *Nature 203*, 1343 – 1345.

Pruppacher, H. R. and *Pflaum, J. C.*, 1975: Some characteristics of ice-nucleation active sited derived from experiments with a ferroelectric substrate. *J. Coll. Interface Sci. 52*, 543 – 552.

Rowland, S. C., Layton, R. G. and *Smith, D. E.*, 1964: Photolytic activation of silver iodide in the nucleation of ice. *J. Atmos. Sci. 21*, 698 – 700.

IDŐJÁRÁS

Az Országos Meteorológiai Szolgálat folyóirata, 86. évf. 2–4. szám, 1982. március–augusztus
Journal of the Hungarian Meteorological Service, Vol. 86. No. 2–4. March–August 1982, Budapest

Investigation on the saturation spectra of ice nuclei

D. STEIN and H.-W. GEORGII, *Universitätsinstitut für Meteorologie und Geophysik, Feldbergstrasse 47, D—6000 Frankfurt/Main — 1*

Jégmagvak túltelítettségi spektrumának vizsgálata. A légköri jégmagvak hatékonysága nemcsak az aktivációs hőmérséklettől, hanem a folyékony víz-, illetve jégfelszínre vonatkoztatott telítettség mértékétől is függ. A szerzők különböző hőmérsékleteken a jégkoncentráció és a telítettség összefüggését tanulmányozták alacsony nyomási diffúziós kamrák segítségével. A berendezéssel ugyanazon szűrő különböző hőmérsékletekre vonatkozó telítettségi spektruma határozható meg. Több szűrővel azonos körülmények között végzett mérések összehasonlítása szerint az eljárás reprodukálhatósága elfogadható. A mérésekhez az aeroszol-mintákat a svájci Alpokban, illetve Frankfurt am Main közelében gyűjtötték. Az eredmények azt mutatják, hogy a jégre vonatkoztatott túltelítettségi spektrumok, illetve a hőmérsékleti spektrumok dőlésének aránya állandó.

*

Investigation on the saturation spectra of ice nuclei. The activity of atmospheric ice nuclei is dependent not only on the activation temperature, but also on the environmen-saturation ratios over water and ice. The relation between the ice-nuclei contal centration and the saturation at different temperatures was investigated with a low-pressure diffusion chamber. With this instrument it is possible to measure the saturation spectra at different temperatures on the same filter. A comparison of the saturation spectra obtained with parallel filters showed good reproducibility. Aerosol samples taken in the Swiss Alps and in the environment of Frankfurt/Main were analysed. A constant ratio was found between the slopes of the ice supersaturation spectra and the respective slopes of the temperature spectra.

*

Introduction. Previous measurements of ice nuclei contentrations performed at a temperature of −18°C and water saturation gave a concentration range from 0.01 ice nuclei/L to 10 ice nuclei/L (*Georgii* and *Stein*, 1981).

Measurements of ice nuclei saturation spectra, made by *Gagin* (1972), *Huffman* (1973) and during the Third Internat. Workshop on Ice Nucleus Measurements 1975, (*Vali*, 1976), yielded a saturation dependency of the ice nuclei concentration at a constant activation temperature, which had a maximum range of three orders of magnitude.

This wide range shows the importance to investigate not only the temperature spectra of ice nuclei but also the saturation spectra.

The aim of our present work was the measurement of the activation of atmospheric ice-nuclei dependence of supersaturation and temperature.

A necessary condition for these measurements is the very accurate control of activation temperature and vapour pressure. The filter method offers good conditions to carry out such measurements, because the filters sampled at different sampling sites can be developed under controlled and comparable

conditions in a laboratory. The disadvantage of this method, the well known volume effect, was reduced so far that a detection in the range of the sampled volumes was not possible when a low-pressure diffusion chamber was used. This type of chamber, first designed at our Institute and presented at the Third Internat. Workshop on Ice Nucleus Measurements in 1975 (*Meyer* and *Gravenhorst*, 1976), shows no volume effect, because the diffusion velocity is enhanced in the low-pressure system.

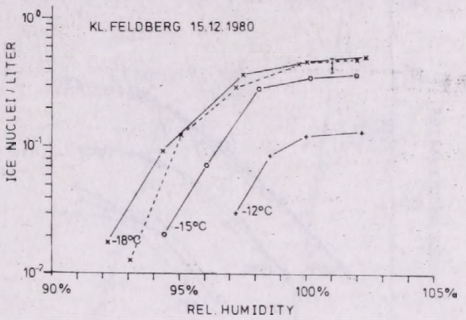

Fig. 1: Comparison of a set of four simultaneously sampled filters: Filters 1 and 2: activated at −18°C (dot); Filter 3: activated at −18°C and different humidities (dashed line); Filter 4: activated at −12°C, −15°C and −18°C and different humidities (solid line)

With the experience obtained by using this chamber, a new low-pressure diffusion chamber was built to attain the necessary reproducibility for these measurements by improving the closeness in the low-pressure system, the temperature control- and measuring system, and the preparation of the filters. (A description of this new chamber is being prepared for publication). This new chamber permits the measurement of saturation spectra of ice nuclei at different temperatures of activation with single exposed filter. A repetition of these measurements with the same filter shows no change in the activation behaviour of the ice nuclei.

Experimental results

An example of the results is shown in *Fig. 1*. In this case, the ice nuclei of the first and second filter of a set of four parallel exposed filters were activated five times at −18°C and 1% water supersaturation marked by two points. The variation of these measurements is shown by a vertical bar. The ice nuclei of the third filter, marked with dashed lines, were activated at −18°C at five different increasing humidities. The ice nuclei of the fourth filter, here marked with full lines, were activated also at five different increasing humidities, but also at three different temperatures, at −12°C, −15°C and −18°C.

To avoid a memory effect, the filter surface was heated up to +15°C at a remaining relative humidity < 1% for some minutes between the subsequent measurements of the single saturation spectra.

A comparison of the ice nuclei concentration at −18°C and 1% water supersaturation shows that there is no change in the activation behaviour when the activation is repeated at different humidities and temperatures.

Usually, two parallel exposed filters were developed to control the variations of such a set and to recognize possible errors of single measurements.

Figure 2 shows the saturation spectra at three different temperatures of two simultaneously exposed filters, plotted with dashed lines. The full lines between them correspond to the computed means of the single spectra of both filters. These means are used in the further treatment of our results.

Plotting the mean spectra of *Fig. 2* in relation to ice supersaturation,

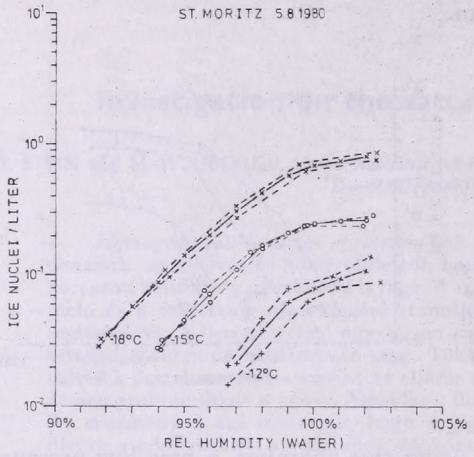

Fig. 2: Saturation spectra of two simultaneously sampled filters at −12°C, −15°C and −18°C (dashed line) and the mean spectra of both filters (solid line)

the three spectra taken at −12°C, −15°C and −18°C lie on one line. Only the values measured at water supersaturation deviate from this line. The deviation can clearly be seen in a double logarithmic diagram *(Fig. 3)*. In this figure the water saturation for each temperature is marked by two vertical bars.

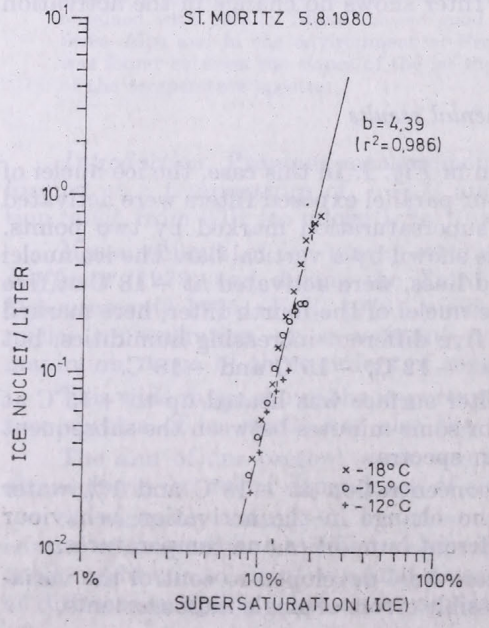

Fig. 3: Ice supersaturation spectrum at −12°C, −15°C and −18°C with the computed slope *b*

In many cases there was no further increase in the ice-nuclei concentration after exceeding water saturation; in other cases there was a smaller increase when water saturation was exceeded. Measurements made up to now did not reveal a clear relationship to a specific parameter of the constitution of the aerosols, the environmental conditions, or the sampled volume.

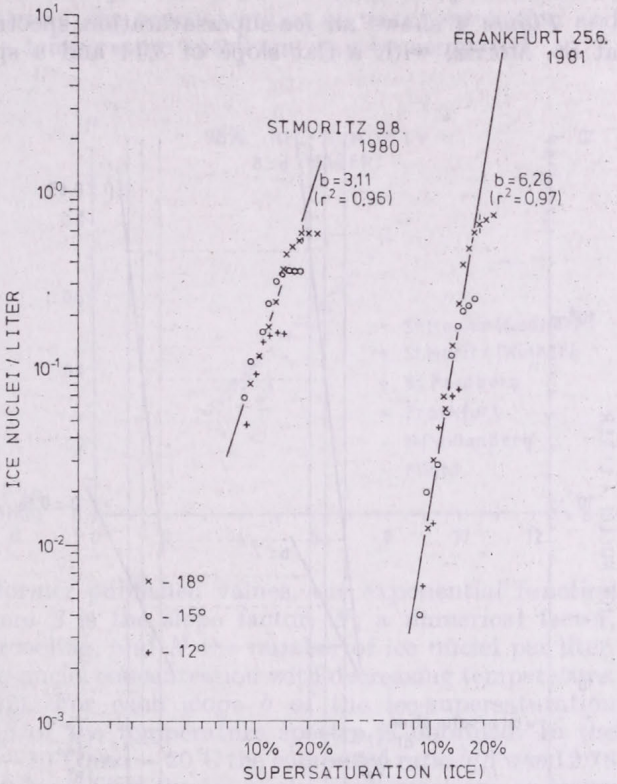

Fig. 4: A typical ice supersaturation spectrum of St. Moritz (Switzerland) and of Frankfurt/Main (FRG)

In the evaluation of our measurements we did not regard results gained at supersaturations above water saturation.

As shown by *Huffman* (1973) it is possible to describe the increase of the ice-nuclei concentration at increasing ice supersaturation by the function $N = C \cdot S_i^b$, where S_i is the supersaturation over ice, C is a constant, b the slope factor and N the number of ice nuclei per liter. To compute the slope b, the three spectra measured at different temperatures were combined into one ice supersaturation spectrum. The straight line in Fig. 3 corresponds to the computed ice supersaturation spectrum of the three plotted single spectra. The good correlation shown in this example is generally existent, the mean r^2 of all ice supersaturation spectra measured up to now yield 0.93. The results of the slopes measured at different sampling sites varied between 3.1 and 12.5.

Samples from St.Moritz, Switzerland, had a mean slope of 4.3; samples from Mt. Kleiner Feldberg near Frankfurt, F. R.Germany, had a mean slope of 6.0 and in Frankfurt the mean slope was 6.8. These results point to an increase of the slope from unpolluted to polluted regions.

The first filters exposed airborne at an altitude of 4,000 ft above the souther part of the FRG gave a mean slope of 6.4 which was also found at a mountain station at 3,000 ft. The trajectories showed that the air masses during the flight period moved slowly within two days over North-Western Europe, and the simultaneously measured sulfate concentrations confirmed the polluted condition of these air masses. At higher altitudes, up to 18,000 ft, the mean slope was 4.9.

Figure 4 shows an ice supersaturation spectrum of a sample, collected at St. Moritz, with a flat slope of 3.11 and a spectrum of Frankfurt with

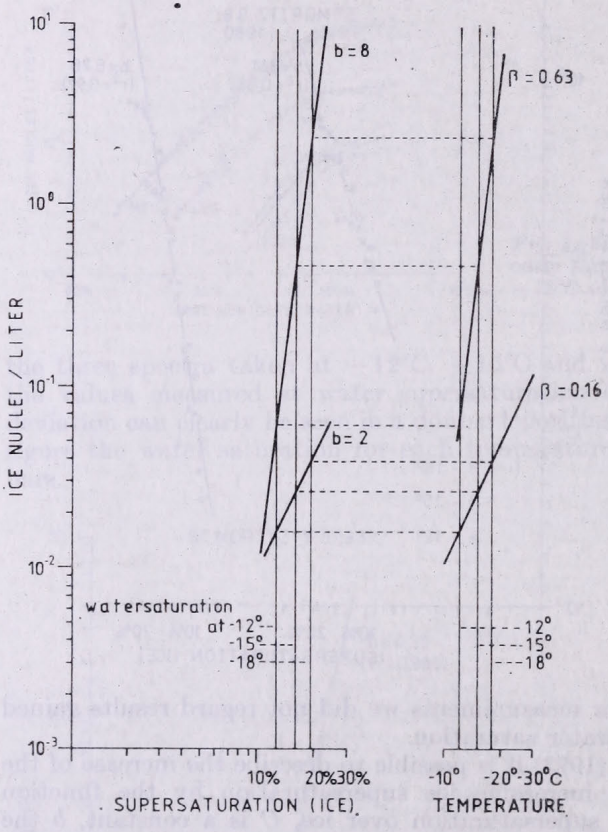

Fig. 5: Representation of the relation between two ice supersaturation spectra and two temperature spectra

a steep slope of 6.26, for comparison. While there is only a small difference in concentration at high ice supersaturations, the difference increases towards low supersaturations.

The mean concentration at -18 °C and water saturation measured in Frankfurt was 0.6 ice nuclei/L and in St. Moritz, Switzerland, 0.55 ice nuclei/L. The mean concentration at -12 °C and water saturation in Frankfurt was 0.04 ice nuclei/L and in St. Moritz 0.1 ice nuclei/L. Taking -18 °C as reference, the concentration was too high in St. Moritz and too low in Frankfurt at high temperatures respectively at low ice supersaturations.

Parallel measurements of the aerosol spectra have shown that neither

the concentration nor the size distribution has a major influence on the ice-nuclei saturation spectra. The chemical composition and surface of the aerosol seems to be decisive.

The relation between supersaturation and temperature spectra

Taking, as demonstrated in *Fig. 5* for the extreme slopes $b=2$ and 8 of an ice supersaturation spectrum, the concentrations at water saturation and at different temperatures, a temperature spectrum may be computed.

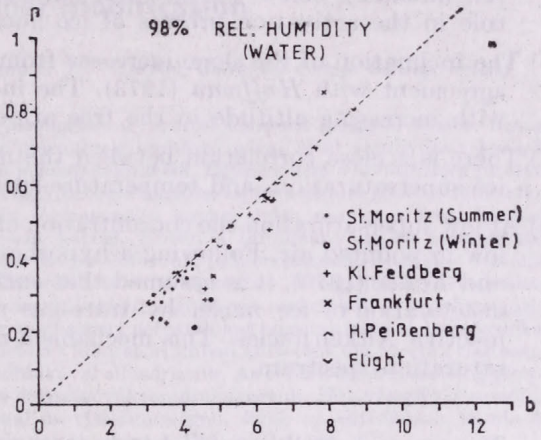

Fig. 6: Computed ratio of slope b to β at 98% rel. humidity (dashed line) and the measured slopes b and β

For comparison with former published values, the exponential function $N=N_0 \cdot \exp[\beta(T_0-T)]$, where β is the slope factor, N_0 a numerical factor, (T_0-T) the degree of supercooling, and N the number of ice nuclei per liter, is fitted to the increase of ice-nuclei concentration with decreasing temperature, according to *Fletcher* (1962). For each slope b of the ice-supersaturation spectra a respective slope β of the temperature spectra is obtained. In the investigated range between -10°C and -20°C the computed ratio b/β was 12.78 for all slopes b from 1 to 10 by taking the ice-nuclei concentrations at water saturation for each temperature. Taking the ice-nuclei concentration at 98% rel. humidity, the quotient was 10.92. The ratio of both slopes of the ice-nuclei concentration at 98% is plotted as a dashed line in *Fig. 6*.

The symbols in Fig. 6 correspond to the measured slopes b of the ice supersaturation spectra and the respective measured slopes β of the temperature spectra of different sampling sites.

Conclusions

(1) The results of the investigations show that the low-pressure diffusion chamber permits to measure saturation spectra of ice nuclei with the same filter at different temperatures. The results are reproducible.

(2) The relation between humidity and the activity of ice nuclei leads to an increase of the ice-nuclei concentration according to a power-law. This increase is independent of the temperature as long as water saturation is not exceeded.

(3) The slope of the ice supersaturation spectra becomes smaller at water supersaturation, independently of the actual concentration of nuclei on the filter. This is in confirmation of the results obtained by *Tanaka* (1980).

(4) The change of the slope at water saturation shows that the computed water saturation is in agreement with the actual water saturation on the filter surface.

(5) The concentrations of activated ice nuclei on the filter at different water subsaturations but at equal ice supersaturations coincide. Therefore the rel. humidity below 100% water saturation does not play a dominant role in the activation process of ice nuclei.

(6) The inclination of the slope increases from unpolluted to polluted areas in agreement with *Huffman* (1973). The inclination of the slope decreases with increasing altitude in the free atmosphere.

(7) There is a close correlation between the measured and computed ratio of ice supersaturation- and temperature-spectra only in unpolluted air.

(8) At low supersaturation the concentration of activated ice nuclei is relatively low in polluted air. Following a hypotheses by *Georgii* (1963) and *Georgii* and *Kaller* (1970), it is assumed that surface poisoning leads to a partial deactivation of ice nuclei by trace-gas adsorption or coagulation with inactive Aitken nuclei. This mechanism may also influence the ice supersaturation spectrum.

*

The research in this paper has been supported by Deutsche Forschungsgemeinschaft through Sonderforschungsbereich 73 "Atmospheric Trace Constituents".

REFERENCES

Fletcher, N. H., 1962: *Physics of rain clouds.* Cambridge University Press, London.

Gagin, A., 1972: The effect of supersaturation on the ice crystal production by natural aerosols. *J. Rech. Atmos. 6*, 175–185.

Georgii, H.-W., 1963: Investigation on the deactivation of inorganic and organic freezing nuclei. *Z. Angew. Math. Physik 14*, 503–510.

Georgii, H.-W. and *Kaller, R. S.*, 1970: Über die Inaktivierung von Gefrierkernen durch die Koagulation mit Aitkenkernen. *Berichte des Instituts für Meteorologie und Geophysik*, Universität Frankfurt/Main Nr. 36.

Georgii, H.-W. and *Stein, D.*, 1981: Die Konzentrationsverteilung atmosphärischer Gefrierkerne in der unteren und mittleren Troposphäre. *Met. Rdsch. 34*, 137–143.

Huffman, P., 1973: Supersaturation dependence of ice nucleation by deposition on silver iodide and natural aerosols. *Res. Rept. No. AR 108. Sept. 1973*, Dept. of Atmospheric Resources, University of Wyoming, Laramie, Wyoming.

Meyer, D. and *Gravenhorst, G.*, 1976: A low pressure diffusion chamber. *The Third International Workshop on Ice Nucleus Measurements.* aramie, Wyoming, 128–148.

Tanaka, T., 1980: Ice nucleating activity and the mode of action of volcanic ash ejected from Mt. Usu in Hokkaido. An improved method to remove hygroscopic materials collected on a membrane filter. *Papers in Meteorology and Geophysics 31*, 153–171.

Vali, G., (ed.) 1976: *The Third International Workshop on Ice Nucleus Measurements. Proceedings*, University of Wyoming, Laramie, Wyoming.

IDŐJÁRÁS

Az Országos Meteorológiai Szolgálat folyóirata, 86. évf. 2–4. szám, 1982, március–augusztus
Journal of the Hungarian Meteorological Service, Vol. 86, No. 2–4, March–August 1982, Budapest

Lead-bearing exhaust aerosol and inadvertent weather modification

B. D. O'REGAN*, A. F. RODDY and C. M. MORAN, *University College Galway, Ireland*

Kipufogó gázokból származó, ólomtartalmú aeroszol időjárást módosító hatása. Számos kutató tapasztalta, hogy ha a gépjárművek kipufogó gázai által szennyezett levegőbe jódgőzt juttatnak, igen nagyszámú jégmag keletkezik. Egyesek arra a konklúzióra jutottak, hogy a kipufogó gázban lévő ólomvegyületek reakcióba lépve a jóddal ólom-jodidot alkotnak, ami tudvalevőleg igen aktív jégmagvasító anyag. Jelen munka a fenti kérdéssel foglalkozó átfogó kutatás egy részét képezi. Ebben a tanulmányban az ólomtartalmú részecskék kémiai természetét, valamint az előforduló jódkoncentráció-értékeket tekintjük át. Tanulmányozzuk a PbI_2 képződési feltételeit a légkörben. Vizsgáljuk a jódvegyületek és a részecske formájú ólom közt, vízcseppekben végbemenő reakciókat. A kipufogó gázokban található ólomvegyületekből monodiszperz aeroszolokat hoztunk létre. A kereskedelemben be nem szerezhető ólomvegyületeket laboratóriumban állítottuk elő, melyek tisztaságát és szerkezetét röntgendiffrakció technikával ellenőriztük. Az előállított aeroszolok jégképző aktivitását termál diffúziós kamra segítségével tanulmányoztuk. Hat vizsgált aeroszolnak volt jégképző aktivitása −20°C-nál és víztelítettségen. Ezek az aktivitások közelítőleg egy nagyságrenddel alacsonyabbak voltak, mint a PbI_2 aktivitása.

*

Lead-bearing exhaust aerosol and inadvertent weather modification. Several researchers have found that the addition of iodine vapour to air polluted by vehicular exhaust led to the production of large numbers of ice nuclei. Some have concluded that lead compounds in the exhaust reacted with iodine to form lead iodide, a well-known ice nucleant. This work is part of a comprehensive study of that phenomenon. The composition and chemistry of lead-bearing particles in the atmosphere is reviewed, in this context. There is also a brief review of iodine levels in the atmosphere. The possibility of the production of PbI_2 in the atmosphere is discussed in some detail. Among processes considered are reactions of iodine compounds with particulate lead in a water droplet environment. Monodisperse aerosols of lead compounds reported in motor vehicle exhaust were prepared. Lead compounds not available commercially were synthesised in the laboratory and examined with regard to purity and structure using X-ray diffraction techniques. The ice nucleation activities of some of these aerosols were investigated using a thermal diffusion chamber. Six aerosols tested had ice nucleation activities at −20°C and nominal water saturation, which were about an order of magnitude less than for PbI_2.

*

Introduction. The work reported in this paper is the first effort in a major investigation of a phenomenon originally discovered by *Schaefer* (1966, 1968). He found that the introduction of iodine vapour into air polluted by vehicular exhaust lead, produced vast numbers of ice nuclei. He inferred that the lead compounds reacted with iodine to form lead iodide (PbI_2) a well-known ice nucleant.

* Present affiliation: Regional Technical College, Carlow, Ireland

The composition of lead-bearing particles

It is worth examining briefly the reports in the literature on the chemistry of lead-bearing exhaust particles in the atmosphere.

Commercial anti-knock fluids contain alkyl lead compounds (formerly tetraethyl lead but more recently also tetramethyl lead). During combustion the Pb additives form halide particulates by combining with ethylene dihalides (bromides and chlorides) which are added to the petrol as lead "scavengers". According to *Hirschler* et al. (1957) the chief constituents of inorganic lead compounds leaving the exhaust system are PbClBr, $NH_4Cl.2PbClBr$ and $2NH_4Cl.PbClBr$. *Habibi* (1970) found PbClBr, 2PbO.PbClBr and small amounts of $PbSO_4$ and $Pb_3(PO_4)_2$ in fresh exhaust particles larger than 200 μm. In the $2-10$ μm range the principal component was PbClBr, while the submicron particles contain PbClBr and $2NH_4Cl.PbClBr$. *Ter Haar* and *Bayard* (1971) reported other populous lead-containing species as $(PbO)_2PbClBr$, $PbCl_2$ and $PbBr_2$ in fresh exhaust; and $PbCO_3$, $(PbO)_2PbCO_3$ and lead oxides PbO_x in aged or rural samples. *Biggins* and *Harrison* (1979), using powder X-ray diffraction techniques found the predominant lead compound at four out of five sites to be $PbSO_4.(NH_4)_2SO_4$. At only one site did they find $2PbBrCl.NH_4Cl$ and $PbBrCl.2NH_4Cl$. $PbSO_4$ and $PbBrCl.(NH_4)_2BrCl$ were also observed. In laboratory experiments the very small vehicle generated PbClBr particles coagulated rapidly with neutral and acid sulphate droplets in the atmosphere to form $PbSO_4(NH_4)_2SO_4$, $PbSO_4$, $PbBrCl.(NH_4)_2BrCl$ and other unidentified lead ammonium halides. According to *Harrison* and *Perry* (1977) approximately $1-4\%$ of atmospheric lead is present as vapour phase tetraalkyl compounds. This arises from evaporation of the antiknock additives in petrol in the vicinity of petrol stations and incomplete combustion within engines. Some of the organolead compounds may be sorbed onto atmospheric particles; generally their fate is little understood.

Lead concentrations and particle sizes

Atmospheric lead levels vary enormously in space and time. Thus to take the more extreme values, *Dams* and *De Jonge* (1976) found mean Pb concentration at the Jungfraujoch (3,752 m altitude) in Switzerland to be 4.4 ng m^{-3} whereas levels of $400-3{,}700$ ng m^{-3} were found for Cambridge, Mass., U.S.A. by *Moyers* et al. (1972).

Chamberlain et al. (1978) have shown that primary vehicle exhaust lead particulate is approximately 0.015 μm in diameter, but grows rapidly by coagulation, especially in an urban environment. In a rural area in Urbana-Champaign, Illinois, *Hudson* et al. (1975) found that 80% of the particles were less than 2 μm with a mean median value of 0.42 μm.

Iodine in the atmosphere

Moyers et al. (1971) give an average value of 8 ± 3.5 ng m^{-3} for gaseous iodine I(g) in an unpolluted marine atmosphere. *Moyers* and *Duce* (1972) have discussed the enrichment of I relative to Cl in sea-salt particles and rain samples in maritime air, by factors of 10^2-10^3 as compared with sea-water. Two possible explanations are that (1) I_2 gas escapes from the sea surface or (2) organic matter on the sea surface is enriched in iodine. *Garland* and *Curtis*

(1981) have found evidence that ozone causes the release of iodine vapour from the sea surface. *Moyers* and *Duce* found mean values of I(g) and particulate iodine I(p) at a Hawaii site to be respectively 5.84 ng m^{-3} and 2.33 ng m^{-3}. They calculated that $I_2(g)$ should be taken up by sea-salt particles, provided IO_3^- is formed,

$$I_2(aq.) + H_2O + \frac{5}{2}O_2 \rightleftharpoons 2IO_3^-(aq.) + 2H^+$$

However, there is also an argument that says that $I_2(g)$ is volatilized from the particles.

The gaseous iodine species in the atmosphere may be I_2, HI, CH_3I, C_2H_5I.

Moyers et al. (1971) give values of 10 -- 18 ng m^{-3} for I(g) and 2 – 15 ng m^{-3} for I(p) in polluted urban air.

The possible production of PbI_2 *in the atmosphere*

Morgan (1967) and *Hogan* (1967), in addition to *Schaefer* (1966, 1968) concluded that the ice nucleation they observed was produced by lead iodide, formed as a result of reaction between particulate exhaust lead and iodine in the atmosphere.

Grant and *Corrin* (1973) calculated that the conversion of PbBrCl to PbI_2 is thermodynamically unfavourable. They also found that the addition of iodine to exhaust products from unleaded gasoline produced more ice nuclei than when leaded gasoline was used, thus casting doubt on PbI_2 as the "exhaust nucleant".

Langer (1970) found some evidence, though not conlusive, that lead oxide produced by the photolytic decomposition of $PbBr_2$ could be the nucleant.

Much attention has been given to the question of halogen loss as the exhaust particles age (*Pierrard* 1969, *Martens* et al. 1973, and many others).

Parungo and *Rhea* (1970) found large increases in the ice nuclei content of Denver air when passed through an iodine chamber. The I_2 concentration used was not stated, but since a saturated I_2 solution was used, there probably was a large excess of I_2 over Pb^{2+}.

Moyers et al. (1971) conclude that the levels of I(g) and I(p) they found in polluted air, 10 – 18 ng m^{-3} and 2 – 15 ng m^{-3}, respectively, should be sufficient to activate all the lead aerosol particles there. But this is doubtful, because it is hardly likely that exhaust particles are all in a reactive form.

Also, *Moyers* et al. (1971) state that the reaction of Pb and I_2 to form PbI_2 as performed by *Schaefer*, under laboratory conditions, had reactant concentrations much in excess of even a polluted atmosphere. Therefore from reaction kinetics alone, the time required to form measurable numbers of "latent ice nuclei" under 'normal' conditions of atmospheric pollution would be long. This is a possible reason why the clouds of ice crystals observed by Schaefer and attributed to PbI_2 nucleation appear downwind of polluted cities and not immediately overhead.

Borys and *Duce* (1979) found a weak positive correlation between lead and ice nuclei in a study over a one-year period in Providence, Rhode Island. However, this may have been due to lead and ice nuclei both being involved with the fine sub-micron particle mode. The main conclusion drawn from the study was that the greatest effect on the ice nuclei concentrations in Providence

was due to the difference in the ice nuclei concentrations existing in the contrasting air masses of continental and marine origin which are advected to the site. The sampling site was located essentially at the point where marine air masses encounter pollution sources. If the gaseous iodine existed largely as CH_3I, then its photodissociation in the atmosphere providing a more reactive source of iodine such as I_2, could, according to *Borys* and *Duce*, lead to the reaction necessary to produce PbI_2 occurring further downwind of the sampling site.

Drop freezing experiments

Reischel (1975) investigated the possibility that interaction between lead aerosols and iodine may not occur until both have become incorporated into liquid water. In drop freezing experiments he found that the presence of NH_4I caused about two orders of magnitude increase in numbers of active nuclei with six lead salts: PbO_2, PbO, $PbCrO_4$, PbS, $[Pb(CO_3)_2Pb(OH)_2]$ and $PbSO_4$. Additional experiments with PbO and NH_4I showed that best results were obtained when the $[NH_4^+]/[I^-]$ ratio was at least 0.5. Such a ratio is certainly present in natural precipitation (*Junge*, 1963; *Winchester* and *Duce*, 1966). The chemical nature of the apparently highly active reaction produce of PbO and NH_4I was not known. This combination (at 0.1 NH_4I) showed better ice nucleation activity than PbI_2 itself.

Reactions of $PbCl_2$, $PbBr_2$ *and* PbClBr *in droplets*

I_2, Br_2, Cl_2 are all thermodynamically able to oxidize SO_2 to SO_3, while being converted to I^-, Br^-, Cl^- themselves. These anions may remain associated with newly formed $SO_4^=$ particles. The association of $SO_4^=$ with NH_4^+ is documented in the literature so that if the halogen anions "live" in the same chemical environment as $SO_4^=$ ions, then species such as $NH_4^+Cl^-$ and NH_4I are possible (see *Winchester* and *Duce*, 1966).

Following the work of *Reischel*, some experiments were performed to investigate the reactivity of the above lead salts:

Mixing a solution of $PbCl_2$ and a solution of NH_4I resulted in an instant yellow precipitation. The reaction is

$$PbCl_2 + 2NH_4I \rightarrow PbI_2 + 2NH_4Cl$$

Similar reactions occurred for PbBr- and PbClBr,

$$PbBr_2 + 2NH_4I \rightarrow \text{yellow precipitation}$$

$$PbClBr + 2NH_4I \rightarrow \text{yellow precipitation}$$

When $PbCl_2$, $PbBr_2$ and PbClBr were reacted with 2KI, a yellow precipitate also resulted. In the case of $PbCl_2$ this reaction product was isolated and shown by X-ray diffraction to be mainly PbI_2 with a small quantity of an unidentified compound (not $PbCl_2$ or KI but possibly $KPbI_3$)

The displacement of Cl^-, Br^- ions by I^- in the above reactions is to be expected for solubility reasons and also because K^+ ions have a much larger electrode

potential than Pb^{2+} ions. However, when very dilute solutions of $PbSO_4$ and either KI or NH_4I are mixed, the appearance of yellow PbI_2 is not recorded. This again is expected for solubility reasons. A similar situation exists for $PbCO_3$. The following would appear to be the order of precipitation of lead salts out of dilute solutions of the constituent ions:

$$Pb(CO_3) \text{ before } Pb(IO_3)_2 \text{ before } Pb(SO_4) \text{ before } PbI_2.$$

Since urban atmospheres would contain higher concentrations of sulphate- than of any iodine-containing species, the chances of preferential PbI_2 formation – in solution – are small.

Laboratory preparation of inorganic lead salts

It was decided to investigate the ice-nucleating ability of aerosols of laboratory-prepared samples of lead compounds. Some of these are reported to be present in exhaust particles, before reaction with iodine and some may be present after reaction with iodine. Among these lead compounds a number were available commercially in Anala R grade; $PbCl_2$, $PbBr_2$, PbI_2, $PbSO_4$ and PbO. Other compounds were synthesized from these available starting materials.

The composition of the exhaust particle compounds depends on conditions such as the composition of the anti-knock mixture, the fuel – air ratio, the temperature of the surface on which it is formed, etc. The laboratory synthesis occurs under controlled conditions of temperature using measured quantities of the lead salts.

TABLE I

Compounds of lead prepared by thermal solid-state reactions

	Reactants	Product	Formation temperature (°C)
1	$PbCl_2 + PbBr_2$	2PbClBr	350
2	$2PbO + PbCl_2$	$2PbO.PbCl_2$	350
3	$2PbO + PbClBr$	2PbO.PbClBr	350
4	$2PbO + PbBr_2$	$2PbO.PbBr_2$	375
5	$PbO + PbClBr$	PbO.PbClBr	375
6	$PbO + PbCl_2$	$PbO.PbCl_2$	300
7	$PbO + PbBr_2$	$PbO.PbBr_2$	375
8	$PbO + PbI_2$	$PbO.PbI_2$	350
9	$NH_4Cl + 2PbClBr$	$NH_4Cl.2(PbClBr)$	300
10	$2NH_4Cl + PbClBr$	$2(NH_4Cl)PbClBr$	300
11	$(NH_4)_2SO_4 + PbSO_4$	$(NH_4)_2SO_4.PbSO_4$	180

Solid-state reactions. Several compounds as listed in *Table I* were prepared by solid-state reactions at appropriate temperatures, using equimolar quantities. The reaction temperatures have been determined by experiment and are well below the melting points of the lead salts (see *Lamb* and *Niebylski*,

1951 and *Calingaert* et al., 1949). Compounds 1 – 7 *(Table I)* were checked for identity and purity by X-ray diffraction. Products were stored in the dark.

Preparations in solution. A sample of $PbO.PbCl_2.H_2O$ was prepared using the basic method given by *Lamb* and *Niebylski* (1951). Preparation of $PbO.PbBr_2 \cdot H_2O$ and $PbO.PbI_2.H_2O$ were conducted along similar lines.

Solution chemistry was also used to prepare $PbI_2.NH_4Cl$, $3PbO.H_2O$, $2PbO.H_2O$, $PbO.H_2O = Pb(OH)_2$, and $PbCO_3$. Details of preparation are given elsewhere. (*O'Regan*, 1978).

Generation of lead compound aerosols

Aerosols of the compounds listed in *Table II* were prepared using a *Berglund – Liu* vibrating orifice monodisperse aerosol generator (Thermo-Systems Inc.), with distilled water as the solvent. A 10 μm orifice was used with a disturbing frequency of 225 kHz and a total air flow rate of 1,125 $cm^3\ s^{-1}$. The concentration of aerosol particles in the exit hose was nominally $2 \times 10^8\ m^{-3}$. The solvent evaporated in the dried dilution air and dry particles were available at the exit tube of the generator. *Table II* gives the diameters of the various particles as calculated from the expressions

$$D_p = C^{1/3} D_d$$

$$D_d = \left(\frac{60}{\pi f}\right)^{1/3}$$

given by *Berglund* and *Liu* (1973). D_d and D_d are particle and droplet diameters, respectively; Q is the liquid flow rate, f is the disturbance frequency and C is the volumetric concentration of the solute in solution.

TABLE II

Calculated diameters of lead compound aerosol particles

Compound	PbI_2	$PbBr_2$	$PbCl_2$	PbBrCl	PbO	$PbSO_4$	$2PbO.PbCl_2$
Particle diameter (μm)	0.94	1.9	1.7	1.8	0.16	0.38	0.23

The presence of non-volatile impurities in the solvent will cause an error in the calculated particle diameter. The distilled water used conformed to British Standard 3,978, which gives the limit for non-volatile residue as 5 mg $litre^{-1}$. For a lead iodide solution this corresponds to 1 part non-volatile impurity to 92.2 parts solute.

Measurement of ice nucleation activity of lead compound aerosols

Nuclepore filters of pore size 0.5 μm were used to sample the aerosol contained in three litres of air exiting in the flexible hose of the *Berglund – Liu* generator.

These filter samples were then processed in a *Meeda* ice diffusion chamber based on the design of *Gagin* and *Aroyo* (1969). The filter temperature was -20°C, the ice plate temperature -17.9°C, thus giving (nominal) water

saturation at the filter surface. Background counts were found for filter batches and subtracted to get results as recorded.

The results are given in *Table III*. The quantity $N/N_0 \times 10^4$ is taken as a measure of the ice nucleating activity of an aerosol, where N is the number of ice crystals measured per filter, and $N_0 = 6 \times 10^5 =$ nominal number of particles in the 3 litres of air sampled. $N/N_0 \times 10^4$ is a mean of at least four values, for each compound.

TABLE III

Ice nucleation activity of lead compound aerosols at −20°C and nominal water saturation

Lead compound	PbBrCl	$PbCl_2$	$PbBr_2$	PbO	$PbSO_4$	$2PbO.PbCl_2$	PbI_2
$N/N_0 \times 10^4$	5.0	2.7	4.5	2.5	4.5	2.4	31.0

These results indicate that aerosols of six compounds tested, all detected in exhaust lead-bearing aerosol, were about an order of magnitude less active than PbI_2 aerosol, under the test conditions.

These are the first results in a continuing comprehensive study in which the ice nucleation activity of lead compounds is being investigated prior to and after reaction (or attempted reaction) with iodine at realistic concentrations.

Acknowledgement. This work was funded by a grant from the National Science Council (now the National Board for Science and Technology, Ireland).

REFERENCES

Berglund, R. N. and *B. Y. H. Liu*, 1973: Generation of monodisperse aerosol standards. *Environ. Sci. Technol. 7*, 147–152.

Biggins, P. D. E. and *R. M. Harrison*, 1979: Atmospheric chemistry of automotive lead. *Environ. Sci. Technol. 13*, 558–565.

Borys, R. D. and *R. A. Duce*, 1979: Relationships among lead, iodine, trace metals and ice nuclei in a coastal urban atmosphere. *J. Appl. Meteor. 18*, 1490–1499.

Calingaert, G., F. W. Lamb and *F. Meyer*, 1949: *J. Am. Chem. Soc. 71*, 3709.

Chamberlain, A. C., M. J. Heard, P. Little, D. Newton, A. C. Wells and *R. D. Wiffen*, 1978: Investigations into lead from motor vehicles. *United Kingdom Atomic Energy Authority Report, AERE-R 9198*, H.M.S.O., London.

Dams, R. and *J. De Jonge*, 1976: Chemical composition of Swiss aerosols from the Jungfraujoch. *Atmospheric Environment 10*, 1079–1084.

Gagin, A. and *M. Aroyo*, 1969: A thermal diffusion chamber for the measurement of ice nuclei concentrations. *J. Rech. Atmos. 4*, 115–122.

Garland, J. A. and *H. Curtis*, 1981: Emission of iodine from the sea surface in the presence of ozone. *J. Geophys. Res. 86*, 3183–3186.

Grant, L. O. and *M. L. Corrin*, 1973: Raw and iodine treated automobile exhaust as a source of ice nuclei. *J. of Weather Modification 5*, 238–248.

Habibi, K., 1970: Characterization of particulate lead in vehicle exhaust—experimental techniques. *Environ. Sci. Technol. 4*, 239–248.

Harrison, R. M. and *R. Perry*, 1977: The analysis of tetraalkyl lead compounds and their significance as urban air pollutants. *Atmospheric Environment 11*, 847–852.

Hirschler, D. A., L. F. Gilbert, F. W. Lamb and *L. M. Niebylski*, 1957: Particulate lead compounds in automobile exhaust gas. *Industrial and Engineering Chemistry 49*, 1131–1142.

Hogan, A., 1967: Ice nuclei from direct reaction of iodine vapor with vapor from leaded gasoline. *Science 158*, 800.

Hudson, J. L., J. J. Stukel and *R. L. Solomon*, 1975: Measurement of the ambient lead concentration in the vicinity of Urbana-Champaign, Illinois. *Atmospheric Environment 9*, 1000–1006.

Junge, C. E., 1963: *Air chemistry and radioactivity*, Academic Press, New York and London.
Lamb, F. W. and *L. M. Niebylski*, 1951: Formation of engine-deposit compounds by solid-state reactions. *Analytical Chemistry 23*, 1388–1397.
Langer, G., 1970: A study of automobile exhaust as a source of ice nuclei. *Preprints of the Second National Conference on Weather Modification*, American Meteorological Society, 45 Beacon St., Boston, Mass. U.S.A., 242–243.
Martens, C. S., J. J. Wesolowski, R. Kaifer and *W. John*, 1973: Lead and bromine particle size distributions in the San Francisco Bay area. *Atmospheric Environment 7*, 905–914.
Morgan, G. M., Jr., 1967: Technique for detecting lead particles in air. *Nature 213*, 58–59.
Moyers, J. L., W. H. Zoller and *R. A. Duce*, 1971: Gaseous iodine measurements and their relationship to particulate lead in a polluted atmosphere. *J. Atmos. Sci. 28*, 95–98.
Moyers, J. L. and *R. A. Duce*, 1972: Gaseous and particulate iodine in the marine atmosphere. *J. Geophys. Res. 77*, 5229–5238.
Moyers, J. L., W. H. Zoller, R. A. Duce and *G. L. Hoffman*, 1972: Gaseous bromine and particulate lead, vanadium and bromine in a polluted atmosphere. *Environ. Sci. Technol. 6*, 68–71.
O'Regan, B., 1978: *Atmospheric Lead – A laboratory study of the related chemistry.* Unpublished internal report, Department of Physics, University College Galway, Ireland.
Parungo, F. P. and *J. O. Rhea*, 1970: Lead measurement in urban air as it relates to weather modification. *J. Appl. Meteor. 9*, 468–475.
Pierrard, J. M., 1969: Photochemical decomposition of lead halides from automobile exhaust. *Environ. Sci. Technol. 3*, 48–51.
Reischel, M. T., 1975: Ice nuclei from reactions involving lead, ammonia and iodine. *Atmospheric Environment 9*, 955–958.
Schaefer, V. J., 1966: Ice nuclei from automobile exhaust and iodine vapor. *Science 154*, 1555–1557.
Schaefer, V. J., 1968: Ice nuclei from auto exhaust and organic vapors. *J. Appl. Meteor. 7*, 148–149.
Ter Haar, G. L. and *M. A. Bayard*, 1971: Composition of airborne lead particles. *Nature 232*, 553–554.
Winchester, J. W. and *R. A. Duce*, 1966: Coherence of iodine and bromine in the atmosphere of Hawaii, northern Alaska, and Massachusetts. *Tellus 14*, 1–18.

IDŐJÁRÁS

Az Országos Meteorológiai Szolgálat folyóirata, 86. évf. 2–4. szám, 1982. március–augusztus
Journal of the Hungarian Meteorological Service, Vol. 86. No. 2–4. March–August 1982, Budapest

Nucleation inhibition of Ice Nuclei Active bacteria

G. CAPLE, G. LAYTON and G. SCALLY,* *Departments of Chemistry and Physics, Northern Arizona University, P.O.B. 5698 Flagstaff, Arizona 86011, U.S.A.*

Jégmag-aktív baktériumok nukleáló hatásának csökkentése Az elmúlt tíz évben számos kutató kimutatta, hogy bizonyos baktériumok viszonylag magas hőmérsékleteken (−2 és −5 °C között) megindíthatják a jégképződést. Ezek az ún. jégmag-aktív baktériumok fontos szerepet játszanak mind a növények fagykárainak kialakításában, mind a légköri jégképződésben. Olyan javaslatok is elhangzottak, hogy ilyen baktériumok időjárás-módosítási kísérletekben is felhasználhatók. Mindez azt bizonyítja, hogy a baktériumok jégnukleációs hatásának tanulmányozása igen fontos kérdés. A kísérletek azt is kimutatták, hogy a fagykároknak kitett növényekben vannak olyan természetes biogén anyagok, amelyek gátolják a jégképződést, beleértve az ezüst-jodid szolok aktivitását is. A szerzők kísérletei szerint ezek a természetes biogén inhibitorok kölcsönhatásba lépnek a *Pseudomonas syringae* és *Herbicola erwina* baktériumok jégképző helyeivel. Az inhibitorok hatékonysága eltűnik a baktérium kultúra növekedésével és a baktériumok ilyenkor visszanyerik jégképző hatékonyságukat. Ez arra mutat, hogy a baktériumok megemésztik a biogén inhibitorokat. Az is kiderült, hogy ezek a természetes fagyás-gátlók oldatokban vannak és fehérjék vagy fehérjeszerű anyagok. Adott inhibitor mind szervetlen, mind szerves részecskék esetén gátolja a fagyást, s ez a körülmény valószínűvé teszi, hogy mindkét esetben hasonló kölcsönhatás lép fel.

*

Nucleation inhibition of Ice Nuclei Active bacteria. Over the past decade several workers have shown that certain bacteria can induce ice nucleation at warm temperatures (−2 to −5°C). These Ice Nuclei Active (INA) bacteria have been shown to be responsible for freeze damage to food crops and may possibly play a significant role in atmospheric ice nucleation. Others have suggested the possibility of using these INA bacteria as weather modification agents; thus there are several reasons to understand the mode of action of bacterially-induced ice nucleation. Experiments have shown that there are natural biogenetic materials, found in many plants subject to freezing stress, which can inhibit ice nucleation, including a significant deactivation of silver iodide sols. We have been able to demonstrate that these naturally occurring biogenetic inhibitors will interfere with the ice nucleation sites produced by the INA bacteria *Pseudomonas syringae* and *Herbicola erwina*. The activity of these inhibitors rapidly dissipates in a growing bacterial culture, and the bacteria recover their ice nucleation abilities, suggesting that the bacteria metabolize the biogenetic inhibitor. Studies indicate that these biogenetic inhibitors are in solution and are denaturable proteins or protein-like compounds. A given inhibitor will inhibit both inorganic and organic ice nucleation sites, suggesting common interactions in both types of ice nucleation.

*

Since *Schnell* and *Vali* (1972, 1973) reported that at least a portion of atmospheric freezing nuclei was of biological origin, there has been an active interest in this area. The fact that bacteria were involved in ice nucleation

* The authors wish to acknowledge support from the Petroleum Research Fund and the NAU Organized Research Committee

processes has been shown by *Maki* et al. (1972); *Maki* and *Garvey* (1975); *Schnell* (1976); *Vali* et al. (1976) and *Maki* and *Willoughby*, (1978). These bacteria have been shown to be Ice Nuclei Active (INA) at temperatures as warm as −1 °C. *Maki* et al. (1974) identified INA bacteria as *Pseudomonas syringae*, a plant pathogen. *Lindow* et al. (1978) showed that frost injury in plants was caused by ice nucleation events initiated by two bacteria, *Pseudomonas syringae* and *Herbicola erwina*.

Levin et al. (1980) suggested that ice nucleating bacteria may have a potential use in weather modification. *Sands* et al. (1981) and *Jayaweera* and *Flanagan* (1981) in elegantly devised experiments were able to show that *Pseudomonas syringae* bacteria were found in the atmosphere and in rain drops. INA bacteria have a direct influence on frost damage in agricultural crops and may play a role in atmospheric processes.

Layton and *Caple* (1980) and *Layton* et al. (1980) have shown that certain biogenic materials can act as nucleation inhibitors on different INA sites. This inhibition was a non-colligative property, and most likely involved inhibition by absorption on the INA site. The current study reported here deals with our experiments using these biogenic inhibitors and the INA bacteria *Pseudomonas syringae* and *Herbicola erwina*. The INA sites on *Pseudomonas syringae* and *Herbicola erwina* are the most active ice nuclei sites known. Elucidation of the structure of these sites and the mechanism by which they cause ice nucleation should deepen our understanding of the physical process of initiating freezing in water.

Procedures and results[1]

Inhibition. The INA bacteria were grown in sterile solutions of Koser citrate (5.7 g/L) as described by *Maki* et al. (1974). The biogenic inhibitors were extracted from the seed materials of *Prunus persica* (peach) by crushing 2 g of seed material and extracting this with the sterile Koser citrate medium; after filtration the resulting solution was used. All dilutions of the active bacteria solutions were done with sterile Koser citrate medium, and all solutions used in the freezing tests were prepared such that the only difference was the biogenic material. Bacterial counts were effected using plating techniques. All freezing tests were performed using the drop freezing method as described by *Vali* (1971).

The results of our study on *Pseudomonas syringae* are shown in *Fig. 1.* These results were obtained with bacterial counts of 10^9 cells/ml and about 10^8 cells/ml after a 1 : 5 and a 1 : 30 dilution, followed by a 1 : 2 dilution with the biogenic inhibitor. The results shown are from freezing experiments performed about 20 min after mixing the biogenic material and the bacteria. Later freezing tests showed that the inhibitory effect was lost upon standing with only 10% of inhibition left in one hour.

The results of our study on *Herbicola erwina* were similar to the *Pseudomonas syringae* experiments with the following differences. The active bacterial culture had to be diluted 1 : 2,000, i.e. the cell count brought down to 10^6 cells/ml prior to the observation of any inhibition. Like with *P. syringae*, we observed less inhibition of the warm temperature sites (−4 °C to −5.5 °C)

[1] We wish to thank *R. C. Schnell* for cultures of the bacteria

than the colder sites (−6°C to −9°C). Also the inhibitor was slightly more efficient (−0.5°C) if the bacteria and biogenic inhibitor were precooled prior to mixing.

Nature of the inhibitor. A distilled water sample with a T_{50} of −8°C was treated with a distilled water extract of *Prunus persica*. (Temperature at which at least 50% of the drops have at least one active nucleus at that temperature or above.) The new T_{50} was now −10°C. This inhibited distilled water sample was heated to 80°C for 5 minutes. A white gelatinous precipitate formed, this was removed by millipore filtration (3.0 μm), dried and weighed. About 30 mg

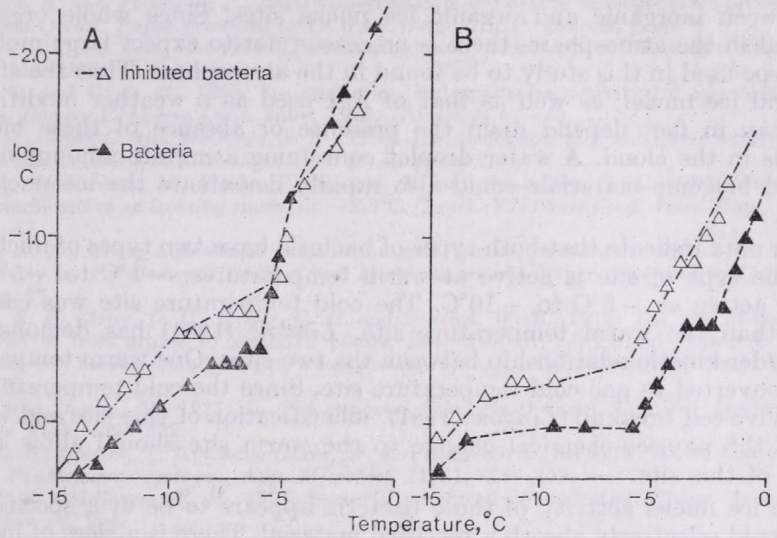

Fig. 1: The inhibition of the bacterial ice nucleation caused by *Pseudomonas syringae* using biogenic inhibitors. Graph A shows the inhibition of a cold temperature (below −5°C) site. Graph B shows the inhibition of two sites, a cold site and a warm (−1°C to −5°C) site at a reduced cell concentration. *C* is the cumulative concentration of ice nuclei active (INA) sites per cm³ at that temperature

of bioorganic material per ml solution was recovered. The freezing spectrum of the supernatant liquid was determined to have a T_{50} of −8°C. A distilled water sample (blank) of T_{50} −8°C was treated in the same manner with no biogenic material added. The T_{50} of this blank remained at −8°C. The biogenic material can be reversibly removed from an active nuclei site, and the site recovers its previous nucleation spectrum. This experiment places the biogenic inhibitor in a class of water-soluble denaturable proteins or glycoproteins. No attempts were made to differentiate between these denaturable proteins.

A growing culture of *Pseudomonas syringae* with a cell count of 10^8 cells per ml and a T_{50} of −12°C was diluted with three volumes of a galactose solution of 3 g/liter (0.0166 M) until the final galactose concentration was 0.0041 M (3 ml galactose and 1 ml bacterial culture). A blank was prepared by diluting 1 ml of the bacterial culture with 3 ml Koser citrate. The solutions were not aereated. Freezing tests on both samples were determined at various time intervals for three hours. During this time T_{50} for the galactose experiment changed to −5°C, for the blank T_{50} changed only to −11.5°C. The

addition of galactose increased the number of warm temperature events dramatically. In a similar test performed with cell counts of 10^{11} cells/ml, T_{50} of -3°C, the number of warm temperature events increased upon a similar galactose experiment, but little net effect was observed on T_{50}.

Discussion

The most obvious result of these experiments was that the biogenic inhibitor could in fact influence the ice nuclei active site on INA bacteria as well as on silver iodide (*Layton* and *Caple*, 1980), indicating certain similarities between inorganic and organic ice nuclei sites. Since whole organisms are found in the atmosphere, there is no reason not to expect large molecules of the type used in this study to be found in the atmosphere. Thus the efficacy of natural ice nuclei, as well as that of AgI used as a weather modification agent may in fact depend upon the presence or absence of these biogenic materials in the cloud. A water droplet containing a minute amount of such dissolved biogenic materials could also rapidly deactivate the ice nucleating particle.

Our data indicate that both types of bacteria have two types of nucleating sites. One type of site is active at warm temperatures, -1°C to -5°C, the other is active at -5°C to -10°C. The cold temperature site was easier to inhibit than the warm temperature site. *Lindow* (1981) has demonstrated a first-order kinetic relationship between the two sites. One warm temperature site is converted to one cold temperature site. Since the cold temperature site will survive cell breakup (*Lindow*, 1981), identification of this site and knowledge of the physico-chemical change to the warm site should allow identification of this site.

The ice nuclei activity of these bacteria appears to be at a specific site, which could selectively absorb a specified material. There is a class of biogenic materials which *Gold* and *Balding* (1975) called receptor-specific proteins, or in some cases lectins, which react with specific sites on cell surfaces. These materials cause specific reactions, most commonly agglutination of cells or clumping. However, other reactions of these materials have also been shown (*Kosloff* and *Lute*, 1979). In some cases the specific effect of these receptor-specific proteins can be reserved (the complex disassociated) by adding an excess of the sugar found in glycoproteins in the binding site (*Lis* and *Sharon*, 1977). Since galactose is one of the sugars commonly involved in cell receptor sites, the change in the ice nucleation activity caused by galactose indicates that galactose may be involved in the specific ice nuclei active site. Although *Pseudomonas syringae* has not been studied in relation to producing receptor-specific proteins, *Gilboa-Garber* (1972a, b) isolated a receptor-specific protein from *Pseudomonas aerugmosa*.

These preliminary results suggest the possibility that the INA bacteria could produce a receptor-specific protein which effectively caps the active sites, at least temporarily. However, other explanations are possible, such as direct metabolic incorporation of galactose into the active site. Receptor-specific proteins can be isolated, structurally identified and such identifications have been used to investigate receptor sites (*Gold* and *Balding*, 1975). These proteins are a sensitive analytical tool for investigating cell surfaces. *Schnell* and *Kosloff* (1981) have also shown a specific receptor protein that binds to

the active bacteria and inhibits the ice nucleation site. These biogenic receptor-specific materials may be the key to unlocking the secrets of the most active ice nuclei site known to science.

REFERENCES

Gilboa-Garber, N., 1972a: Inhibition of broad spectrum hemagglutin from *Pseudomonas aeruginosa* by *D*-galactose and its derivatives. *FEBS Letters 20*, 242.

Gilboa-Garber, N., 1972b: Purification and properties of hemagglutinin from *Pseudomonas aeruginosa* and its reaction with human blood cells. *Biochem. Biophys. 273*, 165.

Gold, E. R. and *Balding, P.*, 1975: *Receptor-specific proteins, plant and animal lectins.* Excerpta Medica, Amsterdam.

Jayaweera, K. and *Flanagan, P.*, 1981: Concentration and nature of biogenic ice nuclei over the Arctic Ocean. *Paper presented to IAMAP Conf., ICCP Abstract*, p. 35.

Kosloff, L. M. and *Lute, M.*, 1979: Lecitin stimulation of bacterio tail fiber attachment. *Virol. 97*, 218–220.

Layton, G. and *Caple, G.*, 1980: Ice nucleation and antifreeze activity by *Simonsida chenisis* link. *Comm. VIII-ème Conf. Inter. Phys. Nuages 1*, 41–43.

Layton, G., Caple, G. and *McCurdy, S. N.*, 1980: Ice nucleation and antifreeze activity due to biological materials. *J. Rech. Atmos. 16*, in press.

Levin, S., Sandlerman, N., Moshe, P., Bertold, T. and *Yankofsky, S. A.*, 1980: *Citrus* derived bacteria active as freezing nuclei at −2.5°C. *Comm. VIII-ème Conf. Inter. Phys. Nuages 1*, 45–47.

Lindow, S. E., 1981: Subcellular localization and partial characterization of ice nucleation activity by *Pseudomonas syringae* and *Herbicola erwina*. Paper presented to IAMAP Conf. Aug. 27.

Lindow, S. E., Arny, D. C., Upper, C. D. and *Barchet, W. R.*, 1978: The role of bacterial ice nuclei in frost injury to sensitive plants, 244–263. In: *Li, P.* and *Sakai, A.* (Editors), *Plant cold-hardiness and freezing stress mechanism and crop implications.* Acad. Press Inc., N. Y.

Lis, H. and *Sharon, N.*, 1977: In *The antigens, Sela, M.* (Editor), Vol. IV, Academic Press, New York, 429–529.

Maki, L. R., Galyan, E. L., Chang-Chein, M. and *Caldwell, D. R.*, 1974: Ice nucleation induced by *Pseudomonas syringae. App. Microbiol. 28(3)*, 456–459.

Maki, L. R. and *Garvey, F. M.*, 1975: Bacterially induced ice nucleation. *Trans. Amer. Geophys. Union, 56*, 994.

Maki, L. R. and *Willoughby, K. J.*, 1978: Bacteria as biogenic sources of freezing nuclei. *J. App. Meteor. 17*, 1049–1053.

Sands, D. C., Laughans, V. W., Scharen, A. L. and *DeSmet, G.*, 1981: The interaction between bacteria and rain and possible meteorological implications. *Paper presented to IAMAP Conf.*, ICCP. *Abstracts, 32.*

Schnell, R. C. and *Vali, G.*, 1972: Atmospheric ice nuclei from decomposing vegetation. *Nature 236*, 163–165.

Schnell, R. C. and *Vali, G.*, 1973: World-wide source of leaf derived freezing nuclei. *Nature 246*, 212–213.

Schnell, R. C., 1976: Bacteria acting as natural ice nucleants at temperatures approaching −1°C. *Bull. Amer. Meteor. Soc. 57*, 1356–1357.

Schnell, R. C. and *Kosloff, L. M.*, 1981: Private communication.

Vali, G., 1971: Quantitative evaluation of experimental results on heterogeneous freezing nucleation of supercooled liquids. *J. Atmos. Sci. 28*, 402–409.

Vali, G., Cristensen, M., Fresh, R. W., Galynn, E. E., Muki, L. R. and *Schnell, R. C.*, 1976: Biogenic ice nuclei: Part II. Bacterial Sources. *J. Atmos. Sci. 33*, 1565–1570.

IDŐJÁRÁS

Az Országos Meteorológiai Szolgálat folyóirata, 86. évf. 2—4. szám, 1982. március—augusztus
Journal of the Hungarian Meteorological Service, Vol. 86. No. 2—4. March—August 1982, Budapest

Heterogeneous nucleation of water vapour on ultrafine monodispersed Ag- and NaCl-particles

J. PORSTENDÖRFER and H. G. SCHEIBEL, *Isotopenlaboratorium der Georg-August-Universität, Burckhardtweg 2, D—3400 Göttingen, F. R. G.*

F. G. POHL, O. PREINING, G. REISCHL and P. E. WAGNER, *Institut für Experimentalphysik der Universität Wien, Strudlhofgasse 4, A—1090 Wien, Austria*

A vízgőz heterogén nukleációja ultrafinom monodiszperz ezüst- és nátrium-klorid részecskéken. A szerzők a vízgőz Ag- és NaCl-részecskéken végbemenő heterogén nukleációját tanulmányozták nagyság-analizáló számláló segítségével. A részecskék nagysága 6, 8, 12 és 18 nm volt. A mérések szerint a heterogén nukleációhoz szükséges telítési arány a részecskenagyság és az arány függvénye. A tanulmány végén a szerzők eredményeiket a makroszkópikus heterogén nukleáció elméletével vetik össze.

*

Heterogeneous nucleation of water vapour on ultrafine monodispersed Ag- and NaCl-particles. The heterogeneous nucleation of water vapour on monodispersed Ag- and NaCl-aerosols was measured by means of a size-analyzing nuclei counter with particle sizes of 6, 8, 12 and 18 nm. The measured saturation ratios necessary for heterogeneous nucleation depend on the particle size and the material. The results were compared with the macroscopic theory of heterogeneous nucleation.

*

During a workshop, performed at the University of Vienna, November 1980, we investigated the heterogeneous nucleation of water vapour on aerosol particles with diameters ranging from 6 to 18 nm. *Fig. 1* is a diagram of the experimental arrangement. The aerosol generation equipment (*Scheibel* and *Porstendörfer*, in preparation) consists of a condensation aerosol generator in connection with an electrostatic aerosol classifier (EAC) (*Knutson*, 1975). Ag-wool and NaCl-salt were vaporized in a tube of inner diameter of 12 mm heated by a constant-temperature tube furnace with a nitrogen carrier gas flowrate of 2 l/min. Homogeneous nucleation and condensation of the Ag- and NaCl-vapor within a linear decreasing temperature gradient behind the furnace generates highly dispersed aerosols. The condensation aerosols have concentrations of more than 10^7 particles/cm^3 and a polydisperse size distribution with a geometric standard deviation σ_g of about 1.5. For the generation of Ag-particles Ag-wool was vaporized at 1,110 °C, for NaCl-particles the furnace temperature was 695 °C. The generated condensation aerosol was subsequently brought into charge equilibrium in a Kr-85 bipolar ion source (neutralizer). A monodisperse unipolar singly charged aerosol fraction was then obtained by means of an electrostatic aerosol classifier (EAC). The number concentrations were measured by means of an aerosol filter electrometer (AE).

The size of the monodisperse Ag- and NaCl-aerosol was checked in previous experiments by means of transmission electron microscopy (TEM) and diffusion batteries, and agreement of calculated size and experiment was

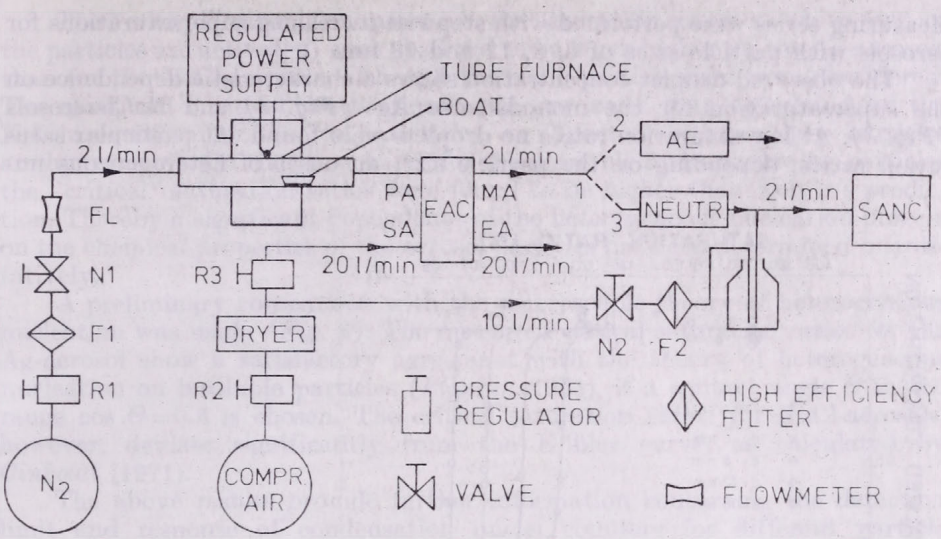

Fig. 1: Experimental arrangement

found. The size distributions of the classified Ag-aerosols, obtained by means of TEM, confirm that the aerosol is monodisperse with a geometrical standard deviation of $\sigma_g \approx 1.1$.

After passing through a second Kr-85 neutralizer (NEUTR., Fig. 1), the monodisperse aerosol entered the process-controlled size-analyzing nuclei counter SANC (*Preining* et al., 1981). In a humidifier the aerosol was vapour-saturated close to 100% relative humidity and supersaturation was then obtained in an expansion cloud chamber with an expansion time of about 5 – 7 ms. Saturation ratios between 102 and 350% were chosen with a reproducibility better than 0.1% in the range below 110%. The growing droplets in the expansion chamber were illuminated by a laser beam and the scattered intensity was monitored under particular forward scattering angles. By comparison with Mie-theory the droplet concentration was determined quantitatively.

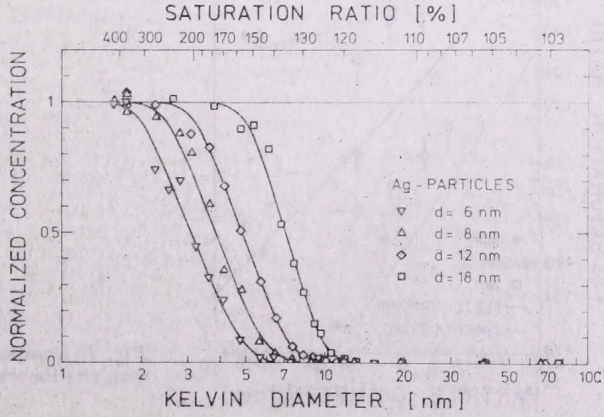

Fig. 2: Droplet concentration of increasing saturation ratios, Ag-aerosol

Measuring series were performed with stepwise increasing supersaturations for aerosols with particle sizes of 6, 8, 12 and 18 nm.

The observed droplet concentration shows a characteristic dependence on the supersaturation for the monodisperse Ag- *(Fig. 2)* and NaCl-aerosols *(Fig. 3)*. At low saturation ratios no droplets were found. At particular saturation ratios, depending on the particle size, an onset of heterogeneous nu-

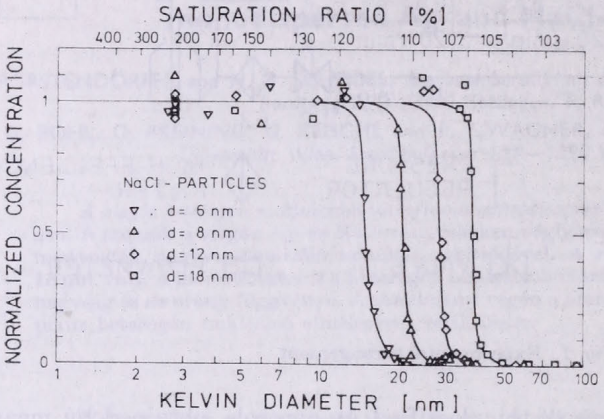

Fig. 3: Droplet concentration for increasing saturation ratios, NaCl-aerosol

cleation was observed. With further increasing saturation ratio the droplet concentration increases until a maximum is reached when all particles are activated as condensation nuclei and become droplets. The onset of heterogeneous nucleation was found to be much steeper for the NaCl-particles than for the Ag-particles.

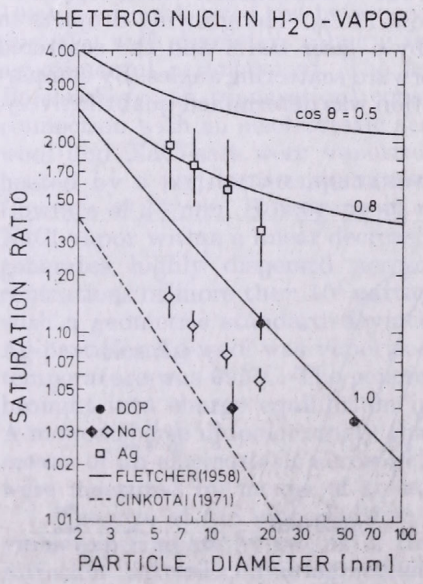

Fig. 4: Comparison of the experimental results with the macroscopic heterogeneous nucleation theory

The "critical" saturation ratios (i.e. the saturation ratios, at which 50% of the particles are activated) were observed to be much higher for the Ag-aerosols than for the NaCl-aerosols, although the same particle sizes were considered. The measured "critical" saturation ratios are lower than calculated by the Kelvin equation for the NaCl-particles, as expected, because these particles are hygroscopic. On the other hand, for the insoluble hydrophobic Ag-particles the "critical" saturation ratios were found to be higher than Kelvin's prediction. Thereby a significant dependence of the heterogeneous nucleation process on the chemical properties of the aerosol particles has been determined quantitatively.

A preliminary comparison with the macroscopic theory of heterogeneous nucleation was made *(Fig. 4)*. The measured critical saturation ratios for the Ag-aerosol show a satisfactory agreement with the theory of heterogeneous nucleation on insoluble particles (*Fletcher*, 1958), if a contact angle Θ in the range $\cos \Theta = 0.8$ is chosen. The critical saturation ratios for NaCl-aerosols, however, deviate significantly from the Köhler curve, as calculated by *Cinkotai* (1971).

The above results provide further information concerning the detection limit and response of condensation nuclei counters for different particle materials.

REFERENCES

Cinkotai, F. F., 1971: The behaviour of sodium chloride particles in moist air. *J. Aerosol Sci. 2*, 325.

Fletcher, N. H., 1958: Size effect in heterogeneous nucleation. *J. Chem. Phys. 29*, 572.

Knutson, E. O., 1975: Aerosol classification by electric mobility: apparatus, theory and applications. *J. Aerosol Sci. 6*, 443.

Scheibel, H. G. and *Porstendörfer, J.*, 1982: Generation of monodisperse hydrophobic Ag- and hydrophilic NaCl-aerosol in the size range between 2 nm to 300 nm. *J. Aerosol Sci.* submitted for publication.

Preining, O., Wagner, P. E., Pohl, F. G. and *Szymanski, W.*, 1981: Heterogeneous nucleation and droplet growth; In: Aerosol research at the Institute for Experimental Physics of the University of Vienna. *O. Preining*, Ed. Vienna, Austria.

IDŐJÁRÁS

Az Országos Meteorológiai Szolgálat folyóirata, 86. évf. 2–4. szám, 1982. március–augusztus
Journal of the Hungarian Meteorological Service, Vol. 86. No. 2–4. March–August 1982, Budapest

The association between bacteria and rain and possible resultant meteorological implications

D. C. SANDS, V. E. LANGHANS, A. L. SCHAREN* and G. de SMET, *Plant Pathology Department, Montana State University Bozeman, Montana 59717 U.S.A.*

A baktériumok és a csapadék közötti kapcsolat és a lehetséges meteorológiai következmények. *Pseudomonas syringae* csoportba tartozó jégmagvasító baktériumokat izoláltunk záporesők cseppjeiből, amelyeket 180 és 2500 m közötti magasságban gabonaföldek fölött gyűjtöttünk. Ezek a jégképző baktériumok valószínűleg növényi környezetben élnek mint kórokozók vagy epifiták, mivel fluoreszcens, hiperérzékenységet kiváltó pszeudomonádokat más környezetben eddig nem találtak. Száraz évek száraz napjain és nedves évek telén végzett mérések nem mutattak ki ilyen jégképző baktériumokat. Kvantitatív eredmények eléréséhez nyilvánvalóan több éven át végzett, számos mérésre lenne szükség. Hipotézisünk szerint ezek a kórokozók vagy epifiták a csapadék-indukcióhoz vezető ciklus egy részét alkotják, amelyet a vegetáció feldúsulása követ, ez viszont megnövekedett jégképző baktérium produkcióhoz vezet. A mikróbák által előidézett csapadék a bio-precipitációs ciklus fontos összetevője. Ez a ciklikus jelenség megnövekedett vegetációt és biomassza-produktivitást eredményezhet adott földrajzi területen, vagy csökkent termékenységet és elsivatagosodást.

⁂

The association between bacteria and rain and possible resultant meteorological implications. Ice-nucleating bacteria, of the *Pseudomonas syringae* group, were isolated from raindrops in rainstorms at elevations from 180 to 2500 meters above cropland. These ice-nucleating bacteria were probably from plant habitats as pathogens or epiphytes, because oxidase negative, fluorescent, hypersensitivity-inducing pseudomonads have not been found in other environments. Overflights in dry years on dry days and all flights during the winter in wet years failed to produce these ice-nucleating bacteria. Clearly, more overflights are needed, over several years, to quantitate these findings. Our hypothesis is that these pathogens or epiphytes are a component of a cycle involving rainfall induction, followed by enhancement of vegetation, leading to increased production of ice-nucleating bacteria. Microbial-induced precipitation is an important component of proposed bio-precipitation cycles. Such cyclic phenomena may result in increased vegetation and biomass productivity of a geographical area or decreased productivity and desertification.

⁂

Introduction. Plant parasitic and epiphytic bacteria in the genera *Pseudomonas* and *Erwina* are capable of nucleating ice formations in supercooled water (*Arny* et al., 1976). Frost injury, initiated by these bacteria, is a problem in temperate agriculture. Data presented here indicate that some of these ice-nucleating bacteria are assimilated into rainstorms and these may be carried long distances. In this paper we present microbiological evidence that supports the existence of a "bio-precipitation" cycle. With this as a mechanism, we speculate as to the influence of activities such as plant disease control, land clearing, and agricultural practices upon the cycle.

* USDA, ARS

Experimental procedures and results

In 1978, in north-eastern Montana, a 360 hectare non-irrigated field test of a chemical seed treatment to control bacterial leaf blight on spring wheat caused by the bacterium *Pseudomonas syringae*, failed when the entire field exhibited symptoms of the disease even though a laboratory assay *(Table I)* had confirmed the effectiveness of the seed treatment. Uniform symptom development in the field indicated that the bacteria had probably been distributed simultaneously throughout the field and had not emanated from a point source over a period of time. Additionally, *P. syringae* could not be isolated from the soil at the time of planting in the spring or from the previous year's wheat crop stubble (Table I). Dry land conditions eliminated irrigation water as an inoculum source.

TABLE I

Soil and plant material samples containing P. syringae *that were taken after the* 1977 *harvest of a Montana spring wheat field*

Date	# Samples	# Samples with *P. syringae**
October, 1977	10 (straw, post harvest)	5 (>1000/gm sample)
April, 1978	10 (straw)	0 (<1000/gm sample)
April, 1978	5 (soil)	0 (<100/gm soil)
May, 1978	1 (seed sample treated)	0 (none on 200 seeds)
June, 1978	10 (seedling samples)	10 (>1000/gm sample)

* BCBRVB Selective Medium and Negative Oxidase Test *(Sands* et al., 1980).

Having eliminated these alternative pathogen sources, samples were taken of the atmosphere at ground level, and at approximately 180 m intervals to 2,500 m above this general area and above similar fields in the Gallatin Valley to determine, if the pathogen was being introduced by wind or rain. Sampling was accomplished using petri plates of the highly selective BCBRVB medium for fluorescent pseudomonads (*Sands* et al., 1980). Plates were exposed to the atmosphere for 10 s in dry air, or until nearly confluent, when exposed during rain. Sampling was done both on the ground and from an airplane at cca 270 km/h airspeed. The exposed plates were incubated at 27 °C for 48 h and the fluorescent pseudomonad colonies were identified using long-wave ultraviolet light (UV). The fluorescent colonies were transferred to petri plates of medium *B* (*King* et al., 1954), to which had been added 100 ppm cycloheximide (Sigma Chemical Co., St. Louis, MO). The fluorescent pseudomonads thus obtained were tested for the presence of oxidase and for hypersensitivity on tobacco (*Sands* et al., 1980).

The test results *(Table II)* show that all the isolates of *P. syringae* obtained from rain clouds in 1978 were oxidase negative, elicited a hypersensitive reaction on tobacco (*Klement*, 1967), and produced toxins on potato dextrose agar that were inhibitory to the growth of *Rhizobium* sp. and *Rhodotorula* sp., thus indicating that they were plant pathogenic or epiphytic members of the *Pseudomonas syringae* group (*Sands* et al., 1970 and 1980). Similar results were obtained during other flights conducted during the same year.

These examples of *P. syringae* were found in the air, rain, and hail samples taken at altitudes ranging from ground level (1,400 m above MSL) to 2,500 m

above ground level. Exceptions were an oxidase positive fluorescent pseudomonad collected inside the cabin of the airplane and a similar isolate collected at ground level at the airport. Also, all but one of the oxidase negative bacteria were able to induce ice nucleation at −4 °C when added to water at a final dilution of 10^6 cells/ml. No fluorescent bacteria were obtained when samples were taken during the winter months of 1978. In 1979 and 1980 the summer months were characterized by a lack of the normal large west to east flowing

TABLE II

Laboratory results of rain and ice samples taken October 6, 1978, *over the Gallatin Valley in Montana*[1]

Sample *N*	AGL Altitude (m)[2]	Condition	Fluorescence	Oxidase test	INA (−4°C)
1	180 m	Rain	+	−	+
2	700 m	Rain	+	+	+
3	700 m	Rain	+	−	+
4	1800 m	Ice	+	−	+
5	2500 m	Ice	+	-	+

[1] In this flight, 10 bacteria were found in cca 80 ml of rain and/or ice
[2] Most specimens taken at the 180 m sampling intervals contained no *P. syringae*

frontal systems. Very infrequent summer rain was from small localized showers. No plant pathogenic fluorescent pseudomonads were obtained during this period with the exception of one isolate in 1980. Only a few non-pathogenic, fluorescent pseudomonads were isolated in these two years.

Previous reports have not documented the occurrence of plant pathogenic bacteria in the atmosphere, except within the canopy of infected field crops or orchard trees (*Walker* and *Patel*, 1964). The presence of microbes in the atmosphere was studied as early as 1878 (*Gregory*, 1961), but most research has concentrated on fungal spores and their long distance dissemination by wind (*Hirst* and *Hurst*, 1967), (*Asai*, 1960). In recent years, aerobiologists have also given much attention to the presence of ice-nucleation active (INA) bacteria in the atmosphere (*Schnell* and *Vali*, 1976), (*Vali* et al., 1976), (*Carney* et al., 1975). INA bacteria have also been found on living and dead plant material (*Schnell* and *Vali*, 1972 and 1973), (*Maki* et al., 1974), (*Lindow* et al., 1978) and are believed to be responsible for initiating frost damage on many crops (*Macellos* and *Single* 1976), (*Arny* et al., 1976). *P. syringae*, a plant pathogen with a wide host range, may also exist as an epiphyte on non-host plants (*Crosse*, 1966 and 1969), (*Dowler* and *Weaver*, 1975) and can survive on plant refuse (*Latorre* and *Jones*, 1979), thus providing an inoculum reservoir even in the absence of host crops. We have found *P. syringae* on fungal spores of rusts and smuts of wheat and barley.

The presence of INA plant pathogenic bacteria in rainstorms leads to the speculation that an inter-relationship may exist between INA plant pathogenic bacteria and the weather. A one-way relationship almost certainly exists wherein the bacterium is dependent on rainstorms for both plant-to-plant and field-to-field spread. But does the reciprocal relationship also exist? Are rainstorms influenced by the presence or absence of INA bacteria? Prerequisites for this are: (1) a mechanism must exist by which bacteria can be readily taken up into the atmosphere; (2) the bacteria must be ice nucleators and

present in sufficient number to be effective; and (3) conditions must sometimes exist such that ice nucleation is the limiting factor for rainfall initiation.

The upward movement of bacteria into the atmosphere was demonstrated by *Schnell* and *Vali* (1976) who found that plant litter releases INA bacteria into the atmosphere as does water splash (*Walker* and *Patel*, 1964). Once free of plant surface, the bacteria might be easily carried to high altitudes by the updrafts which usually occur during rainstorm formation. Bacteria may also be carried into the atmosphere on the surface of fungal spores (*Sands* and *Scharen*, 1978).

Not as well documented, but still probable, is the ability of INA bacteria to induce rain. Some strains of *P. syringae* can induce ice nucleation at temperatures as high as -1 °C to -4 °C (*Maki* and *Willoughby*, 1978). Ice formation in the absence of nucleating agents normally requires temperatures as low as -40 °C. Thus, INA bacteria could induce water vapor to nucleate, forming ice crystals and rain. This has been demonstrated in cloud chamber experiments (*Maki* and *Willoughby*, 1978). The association of bacteria with fog (*Carney* et al., 1975) and rain and hail give circumstantial evidence that bacteria can induce rain.

The implications of a two-way relationship between rain and bacteria are far-reaching. It is possible that the reduction of bacterial populations on cultivated crops could actually affect the climate. Therefore we may ask, is it possible that the desertification occurring in eastern Africa (the Sahel) may be due in part to the destruction of sources of INA bacteria by overgrazing with a subsequent decrease in rainfall, thus initiating a cycle which allows neither the vegetation nor the climate to return to normal?

REFERENCES

Arny, D. C., Lindow, S. E. and *Upper, D. C.*, 1976: Frost sensitivity of *Zea mays* increased by application of *Pseudomonas syringae*. *Nature (London) 262*, 282–284.

Asai, G. N., 1960: Intra- and interregional movement of urediospores of black stem rust in the upper Mississippi Valley. *Phytopathology 50*, 535–546.

Carney, J. F., Schnell, R. C. and *Carty, C. E.*, 1975: Active ice nuclei associated with viable bacteria in Nova Scotia marine fogs. *Trans. Amer. Geophys. Union 56*, 994.

Crosse, J. E., 1966: Epidemiological relations of the pseudomonad pathogens of deciduous fruit trees. *Ann. Rev. Phytopathol. 4*, 291–310.

Crosse, J. E., 1969: Inhibition of leaf scar infection of cherry by a saprophytic bacterium from leaf surfaces. *Ann. Appl. Biol. 56*, 149–160.

Dowler, W. M. and *Weaver, D. J.*, 1975: Isolation and characterization of fluorescent pseudomonads from apparently healthy peach trees. *Phytopathol. 65*, 223–236.

Gregory, P. H., 1961: *The microbiology of the atmosphere*. Leonard Hill, London.

Hirst, J. M. and *Hurst, G. W.*, 1967: Long distance spore transport. In: *Gregory* and *Monteith* (ed.), Airborne microbes, *Soc. Gen. Microbiol. Symp. 17*, 307–344.

King, E. O., Ward, M. K. and *Raney, D. E.*, 1954: Two simple media for the demonstration of pycocyanin and fluorescein. *J. Lab. Clin. Med. 44*, 301–307.

Klement, A., 1967: Rapid detection of the pathogenicity of some phytobacteria by the hypersensitive reaction in plants. pp. 61–62 In: *R. N. Goodman* (ed.) *Proc. 1st Workshop in Phytobacteriology*, University of Missouri, Columbia.

Latorre, B. A. and *Jones, A. L.*, 1979: Evaluation of weeds and plant refuse as potential sources of inoculum of *Pseudomonas syringae* in bacterial canker of cherry. *Phytopathol. 69*, 1122–1125.

Lindow, S. E., Arny, D. C. and *Upper, C. D.*, 1978: Distribution of ice nucleation-active bacteria on plants in nature. *Appl. Env. Mircobiol. 36*, 831–838.

Macellos, H. and *Single, W. V.*, 1976: Ice nucleation on wheat. *Agric. Meterol. 16*, 125–129.

Maki, L. R., Galyan, E. L., Chang-Chien, M. and *Caldwell, D. R.*, 1974: Ice nucleation induced by *Pseudomonas syringae*. *Appl. Microbiol. 28*, 456–459.

Maki, L. R. and *Willoughby, K. J.*, 1978: Bacteria as biogenic sources of freezing nuclei. *J. Appl. Meterol. 17*, 1049–1053.
Sands, D. C., Schroth, M. N. and *Hildebrand, D. C.*, 1970: Taxonomy of phytopathogenic pseudomonads. *J. Bacteriol. 27*, 132–134.
Sands, D. C. and *Scharen, A. L.*, 1978: A selective medium for the *Pseudomonas syringae* group of plant pathogens. *Phytopathology News 12*, 137 (abstract).
Sands, D. C., Schroth, M. N. and *Hildebrand, D. C.*, 1980: Pseudomonas. In: *Laboratory guide for identification of plant pathogenic bacteria*, University of Georgia, 1980, 36–44.
Schnell, R. C. and *Vali, G.*, 1972: Atmospheric ice nuclei from decomposing vegetation. *Nature (London) 236*, 163–165.
Schnell, R. C. and *Vali, G.*, 1973: World-wide source of leaf-derived freezing nuclei. *Nature 246*, 212–213.
Schnell, R. C. and *Vali, G.*, 1976: Biogenic ice nuclei. Part 1. Terrestial and marine sources. *J. Atmos. Sci. 33*, 1554–1564.
Vali, G., Christenson, M., Fresh, R. W., Gaylon, E. L., Maki, T. R. and *Schnell, R. C.* 1976: Biogenic ice nuclei. Part 2. Bacterial sources. *J. Atmos. Sci. 33*, 1565–1570.
Walker, J. C. and *Patel, P. N.*, 1964: Splash dispersal and wind as factors in epidemiology of halo blight of bean. *Phytopathology 54*, 140–141.

IDŐJÁRÁS

Az Országos Meteorológiai Szolgálat folyóirata, 86. évf. 2–4. szám, 1982. március–augusztus
Journal of the Hungarian Meteorological Service, Vol. 86. No. 2–4. March–August 1982, Budapest

Concentration and nature of biogenic ice nuclei over the Arctic Ocean

K. JAYAWEERA, *Geophysical Institute, and* P. FLANAGAN, *Institute of Arctic Biology, University of Alaska, Fairbanks, Alaska 99701, U.S.A.*

Biogén jégmagvak koncentrációja és természete az Északi-Jeges-tenger fölött. A tenger fölött különböző magasságokban gyűjtött levegőmintákban legalább kétfajta baktérium és öt különböző gombaspóra található, amelyek vízcseppek fagyását magas hőmérsékleten kiválthatják. A megfigyelések szerint a fagyási hőmérséklet logaritmikusan emelkedik az egy cseppben lévő sejtek számának növekedésével, majd a fajtától függően maximális értéket ér el. A baktériumok hatékonyabbak, mint a gombaspórák, de a spórákkal ellentétben laboratóriumi növesztés esetén elvesztik aktivitásukat. A mikroba-sejtek maximális koncentrációja felhőkben 10 l^{-1}, míg felhőkön kívül 1 l^{-1}. Ennél azonban jóval nagyobb koncentrációkat figyeltek meg 7 km-es magasságig, jéggel borított tengerek fölött.

*

Concentration and nature of biogenic ice nuclei over the Arctic Ocean. Air samples collected at several heights above the Arctic Ocean contained at least two types of bacteria and five different fungal spores which could elevate the freezing temperature of water droplets. It was observed that the freezing temperature increased logarithmically with the number of cells per drop up to a maximum temperature dependent upon species. Bacteria were more effective than fungal spores but, unlike the spores, they lost their activity under laboratory growth conditions. Maximum concentration of nearly 10 microbial cells l^{-1} occurs in clouds and one cell l^{-1} in air outside clouds. However, numbers and varieties of microbial cells in excess of those found near sea ice surface level were observed up to 7 km.

*

Introduction. During the past decade, research on composition of ice nuclei has shown that certain bacteria act as effective ice nuclei. *Soulage* (1957) suggested that bacteria may act as ice nuclei and showed that bacteria cells nucleated ice crystals in a cloud chamber. Recently *Schnell* and *Vali* (1972, 1973, 1976) have shown the presence of freezing nuclei associated with decaying leaves and marine plankton. They suggested that these biogenic nuclei may constitute a significant fraction of the atmospheric ice nuclei. Investigations by *Vali* et al. (1976), *Maki* and *Willoughby* (1978) have shown that the development of these biogenic nuclei depended upon the presence of bacteria of the genus *Pseudomonas*. The activity of this particular genus in ice nucleation had been shown earlier in the laboratory by *Maki* et al. (1974).

Bacteria active as ice nuclei have been isolated in laboratory cultures from plant surfaces (*Lindow* et al, 1978a), rain or snow (*Maki* and *Willoughby*, 1978), and hail (*Mandrioli* et al., 1973). The type of bacteria isolated in these instances also belongs to the genus of *Pseudomonas* and in the case of plant surfaces, *Lindow* et al. (1978b) isolated strains of *Erwina herbicola* as well.

Presence of a variety of genera of bacteria in the atmosphere is well documented. Early description of microbiological studies in the atmosphere over the non Arctic regions in Canada is reported by *Kelley* and *Paddy* (1953) and for the upper atmosphere by *Fulton* (1966). A summary of these invetigations is found in *Gregory* (1961). These bacteria were alive and their concentration, although depended on the type of air mass, varied from 0.2 to about 0.01 per liter.

Although the ice-nucleating activity of *Pseudomonas* has been confirmed in the laboratory and variety of different species including *Pseudomonas* has been found in the atmosphere, there are no reports of ice-nucleating bacteria being isolated from the atmosphere. Clearly biogenic ice nuclei derived from leaf, soil, and marine sources should be expected in the atmosphere carried aloft with air masses. Mechanisms for injecting these nuclei to the atmosphere, especially from the ocean, are well documented (*Blanchard* and *Syzdek*, 1972, 1974).

In this paper we describe the isolation of ice-nucleating cells (I.N.C.) from air samples collected over the Arctic Ocean up to an altitude of 7 km. Many varieties of bacteria and fungal spores were isolated in clouds in proximity to clouds and in clear air. We present here results of experiments to induce water freezing using a variety of such bacterial cells and fungal spores. It is clear from our data that many of these I.N.C. are viable and active to a greater or lesser extent in initiating ice formation in clouds.

Approach and methods

Sampling of air for the presence of bacteria was done as a part of the Arctic stratus experiment conducted in the Beaufort Sea area of the Arctic Ocean during June 1980. The National Center of Atmospheric Research (U.S.A.) aircraft 'Electra' flew six missions into this region.

The aircraft carried an air sampling device, where microbial cells can be collected on sterilized filters. With this system, the only possibility that aircraft air could contaminate the filters was during the transfer of filters from their box into the holder of the sampler. As such, some filters were left exposed in the aircraft cabin and few others were moved about the cabin to determine the possible contaminants. Sampling for microbial cells was done during two flights on June 28 and 30, 1980. The June 28th flight was from Eielson AFB, Alaska to Barrow, Alaska and then to a location of approximately 78°N and 155°W. The June 30th flight was from Eielson AFB to Prudhoe Bay, Alaska and then on to a location of approximately 73.5°N and 134°W *(Fig. 1)*. During both these flights air was sampled for microbes at regular intervals during the entire flight which lasted about 7 h at altitudes of 30 m to 7 km. The sampling rate was maintained at an indicated 20 liters per minute and air flow rates were calculated from recordings of incoming and outgoing pressures. The sampling duration was chosen to coincide with the length of a flight leg, in which the aircraft flew at a constant altitude and heading.

(a) *Preparation of the specimens.* Membrane filters with samples from clouds and air and the background (control) filters were cut in half, and one half each was split in three, placed on agar growth medium and examined for microbial growth. The other half was also split in three. One third was examined for the presence of bacteria using a scanning electron microscope (SEM), while the

other two were suspended in liquid nutrient broth of either sea water, potato extract, or blood infusion.

Bacteria that grew in the nutrient solutions and agars were suspended in triple distilled water and enumerated using a Klett densitometer, calibrated using a haemocytometer.

Fungal spores were separated from fungi by growing on solid agar by tapping the back of the plates being held over glass slides and then adding

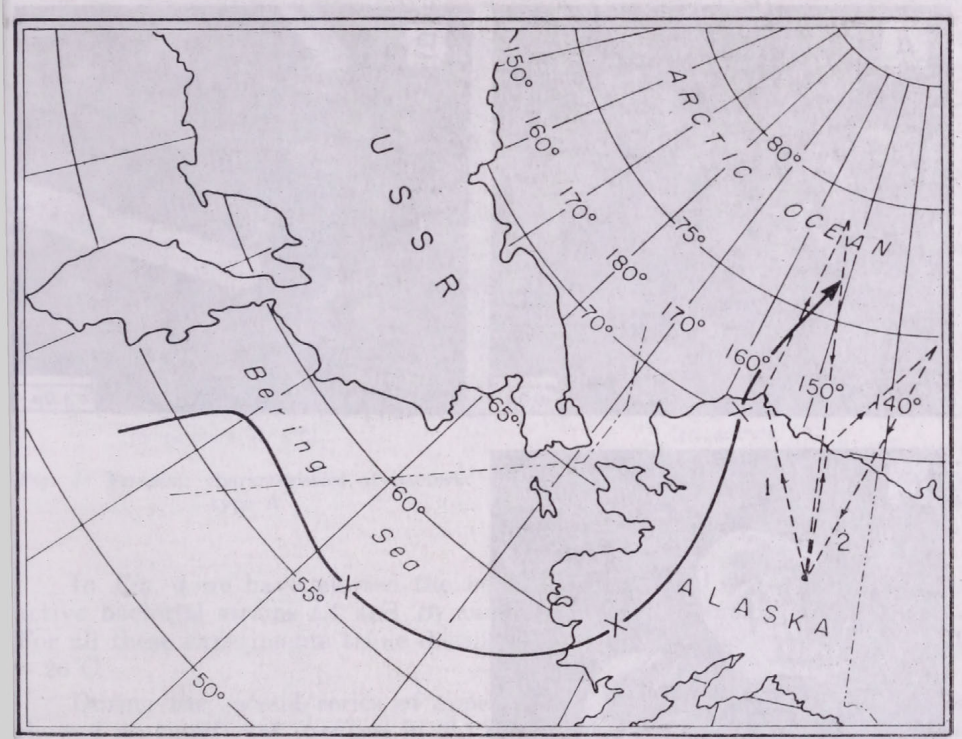

Fig. 1: A map showing the flight paths (dashed lines) on June 28, 1980 (1) and June 30, 1980 (2). The solid line shows the air trajectory at 850 mb on June 28, 1980. Crosses denote the location of the air mass on the three previous days

a few drops of sterile water to float the spores. Subsequently, spores were treated in the same manner as the bacteria to calculate spore concentration per volume of water.

(b) *Drop freezing*. The ice-nucleating activity of microbial cells was measured using the drop-freezing technique developed by *Vali* (1971) and modified later by *Schnell* (1979).

Control experiments were done by measuring the freezing temperature of triple distilled water drops of size 0.5 μl. The freezing temperature was defined as that temperature (T_{96}) at which 48 of the 50 drops froze.

Determination of the freezing temperature of drops containing bacterial cells or fungal spores was performed as above for pure water. For each cell concentration experiment was replicated ten times. Experiments were performed for all the different species of bacteria and spores isolated from the filters.

Initially, a concentration of 100 cells per drop was used to distinguish those that act as biogenic nuclei. Active cells were further tested using concentrations from 2 to 10^4 cells per drop.

The freezing experiments were done in two series, the first about 3 months after the samples were collected, and the second 10 months afterwards. Between series, bacterial and fungal spores were maintained in refrigerated cultures.

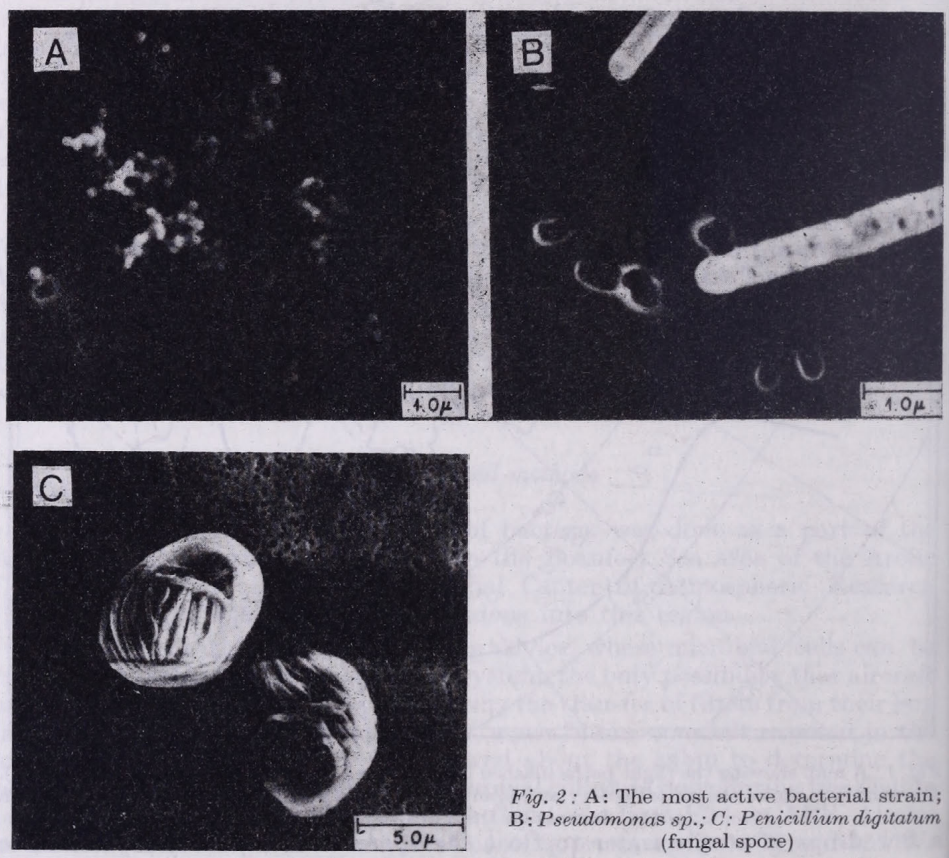

Fig. 2: A: The most active bacterial strain; B: *Pseudomonas sp.; C: Penicillium digitatum* (fungal spore)

Results

(a) *Ice-nucleating activity.* In the first series of experiments we found two strains of bacteria and five different fungal spores capable of elevating the freezing temperature of water. The most active was an unidentified microbacterium shown in *Fig. 2a*. The T_{96} for this strain as a function of the number of cells per 0.5 μl drop is shown in *Fig. 3*. It is noteworthy that when the cell concentration/drop was >20, the T_{96} remained constant to within 0.5°C. For concentrations <20 cells/drop, an exponential curve can be fitted for T_{96} as shown in *Fig. 3*.

The constancy of T_{96} for more than 20 cells per drop indicates that this strain of bacterium under conditions of the first experiment has a 5% proba-

bility of nucleating a water drop at -4.0°C, an elevation of more than 20°C over that of pure water under identical conditions. The *Pseudomonas* strain *Fig. 2b* was also active as an ice nucleus with about a 10% probability of nucleating a water drop at -9°C.

The fungal spores were generally less effective than bacteria. In *Table I* we have listed the T_{96} temperature for effective fungal spores having 100 spores per drop.

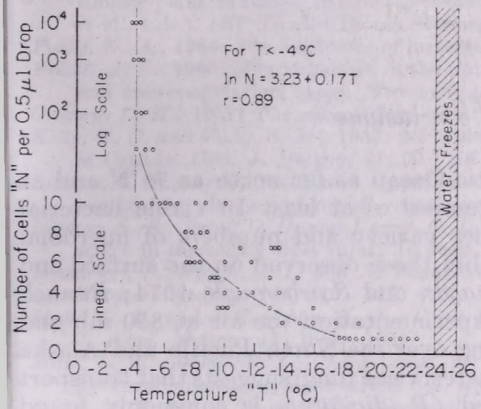

Fig. 3: Freezing characteristics of bacteria type A

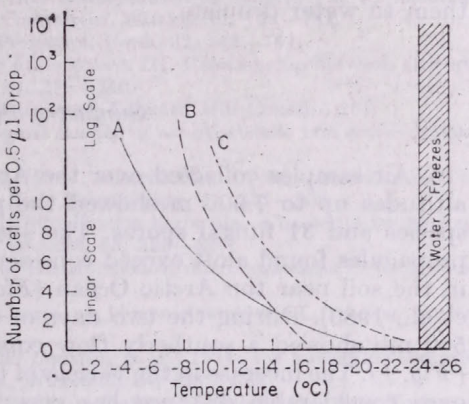

Fig. 4: Comparison of freezing temperatures for two strains of bacteria and one fungal spore

In *Fig. 4* we have plotted the best fit exponential curves for the two, active bacterial strains (*A* and *B*) and for the *Penicillium* spore *(Fig. 2c)*. For all these experiments triple distilled water T_{96} was between -24°C and -26°C.

During the second series of experiments, the original bacterial strains showed no significant increase in T_{96} over that of pure water. On the other hand, no loss in activity was found for fungal spores.

Comparison of the results for the first and second series of experiments showed that long-term growth in nutrient cultures does not affect the activity of spores, but markedly deactivates bacterial cells.

TABLE I

T_{96} *for five ice-nucleating fungal spores found in the Arctic atmosphere*

Species	Color	T_{96} °C
Penicillium digitatum	beige	-10.0
Cladosporium herbarum	beige	-15.0
Penicillium rotatum	dark green	-22.0
Penicillium frequenten	light green	-22.5
Rhizopus stolmifera	brown	-23.0

[Tripple distilled water $T_{96} = -24$ to -26 °C]

(b) *Concentration of bacteria and spores.* It can be estimated from the SEM counts of microbes, after correction for the sampling effects as indicated by *Fuchs* (1964), that concentrations (10 cells l^{-1}) were highest inside clouds. Outside clouds, the concentrations were lowest, particularly above the ice surface, then reached a maximum of about 1.0 cell l^{-1} near the cloud heights, and decreased slowly up to the maximum sampled level of 7 km.

The most significant observation here is the substantial difference that occurs between the concentration within and without clouds. It is conceivable that cloud movement through air may concentrate microbial cells by adhering them to water droplets.

Summary and conclusions

Air samples collected over the Arctic Ocean as far north as 76°N and at altitudes up to 7,000 m showed the presence of at least 10 viable bacterial species and 31 fungal spores. The species variety and numbers of microbial propagules found aloft exceed considerably those observed on the surface and in the soil near the Arctic Ocean (*Flanagan* and *Scarborough*, 1974; *Bunnell* et al., 1980). During the two days of experimentation the air at 850 mb and 500 mb showed a southerly flow coming over the North Pacific and Alaska *(Fig. 1)*. The incerase in the variety of bacteria and fungi suggests that transport over considerable distance has occurred *(P. digitatum* is commonly found associated with citrus fruit disease and other temperate and sub-tropical crops, *Raper* and *Thom*, 1968) and that the species have survived such transport under the temperature and pressure conditions aloft.

The activity of bacteria as ice nuclei seems to depend very heavily on the morphology and/or physiological state. This is evident in the substantial decrease of the ice-nucleating activity of types shown in *Fig. 2a* and *b* after a ten-month incubation in a culture collection, where the culture was transferred twice. During this period the average length of these cells had increased from 0.2 μ *(Fig. 2a)* to 1.1 μ. Cells were more elongate, though their colorations were identical.

We believe that our present experiments are noteworthy because (1) a wide variety of bacteria exists in the atmosphere of which some may nucleate water droplets at temperatures as high as −4°C; (2) because of their hydrophilic nature bacteria and especially fungal spores readily form water droplets, hence nucleation could occur through the more efficient condensation freezing process; (3) ice nucleation of microbial cells *in vitro* is determined by some surface morphology and is influenced by some unknown growth phenomena occurring during culturing. Whether this is a reversible process or not may become clear from our planned future experiments; (4) fungal spores can constantly nucleate water droplets. Although they are not as active as bacteria, the spores retain their activity during successive cultivation transfers in nutrient agar.

Acknowledgements. The research described in this paper was carried out by the State of Alaska funds. The authors are indebted to the National Science Foundation grant DPP 77-20887 for sponsoring the Arctic Stratus Experiment.

REFERENCES

Blanchard, D. C. and *L. D. Syzdek*, 1972: Concentration of bacteria in jet drops from bursting bubbles. *J. Geol. Res., 77*, 5087–5099,

Blanchard, D. C. and *L. D. Syzdek*, 1974: Importance of bubble scavenging in the water-to-air transfer of organic material and bacteria. *J. Rech. Atmos., 8*, 529–540.

Bunnell, F., O. K. Miller, P. W. Flanagan and *R. E. Benoit*, 1980: Tundra microflora: composition, biomass and environmental relations. In: *An arctic ecosystem: The coastal tundra of Northern Alaska, Brown* et al., Eds.). Hutchinson and Ross Inc., Strandsburg, Penn., 255–290.

Flanagan, P. W. and *A. M. Scarborough*, 1974: Physiological groups of decomposed fungi in tundra plant remains. In: *Soil organisms and decomposition in tundra, (A. J. Holdings* et al., Eds.). IBP Tundra Biome Steering Committee, Stockholm, 159–181.

Fuchs, N. A., 1964: *The mechanics of aerosols.* Pergamon Press, 32, 142–151.

Fulton, J. D., 1966: Microorganism of the upper atmosphere. III. Relationship between altitude and micropopulation. *Appl. Microbiology, 14*, 237–240.

Gregory, D. H., 1961: *The microbiology of the atmosphere*, Leonard Hill London, 251.

Kelly, C. D. and *Pady, S. M.*, 1953: Microbiological studies of air over some non arctic regions of Canada. *Can. J. Botany, 31*, 90–106.

Lindow, S. E., Arny, D. C. and *Upper, C. D.*, 1978a: Distribution of ice nucleation-active bacteria on plants and nature. *Appl. and Env. Microbiology, 36*, 831–838.

Lindow, S. E., Arny, D. C. and *Upper, C. D.*, 1978b: Erwina herbicola: a bacterial ice nucleus active in increasing frost injury to corn. *Phytopath, 68*, 523–527.

Mandrioli, P., Puppi, G. L. and *N. Bagni*, 1973: Distribution of microorganisms in hailstones. *Nature (London), 246*, 416–417.

Maki, L. R. and *Willoughby, K. J.* 1978: Bacteria as biogenic sources of freezing nuclei. *J. Appl. Meteor., 17*, 1049–1053.

Maki, L. R., Galyan, E. L., Chang-Chien, M. and *Cadwell, D. R.*, 1974: Ice nucleation induced by Pseudomonas syringae strain C-9. *Appl. Microbiol, 28*, 456–459.

Raper, K. B. and *C. Thom*, 1968: *A manual of Penicillia.* Hafner Publishing Co., New York and London.

Schnell, R. C. and *Vali, G.*, 1972: Atmospheric ice nuclei from decomposing vegetation. *Nature (London), 236*, 163–165.

Schnell, R. C. and *Vali, G.*, 1973: Worldwide sources of leaf derived freezing nuclei. *Nature (London), 246*, 212–213.

Schnell, R. C. and *Vali, G.*, 1976: Biogenic ice nuclei Part I–Terrestrial and marine sources. *J. Atmos. Sci., 33*, 1544–1564.

Schnell, R. C., 1979: A new technique for measuring atmospheric ice nuclei active at temperatures from −20°C to approaching 0°C with results. *Proc. Seventh Int. Conf. on Inadvertant and Planned Wea. Mod.*, Banff, Canada, 110–111.

Soulage, G., 1957: Les noyaux de congelation de l'atmosphère *Ann. de Geophysique, 13*, 103–134.

Vali, G., 1971: Quantitative evaluation of experimental results on the heterogeneous freezing nucleation of supercooled liquids. *J. Atmos. Sci., 28*, 402–409.

Vali, G., Christensen, M., Fresh, R. W., Galyau, E. L., Maki, L. R. and *Schnell, R. C.*, 1976: Biogenic nuclei. Part II-Bacterial sources. *J. Atmos. Sci., 33*, 2565–2570.

IDŐJÁRÁS

Az Országos Meteorológiai Szolgálat folyóirata, 86. évf. 2–4. szám, 1982. március–augusztus
Journal of the Hungarian Meteorological Service, Vol. 86. No. 2–4. March–August 1982, Budapest

The 1980 International Cloud Condensation Nuclei Workshop

W. C. KOCMOND, C. F. ROGERS, U. KATZ and J. G. HUDSON, *Desert Research Institute University of Nevada System, P.O.B. 60220 Reno, Nevada 89506 and* J. E. JIUSTO, *Atmospheric Sciences Research Center State University of New York, Albany, New York, 12222, U.S.A.*

Nemzetközi munkaülés 1980-ban a felhő-kondenzációs magvak mérő módszereinek összehasonlítására. A felhő-kondenzációs magvak (Cloud Condensation Nuclei, CCN) témával foglalkozó harmadik nemzetközi munkaülést 1980. október 6–17. között rendezték meg a Reno-i (Nevada állam) Sivatag Kutató Intézetben. A munkaülés célja – melyen 20 intézet képviseletében 39 szakember vett részt – a különböző CCN mérő módszerek összehasonlítása volt, emellett néhány alapvető tudományos kísérlet elvégzése. Huszonöt műszert hasonlítottak össze, beleértve a részecskenagyság meghatározására szolgáló műszereket és két Aitken-számlálót. A teszt aeroszolt a rendszerbe kapcsolt generátor szolgáltatta, ezzel elkerülhetővé vált a tároló tartályok használata. A munkaülés két hete alatt nyert legfontosabb megállapítások a következők: 1. Monodiszperz és polidiszperz teszt aeroszolok állíthatók elő tiszta oldódó sóból 3% óránkénti stabilitással. 2. A kilenc statikus diffúziós kamrából (SDC) az öt legjobb átlagban 20%-on belül egyezett meg az NRL mozgékonyság-analizátorral és 10%-on belül, ha a túltelítettség 1% volt. 3. Az öt folyamatos áramú diffúziós kamra (CFD) közül négy 15% és 20%-on belül egyezett meg egymással, ha a túltelítettség rendre 0,7% és 0,3% volt. 4. A legjobb CFD-k és SDC-k 15%-on belül egyeztek meg egymással. 5. A négy izotermikus ködkamra közül kettő megegyezik egymással 40%-on belül. 6. Az eredmények analízise szerint a műszerek többsége alapján megbecsült felhő-kondenzációs mag spektrum dőlése (k) és a száraz aeroszolnagyság spektrumának ismert dőlése (β) megközelítette a $k=2/3\ \beta$ elméleti összefüggést.

*

The 1980 International Cloud Condensation Nuclei Workshop. The Third International Cloud Condensation Nuclei Workshop was held at the Desert Research Institute, Reno, Nevada, October 6–17, 1980. The goals of the Workshop were to intercompare CCN measurement technologies and to perform a limited number of experiments of fundamental scientific interest. A total of 39 scientists representing 20 institutions were in attendance. Twenty-five instruments were tested including size characterization devices and two Aitken counters. The test aerosols were supplied to the instruments by an on-line generation system, thereby eliminating the need for storage bags. Some of the main conclusions reached during the two-week Workshop were as follows: (1) Test aerosols of pure soluble salts, both monodisperse and polydisperse, can be provided with stability in output concentration to about ±3% per hour; (2) Of nine static diffusion chambers (SDC), the five best units (averaged) agreed to within 20% of the NRL mobility analyzer and to within 10% at 1% supersaturation; (3) Four of the five continuous flow diffusion (CFD) chambers agreed with each other to within about 15% at 0.7% supersaturation and about 20% at 0.3% supersaturation; (4) The best CFD's and SDC's agreed to within about 15%; (5) Two of four isothermal haze chambers agreed with each other to within about 40%; (6) Analysis of the results showed that most instruments' estimation of the CCN spectral slope, k, and the known dry aerosol size distribution slope, β, confirmed the theoretical relationship $k=2/3\ \beta$.

*

Introduction. The 1980 International Cloud Condensation Nuclei (CCN) Workshop was the third meeting of its kind, continuing in the tradition of the first and second workshops held at Lannemezan, France, in 1967, and at

Fort Collins, Colorado, U.S.A., in 1970. Ice nuclei counters were not included, as a separate workshop to assess progress in their technology was held in 1975 at Laramie, Wyoming, U.S.A. The earliest planning for the 1980 Workshop was carried out by an Ad Hoc Commission of the International Committee on Cloud Physics (ICCP), appointed by Professor *H.-W. Georgii* and with *Dr. J. Jiusto* as chairman. Following acceptance of an offer by the Desert Research Institute to host the meeting, a Steering Committee *(A. Gagin, J. Jiusto, J. Kassner, W. Kocmond, J. Megaw, L. Radke, R. Ruskin)* was appointed by the Ad Hoc Commission, to proceed with the planning of the specific logistical and scientific details of the meeting. Funding was provided by the National Aeronautics and Space Administration and the National Science Foundation.

The Steering Committee in its deliberations had a number of scientific questions to consider. First, the stated goals of the Workshop included not only instrument intercomparisons, but also utilization of the large number of instruments expected to be present at the Workshop to perform one or two experiments of basic relevance to aerosol science. In the first case, CCN counter technology had advanced considerably since the 1970 Workshop, as for example illustrated by the appearance in several laboratories of continuous-flow diffusion (CFD) CCN counters in the intervening years. Comparison of these devices to the older standard Twomey-type "static" diffusion chambers was identified as a Workshop goal, as well as evaluation of isothermal haze chamber (IHC) performance.

In addition, the Steering Committee addressed the question of experiments of basic scientific relevance by suggesting tests of the Kohler theory of pure soluble aerosols and the Volmer theory of insoluble, wettable aerosols, and examination of the theoretical relationship between the slope, k, of the cumulative number-*versus*-critical supersaturation spectrum curve, and the slope of the dry aerosol size distribution.

The advances in CCN counter technology were matched by advances in the technology of generating and size-characterizing of aerosols; an early Steering Committee decision was to generate aerosols "on-line" during the experiments, without recourse to a storage bag. The Naval Research Laboratory's electrical mobility analyzer was adopted as the aerosol sizing standard. Further Steering Committee recommendations included: (a) that aerosol concentrations should be in the range of $1{,}000 - 2{,}000$ cm^{-3} to a few hundred cm^{-3} over the supersaturation range of 1.0% to 0.1%; (b) aerosol composition should include NaCl, $(NH_4)_2SO_4$, and AgI; and (c) aerosols would be provided *via* a sampling duct to each instrument, under slight positive pressure. The Steering Committee recommendations were passed on to a local committee at the Desert Research Institute for implementation.

TABLE I

CCN *Workshop participants*

Name/Affiliation	*Instrument*	*Name/Affiliation*	*Instrument*
Dr. Jeffrey B. Anderson NASA-MSFC	–	*Mr. R. Leaitch* York University	Diffusion Tube
Dr. Greg Ayers CSIRO	SDC	*Dr. Ray McKenzie* National Bureau of Standards	Pollak TSI

(Continuation on the next page)

Name/Affiliation	*Instrument*	*Name/Affiliation*	*Instrument*
Dr. Darryl Alofs Univ. of Missouri-Rolla	CFD	*Dr. William H. Mach* Florida State University	CFD Impactor
Mr. Randolph D. Borys Colorado State University	SDC	*Mr. Thomas R. Mee* Mee Industries, Inc.	SDC
Mr. Jack Dea Desert Research Institute	Aero. Gen.	*Dr. W. J. Megaw* York University	Diffusion Tube
Dr. S. Domonkos University of Washington	4SS CFD	*Dr. Sherm Neste* General Electric Company	–
Dr. L. R. Eaton General Electric Company	–	*Ms. Hana Nuzitsa* Hebrew University	SDC
Dr. J. Fitzgerald Naval Research Laboratory	IHC	*Dr. T. Ohtake* University of Alaska	Impactor Photomicro.
Dr. Abe Gagin Hebrew University	SDC	*Dr. Myron Plooster* Denver Research Institute	–
Dr. Herman E. Gerber Naval Research Laboratory	–	*Ms. Marsha Politovitch* University of Wyoming	SDC
Dr. Edward Hindman II Colorado State University	IHC	*Dr. Lawrence F. Radke* University of Washington	4SS CFD
Dr. W. A. Hoppel, Code 4320 Naval Research Laboratory	Aero. Sizing	*Dr. C. Fred Rogers* Desert Research Institute	DRI-NASA CFD
Mr. Richard Hucek Florida State University	CFD Impactor	*Dr. David Rogers* University of Wyoming	SDC Aero. Siz.
Dr. James G. Hudson Desert Research Institute	CFD, 3SS, CFD IHC	*Dr. R. Ruskin* Naval Research Laboratory	SDC
Dr. James Jiusto State Univ. of NY at Albany	SDC	*Dr. V. J. Schaefer* State University of New York	–
Dr. J. Kassner Univ. of Missouri-Rolla	CFD	*Dr. R. Serpolay* Université de Clermont	SDC
Dr. Ulrich Katz Desert Research Institute	Aero. Gen.	*Dr. Patrick Squires* NCAR	–
Dr. Vernon Keller NASA-MSFC	–	*Dr. D. Stein* Institut für Met. und Geophy.	–
Mr. Gary Keyser Desert Research Institute	DRI-NASA CFD	*Mr. M. Trueblood* Univ. of Missouri-Rolla	CFD
Mr. Malcolm Kitchen British Meteorological Office	SDC	*Dr. Sean Twomey* University of Arizona	–
Prof. Warren C. Kocmond Desert Research Institute	DRI-NASA CFD	*Mr. C. H. Wilson* NASA Langley Research Center	–
Dr. G. G. Lala State Univ. of NY at Albany	SDC	*Mr. T. Wojciechowski* Naval Research Laboratory	SDC

The participants and their instruments are listed in *Table I*. There were 39 participants representing 20 institutions, and 25 total instruments including size characterization devices, and two Aitken counters.

1. Experimental facilities

Figure 1 shows the aerosol supply duct in plan view; the duct itself was aluminum tubing 8.2 cm in inside diameter. Participants sampled aerosols over a 16 meter length of the duct, through which the volume flow rate was in the

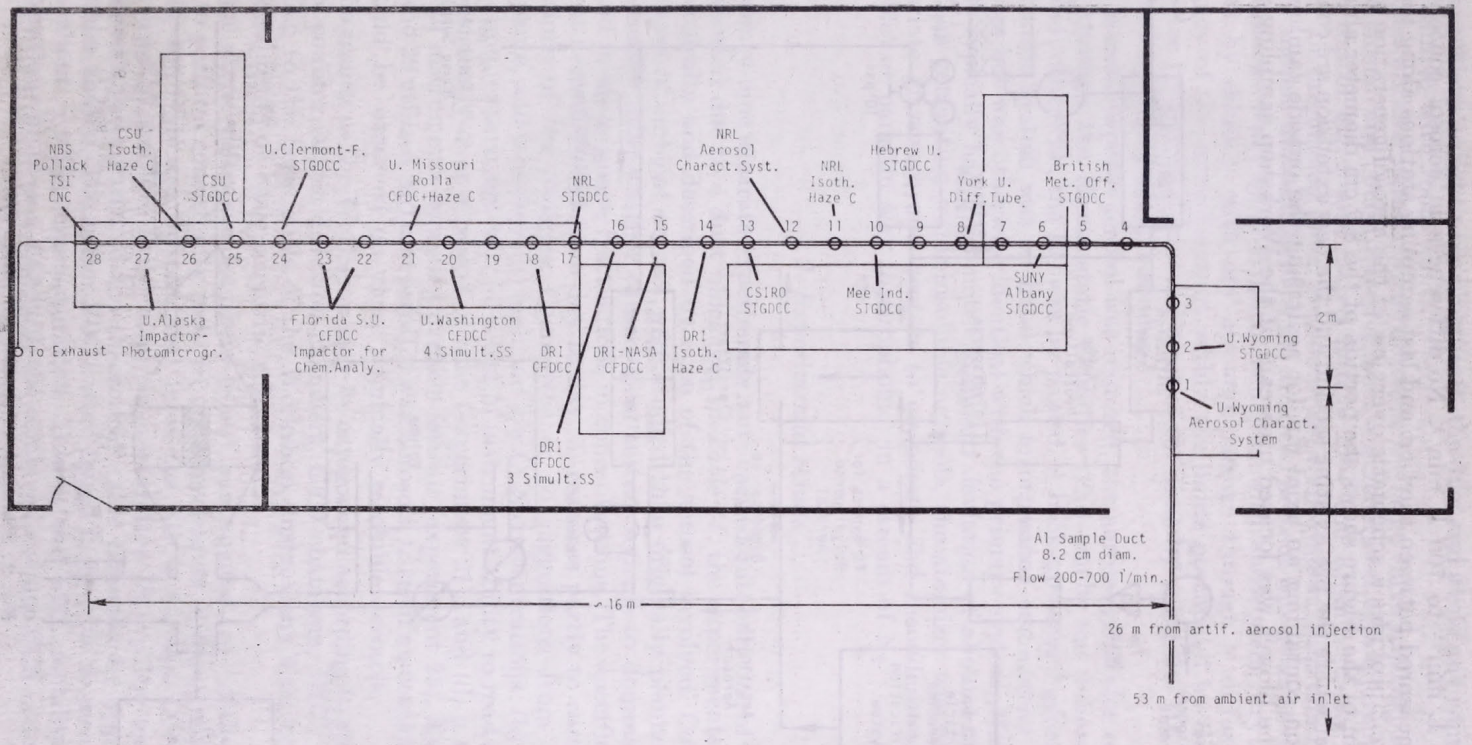

Fig. 1: Layout of sampling duct and instruments in workshop area

range 200 L min^{-1} to 700 L min^{-1}. No differences in aerosol concentration could be measured between the first and last sampling stations along the duct.

Figure 2 provides a schematic overview of the aerosol generation system. The bottom of the Figure shows the portion of the 8.2 cm diameter aluminum sample duct where the pre-existing section and the new extension are connected by a section containing an axial fan for aspirating the outside (ambient) air sample. The blower was located upstream of the Workshop sampling area in

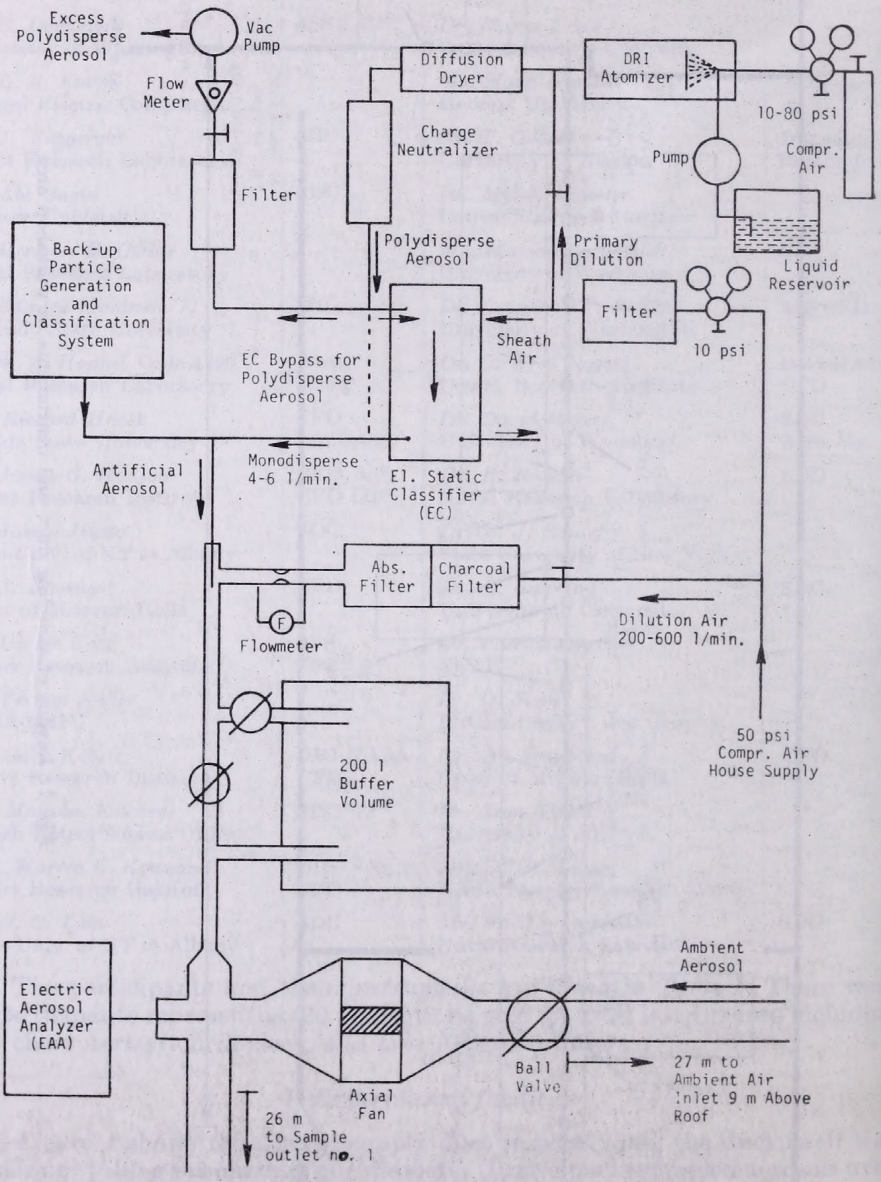

Fig. 2: Schematic of aerosol generation system

order to achieve a slight over-pressure in the duct and avoid any contamination of the sample with room air.

When working with artificial aerosols, the large valve adjacent to the axial fan was closed, and concentrated aerosol was generated with equipment shown on the top of Fig. 2 and mixed into a $200-600$ Lmin^{-1} stream of filtered dilution air originating from the compressed air system (thus eliminating the need for another blower). Most of the artificial aerosol was generated by atomizing aqueous NaCl or $(NH_4)_2SO_4$ solutions with subsequent drying of the droplets by dilution with dry air and passage through a diffusion dryer. Constancy of the aerosol output within the limits postulated by the Steering Committee ($\pm 3\%$) was achieved most of the time by using the DRI atomizer developed under NASA sponsorship.

If a monodisperse aerosol was required, the aerosol generator output was passed through the Electrostatic Classifier (EC) where the desired size was extracted; otherwise, the EC was by-passed. A back-up aerosol generation and classification system was on hand which incorporated commercial inhalation atomizers but was otherwise identical with the primary system. Monodisperse aerosols typically had a geometric standard deviation of about 1.2.

When generating water-insoluble aerosols, the atomizer was replaced by appropriate glassware and heaters to evaporate and recondense either AgI (insoluble) or paraffin wax (hydrophobic) in a stream of N_2.

2. Experimental results

Twenty-nine separate experiments were carried out, only one of which had to be aborted due to a duct blockage. In *Table II*, the experiments are listed chronologically and described by type of the aerosol involved. Considerably fewer cases of ambient aerosol were studied than originally planned because the unusually calm weather caused local aerosol sources to dominate the air mass and produce severe fluctuations in concentrations. The specifications for each test aerosol varied from day to day, in response partly to earlier recommendations of the Steering Committee or to suggestions from individual participants, and included: (a) high and low CCN concentrations; (b) a bimodal distribution (experiment 10); (c) a test of instrument ability to read accurately and consistently over a period of time (experiment 21); and (d) a test of the "zero" of instruments sampling particle-free air (experiment 25). Experiments 27, 28 and 29 utilized AgI and paraffin wax aerosols, to see if nucleation phenomena could be observed on these nominally insoluble aerosols.

The results of the Workshop may be categorized according to generic type of CCN counter (static diffusion chambers, CFD chambers, IHC's, etc.) and according to the basic goals of the Workshop (instrument intercomparisons, and experiments of basic scientific relevance).

Nine static diffusion chambers (SDC) participated, of which five were found to perform consistently well. In the experiments utilizing monodisperse aerosols, the CCN spectra obtained from the SDC's (or any CCN counter) can be used to measure the critical supersaturation (S_c) of the test aerosol, and the result compared to the theoretical value obtained by application of the Kohler theory. The better SDC's were found to be able to measure S_c to within about $\pm 0.1\%$ supersaturation. Taking the NRL mobility analyzer concentration values as a standard, the combined average CCN concentrations

from the five best SDC's agreed with this device to within 10% at 1% supersaturation, and no worse than 20% at other settings. The SDC's were also found to agree with the CFD chambers to within about 15% over their common supersaturation range. The general spread of the SDC data was in excess of that at the Fort Collins Workshop (1970), but this may be attributed to the greater number of SDC's present at the 1980 Workshop, many of which had been previously untested.

TABLE II

List of experiments

No.	Date			Aerosol A – Ambient; M – Monodisperse; P – Polydisperse
0	Tues	7 Oct	AM	M – $(NH_4)_2SO_4$
1	Tues		PM	P – NaCl – oscillating concentration
2	Tues		PM	P – NaCl – higher concentration
3	Wed	8 Oct	AM	A – quite fluctuating
4	Wed		AM	M – NaCl – low concentration
5	Wed		PM	M – NaCl – medium concentration
6	Wed		PM	A
7	Thurs	9 Oct	AM	A – aborted – duct blockage
8	Thurs		AM	M – NaCl – slight drift down
9	Thurs		AM	M – NaCl – higher concentration
10	Thurs		PM	Bimodal – NaCl – "flat k"
11	Thurs		PM	A
12	Fri	10 Oct	AM	A
13	Fri		AM	P – $(NH_4)_2SO_4$
14	Fri		PM	P – $(NH_4)_2SO_4$
15	Fri		PM	M – $(NH_4)_2SO_4$
16	Fri		PM	A
17	Mon	13 Oct	AM	A
18	Mon		AM	M – $(NH_4)_2SO_4$
19	Mon		AM	M – $(NH_4)_2SO_4$
20	Mon		PM	M – $(NH_4)_2SO_4$
21	Mon		PM	M – $(NH_4)_2SO_4$ – time variations
22	Tues	14 Oct	AM	P – $(NH_4)_2SO_4$ – medium concentration
23	Tues		PM	P – $(NH_4)_2SO_4$ – low concentration
24	Tues		PM	P – $(NH_4)_2SO_4$ – high concentration
25	Wed	15 Oct	AM	Filtered air – noise check
26	Wed		AM	A
27	Wed		PM	P – AgI, "insoluble"
28	Wed		PM	M – AgI, "insoluble"
29	Wed		PM	P – paraffin, hydrophobic

Five continuous-flow diffusion (CFD) CCN counters were present; two of these (from the University of Washington, and from the Desert Research Institute) were arranged to simultaneously yield three or four points on a CCN spectrum. One device was only very recently designed and constructed before the Workshop and did not always provide data. The other four devices were often in good agreement with theory and with each other. In measuring the S_C of monodisperse aerosols (as discussed above for SDC's), the CFD chambers gave values agreeing with theory to within an average of about 0.05% supersaturation. The total count data of four of the CFD chambers (excluding the most recently constructed device) for these monodisperse cases showed that the CFD's agreed with each other to within about 15% (5% when diffusion losses were properly accounted for). In polydisperse and ambient cases, the

CFD chambers agreed with each other to within about 15% at 0.7% supersaturation, and about 20% at 0.3% supersaturation. Most of the discrepancies could also be explained in terms of aerosol diffusion losses in the sample inlet systems of some of the CFD chambers.

Only four isothermal haze chambers (IHC) were present, one of which was newly-constructed at the time of the Workshop. These devices typically showed a large spread (many tens of percent) in indicated number concentration, as well as in their measurements of the S_C of monodisperse aerosols. Two of the devices (one of which is a "second-generation" device, technologically, and the other of which is a "dual-mode" CFD – IHC) agreed to within about 40% with each other and the NRL mobility analyzer. A third IHC showed this type agreement only at the lower end of the S_C spectrum and a factor of 2 agreement otherwise. The counts of all four of the instruments were generally at least proportional to the count of the NRL mobility analyzer. It was concluded that the calibration of, and interpretation of the data from the optical particle counting-sizing sensors in use on the IHC's was a major factor in analyzing their data, and in comparing two or more IHC's.

There were three novel and prototype devices in operation at the Workshop: a "diffusion tube" CCN counter from York University; a CFD chamber delivering its output to an impactor (from Florida State University); and an impactor combined with a humidifying chamber, from the University of Alaska. It is especially noteworthy that the Florida State University group used their samples for PIXE analysis, to check the purity of aerosols generated during the Workshop. These devices all performed reasonably well and detailed discussions of their design and construction may be found in the complete Workshop Proceedings volume (as also may be found detailed discussions of the SDC, CFD, and IHC devices).

Two Aitken counters were also present, and served the practical purpose of monitoring the output of the test aerosol generation system. When monodisperse aerosols were being sampled, these devices agreed rather well with the CCN counters.

The remaining goals of the Workshop – experiments of basic scientific interest – were addressed in part by examination of silver iodide and paraffin wax aerosols. Both monodisperse and polydisperse silver iodide aerosols were found to be active as CCN. Use of the monodisperse aerosol allowed a comparison of the measured and theoretical S_C, which were found to be approximately 0.6% and 4%, respectively. The reason for the discrepancy is still a matter of debate, but the resulting lowering of the S_C from the theoretical value has been observed in similar experiments before, and point to the likelihood that silver iodide prepared for cloud seeding experiments is active as CCN as well. The paraffin wax aerosol was found to be inactive as CCN.

Drs. J. Jiusto and *G. Lala* have addressed one of the other questions of basic scientific interest, whether the CCN spectrum slope, k, is consistently related to the exponent, β, in the power function expression of cumulative particle concentration: $N_{cum} \propto r^{-\beta}$. Workshop results did tend to verify the theoretical relationship $k = 2/3\ \beta$, when β was deduced from the size distribution data provided by the NRL mobility anlayzer. It was, however, sometimes necessary to evaluate k twice on any given CCN spectrum, depending on whether or not the determination was made above or below the inflection point usually occurring on the spectrum curve in the vicinity of 0.1% to 0.2% supersaturation.

3. Conclusions

The 1980 International CCN Workshop provided an occasion for users of SDC's, CFD chambers, and IHC's to intercompare their instruments and to perform experiments of basic scientific relevance. Salient points to be made from the twenty-nine experiments include the following:

(a) Test aerosols of pure soluble salts, both monodisperse and polydisperse, were provided with stability in output concentration to about 3% per hour;

(b) Five of the best SDC's (averaged) agreed to within at least 20% of the NRL mobility analyzer and to within 10% at 1% supersaturation. The coefficient of variation ($\sigma/\bar{N}$) of the five instruments was 0.42 at 0.2% supersaturation 0.31 at 0.5% and 0.24 at 1.0%. These devices could measure the S_C of monodisperse aerosols to within about $\pm 0.1\%$ supersaturation;

(c) Four CFD chambers agreed with each other to within about 15% at 0.7% supersaturation and to 20% at 0.3% supersaturation, with most of this discrepancy being accounted for by diffusion losses. All four CFD chambers could measure the S_C of the monodisperse aerosols to within about $\pm 0.05\%$ supersaturation;

(d) The best SDC's and CFD chambers agreed to within about 15%;

(e) Two of four IHC's agreed with each other to within about 40%;

(f) Workshop results were generally in confirmation of the theoretical relationship between the CCN spectral slope, k, and dry aerosol size distribution slope, β, in the form $k = 2/3\ \beta$. It was necessary, however, to evaluate k on each side of inflection points in the CCN spectra, which typically occurred around $S_C = 0.1\%$ to 0.2%.

Acknowledgements. This work was sponsored by the National Aeronautics and Space Administration, Grant No. NAS8 – 33820, and the National Science Foundation, Grant No. ATM79 – 21558.

IDŐJÁRÁS

Az Országos Meteorológiai Szolgálat folyóirata, 86. évf. 2—4. szám, 1982. március—augusztus
Journal of the Hungarian Meteorological Service, Vol. 86. No. 2—4. March—August 1982, Budapest

A new cloud condensation nucleus counter

T. OHTAKE, *Geophysical Institute University of Alaska, Fairbanks, Alaska 99701, U.S.A.*

Új felhő-kondenzációs mag számláló. Az individuális felhő-kondenzációs magvak (CCN) kémiai összetételének tanulmányozása végett aeroszol részecskéket gyűjtöttünk mikroszkóp lemezeken elektrosztatikus precipitátor segítségével. A részecskéket ezután egy kis kamrában higroszkópossági vizsgálatnak vetettük alá különböző nedvességi feltételek között. A részecskéken kondenzálódott vízcseppek számából határoztuk meg a CCN koncentrációt. A kondenzációs magvakat elektron energia-spektrométerrel vizsgálva azt tapasztaltuk, hogy az Alaszkában gyűjtött CCN-ek ammónium-szulfátot tartalmaznak. Az energia diszperzív röntgen spektrométerrel végzett mérések szintén kén jelenlétére utaltak a kondenzációs magvakban.

*

A new cloud condensation nucleus counter. In order to investigate the chemical composition of individual cloud condensation nuclei, aerosols are collected on slide glasses by an electrostatic precipitator. The particles are later subjected to hygroscopicity tests in a small chamber under various humidity conditions. Optical micrographs showing numbers of water droplets condensed on the aerosol particles give concentrations of CCN. Examination of the CCN by an electron energy loss spectrometer revealed that a CCN particle collected in Interior Alaska contained $(NH_4)_2SO_4$. The X-ray energy dispersive spectrometer technique independently identified sulfur in the CCN particles.

*

Unlike typical cloud condensation nucleus (CCN) counters, this device counts the numbers of water droplets condensed on aerosol particles sampled on a microcover glass at various different relative humidities. The relative humidities ranged from 75% to a calculated value of 110%. A schematic of the apparatus is shown in *Fig. 1.* The individual CCN can be identified in an

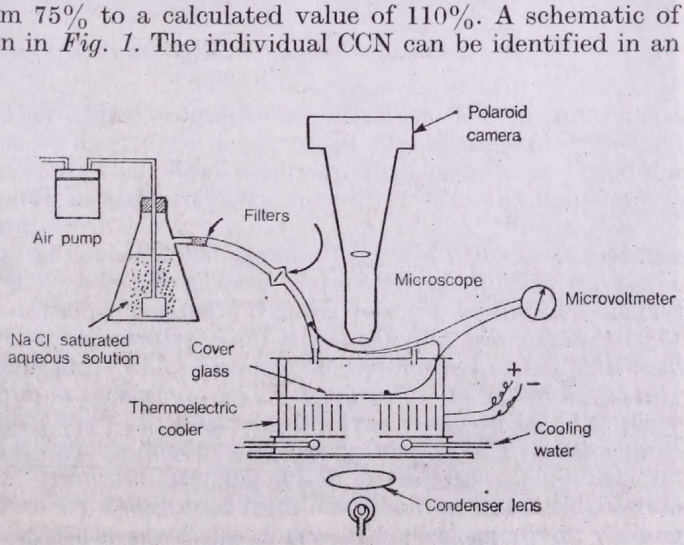

Fig. 1: Schematic of apparatus showing humidifying chamber and operational mode

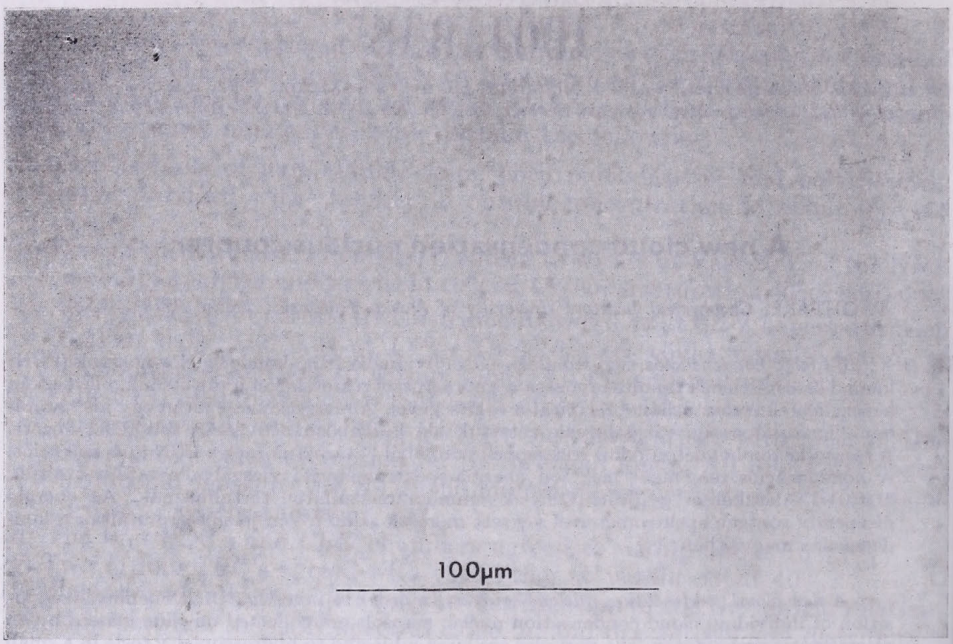

Fig. 2a : Photo micrograph of aerosols collected by electrostatic sampler under conditions of 75% relative humidity

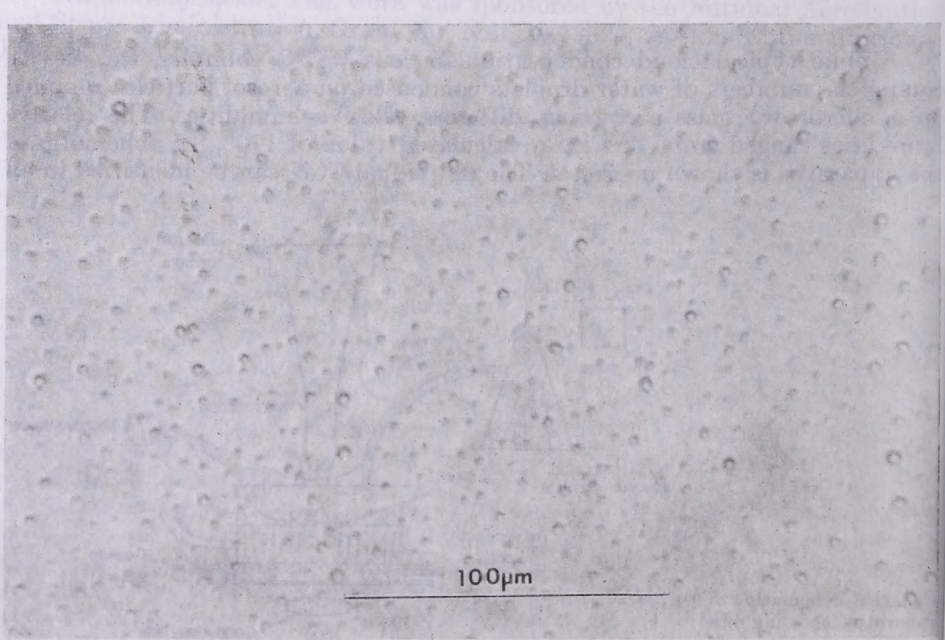

Fig. 2b : Same as *Fig. 2a* except relative humidity is 98%

optical micrograph and an electron micrograph for finding their size distributions and their growth rates, and may be inspected for their chemical composition later.

Sampling is made onto microcover glasses or electron microscope grids by means of an electrostatic precipitator and a vacuum pump. The sampling system allows collection of particles between 0.01 and 10μm diameter in an air volume of 0.001 to 1 cm^3 on an area of 0.2 mm by 0.3 mm of a substrate (0.25 mm thick) as a uniform distribution (*Liu*, et al., 1967). The cover glass is then transferred to the small humidifying chamber, where temperature is controlled

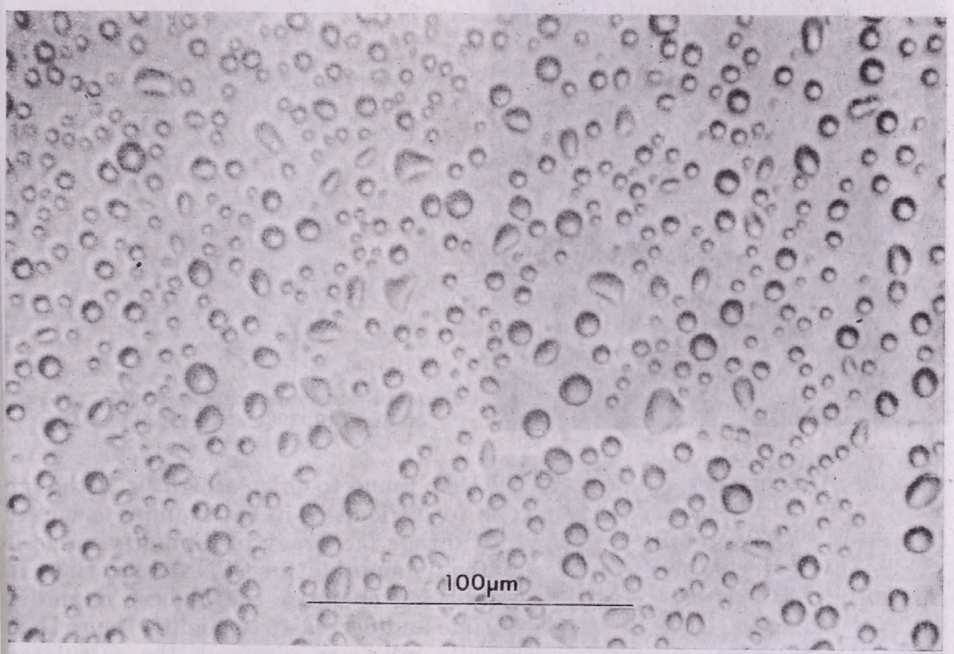

Fig. 2c: Same as *Fig. 2b* except calculated relative humidity is 101%

by a thermoelectric cooler at the bottom of the chamber. The chamber has a closed glass top and is connected to a controlled humid air supply, which consists of an air pump and a bottle with saturated aqueous solution of sodium chloride, giving an equilibrium relative humidity of 75% in the temperature range between 20°C and 70°C.

As the cover glass is cooled down by applying a direct current to the thermoelectric cooler, it is chilled to a lower temperature producing a relative humidity of 100%. Additional current produces relative humidities beyond water saturation. The exact saturation point is identified by the observation of dew on the cleaned cover glass which was previously cleaned and coated with aluminum, using vacuum evaporation to form a mirror on its backside, leaving the center portion uncoated. Simultaneously, the temperature difference between the cover glass and the air is observed by means of a thermocouple and a microvolt meter from the starting point of cooling, giving the "0" reading. Humidity values are determined from interpolation and extrapolation of the microvolt reading at the point dew forms. A typical microvolt reading

at the dew point is about 100 μV, representing a 25% humidity difference. In this case, every 4 μV change indicates a 1% relative humidity change. Consequently, an 8 μV reading, higher than that necessary to obtain the dew point, gives a nominal 2% supersaturation. Due to various cooling water tempera-

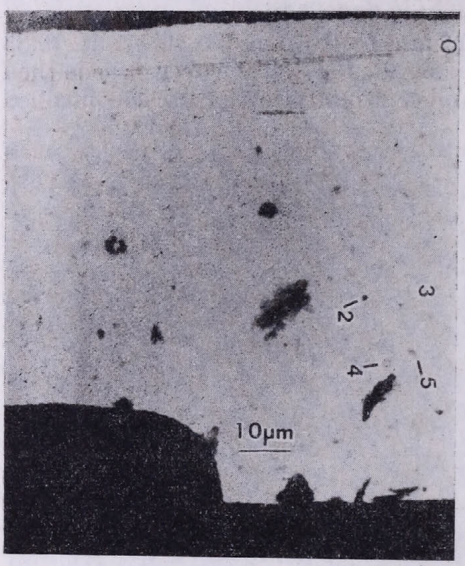

Fig. 3: Electron micrograph of CCN collected on June 19, 1981 at Fairbanks, Alaska

tures, the reading at the dew point has been found to change slightly. Although poor resolution of supersaturation due to difficulties in determining accurate temperatures was found to be a disadvantage (accuracy of humidity value is 2% RH), the technique seemed practically suitable for CCN observations in the natural atmosphere. In the humidifying chamber the highest humidity seems to reach 102% RH for a short time and decreases to slightly more than 100% RH after water droplets form on a substrate, although the calculated humidity slightly exceeds water saturation. This condition could be very similar to that found in natural clouds.

The condensed water droplets are photographed for counting by a Polaroid micrograph camera or a normal microscope camera. Since the sizes of the water drops on a cover glass are larger than 5 μm, the resolution of an optical microscope is adequate. An example of micrographs of growing particles can be seen in *Fig. 2a–c*.

The problem on the previous model with humidifying chamber, which had humid air standing still, was the humidity value on a substrate where the aerosols were sampled. Water vapor molecules tend to diffuse to the particles, and some condensed water drops will restrict many adjacent aerosols from condensing to water drops as pointed out by *Lala* and *Jiusto* (1972) for the case of ice nucleation. Effective relative humidity on the substrate may therefore never have reached water saturation. In order to break the microscale boundary layer over hygroscopic particles, ventilation of air at the controlled humidity of 75% RH is supplied to the chamber. The amount of air at 1.5 liter/min or 7 cm/s air movement in the chamber seems to be adequate for activation of all effective CCN particles.

The greatest advantage of this technique is to allow the inspection of sizes and chemical composition of the individual nuclei by electron microscopes combined with an X-ray energy spectrometer (XES) or an electron energy loss spectrometer with a specimen cooling device to prevent possible heating on

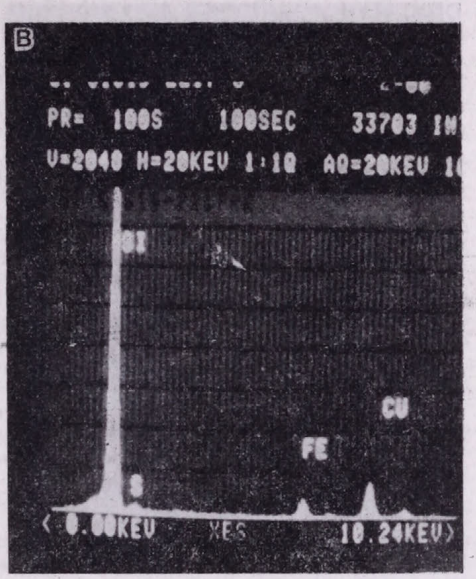

Fig. 4: XES display of particle 2 shown in *Fig. 3*

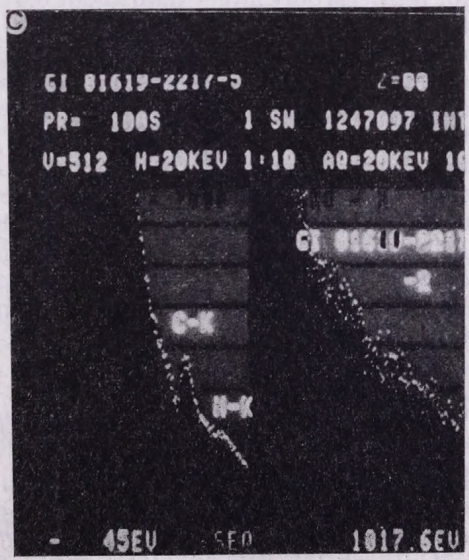

Fig. 5: EELS display of a portion of particle 2 (as shown in *Fig. 3*)

volatile nuclei. Such analysis is in progress for aerosols sampled over the Arctic Ocean and Interior Alaska. The second advantage is that aerosols sampled can be stored for a long time and their condensation ability can be examined later.

For example, although the aerosols were previously collected by means of

an impactor which obtains particles with a minimum size of 0.3 μm diameter, most of the CCN over the Arctic Ocean contained sulfur for the particle range of 0.3 to 15 μm according to XES analysis. However, XES can detect the chemical composition of elements with an atomic number larger than 10 and

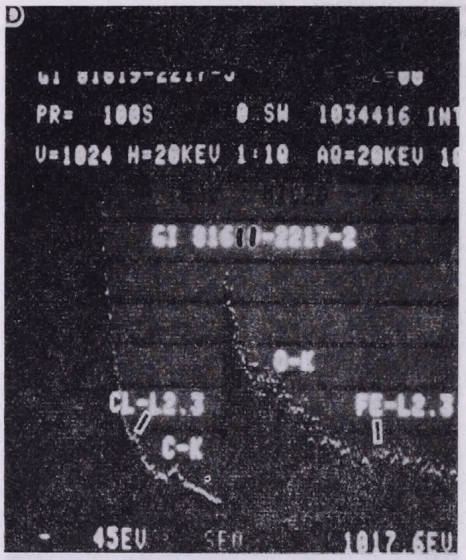

Fig. 6: EELS display of another portion of particle 2 (as shown in *Fig. 3*)

for particles only larger than about 0.3 μm. So, the indication of S does not mean that a particle consists of pure sulfur, but could be H_2SO_4 or $(NH_4)_2SO_4$ as a sulfuric compound. On the other hand, electron energy loss spectrometer (EELS) combined with a scanning transmission electron microscope (STEM) can expand the detectable elements with atomic numbers smaller than 10. Using an electron beam size of 0.03 μm, resolution of analysis is sufficient to analyze the smallest CCN particles. *Figure 3* is a STEM micrograph showing the particles with the numbers collected on a specimen grid coated with collodion/carbon film. *Figure 4* is an XES display of particle 2 showing Si, S and Fe overlapping with Cu from copper grid and C from carbon coating. *Figures 5* and *6* are EELS displays showing that the particle contained S, Cl, N, O and Fe. From these figures particle 2 contained qualitatively $(NH_4)_2SO_4$ rather than H_2SO_4.

Acknowledgements. The author is indebted to JEOL Ltd. for the opportunity to inspect Alaskan CCN particles by EELS and STEM. The work was supported in part by the National Science Foundation Grant ATM 77-27748 and State of Alaska funds.

REFERENCES

Liu, B. Y. H., Whitby, K. T. and *Yu, H. H. S.*, 1967: Electrostatic aerosol sampler for light and electron microscopy, *Review Sci. Instr. 38*, 100–102.

Lala, G. G. and *Jiusto, J. E.*, 1972: Numerical estimates of humidity in a membrane-filter ice nucleus chamber, *Jour. Appl. Meteor. 11*, 674–683.

IDŐJÁRÁS

Az Országos Meteorológiai Szolgálat folyóirata, 86. évf. 2–4. szám, 1982. március–augusztus
Journal of the Hungarian Meteorological Service, Vol. 86. No. 2–4. March–August 1982, Budapest

Nature of fog nuclei from measurements of relative humidity

H. GERBER, *Naval Research Laboratory, Washington, D.C., 20375, U.S.A.*

Köd-kondenzációs magvak természetének tanulmányozása relatív nedvesség mérés alapján. A relatív nedvesség meghatározására érzékelőként szubmikron méretű sóoldat-cseppekkel bevont hidrofób felületet használtunk, amelyet sűrű kisugárzási ködbe helyeztünk ki. A sóoldat-cseppek által szórt fényből számítottuk a relatív nedvességet, amely igen gyorsan fluktuált a telítetlen és a túltelített állapot között, de középértékben alacsonyabb volt 100%-nál. A mérések során tapasztaltak szerint a turbulencia nagy hatással van a köd mikrostruktúrájára. Így a kondenzációs mag-spektrum és a ködcsepp-spektrum Euler-típusú méréséből meghatározott „effektív túltelítettség" félrevezető lehet. Ezért fontosnak tűnik a ködben kialakuló turbulens örvények szerepének földerítése, mert ezáltal, hogy időszakosan jelentős túltelítettség alakulhat ki, nagyobb kritikus túltelítettséghez tartozó köd-kondenzációs magvak (nagyobb számban) aktivizálódhatnak, mint azt korábban gondoltuk.

*

Nature of fog nuclei from measurements of relative humidity. A hydrophobic substrate coated with salt-solution haze droplets is a sensor which was exposed in dense radiation fog. Light scattered by the haze droplets was used to obtain the relative humidity (RH) which fluctuated rapidly between unsaturated and supersaturated conditions, but which had a time-averaged value of less than 100%. These measurements suggest that turbulence has a strong influence on the microphysics of the fog. Thus the "effective supersaturations" determined from Eulerian-type measurements of nuclei spectra and droplet size distributions may be misleading. Instead, it becomes important to understand the role of turbulent eddies in the fog where sporadic excursions into the supersaturation regime activate fog nuclei at greater supersaturations (and numbers) than previously thought.

*

1. Instrumentation.

A new saturation hygrometer has recently been described (*Gerber*, 1980) which is capable of measuring relative humidity over the range of about 95% to 105% RH. The performance of the hygrometer depends on the reaction of small salt particles to the ambient RH. These particles are situated on a thin hydrophobic mirror which was designed to cause a minimal interference on the response of the particles to changes in RH. As the ambient RH exceeds the deliquescent point of the salt particles, $\approx 80\%$ RH for the $(NH_5)_2SO_4$ particles used here, the particles become salt solution droplets and swell in size. This size is monitored optically by measuring the light scattered from the droplets on the mirror. The intensity of the scattered light is related to the ambient RH up to a value of RH = 100%. Above 100% RH the function of the instrument becomes similar to that of the familiar dew point hygrometers, except that now the mirror is heated to control the droplet deposit instead of being cooled. Enough heat is applied to the mirror to cause the solution droplets to remain at their 100%-RH size. The temperature increase of the mirror is directly related to the ambient RH (supersaturation S in this

case). The choice of RH = 100% above which the hygrometer employs the thermo-optical feedback loop is dictated by convenience: of all large values of RH, RH = 100% can be most easily generated to calibrate the hygrometer; the hygrometer is placed in an insulated sealed box with interior walls wetted with distilled water.

For RH > 100% the saturation hygrometer was calibrated in the laboratory using a large continuous-flow thermal-gradient diffusion chamber. These calibrations showed that the solution droplet deposit on the hydrophobic mirror had a strong resilience to change, which was a critical aspect in the successful application of this technique. The droplet deposit was also stable, i.e., it showed no changes in its light-scattering properties, during its 10 hours of exposure in radiation fog. This desirable stability was suggested in similar work with hydrophobic substrates by *Wylie* et al. (1965).

2. Measurements

The first field test of the new hygrometer was described by *Gerber* (1981). Measurements were made on two successive nights in radiation fog which formed over a flat grassy area in rural Virginia. The hygrometer was situated 1 m above the ground. *Figure 1* shows the measured RH for a typical 1-hour period of the fog in which the visual range remained less than 1 km at nearly all times. Rapid fluctuations in RH are evident in this Figure, suggesting (along with the temperature, light transmission, and droplet-size-spectra records) that turbulence played a significant role in controlling this fog. The humidity only sporadically exceeded 100%, which is consistent with the highly structured nature of the fog, where patches containing activated droplets appeared to be separated by areas containing just haze droplets. (The difference in the record in Fig. 1 for RH > 100% and RH < 100% is due to the different time response of the hygrometer for those two ranges.)

The frequency distribution of RH in the radiation fog is shown in *Fig. 2*. The curve was constructed from values of RH measured in the fog every

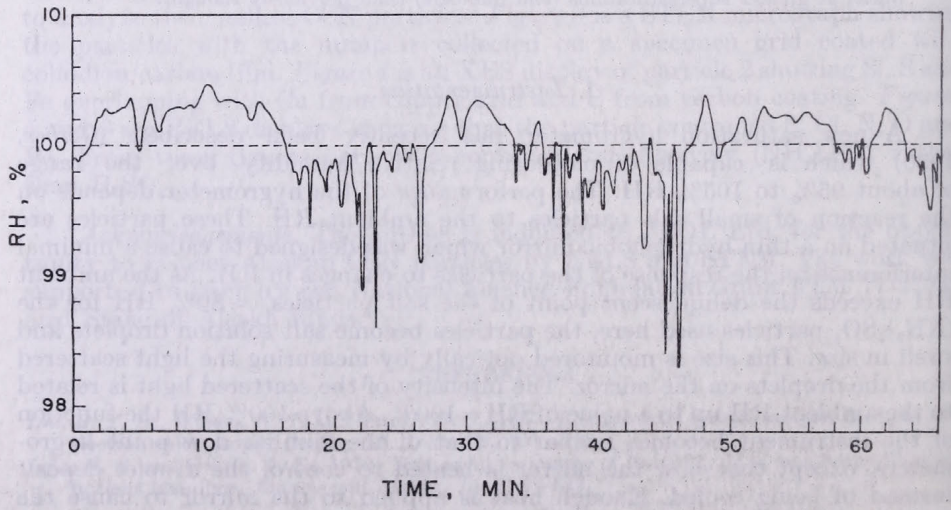

Fig. 1: Time dependence of the relative humidity (RH) measured in radiation fog from 0400 to 0506 LST on 20 November 1979 in Lake Fairfax County Park, Virginia

30 seconds over a four-hour period. The similarities of this curve to the spectrum calculated by *Warner* (1968) for moderately-sized cumuli is noteworthy. A major difference is that the average RH in the radiation fog was less than 100%.

3. Interpretation

The measurements described in the preceding show that it is difficult to define an "effective supersaturation" for this fog. Not only is the fog unsaturated on the average, but it also has a spectrum of supersaturations. For this fog the technique used by *Hudson* (1980) to determine the "effective supersaturation" would not be accurate. Essentially he compared isothermal-haze-chamber measurements with droplet size spectra measured with an optical particle counter to arrive at the critical or "effective" supersaturation in the fog; fog inhomogeneities were not considered. However, the possibility exists that Hudson's measurements along the US Pacific coast were in fogs of much more homogeneous nature than the described radiation fog, so that his approach is valid. Of course, the possibility also exists that most fogs are strongly inhomogeneous and that unsaturated fogs often exist. The latter would be consistent with the many earlier (and mostly forgotten) measurements of RH in fogs which showed unsaturated conditions the majority of the time (see the list of references in *Pruppacher* and *Klett*, 1978).

The similarity in the shape of the spectra in Fig. 2 comes from the same cause: drier air mixed by turbulent exchange with the moist air in the cumuli/fog causes a substantial fraction of the cumuli/fog to be unsaturated. This fact is well known for cumuli where a submoist adiabatic lapse rate is

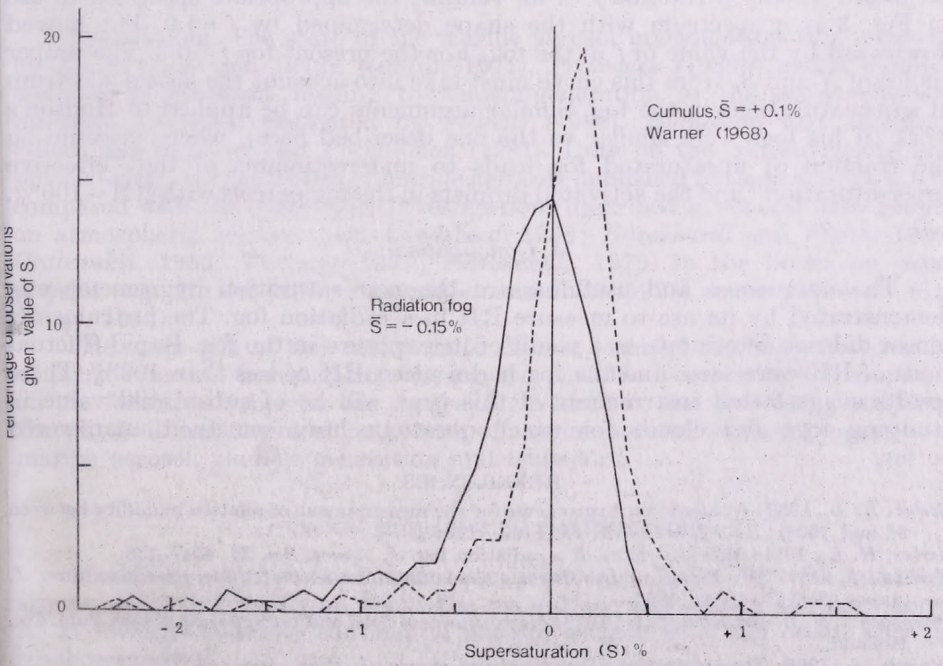

Fig. 2: Frequency distribution of water vapor supersaturation in moderately-sized cumuli (*Warner*, 1968) and in one case of radiation fog; $\bar{S}$ = average supersaturation

generally the rule. The mixing of drier air above the fog with the fog layer gives the same results. It is thus necessary (at least for the present fog) to differentiate between the saturated and unsaturated portions of the fog when discussing "effective supersaturations".

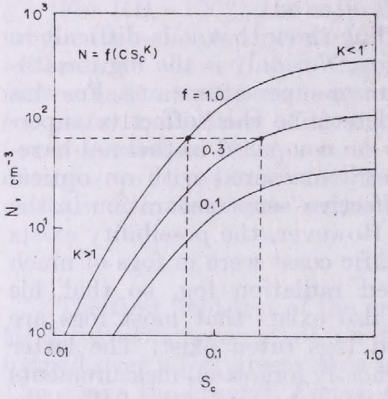

Fig. 3: Hypothetical fog condensation nuclei spectra: N = number of active nuclei, S_c = critical supersaturation; given a fog in which only a fraction $f = 0.3$ of the volume is supersaturated, an estimate of the effective supersaturation in the supersaturated regions is given by the larger value of S_c

In *Fig. 3* the curve for $f = 1.0$ represents a hypothetical FCN (fog condensation nuclei) spectrum measured in the atmosphere with, for example, an isothermal haze chamber and a thermal-gradient diffusion chamber. This spectrum reflects the concentration N of nuclei active at the given critical supersaturation S_c per unit volume of air. However, since the fog is supersaturated in only a fraction f of its volume, the appropriate spectrum to use in Fig. 3 is a spectrum with the shape determined by $f = 1.0$, but moved downward by the value of f in the fog. For the present fog $f \approx 0.3$. The proper choice of N and S_c from this curve must take into account the actual spectrum of supersaturations in the fog. Similar arguments can be applied to Hudson's work (if his fogs were similar to the one described here), where discounting the fraction of unsaturated fog leads to underestimates of the "effective supersaturation" and the activated droplets in the fog parcels with RH > 100%.

4. Conclusions

The uniqueness and usefulness of the new saturation hygrometer was demonstrated by its use to measure RH in a radiation fog. The instrument's sensor did not deteriorate as a result of its exposure in the fog. Rapid fluctuations of RH were seen, and the fog had a mean RH of less than 100%. These results suggest that instruments of this type will be of substantial value in studying fogs and clouds for which questions have remained unanswered so far.

REFERENCES

Gerber, H. E., 1980: A saturation hygrometer for the measurement of relative humidity between 95 and 100%. *J. Appl. Meteor. 19*, 1196–1208.

Gerber, H. E., 1981: Microstructure of a radiation fog. *J. Atmos. Sci. 38*, 454–458.

Hudson, J. G., 1980: Relationship between condensation nuclei and fog microstructure. *J. Atmos. Sci. 37*, 1854–1867.

Pruppacher, H. R. and *Klett, J. D.*, 1978: *Microphysics of cloud and precipitation.* Reidel Publ. Co., Holland.

Warner, J., 1968: The supersaturation in natural clouds. *J. Rech. Atmos. 3*, 233–237.

Wylie, R. G., Davies, D. K. and *Caw, W. A.*, 1965: The basic process of dew-point hygrometer. *Humidity and moisture, Vol. 1*, R. E. Ruskin, Ed., Reinhold Publ. Co., New York.

IDŐJÁRÁS

Az Országos Meteorológiai Szolgálat folyóirata, 86. évf. 2–4. szám, 1982. március–augusztus
Journal of the Hungarian Meteorological Service, Vol. 86. No. 2–4. March–August 1982, Budapest

Marine aerosol research

J. PODZIMEK, *Department of Mechanical and Aerospace Engineering and Graduate Center for Cloud Physics Research, University of Missouri-Rolla, Rolla, MO 65401, U.S.A.*

Tengeri aeroszol-kutatások. A tanulmány összefoglalja a tengeri és óceáni levegőben lévő aeroszol részecskék koncentrációjára, nagyság szerinti eloszlására, optikai tulajdonságaira és kémiai összetételére vonatkozó legújabb eredményeket. Tárgyalja a részecskék keletkezésének és terjedésének lehetséges módjait, végül a tengeri aeroszol-kutatások jövőjét vázolja fel.

*

Marine aerosol research. The aim of this paper is to give a review of recent research carried out in the field of marine aerosols. New results concerning the concentration, size distribution, optical properties and chemical composition of the aerosol particles in maritime and oceanic atmosphere are summarized. The formation and transport mechanisms of marine particles as well as the future of marine aerosol research are also discussed.

*

Introduction. The state of the marine aerosol investigation was reviewed by *Junge* (1969 and 1972), *Georgii* (1975), *Podzimek* (1980b) and a detailed analysis of processes leading to aerosol generation at the sea-atmosphere interface has been presented by *Morelli* (1980), *Blanchard* and *Woodcock* (1980) and by *Lord* and *Pocklington* (1981). Data on the concentrations and physico-chemical properties of marine aerosols published in these studies can be compared with the other older investigations described in several monographs on atmospheric aerosols (e.g. *Landsberg*, 1938; *Burckhardt* and *Flohn*, 1939; *Grabovskii*, 1956; *Twomey*, 1977; *Petrenchuk*, 1979) in the books on cloud physics (e.g. *Mason*, 1971; *Pruppacher* and *Klett*, 1978) or air chemistry (e.g. *Junge*, 1963).

The main aim of this review is to discuss some of the important results of marine aerosol investigation during the past ten years with the emphasis on the following subjects: the geographical location and art of the sampling, the physical and chemical properties of marine aerosol, optical properties of marine aerosol, particle generation and transport.

Physical properties of marine aerosol

Marine aerosol discussed in this study covers all particles with minimum size around 0.002 μm found above the sea surface and in high altitudes above it. It includes also the continental aerosol drifted over the ocean and the seashore aerosol.

Glancing over the plotted data on worldwide distribution of AN concentrations (e.g. *Podzimek*, 1980b), the most interesting is the fact that in spite

of the dramatic change in the use of fossil fuels during the past fifty years and the alteration of the mode of transportation, the AN concentrations measured now over the North Atlantic do not deviate much from the "Carnegie" expedition measurements. The impact of large cities and industrialized areas in the

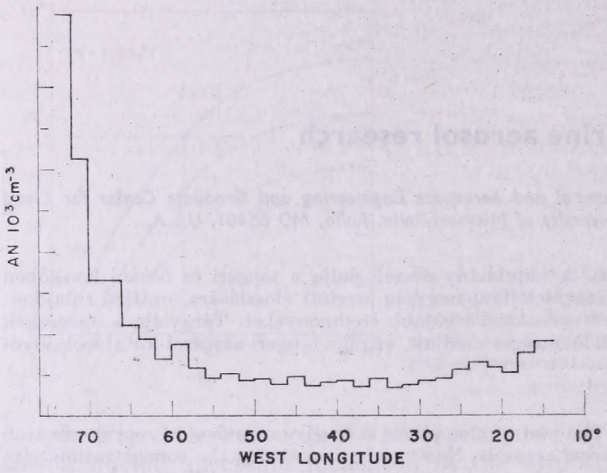

Fig. 1: Mean Aitken nucle concentration measure d ove the North Atlantic betw e en 36 and 44°N latitude during th period 1966–1973 *(Hog an, A.* 1976, ASRC, Pub. 408, SUNY Albany)

USA and Europe on the AN counts over the Atlantic Ocean is documented by many authors (*Hogan* et al., 1967; *Hogan* et al., 1973; *Schaefer*, 1972) who found in very clean environment over the North Atlantic concentrations

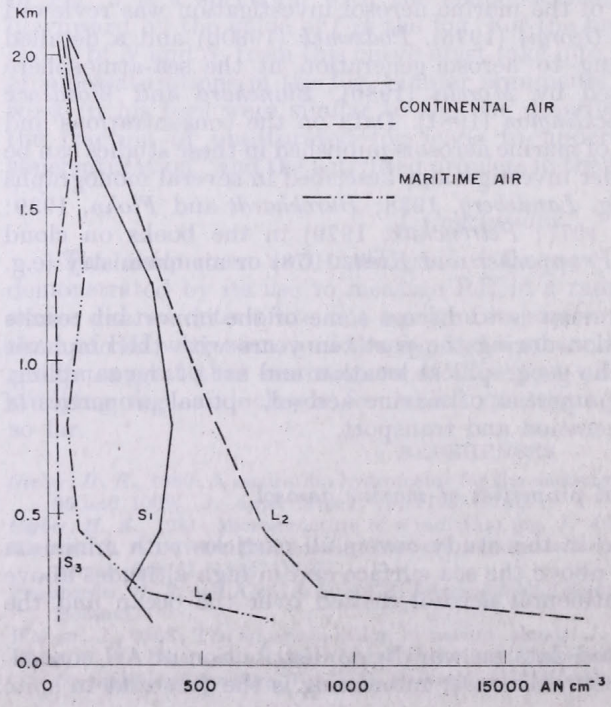

Fig. 2: Aitken nuclei concentration profiles measured over southern Texas (*L*) and 50 km offshore over the Gulf of Mexico (*S*) in the continental (S_1, L_2) and maritime (S_3, L_4) air mass (*Podzimek*, 1980c)

between 200 and 500 AN cm^{-3}. Close to the seashore the concentrations rose up to several thousands of AN cm^{-3} *(Fig. 1)*. A similar picture was obtained in the Pacific Ocean eastwards of Japanese seashore.

The vertical distribution of AN over the ocean shows a strong dependence on the air mass origin and air stability. A typical AN concentration vertical profile is presented in *Fig. 2*, which includes four different curves deduced from the sampling 50 km off shore of South Texas (S) and 50 km over the continent (L) in continental (S_1 and L_2) and maritime air (S_3 and L_4). In both situations there was a strong temperature inversion in the PBL over land. Over the sea surface there was almost an indifferent stratification with very little change in AN concentration through the PBL (*Podzimek*, 1980c). A similar picture has been obtained by *Allee* (1974) in the proximity of Barbados Island where AN concentration varied within 200 and 300 AN cm^{-3} almost up to 3.7 km altitude. Another challenging subject reflecting the complexity of AN measurements in high altitudes over the ocean seems to be the increased AN concentration above and between the clouds of Intertropical Convergence Zone discussed by *Podzimek* et al. (1975; 1977) and recently stressed by *Hogan* (1981) who found higher AN counts in the ITCZ region than on the ocean surface.

One of the most detailed investigations of the AN size distribution over the Atlantic Ocean has been made by *Jaenicke* et al. (1971) and *Jaenicke* (1978a). They concluded that besides the large concentration of particulates of 10^{-3} μm in radius there is a distinct maximum at $r = 3.10^{-2}$ μm. This does not contradict the finding by *Schultz* et al. (1978) who measured AN in the same environment. Some discrepancies have been found, however, between the filter technique and diffusion battery technique (*A. Mészáros* and *Vissy*, 1974; *Prahm* et al., 1976; *Tymen* et al., 1975; *Jaenicke* and *Schütz*, 1977). In *Fig. 3*, which was published by *Jaenicke* (1978a), there are plotted, besides the AN size distributions measured by different authors on the high sea, also the data from continental stations and our data (*Podzimek*,

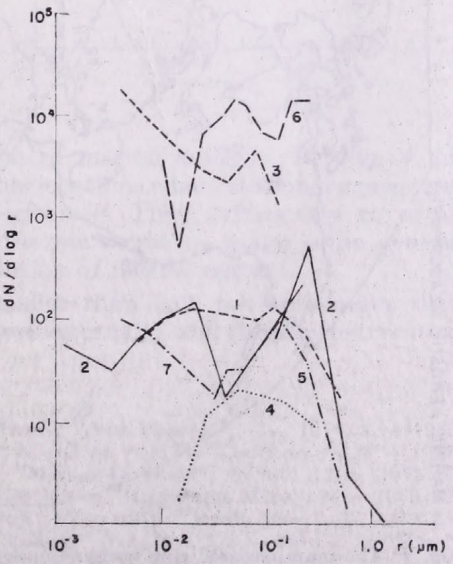

Fig. 3: Aitken nuclei size distribution reported by different authors (the total nuclei concentration – if measured — is indicated in paranthesis): *1* – *Tymen* et al., 1975 – 242 cm^{-3}; *2* – *Jaenicke*, 1978a – 370 cm^{-3}; *3* – *Sverdrup*, 1977, (*see Jaenicke*, 1978a) – 12,800 cm^{-3}; *4* – *Prahm* et al., 1976; *5* – *Mészáros A.* and *Vissy*, 1974 – 440 cm^{-3}; *6* – *Tanner* et al., 1977, (*see Jaenicke*, 1978a); *7* – *Podzimek*, 1980c – 550 cm^{-3}

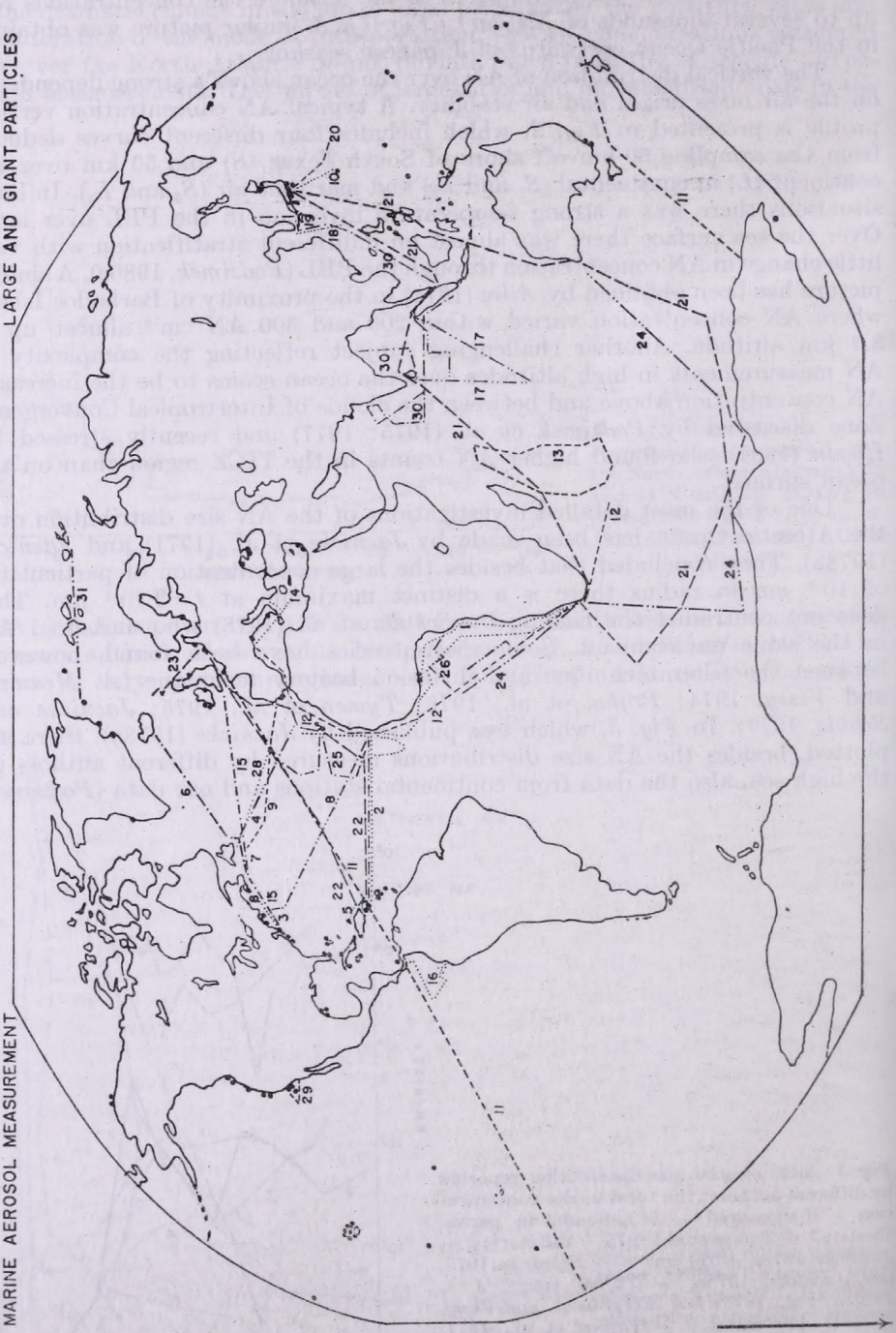

Fig. 4: The main research ship cruises (marked with lines) and the sites of stationary marine

1980c) deduced from the measurement with the diffusion battery on the South Padre Island (Texas) at very high humidity (haze or dissipating fog). Comparison of the AN size distribution curves leads to the conclusion that the curve shapes are quite different – depending on the aerosol dynamics and interaction and probably the measuring techniques – although the measured concentrations do not deviate considerably.

The size distribution of particulates with diameters larger than 0.2 μm has been done frequently during the cruises of research vessels and in rela-

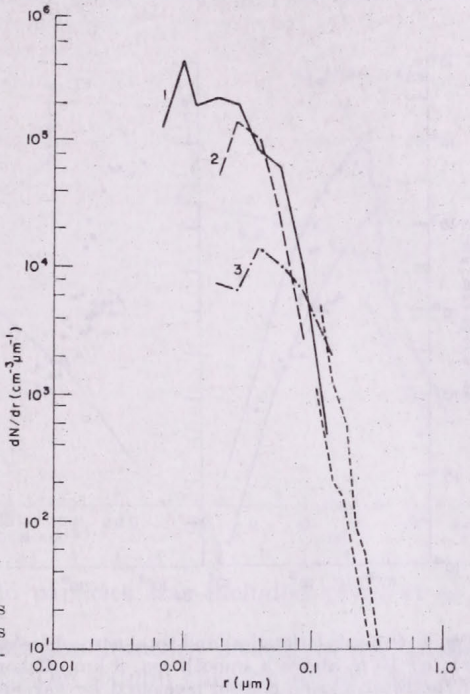

Fig. 5: Size distributions of aerosol particles measured in Norfolk, VA harbor (1), 100 miles off the New Jersey coast (2) and in the Mid-Atlantic (3). *Hoppel* (1979)

tionship with investigation of the origin of marine aerosols. In *Fig. 4* are marked the main ship cruises and with dots locations where stationary measurements of marine aerosols have been performed. They sufficiently cover all important areas on our Earth. Therefore one ought to make some general conclusions about the model size distribution of marine aerosol.

With exclusion of particle sizes smaller than 0.05 μm and larger than 5 μm, Junge's power distribution law describes usually well the size distribution

---

aerosol measurements (marked with dots). – *French:* "Jean Charcot", *1* – 1971, *9* – 1969, *25* – 1974; "James Gillis", *2* – 1972; "Gallieni", *11* and *14* – 1973; "Capricorne", *26* – 1977; "Korotneff" and "Lutin", *27* – 1973 and 74; "Marion Dufresne", *12* and *13* – 1973. – *German:* "Meteor", *22* and *23* – 1968 to 1973. – *Japanese:* "Kogoshima Maru", *17* – 1963–67 and *18* – 1967; "Hakuho Maru", *19* – 1973; "Fuji", *21* – 1970; "Ryofu Maru", *20* – 1972–74; – *Swedish:* "Ymer", *31* – 1980. – *USA:* "Trident", 3, 4, 5, 6, 7, 8 – 1970–72; "Hyes", 15, 16 – 1975; 28 – 1977. – *USSR:* "Profesor Vize", 24 – 1971–72; "Okean", 30 – 1977

of an aged mixed aerosol. Large deviations can be expected, however, in the case of one predominant source, such as sea spray. *Jaenicke* (1977) found large concetrations of very small particulates in the marine atmosphere, which is supported by other investigators as was mentioned earlier. The location of the peak around the particle radius of 0.01 μm or 0.02 μm depends upon the character of the maritime air mass (*Hoppel*, 1979). With decreasing influence of continental aerosol it is shifted from $r = 0.01$ μm to $r = 0.04$ μm *(Fig. 5)*. There seems to be also an impact of continental sources on the shape of the curve between $r = 0.005$ μm and $r = 0.05$ μm as documented by *Mészáros* and *Renoux* (1978), *Tymen* et al. (1975) and *Butor* (1980).

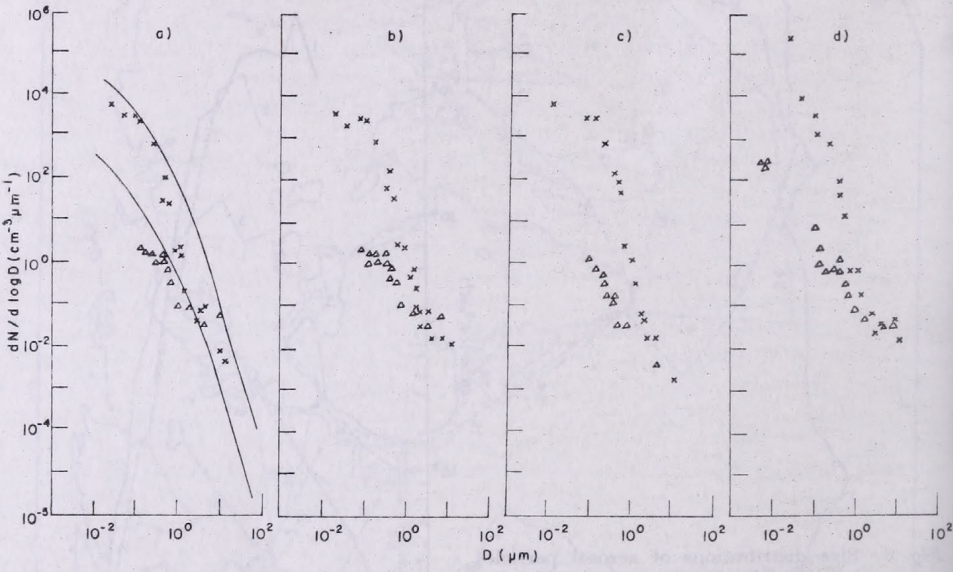

Fig. 6 : Sea salt (triangles) and total aerosol (crosses) size distributions measured by *Radke* (1977) at: *(a)* 10 m above a smooth sea, 8 km offshore – the overprinted curves repsent the bounds of the total marine aerosol measured by various authors; *(b)* at 30 m above the sea surface; *(c)* at 310 m altitude; *(d)* 15 m above a surf breaking over a harbor entrance sand bar (at a wind speed 2 m s^{-1})

On the other hand, the slope of size distribution curves for particulates with $r > 2.0$ μm deviate considerably from the ideal slope of the Junge distribution ($\beta \cong 3.0$). In the maritime atmosphere it was proven by *Podzimek* (1973), *Podzimek* and *Stampfer* (1977), *Levkov* and *Valdes* (1981) for giant sodium chloride particles and by *Schütz* and *Jaenicke* (1974) and by *Prodi* and *Fea* (1979) for Saharan dust. One of the main factors determining the value of the exponent is the wind speed and its impact on the mechanism of bubble bursting and salt particle generation. An attempt to include wind speed in the particle size distribution has been made by *Lovett* (1975).

Besides Junge's formula, the gamma distribution function (including its special case: Nukiyama – Tanassava distribution function – see e.g. *Podzimek*, 1980c) was also applied in marine aerosol studies. Deirmendjian's models for haze and dust in the marine atmosphere have been used by *Gal* (1976) and by *Wells* et al. (1976). These sophisticated models include the influence of

wind velocity, relative humidity and the change of a mixture of an ideal continental and maritime air with altitude. Another attempt to model the maritime and continental aerosol size distribution has been made by *Tomasi* and *Tampieri* (1977) who based their model on collected data from tropospheric aerosol measurements. An interesting application of a general gamma distribution function for describing the behavior of marine aerosols has been made by *Goroch* (1980). Finally, *Podzimek* (1980a) confronted the size distribution curves from the marine aerosol measurements at the seashore with Firedlander's self-preserving mechanism of aerosol production (e.g. *Friedlander* and *Hidy*, 1969) and obtained a reasonable agreement if the additional term

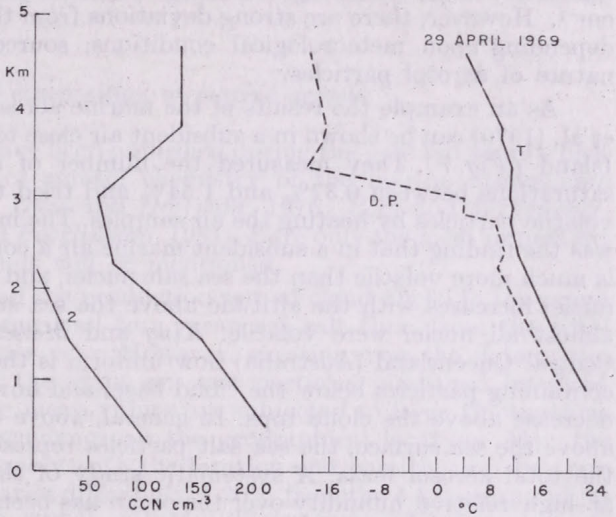

Fig. 7: Aerosol concentration vertical profile in maritime air for unheated (1) and heated (2) air samples. The sampled air was heated around 320°C. The curves of dry temperature (*T*) and dew point (*D.P.*) show the level of temperature inversion. *Dinger* et al. (1970)

for water condensation on hygroscopic particles was included (*Pich* et al., 1970).

Radke (1977) evaluated the aircraft simultaneous measurements of the size distribution of the total aerosol and the sodium chloride nuclei from 0.1 to 10 μm diameter *(Fig. 6)*. He concluded that off-shore of Washington State up to 30 m the aerosol is very well mixed, however, at an altitude of 310 m the seasalt fraction is substantially reduced (4 : 1). Further, it was apparent that almost all particles with diameters larger than 10 μm were composed of sea salt and those smaller than 0.1 μm contained a negligible sea salt fraction. *Podzimek* (1973) identified many salt nuclei with diameters smaller than 0.1 μm at the seashore of Padre Island (Texas). A similar observation has been made in the Federal Republic of Germany by *Doman* (1976) who found the concentration of sodium chloride nuclei with $d < 0.1$ μm around 10 cm^{-3} on the seashore.

The vertical distribution of sea salt particles up to 10 m above the ocean's surface has been calculated by *Toba* (1965a) and for salt nuclei with masses between 10^{-11} to 10^{-7} g up to 13 m altitude by *Chaen* (1973). The latter author found that the salt particle concentration increases linearly on a logarithmic diagram with a dimensionless parameter u^*L/ν (u^* = the friction velocity, L = the significant wavelength and ν = the kinematic viscosity of the air). *Morelli* (1968, 1977) found over the Mediterranean a considerable decrease in

sodium concentration (from 5 μgm^{-3} to 2 μgm^{-3} or from 60 μgm^{-3} to 6 μgm^{-3}) in the lowest 8 m above the sea surface and a slight decrease or constant values in the layer up to 15 m. For higher altitudes in the PBL *Toba* and *Tanaka* (1963) deduced a relationship

$$n = n_0 \exp\{-[(w/D) + (g/RT)]z\}$$

(n_0 is the particle concentration above the sea surface: $z = 0$; w is the terminal particle settling velocity; D is the eddy diffusivity; g is the acceleration in gravitational field, R is the gas constant and T is the absolute temperature). For dry adiabatic lapse conditions *Podzimek* and *Stampfer* (1977) obtained the numerical value of the expression in the broken parenthesis close to 7.0×10^{-6} cm^{-1}. However, there are strong deviations from the ideal aerosol distribution depending upon meteorological conditions, source and the physico-chemical nature of aerosol particles.

As an example the results of the marine aerosol measurements by *Dinger* et al. (1970) can be shown in a subsident air close to Puerto Rico and Barbados Island *(Fig. 7)*. They measured the number of activated nuclei for supersaturations between 0.37% and 1.54% and tried to determine the portion of volatile particles by heating the air samples. The main conclusion of this study was the finding that in a subsident marine air a considerable fraction of nuclei is much more volatile than the sea salt nuclei, and that the number of volatile nuclei increases with the altitude above the sea surface. Above the inversion almost all nuclei were volatile. *King* and *Maher* (1976) showed also over Central Queensland (Australia) how uniform is the concentration of sea salt-containing particles below the cloud base, and how steep is the concentration decrease above the cloud tops. In general, above the altitude of 2.0 – 3.0 km above the sea surface, the sea salt particles represent an insignificant part of the total aerosol mass. A systematic study of the changing aerosol spectra at high relative humidity over the ocean has been recently reported from the Texas seashore (*Podzimek*, 1980c) and over Pacific Ocean off-shore of southern California (*Noonkester*, 1981).

The formation of fog and cloud droplets is determined by the number of condensation nuclei activated at a specific supersaturation. Two main lines of research evolved during the past two decades, the goal of which is to investigate the behavior of aerosol – including marine aerosol – at different relative humidities: the study of the bulk properties of specific size groups of aerosol, and the analysis of the measured spectrum of cloud condensation nuclei with the aim to calculate the evolution of the cloud droplets. The first group yielded very interesting information on the marine aerosol in coastal regions (e.g. *Winkler* and *Junge*, 1972; *Winkler*, 1973; *Hänel* and *Bulrich*, 1978) and brought very useful information on the hysteresis in the growth of nuclei at increasing and decreasing humidities and also on the behavior of delinquescent particles in marine atmosphere (*Winkler*, 1977). The second group concentrated mainly on finding appropriate values of the "constants" C and k in the Twomey relationship between the nucleus concentration n and supersaturation S; $n = C \cdot S^k$ for specific meteorological situations, site of measurement and nuclei composition (e.g. *Fitzgerald*, 1972; *Braham*, 1974; *Goodman*, 1977; *Hoppel*, 1978; *Desalmand*, 1980). Parameters obtained from the measurements over the ocean are featured by low values of the parameter $C (< 800\ cm^{-3})$ and by k values of around 0.55, except one series of measurements made by *Hoppel* et al. (1973) over the Pacific Ocean ($k \cong 1.2$). Several articles with

the calculations of the equilibrium size of an aerosol particle as a function of its dry size, composition and ambient relative humidity have been published (e.g. *Junge* and *McLaren*, 1971; *Fitzgerald*, 1975; *Hoppel*, 1978) and a reasonable agreement with the measurement was obtained (*Hoppel*, 1978, 1979). The results of a systematic measurement of the size distribution and supersaturation spectrum of aerosols over the Atlantic Ocean and the Mediterranean were published recently by *Hoppel* (1979). He suggested an indirect method for determining the supersaturation spectrum from the measurement of the aerosol size distribution together with the measurement of the relationship between particle dry size and critical supersaturation, and obtained a good agreement with the thermal gradient diffusion cloud chamber measurement.

Chemical composition of marine aerosol

Several review articles have been published during the past ten years which deal with specific subjects of aerosol chemistry of the marine atmosphere (e.g. *Chesselet* et al., 1972a; *Duce* and *Hoffman*, 1976; *Berg* and *Winchester*, 1978; *Morelli*, 1980; *Lord* and *Pocklington*, 1981). Here only the most important discoveries and research trends will be mentioned.

Blanchard (1969) assumed the production rate of cloud nuclei in the range of $25-100\ cm^{-2}\ s^{-1}$, which can lead to a mean sea salt flux, from the total ocean surface, of 10^{10} tons per year. However, glancing over the data of the content and distribution of the giant sea salt particles published by *Toba* (1965b), one realizes that the mean values are subjected to large fluctuations during the year, and in dependence on the geographical location. Also the ratio of Cl/Na varies considerably with the location and particle size. In spite of the fact that most of the ratios differ only $\pm 20\%$ from the 1.8 corresponding to sea water, *Tsunogai* et al. (1972) and *Morelli* (1980) found values as high as 3 and 4 over the Pacific and Atlantic Ocean. On the other hand, many scientists believe that a part of Cl is converted into gaseous chlorine (e.g. *Duce*, 1969; *Buat-Menard*, 1970) which often causes lower values of the Cl/Na ratio.

TABLE I

Constituent X	(X/Na) sea water	(X/Na) marine aerosol	Mean concentration of marine aerosol (μgm^{-3})	E_x marine aerosol		
				minimum	values most frequent	maximum
Cl	1.80	1 – 4	2.5 – 70	– 0.5	0.8 – 1.2	2.5
SO_4	0.252	0.3 – 2.3	1.0 – 5.0	1.2	1.5 – 3	9
Mg	0.120	0.1 – 0.6	0.1 – 1.0	0.9 – 1	1 – 1.2	– 5
Ca	0.038	0.035 – 0.4	0.1 – 1.0	– 1	1 – 1.2	– 10
K	0.037	0.035 – 0.2	0.1 – 1.0	– 1	1 – 1.5	– 5

Other substances in the marine aerosols are subjected to the same fluctuation of ion ratios like sea salts. *Table I* was taken from the study of *Morelli* (1980). It contains the ratios for sea water, fog aerosols and the corresponding enrichment factors referred to the concentration of sodium, which represent

approximately 84% of all cations in the sea water. For chlorides the data of thefollowing authors were used: *Chesselet* et al. (1972b); *Willkniss* and *Bressan* (1972); *Willkniss* et al. (1974); *Morelli* (1968); *Buat-Menard* (1970); *Tsunogai* et al. (1972). Data on sulfates were taken from *Morelli* (1977); *Bonsang* et al. (1979); *Buat-Menard* et al. (1974); *Bonsang* (1980); *Gravenhorst* (1978). The concentrations of Mg, Ca and K were excerpted from the studies by *Morelli* (1977); *Buat-Menard* et al. (1974); *Hoffman* and *Duce* (1972); *Hoffman* (1975); *Chesselet* et al. (1975); *Willkniss* et al. (1974); *Tsunogai* et al. (1972).

Strong fluctuation and the highest enrichment show sulfates which are investigated mainly with regard to the impact of continental air pollution on the composition of marine aerosols. There seems to be several different sources of sulfates in marine particulate matter: in general, ocean can act as a source or a sink of SO_2. We assume now that it is usually a sink (e.g. *Georgii* and *Gravenhorst*, 1977), unlike for NH_3 when it may be a source. A mechanism which was suggested for the further evolution of SO_2 into sulfates is gas-to-particle conversion *via* photo-oxidation of SO_2 and heteromolecular nucleation in the presence of water vapor (e.g. *Stauffer* et al. 1973; *Takahashi* et al. 1975). This aerosol was found in the antarctic and subantarctic atmosphere by *Ono* et al. (1981) in the summer months. It was alternated mostly in winter months during the intrusion of maritime air by the aerosol composed of sea salt and ammonium sulfate aerosol (which might be the result of chemical reactions within cloud droplets in the presence of ammonia gas). *Winkler* (1980) found that aerosol particles with $r > 0.3$ μm radius contain very little free acid, unlike particles with radii between $0.1 < r < 0.3$ μm. In the Aitken nuclei region the majority of particulates contain ammonium sulfate (*Mészáros* and *Renoux*, 1978), and there is a considerable difference in their concentrations in different geographical locations: over the Atlantic Ocean ($0° < \varphi < 20°$) 69% (of the total particle concentration), the Atlantic Ocean ($\varphi > 40°$) 35%, and the Indian Ocean 18%. *Mészáros* (1982) also concluded from a comparison of the measurements of different authors that a considerable part (0.19 μgm^{-3}) of sulfate-containing particulates can be found on larger sea salt particles *(Fig. 8)*. The carrier giant particles in the marine atmosphere can also be represented by the desert dust showing a relatively high content of sulfates (0.1 g sulfate per 1.0 g of desert particles), as measured by *Mamane* et al. (1980) over the Mediterranean. The author hypothesized that the active nuclei originated through heterogeneous nucleation of SO_2 on the surface of insoluble large dust particles.

Several other mechanisms have been suggested as effective in generating SO_2 in the marine atmosphere such as the oxidation of organic sulfides (e.g. dimethyl sulfide) produced by the biological activity on the ocean surface (*Nguyen* et al., 1978; *Bonsang* et al., 1980). In coastal regions SO_2 or H_2S might be emitted by algae or other biological objects, oxidized and transformed into Aitken nuclei of a very high concentration (*Bonsang* et al., 1976; *Renoux* et al., 1977; *Renoux* et al., 1978). The attempt to prove experimentally the finding of high sulfate-to-sodium ratio in aerosols in certain ports of the ocean (e.g. Scandinavia) yielded only 10% to 30% excess compared with sea water (*Garland*, 1981).

Many studies of chemical fractionation at the ocean's surface are discussed in a review article by *Duce* and *Hoffman* (1976). There are discussed especially the goals of the SEAREX Program in the North and South Pacific in the unpolluted, well controlled area where aerosol flux experiments and studies of

the sea surface microlayer can be performed (*Duce*, 1980). Many measurements of trace metals in the Atlantic Ocean have been performed (*Hoffman* et al., 1972; *Duce* et al., 1976a; *Duce* et al., 1976b; *Hoffman* and *Duce*, 1977; *Hoffman*, 1975; *Hoffman* et al., 1977; *Hoffman* et al., 1980). The elements of Na, Al, Fe, Mn, Sc, Th and Co were found primarily on particles with radii of approximately 1 μm or greater, whereas Cu, Sn, As, Cd, Pb, Sb, Se, Hg are concentrated on particulates with radii smaller than 1 μm. These results do

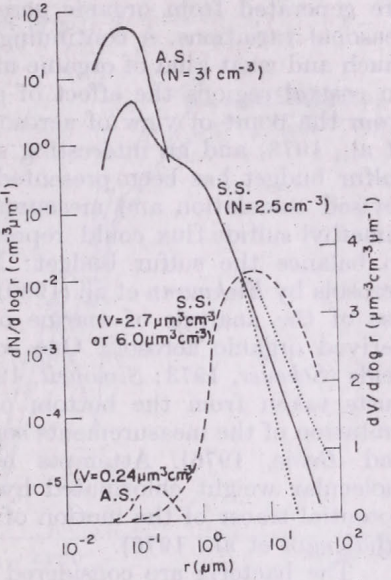

Fig. 8: Average size distribution of ammonium sulfate (A.S.) and sea salt (S.S.) particles *(A. Mészáros* and *Vissy*, 1974) plotted as a Junge's distribution and as a particle volume distribution. Dotted curves and the laver value for total salt particle volume concentration indicate the corrected data for isokinetic sampling conditions *(E. Mészáros*, 1982)

not differ basically from the findings of French scientists (*Crozat* et al., 1973; *Buat-Menard* et al., 1974; *Hoang* and *Servant*, 1974; *Chesselet* et al., 1972 and *Buat-Menard*, 1979). *Hoffman* and *Duce* (1977) proved that only the addition of natural surfactants led to an enrichment of the metals in aerosols over the seawater ratio. In other articles was studied particulate iodine in the marine atmosphere (1 – 5 ng m^{-3} – *Moyers* and *Duce*, 1972a), bromine (5 – 12 ng m^{-3} – *Moyers* and *Duce*, 1972b), phosphorus (*Graham* and *Duce*, 1979), vanadium (*Walsh* and *Duce*, 1976; *Duce* and *Hoffman*, 1976) and arsenic (*Walsh* et al., 1979a; *Walsh* et al., 1979b).

In the SEAREX Program the large scale transport of soil dust from China is investigated in a systematic way. At Enewetak Atoll (11°N; 162°E), e.g., 2.3 μg m^{-3} of soil dust was observed in April 1979 which overrides more than 100 times the normal concentration (*Duce*, 1980). This value can be compared with the earlier study by *Prospero* and *Bonatti* (1969) from the Eastern Equatorial Pacific and by *Fergusson* et al. (1970) who found dust concentrations between 0.1 and 1.0 μg m^{-3}. *Prospero* et al. (1970) measured nearly the same concentrations in the Caribbean area and traced the aerosol to an African dust storm. Similar findings were later reported by *Chester* and *Johnson* (1971), *Jaenicke* et al. (1971) and *Prospero* and *Carlson* (1972).

Much attention has been paid to organic aerosols during the past decade (reviewed by *Hahn*, 1980). Organic particulates contribute for instance 30%

to 40% to the total aerosol count on Hawaiian islands (*Parungo* et al., 1981). The investigators concentrated mainly on the presence of surface active organic material and its role in the air/sea mass transfer (*Barger* and *Garrett*, 1970 and 1976; *MacIntyre*, 1974a; *Baier* et al., 1974; *Hoffman* and *Duce*, 1974, 1977; *Russell* and *Stampfer*, 1976; *Wallace* et al., 1977; *Marty* et al., 1979). Debated is still the nature of organic material (fatty acids, lipids) which is usually concentrated on small particulates. In total, *Ketseridis* and *Eichmann* (1978) found on the west coast of Ireland 1 μg of carbon-containing material per m^3 and *Jaenicke* (1978b) concluded that most of the Aitken nuclei are generated from organic gases and therefore are subjected to daily and seasonal variations. A continuing investigation is going on to determine how much and what kind of organic material in aerosols is generated by the ocean. In coastal regions the effect of algae on nuclei production was investigated from the point of view of aerosol dynamics (*Paugam*, 1975a, 1975b; *Renoux* et al., 1978) and an interesting study on the role of dimethyl sulfide in the sulfur budget has been presented by *Nguyen* et al. (1978). According to the revised calculation and measurements performed in the Atlantic Ocean the dimethyl sulfide flux could represent more than 30% of the amount needed to balance the sulfur budget: N-alkanes were identified in ocean-derived aerosols by *Eichmann* et al. (1980). Another challenging subject seems to be the use of the analysis of marine organic sediments as a tracer of continent-derived organic aerosols. One concentrated on triterpenes and triterpenoic acids (*Scheuer*, 1973; *Simoneit*, 1974) and lipids (*Simoneit*, 1977) in the éolien dusts taken from the bottom of the Atlantic Ocean. However, the interpretation of the measurements sometimes is not void of contradictions (*Lepple* and *Brine*, 1976). Attempts have been also made to investigate high molecular weight chlorinated hydrocarbons in the marine atmosphere as a potential tracer of the motion of the polluted air coming from the continent (*Bidleman* et al., 1976).

The bacteria are considered to play a secondary but important role in the marine aerosol composition (*Carlucci* and *Williams*, 1965; *Aubert*, 1974; *Blanchard* and *Syzdek*, 1970). There is little information on this subject except rough calculation of the virus transfer and drop enrichment of bacteria and dissolved organic material (*Baylor* et al., 1977). The investigator assumed, for instance, that a surf zone 25 m wide and 100 km long would supply each second 7.5×10^{11} bacteria into the marine air advancing over the mainland.

Optical properties of marine aerosol

Marine aerosol has an important role in the propagation of optical signals and radiative transfer. The key role is the susceptibility of marine aerosol to the changes of relative humidity and the dynamics of aerosol evolution above the sea's surface (*Kasten*, 1969; *Winkler* and *Junge*, 1971 and 1972; *Hänel*, 1971 and 1972; *Tang*, 1976; *Tang* et al., 1977a, 1977b, 1978). The real and imaginary parts of the mean refractive index of specific kind of atmospheric aerosol have been investigated by *Hänel* (1968), *Fischer* (1970, 1976) in visible light, and by *Volz* (1972) for the infrared domain. *Fischer* and *Hänel* (1972) determined the mean aerosol properties—including the index of refraction during a cruise of a research vessel over the North Atlantic. The values of the real part of the index of refraction were 1.35 and 1.55, and of the imaginary part 0.003 and 0.047 for the wavelength of 0.589 μm, when the relative humid-

ity increased from 20% to 96%. An approximate formula to calculate infrared extinction for a Junge aerosol size distribution was suggested by *Fitzgerald* (1979). The agreement with measurement was good *(Fig. 9)*.

Several new trends of research of the optical properties of marine aerosol evolved: the change in mean optical properties due to the water uptake by particles composed of different salts (*Thudium*, 1978; *Hänel*, 1976, 1981) and the effect of fluctuating humidity, particulate composition and concentration

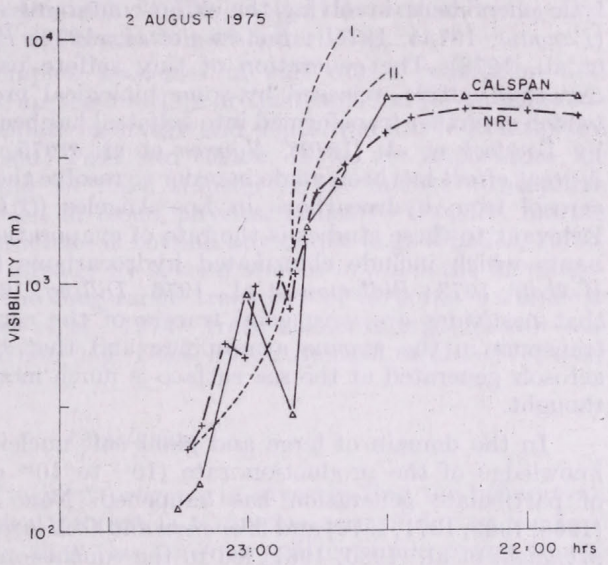

Fig. 9: Comparison of measured (triangles – by CALSPAN; crosses – by NRL) and model predicted visibilities in a maritime fog of 2 August 1975 *(Hoppel* and *Fitzgerald*, 1976; *Fitzgerald*, 1979). Two different model assumptions (I. and II.) about droplet (nuclei) behavior led almost to the same predicted onsetting of fog

on the scattering or extinction coefficient (*Fitzgerald*, 1980; *Goroch* and *Burk*, 1980). *Hänel* and *Lehmann* (1981) investigated the properties of mixed particles (composed of different mixtures of Na_2SO_4, $NaNO_3$, NH_4NO_3, $(NH_4)_2SO_4$, H_2SO_4 and sea salt) and stressed the importance of the knowledge of the particle composition for cloud droplet growth. *Hänel* and *Zankl* (1979) concluded that the water uptake of a multicomponent electrolyte solution is almost the same as the sum of the water uptakes of the separated pure components. This helps to establish simplified formulas for the prediction of a visual range at a high relative humidity (*Hänel*, 1980). Other interesting measurements of the optical properties of marine aerosols have been made recently by *Heintzenberg* (1977), *Gerber* (1979), *Hughes* (1980) and *Noonkester* (1981).

Generation and transport of marine aerosol

The mechanisms of generation and transport from the air-water interface is the subject of several review articles published recently (*Winchester* and *Duce*, 1977; *Blanchard* and *Woodcock*, 1980; *Pozdimek*, 1980b; *Morelli*, 1980; *Lord* and *Pocklington*, 1981). As several of these mechanisms were mentioned in the previous parts of this study, a brief survey should summarize the main avenues of current research.

In the domain of Aitken nuclei the main attention is paid to the kinetic models of aerosol generation and transformation (e.g. *Middleton* and *Kiang*, 1978; *Jaenicke*, 1978c; *Perrin* et al., 1980) with the emphasis on the new techniques used for ultrafine particle size determination. In coastal regions, where oceanic and polluted continental air masses interact (e.g. Los Angeles area), is accentuated the formation of new particles in the presence of an aerosol and gas-to-particle conversion in photochemical smog (*McMurry* and *Friedlander*, 1979; *Heisler* and *Friedlander*, 1977). The production of a large concentration of Aitken nuclei seems to be documented and explained by the photolytic phenomena involving the sulfur-containing substances released by algae (*Paugam*, 1975a, 1975b; *Bonsang* et al., 1976; *Paugam* et al., 1977; *Renoux* et al., 1978). The generation of tiny sulfate particles by the oxidation of dimethyl sulfide, released by some biological processes in the sea, into SO_2 (which is further transformed into sulfates) has been suggested and documented by *Lovelock* et al. (1972), *Nguyen* et al. (1975, 1977) and *Bonsang* (1980). A great effort has been made in order to resolve the formation of photochemical aerosol from hydrocarbons in Los Angeles (*O'Brien* et al., 1975a, 1975b). Relevant to these studies is the rate of evaporation of low-solubility contaminants which include chlorinated hydrocarbons (PCB, DDT) (*MacKay* and *Wolkoff*, 1973; *Bidleman* et al., 1976; *Dilling*, 1977). The main conclusion is that pesticides are very good tracers of the continental particulate matter transport in the marine atmosphere and that their interaction with other aerosols generated at the sea surface is much more important than originally thought.

In the domain of large and giant salt nuclei no dramatic change in our knowledge of the production rate (10^{15} to 10^{16} g per year) and mechanism of particulate generation has happened. New investigations by *Monahan* (1968, 1969, 1971, 1979) and *Monahan* and *O'Muircheartaigh* (1980) as well as by *Monahan* et al. (1980, 1981) led to the conclusion that whitecaps, as a source of salt nuclei, begin to appear at wind speeds larger than 3 m s^{-1} and that at a wind speed of 8 m s^{-1} about 1% of the sea is covered with whitecaps. This value indicates that, on the average, the ocean has a whitecap coverage less than originally assumed (3.5%). On the other hand, this smaller coverage is partly compensated by *Johnson*'s (1979) and *Johnson* and *Cooke*'s (1979) finding that small bubbles exist also in areas not covered by whitecaps. The basic question if jet drops (1 to 10 drops per bubble) are more important for salt nuclei production than film drops (6 mm bubble can produce up to 1,000 drops) remains still to be answered. The process depends not only on the bubble size and its hydro- and thermodynamical parameters, but also on the amount of organic carbon dissolved in the sea water (*Lee*, 1972; *Blanchard* and *Hoffman*, 1978; *MacIntyre*, 1974b). *Blanchard* and *Woodcock* (1980) discuss in detail the vertical distribution of sea salt mass concentration. They found a sea salt inversion layer around a level of 300 m with a slight increase of sea salt mass concentration up to the height of cloud base. Similar profiles both in Na and Cl concentrations were found near the Bahamas by *Gordon* et al. (1977).

The existence of sea salt concentration inversion seems to be closely related rather to the whole complex mechanism of droplet production at the sea surface, the state of their coating and its change after bubble bursting (*Garrett*, 1968, 1971; *Wallace* and *Duce*, 1975, 1978a, 1978b; *Morelli* et al., 1974; *Piotrowicz* et al., 1979), than to a standard model: in reality, to particle

sedimentation, droplet evaporation, wash-out, gas entrainment by water drops, turbulent exchange influence particle size distribution and residence time (*Monahan*, 1968; *Sehmel* and *Sutter*, 1974; *Slinn* et al., 1978; *Schütz* and *Davidson*, 1980). Two main lines of research can be found in the literature: attention is paid to a more complex modelling of the multiphase fluxes over the ocean (*Ling* et al., 1979), others investigate in detail droplet production and dispersion above the breaking waves (*Koga*, 1981a, 1981b, 1981c). The latter author showed in his experiments simulating direct droplet generation what main mechanism governs the obtained droplet spectra: turbulent diffusion is dominant for droplets with $d < 120$ μm and the vertical free motion of ejection is responsible for the generation of larger ones.

The aforementioned complex processes of salt nuclei generation and droplet transport through the air/sea interface are instrumental for understanding the large scale salt particulate exchange and deposition in the atmosphere (e.g. *Toba*, 1965a, 1965b, 1966; *Toba* and *Chaen*, 1973). Its importance for describing the particulate and air mass transfer in the marine atmosphere – with its practical application in cloud physics, radiative transfer, marine biology and environmental studies – is beyond any doubt (e.g. *Winkler*, 1977). A similar trend is indicated already by several studies in which the investigators attempted to analyze the long-range transport of airborne particulate matter to Great Britain (*Lee* et al., 1974), trace elements (e.g. *Husain* and *Samson*, 1979) or organic carbon (e.g. *Duce*, 1978; *Björseth* et al., 1979) over the ocean.

Conclusion

This survey documents a great progress in investigating the generation, transport and physico-chemical properties of marine aerosol during the past decade. One feels intuitively that this progress will continue owing to the importance of these investigations for meteorology and geology, marine biology, the study of material degradation, and the interaction with atmospheric pollutants. There is an indication that some phases of marine aerosol research will develop faster or that they will cover areas not yet sufficiently investigated:

In measuring techniques the main emphasis will be put on developing instrumentation to measure reliably the particulate concentration and size distribution down to particle sizes of 0.001 μm. These techniques will be necessary for following the whole process of gas-to-particle conversion and preferentially should include the possibility to yield some information about the chemical nature of the main ultrafine particle size classes. A standard technique will be probably used for the measurement of deliquescence properties and supersaturation spectra of large and giant particles. Attention will be paid to the statistical representativeness of the measurements of large, giant and "ultragiant" particles and to specific conditions of sampling on the ocean's surface.

The surface microlayer will be intensively investigated with regard to bubble bursting mechanism, element fractionation, fractionation of biological materials and potential impact of gaseous substances on particle generation and transformation. One will probably ask the question if the jet drop and film drop mechanisms are the only dominant ones and whether other processes (e.g. direct emission of droplets from the whitecaps or waves) are competitive

at specific atmospheric conditions. One will try to simulate as truly as possible the very complex processes at the ocean's microlayer in the laboratory.

The transport of sea salt and other particles will require more sophisticated models of the main processes governing the particle behavior in the layer up to several meters above the sea surface. This model should provide a transition into the modelling of particulate transport in the planetary boundary layer with its specific features around temperature inversions and clouds. A special approach will be used for modelling the particulate generation and transfer at the seashore. Finally, for long-range transport of particulates and the assessment of the deposited particle mass it will be very beneficial to adapt several techniques used now for plotting the trajectories of atmospheric pollutants under specific conditions prevailing in the maritime atmosphere.

Acknowledgement. The author is indebted to many of his colleagues from the U.S.A. and from abroad who supplied him with information on their current investigations. He appreciates also the able assistance of Mrs. *Vickie Maples* and *Cindy Turek* while preparing this manuscript for print.

REFERENCES

Allee, P. A., 1974: *J. Rech. Atmos. 8*, 947—955.

Aubert, J., 1974: *J. Rech. Atmos. 8*, 541—554.

Baier, R. E., Goupil, D. W., Perlmutter, S. and *Wing, R.*, 1974: *J. Rech. Atmos. 8*, 571—600.

Barger, W. R. and *Garrett, W. D.*, 1970: *J. Geophys. Res. 75*, 4561—4566.

Barger, W. R. and *Garrett, W. F.*, 1976: *J. Geophys. Res. 81*, 3151—3157.

Baylor, E. R., Baylor, M. B., Blanchard, D. C., Syzdek, L. D. and *Appel, C.*, 1977: *Science 198*, 575—580.

Berg, W. W. and *Winchester, J. W.*, 1978: Aerosol chemistry of marine atmosphere, *Chemical Oceanography, 7*, 2nd Ed., by *J. P. Riley* and *R. Chester*, Academic Press, London, New York, 173—226.

Bidleman, T. F., Rice, C. P. and *Olney, C. E.*, 1976: High molecular weight chlorinated hydrocarbons in the air and sea, rate and mechanisms of air/sea transfer, *Marine Pollutants Transfer*, Ed. *R. A. Duce* and *H. L. Windom*, Lexington, Massachusetts, D. C. Heath and Co.

Björseth, A., Lunde, G. and *Linkskog, A.*, 1979: *Atmos. Envir. 13*, 45—53.

Blanchard, D. C., 1969: *J. Rech. Atmos. 4*, 1—6.

Blanchard, D. C. and *Hoffman, E. J.*, 1978: *J. Geophys. Res. 83*, 6187—6191.

Blanchard, D. C. and *Syzdek, L. D.*, 1970: *Science 170*, 626—628.

Blanchard, D. C. and *Woodcock, A. H.*, 1980: The production concentration, and vertical distribution of the sea-salt aerosol, *Annals New York Acad. Sci. 338*, 330—347.

Bonsang, B., 1980: *Le cycle atmosphérique du soufre d'origine marine*, Thèse de doctorat d'état, Université de Picardie.

Bonsang, B., Nguyen, B. C., Gaudry, A. and *Lambert, G.*, 1979: Sulfate enrichment in marine aerosols due to biogenic gaseous sulfur compounds, Paper Presented at the *CACGP Symposium on Trace Gases and Aerosols*, Boulder, USA, August, 1979.

Bonsang, R., Nguyen, B. C., Gaudry, A. and *Lambert, G.*, 1980: *J. Geophys. Res. 85*, 7410—7416.

Bonsang, B., Nguyen, B. C. and *Paugam, J. Y.*, 1976: *C. R. Acad. Sci. Paris, Serie D, 283*, 1285—1289.

Braham, R. R., 1974: Information content of CCN spectra vs. measments at single supersaturation, *Preprints Conf. on Cloud Physics*, Tucson, October; AMS, Boston, 9—12.

Buat-Menard, P., 1970: *Contribution à l'étude du cycle géochimique du chlore d'origine marine*, Thèse de doctorat 3ème cycle, Faculté des Sciences, Paris.

Buat-Menard, P., 1979: *Influence de la retombée atmosphérique sur la chimie des métaux en trace dans la matière en suspension de l'Atlantique Nord*, Thèse de doctorat d'état, Université de Paris, VII.

Buat-Menard, P., Morelli, J. and *Chesselet, R.*, 1974: *J. Rech. Atmos. 8*, 661—673.

Burckhardt, H. and *Flohn, H.*, 1939: *Die atmosphärischen Kondensations-Kerne in ihrer physikalischen und klimatologischen Bedeutung*, J. Springer, Berlin.

Butor, J. F., 1980: *Contribution à l'étude de l'aerosol atmosphérique en zones urbaine, maritime et océanique*, Thèse de doctorat, University of Brest, July, 130.

Carlucci, A. F. and *Williams, P. M.*, 1965: *J. du Conseil Cons. Perma. Int. Explor. Met. 30*, 28—33.

Chaen, M., 1973: Studies on the production of sea-salt particles on the sea surface, *Mem. Fac. Fisheries, Koaoshima Univ. 22*, 49—107.

Chesselet, R., Buat-Menard, P. and *Lesty, M.*, 1975: *Trace element chemistry in aerosols over Eastern Tropical Atlantic*, Progress Report, Midlante „Jean Charcot" Cruise 1974, CFR/CNRS, Gif-sur-Yvette.

Chesselet, R., Morelli, J. and *Buat-Menard, P.*, 1972a: *J. Geophys. Res. 77*, 5116—5131.

Chesselet, R., Morelli, J. and *Buat-Menard, P.*, 1972b: Some aspects of the geochemistry of marine aerosols, *The changing chemistry of the Oceans, Proc. 20th Nobel Simp., Aspenäsgarden, 1971*, Sweden, Ed. by *B. Dyrssen* and *D. Jagner*, Stockholm, 93—114.

Chester, R. and *Johnson, L. R.*, 1971: *Nature 229*, 105—107.

Crozat, G., Domergue, J. L., Bogui, V. and *Fontan, J.*, 1973: *Atmos. Envir. 7*, 1103—1106.

Désalmand, F. Baudet, J., and *Serpolay, R.* 1980: *J. Res. Atmos. 14*, 207—215.

Dilling, W. L., 1977: *Envir. Sci. Technol. 11*, 405—409.

Dinger, J. E., Howell, H. B. and *Wojciechowski, T. A.*, 1970: *J. Atmos. Sci. 27*, 791—797.

Doman, M. H., 1976: On the size spectrum of sea-salt nuclei as determined with the Sartorius scintillation counter, *Aerosols in Naturwissenschaft, Medizin und Technik, 4*, Tagung GAF, 106—111.

Duce, R. A., 1969: *J. Geophys. Res. 74*, 4597—4599.

Duce, R. A., 1978: *Pageoph. 116*, 244—273.

Duce, R. A., 1980: *Sea/air exchange of pollution and natural substances : The Searex Program*, Sepc. Envir. Rep. No. 14, WMO., No. 549, Geneva, 235—242.

Duce, R. A. and *Hoffman, E. J.*, 1976: *Ann. Rev. Earth Planet Sci. 4*, 187—228.

Duce, R. A., Hoffmun, G. L., Ray, B. J., Fletcher, I. S., Wallace, G. T., Fashing, J. L. Sr., Piotrowicz, R., Walsh, P. R., Hoffman, E. J., Miller, J. M. and *Heffter, J. L.*, 1976a: Trace metals in the marine atmosphere: sources and fluxes, *Marine pollutants transfer*, ed. *R. A. Duce* and *H. L. Windom*, Lexington, Massachussets: D. C. Heath and Co.

Duce, R. A., Ray, B. J., Hoffman, G. L. and *Walsh, P. R.*, 1976b: *Geophys. Res. Letters 3*, 339—342.

Eichmann, R., Ketseridis, G., Schebeske, G., Jaenicke, R., Hahn, J., Warneck, P. and *Junge, E.*, 1980: *Atmos. Envir. 14*, 695—703.

Fergusson, W. S., Griffin, J. J. and *Goldberg, E. D.*, 1970: *J. Geophys. Res. 75*, 1137—1139.

Fischer, K., 1970: *Beitr. Phys. Atmos. 43*, 244—254.

Fischer, K., 1976: *Tellus 13*, 266—274.

Fischer, K. and *Hänel, G.*, 1972: Bestimmung physikalischer Eigenschaften atmosphärischer Aerosolteilchen über dem Atlantik, *"Meteor" Forsch. Erg. B. 8*, 59—62.

Fitzgerald, J. W., 1972: *A study of the initial phase of cloud drop growth by condensation ; comparison between theory and observation*, Tech. note 44, Cloud Physics Laboratory, Univ. of Chicago, June.

Fitzgerald, J. W., 1975: *J. Appl. Meteor. 14*, 1044—1049.

Fitzgerald, J. W., 1979: *J. Appl. Meteor. 18*, 931—939.

Fitzgerald, J. W., 1980: *Atmos, Envir. 14*, 71—77.

Friedlander, S. K. and *Hidy, G. M.*, 1969: New concepts in aerosol size spectrum theory, *Proc. 7-th Int. Conf. Condens. Ice Nuclei, Prague-Vienna, 1969*, Academia, Prague, 21—25.

Gal, G., 1976: *Particulate cloud diagnostics with optical measurements (mathem. model)*, Lockheed Palo Alto Research Laboratory, LMSC-D502379, April.

Garland, J. A., 1981: *Atmos. Environ. 15*, 787—791.

Garrett, W. D., 1968: *J. Geophys. Res. 73*, 5145—5150.

Garrett, W. D., 1971: Impact of natural and man-made surface films on the properties of the air-sea interface. In: *The changing chemistry of the Oceans, Proc. 20-th Nobel Symp., Aspenasgärden*, Sweden, Editor: *D. Dyrssen* and *D. Jagner*, Stockholm, 75—91.

Georgii, H. W., 1975: Recent research on atmospheric cloud nuclei, *Proc. 8th Int. Conf. on Nucleation, Leningrad*, Gidrometizdat, Moscow, 398—403.

Georgii, H. W. and *Gravenhorst, G.*, 1977: *Pure and Appl. Geophys. (Pageoph) 115*, 503—511.

Gerber, H. E., 1979: *J. Atmos. Sci. 36*, 2502—2523.

Goodman, J., 1977: *J. Appl. Meteor. 16*, 1056—1067.

Gordon, C. M., Jones, E. C. and *Larson, R. E.*, 1977: *J. Geophys. Res. 82*, 988—990.

Goroch, A. K., 1980: Calculation of gamma function parameters from aerosol size distribution measurements, *Preprint 2nd Conf. Coastal Meteorology*, Los Angeles, AMS, Boston, Jan.

Goroch, A. K. and *Burk, S. D.*, 1980: Height dependent stability effects on optical propagation in the marine planetary boundarry layer, *Aerosols in science, medicine and technology 8*, GAF, Schmallenberg, 178—183.

Grabovski, R. I., 1956: *Atmosfernye iadra kondensatsii*, (Atmospheric condensation nuclei), Gidrometizdat, Leningrad.

Graham, W. F. and *Duce, R. A.*, 1979: *Geochim. et Cosmochim. Acta, 43*, 1195—1208.

Gravenhorst, G., 1978: *Atmosph. Envir. 12*, 707—713.

Hahn, J., 1980: *Annals New York Acad. Sci. 338*, 359—376.

Hänel, G., 1968: *Tellus 20*, 371—379.

Hänel, G., 1971: *Beitr. Phys. Atmosph. 44*, 137—167.

Hänel, G., 1972: *Aerosol Sci. 3*, 377—386.

Hänel, G., 1976: *Advances is Geophysics 19*, 73—188.

Hänel, G., 1980: *Beitr. Phys. Atmosph. 53*, 539—541.

Hänel, G., 1981: *Beitr. Phys. Atmosph. 54*, (to be published).

Hänel, G. and *Bulrich, K.*, 1978: *Beitr. Phys. Atmosph. 51*, 129—138.

Hänel, G. and *Lehmann, M.*, 1981: *Beitr. Phys. Atmosph. 54*, 57—71.

Hänel, G. and *Zankl, B.*, 1979: *Tellus 31*, 478—486.

Heintzenberg, J., 1977: Light scattering and the atmospheric aerosol over the Atlantic, "*Meteor*" *Forsch.-Ergebnisse, R. B. 12*, 1—9.

Heisler, S. L. and *Friedlander, S. K.*, 1977: *Atmos. Envir. 11*, 157—168.

Hoang, Chi Trach and *Servant, J.*, 1974: *J. Rech. Atmosph.* 8, 791—805.

Hoffman, E. J., 1975: *Chemical fractionation at the air sea interface: alkali and alkaline earth metals and total organic carbon*, Ph.D. Thesis, Univ. of Rhode Island, USA.

Hoffman, G. L. and *Duce, R. A.*, 1972: *J. Geophys. Res. 77*, 5161—5169.

Hoffman, E. J. and *Duce, R. A.*, 1974: *J. Geophys. Res. 79*, 4474—4477.

Hoffman, E. J. and *Duce, R. A.*, 1977: *Geophys. Res. Lett. 4*, 449—452.

Hoffman, G. L., Duce, R. A. and *Hoffman, E. J.*, 1972: *J. Geophys. Res. 77*, 5322—5329.

Hoffman, E. J., Hoffman, G. L. and *Duce, R. A.*, 1980: *J. Geophys. Res. 85*, 5499—5502.

Hoffman, E. J., Hoffman, G. L., Fletcher, I. S. and *Duce, R. A.*, 1977: *Atmos. Environ. 11*, 373—377.

Hogan, A. W., 1981: (Private Communication) — Chapter V in the *Final Report to the GASP.*

Hogan, A. W., Bishop, J. M., Aymer, A. L., Harlow, B. W., Klepper, J. C. and *Lupo, G.*, 1967: *J. Appl. Meteor. 6*, 726—727.

Hogan, A. W., Mohnen, V. A. and *Schaefer, V. J.*, 1973: *J. Atmos. Sci, 30*, 1455—1460.

Hoppel, W. A., 1978: Relationship between dry aerosol size, critical supersturation and size at high relative humidity, *Preprints Conf. on Cloud Physics and Atmos. Electricity*, Issaquah, July—August, 16—19.

Hoppel, W. A., 1979: *J. Atmos. Sci. 36*, 2006—2015.

Hoppel, W. A., Dinger, J. E., Ruskin, R. E., 1973: *J. Atmos. Sci. 30*, 1410—1420.

Hoppel, W. A. and *Fritzgerald, S. W.*, 1976: Measurament of CCN spektra at low supersaturations in relation to fog formation of the coast of Nova Scotina. *Proc. Sympos.on Radiation in the Atmosphere*, Garmisch-Partenkirchen, Science Press, Princeton, N. J., 62—64.

Hughes, H. G., 1980: *J. Appl. Meteor. 19*, 803—808.

Husain, L. and *Samson, P. J.*, 1979: *J. Geophys. Res. 84*, 1237—1240.

Jaenicke, R., 1977: The size distribution of Aitken nuclei in background aerosols. *Abstr. Conf. on Atmos. Aerosols, Cond. and Ice Nuclei*, Galway, 131.

Jaenicke, R., 1978a: Aitken particle size distribution in the Atlantic North East trade winds, "*Meteor*" *Forsch.-Ergebnisse, R. B. 13*, 1—9.

Jaenicke, R., 1978b: *Pageoph. 116*, 283—292.

Jaenicke, R., 1978c: *Ber. Bunsen-Ges. F. Phys. Chemie 82*, 1198—1202.

Jaenicke, R., Junge, C. and *Kanter, H. J.*, 1971: Messungen der Aerosolgrössenverteilungen über dem Atlantik. "*Meteor*" *Forsch.-Ergebn. B. 7*, 1—54.

Jaenicke, R. and *Schütz, L.* 1977: *Tellus, 29*, 189—190.

Johnson, B., 1979: Ph. D. Thesis, Dalhousie Univ., Halifax, Nova Scotia.

Johnson, B. D. and *Cooke, R. C.*, 1979: *J. Geophys. Res. 84*, 3761—3766.

Junge, C. E., 1963: *Air chemistry and radioantivity*, Academic Press, New York and London.

Junge, C. E., 1969: The physical and chemical properties of atmospheric aerosols and their celation to condensation processes, *7th Int. Conf. Condens. and Ice Nuclei, Prague-Vienna, Sept. 1969;* published in Supplem. Volume of the Proc., Academia-Prague, 1971.

Junge, C. E., 1972: Our knowledge in the physico-chemistry of aerosols in the undisturbed marine environment, *J. Geophys, Res. 77*, 5183—5200.

Junge, E. and *McLaren, E.*, 1971: *J. Atmos. Sci. 28*, 382—390.

Kasten, F., 1969: *Tellus 21*, 631—635.

Ketseridis, G. and *Eichmann, R.*, 1978: *Pageoph. 116*, 274—282.

King, W. D. and *Maher, C. T.*, 1976: *Tellus 27*, 11—23.

Koga, M., 1981a: On the bubble entrainment by wind wave breaking, submitted to *Tellus*.

Koga, M., 1981b: *Sci. Rep. Tohoku Univ. s. 5*, 28.

Koga, M., 1981c: Direct production of droplets from breaking wind waves — its observation by a multi-colored overlapping exposure photographing technique, *Tellus* (in press).

Landsberg, H., 1938: Atmospheric condensation nuclei, *Ergebn. Kosm. Physik 3*, 155—252.

Lee, T. M. S., 1972: *An investigation of the effect of bubble age and organic contamination of the ejection height and size of jet drops*, Master's Thesis, State Univ. of New York, Albany.

Lee, R. E., Caldwell, J., Akland, G. G. and *Fankhauser, R.*, 1974: *Atmos. Envir. 8*, 1095—1109.

Lepple, F. K. and *Brine, C. J.*, 1976: *J. Geophys. Res. 81*, 1141—1147.

Levkov, L. and *Valdes, M.*, 1981: A study of maritime aerosol in a tropical region, *IAMAP, Hamburg, Programs and Abstracts*, August, p. 45.

Ling, S. C., Kao, T. W. and *Saad, A.*, 1979: The role of micro-water droplets in the transport of heat and moisture from the ocean and lake, *JASCE* (in press).

Lord, G. and *Pocklington, R.*, 1981: Composition chimique de l'atmosphère en hydrocarbures terrigènes et transfert de ces composés à l'interface air-océan, *J. Rech. Atmos. 15*, 53—79.

Lovelock, J. E., Maggs, R. J. and *Rasmussen, R. A.*, 1972: *Nature 237*, 452—453.

Lovett, R. F., 1975: *The occurrence of airborne sea salt and its meteorological dependence*, Thesis, Heriot-Watt Univ., United Kingdom.

MacIntyre, F., 1974a: Chemical fractionation and sea-surface microlayer processes. In *The Sea 5*, ed. by *E. D. Goldberg*, Wiley-Interscience, p. 245—299.

MacIntyre, F., 1974b: *J. Rech Atmos. 8*, 515—527.

MacKay, D. and *Wolkoff, A.*, 1973: *Envir. Sci. Technol. 7*, 611—614.

Mamane, Y., Ganor, E. and *Donagi, A. E.*, 1980: *Water air, soil pollution 14*, 29—43.

Marty, J. C., Saliot, A., Buat-Menard, P., Chesselet, R. and *Hunter, K. A.*, 1979: *J. Geophys. Res. 84*, 5707—5716.

Mason, B. J., 1971: *The physics of clouds*, Clarendon Press, Oxford, 2nd edition (1st ed., 1957),

McMurry, P. H. and *Friedlander, S. K.*, 1979: *Atmos. Environment 13*, 1635—1651.

Mészáros, A. and *Vissy, K.*, 1974: *J. Aerosol Sci. 5*, 101—109.

Mészáros, E., 1982: On the atmospheric input of sulfur into the ocean. To be published in *Tellus* vol. *34*.

Mészáros, E. and *Renoux, A.*, 1978: *Pollution Atmosph. 79*, 177—181.

Middleton, P. and *Kiang, C. S.*, 1978: *J. Aerosol Sci. 9*, 359—385.

Monahan, E. C., 1968: *J. Geophys. Res. 73*, 1127—1137.

Monahan, E. C., 1969: *J. Atmos. Sci. 26*, 1026—1029.

Monahan, E. C., 1971: *J. Phys. Oceanography 1*, 139—144.

Monahan, E. C., 1979: Whitecapping, a manifestation of air-sea interaction with implications for remote sensing. *Proceedings, Workshop on Processes in Marine Remote Sensing, Primars-1*, University of South Carolina Press, Columbia (in press).

Monahan, E. C., Bowyer, P. A., Doyle, D. M., Fitzgerald, M. P., O'Muircheartaigh, I. G., Spillane, M. C. and *Taper, J. J.*, 1981: *Whitecaps and the marine atmosphere*, Annual Report, Univ. College, Galway, 1981, 1—114.

Monahan, E. C., O'Regan, B. O. and *Doyle, D. M.*, 1980: *The influence of whitecaps on the marine atmosphere*, Annual Report, Univ. College, Galway, 1—123.

Monahan, E. C. and *O'Muircheartaigh*, 1980: *J. Phys. Oceanography 10*, 2094—2099.

Morelli, J., 1968: *Contribution à l'étude de la composition des aérosols formés à la surface de la mer; leur rôle dans les échanges de matière entre l'océan, l'atmosphère et le continent.* Thése de doctorat 3-*ème* cycle, Faculté des Sciences, Paris.

Morelli, J., 1977: *Contribution á l'étude du cycle atmosphérique du potassium marin*, Thése de doctorat d'état, Univ. de Paris VI.

Morelli, J., 1980: Données sur les échanges de matière à l'état particulaire à l'interface air-mer: *Implacations géochimiques, océanis 6*, 2.

Morelli, J., Buat-Menard, P. and *Chesselet, R.*, 1974: *J. Rech. Atmosph. 8*, 961—986.

Moyers, J. L. and *Duce, R. A.*, 1972a: *J. Geophys. Res. 77*, 5229—5238.

Moyers, J. L. and *Duce, R. A.*, 1972b: *J. Geophys. Res. 77*.

Nguyen, B. C., Bonsang, B., Gaudry, A. and *Lambert, G.*, 1977: Oxidation processes of sulfure components in the marine atmosphere: paper presented at the *IAGA/IAMAP Joint Assembly, Seattle*, USA, August 22—September 3, 1977.

Nguyen, B. C., Bonsang, B., Lambert, G. and *Pasquier, J. L.*, 1975: *Pure and Applied Geophysics (Pageoph). 123*, 489—500.

Nguyen, B. C., Gaudry, A., Bonsang, B. and *Lambert, G.*, 1978: *Nature 275*, 637—639.

Noonkester, V. R., 1981: Aerosol size spectra in a convective marine layer with stratus: results of airborne measurements near San Nicolas Island, California; Submitted to *J. Appl. Meteor.*

O'Brien, R. J., Holmes, J. R. and *Bockian, A. H.*, 1975a: *Envir. Sci. Technol. 9*, 568–576.

O'Brien, R. J., Crabtree, J. H., Holmes, J. R., Hoggan, M. C. and *Bockian A. H.*, 1975b: *Envir. Sci. Technol. 9*, 577–582.

Ono, A., Ito, T. and *Iwai, K.*, 1981: A note on the origin and nature of the Antarctic aerosol, prepared for publication.

Parungo, F., Nagamoto, C., Schnell, R., Nolt, I., Nickerson, E. and *Caldwell, W.*, 1981: *Hawaii mesoscale energy and climate project (HAMEC)—III. Atmospheric aerosol and cloud microphysics measurements.* U. S. Dept. of Commerce, NOAA, Envir Res. Labor., Boulder, March.

Paugam, J.-Y., 1975a: *C. R. Acad. Sci. Paris 280*, 821–824.

Paugam, J.-Y., 1975b: *J. Rech. Atmos. 9*, 67–75.

Paugam, J.-Y., Nguyen, B. C., Bonsang, B. and *Fongang, S.*, 1977: *Chemosphère 6*, 333–339.

Perrin, M. L., Madelaine, G. and Renoux, A., 1980: Evolution of fine particles naturally generated in a marine atmosphere, *Aerosols in Science, Medicine and Technology 8*, GAEF, Schmallenberg, 204–210.

Petrenchuk, O. P., 1979: *Eksperimentalnye issledovania atmosfernogo aerozolia*, Gidrometeoizdat, Leningrad.

Pich, J., Friedlander. S. K. and *Lai, F. S.*, 1970: *Aerosol Sci. 1*, 115–126.

Piotrowicz, S. R., Duce, R. A., Fasching, J. L. and *Weisel, C. P.*, 1979: *Marine Chemistry 7*, 307–324.

Podzimek, J., 1973: *J. Rech. Atmos. 7*, 137–152.

Podzimek, J., 1980a: Seashore aerosol at high relative humidity, *2nd Conf. on Coastal Meteor.* Preprint Vol. Los Angeles, Jan., AMS, 29–135.

Podzimek, J., 1980b: Advances in marine aerosol research, *J. Res. Atmos. 14*, 35–61.

Podzimek, J., 1980c: *The role of sea salt nuclei in the formation of precipitation in warm clouds*, Tech. Rep. AG–10 GCCPR, Univ. of Missouri-Rolla, 110.

Podzimek, J., Sedlacek, W. A. and *Haberl, J. B.*, 1975: *Peculiarities in Aitken nuclei counts in the tropical and subtropical stratosphere*, Tech. Rep. GCCPR, Univ. of Missouri, Rolla, Nov.

Podzimek, J., Sedlacek W. A. and *Haberl, J. B.*, 1977: *Tellus 29*, 116–127.

Podzimek, J. and *Stampfer, J. F.*, 1977: *Vertical distribution of marine aerosols above the seashore*, Tech. Rep. No. AG–7 GCCPR, Univ. of Missouri-Rolla.

Prahm, L. P., Torp, U. and *Stern, R. M.*, 1976: *Tellus, 28*, 355–372.

Prodi, F. and *Fea, G.*, 1979: *J. Geophys. Res. 84*, 6951–6960.

Prospero, J. M. and *Bonatti, E.*, 1969: *J. Geophys. Res. 74*, 3362–3371.

Prospero, J. M., Bonatti, E., Schubert, C. and *Carlson, T. N.*, 1970: *Earth and Planet Sci. Let. 9*, 287–293.

Prospero, J. M. and *Carlson, T. N.*, 1972: *J. Geophys. Res. 77*, 5255–5265.

Pruppacher, H. R. and *Klett, J. D.*, 1978: *Microphysics of clouds and precipitation*, D. Reidel, Dordrecht.

Radke, L. F., 1977: Marine aerosol: Simultaneous size distributions of the total aerosol and the sea salt fraction from 0.1 to 10 micron diameter, *Proc. 9-th Int. Conf. on Atmos. Aerosols*, Cond. and Ice Nuclei, Galway (pub. 1981).

Renoux, A., Paugam, J. Y. and *Madelaine, G.*, 1978: Phenomènes photolytiques de création d'aerosols en bord de mer. In *Aerosole in Naturwissenschaft, Medizin und Technik — Dynamik und Nachweis Ultrafiner Aerosole*, Jahreskongress der GAF, Wien, 15–20.

Renoux, A., Paugam, J. Y., Madelaine, G., Fongang, S., 1977: A production of very high condensation nuclei concentration at a tidal seashore, *Abstr. 9th Int. Conf. on Atmos. Aerosols, Cond. and Ice Nuclei*, Galway.

Russel, C. A. and *Stampfer, J. F.*, 1976: The dependence on particle size of the organic content of marine aerosols, Paper presented at the *Annual Meeting of the Missouri Academy of Science*, Rolla, April 23–24.

Schaefer, V. J., 1972: *J. Rech. Atmos. 37*, 507–518.

Scheuer, P. J., 1973: *Chemistry of marine natural products*, Academic Press, New York.

Schultz, A., Fritz G. and *Schumann, G.*, 1978: Size distribution of Aitken-nuclei over the North Atlantic Ocean. "*Meteor*" *Forsch.-Ergebn. B. 13*, 10–13.

Schütz, L. and *Davidson, K. L.*, 1980: Observation results on the influence of stability on surface layer marine aerosol concentrations, *Aerosols in Science, Medicine and Technology 8*, GAF, Schmallenberg, 211–216.

Schütz, L. and *Jaenicke, R.*, 1974: *J. Appl. Meteor. 13*, 863–870.

Schmel, G. A. and *Sutter, S. L.*, 1974: *J. Rech. Atmos. 8*, 911–920.

Simoneit, B. R. T., 1974: *Chem. Oceanography 7*, 233–311.

Simoneit, B. R. T., 1977: *Mar. Chem. 5*, 443–464.

Slinn, W. G., Hasse, L., Hicks, B. B., Hogan, A. W., Lat, D., Liss, P. S., Munnich, K. O., Sehmel, G. A. and *Vittori, O.*, 1978: *Atmos. Envir. 12*, 2055–2087.

Stauffer, D., Mohnen, V. A. and *Kiang, C. S.*, 1973: *J. Aerosol Sci. 4*, 461–471.

Tahahaski, K., Kasahara, M. and *Itoh, M.*, 1975: *J. Aerosol Sci. 6*, 45–56.

Tang, I. N., 1976: *J. Aerosol Sci. 7*, 361—371.
Tang, I. N., Munkelwitz, H. R., Davis, J. G., 1977a: *J. Aerosol Sci. 8*, 149—159.
Tang, I. N., Munkelwitz, H. R., 1977b: *J. Aerosol Sci. 8*, 321—330.
Tang, I. N., Munkelwitz, H. R., Davis, J. G., 1978: *J. Aerosol Sci. 9*, 505—511.
Thudium, J., 1978: *Pageoph. 116*, 130—148.
Toba, Y., 1965a: *Tellus 17*, 365—382.
Toba, Y., 1965b: *Tellus 17*, 131—145.
Toba, Y., 1966: *Tellus 18*, 132—145.
Toba, Y. and *Chaen, M.*, 1973: *Rec. Oceanogr. Works in Japan 12*, 1—11.
Toba, Y. and *Tanaka, M.*, 1963: *J. Met. Soc. Japan 41*, 135—144.
Tomasi, C., Tampieri, F., 1977: *Tellus 29*, 66—73.
Tsunogai, S., Saito, O., Yamada, K. and *Nakaya, S.*, 1972: *J. Geophys. Res. 77*, 5283—5292.
Twomey, S., 1977: *Atmospheric Aerosols*, Elsevier Sci. Publ. Comp., Amsterdam.
Tymen, G., Butor, J. F., Renoux, A. and *Madelaine, G.*, 1975: *Chemosphère 4*, 357—360.
Volz, F. E., 1972: *Appl. Optics 11*, 755—759.
Wallace, G. T., Jr. and *Duce, R. A.*, 1975: *Mar. Chem. 3*, 157—181.
Wallace, G. T., Jr. and *Duce, R. A.*, 1978a: *Deep-Sea Res. 25*, 827—835.
Wallace, G. T., Jr. and *Duce, R. A.*, 1978b: *Limnol. Oceanogr. 23*, 1155—1167.
Wallace. G. T., Jr., Hoffman, G. L. and *Duce, R. A.*, 1977: *Mar. Chem. 5*, 143—170.
Walsh, P. R. and *Duce, R. A.*, 1976: *Geophys. Res. Let. 3*, 375—378.
Walsh, P. R., Duce, R. A. and *Fasching, J. L.*, 1979a: *J. Geophys. Res. 84*, 1710—1718.
Walsh, P. R., Duce, R. A. and *Fasching, J. L.*, 1979b: *J. Geophys. Res. 84*, 1719—1726.
Wells, W. C., Gal, G. and *Munn, M. W.*, 1976: *Aerosol distribution in maritime air and predicted scattering coefficient in the infrared*, LMSC/D45789 Lockheed, Palo Alto Res. Lab, June.
Willkniss, P. E. and *Bressan, D. J.*, 1972: *J. Geophys. Res. 77*, 5307—5315.
Willkniss, P. E., Bressan, D. J., Carr, R. A. and *Larson, R. E.*, 1974: *J. Rech. Atmos. 8*, 883—893.
Winchester, J. W. and *Duce, R. A.*, 1977: The air-water interface: particulate matter exchange across the air-water interface, In *Fate of pollutants in the air and water environment, Part 1, 8*, Ed. I. H. Suffet, John Wiley and Sons, Inc., New York, 27—47.
Winkler, P., 1973: *J. Aerosol Sci. 4*, 373—387.
Winkler, P., 1975: *Geoph. Res. Let. 2*, 45—48.
Winkler, P., 1977: On production rates in marine aerosols, In *Radiation in the Atmosphere*, 50—53, Sci. Press, Princeton.
Winkler, P., 1980: *J. Geophys. Res. 85*, 4481—4486.
Winkler, P. and *Junge, C.*, 1971: *J. Appl. Meteor. 10*, 159—163.
Winkler, P. and *Junge, C.*, 1972: *J. Rech. Atmos. 6*, 617—638.

IDŐJÁRÁS

Az Országos Meteorológiai Szolgálat folyóirata, 86. évf. 2–4. szám, 1982, március–augusztus
Journal of the Hungarian Meteorological Service, Vol. 86. No. 2–4. March–August 1982, Budapest

Airborne measurements of cloud condensation nuclei active at supersaturations $\leq 0.15\%$

E. E. HINDMAN*, *Research Institute of Colorado, Fort Collins, CO 80526, U.S.A. and* P. C. SINCLAIR, *Dept. Atmospheric Science, Colorado State University, Fort Collins, CO 80523, U.S.A.*

Repülőgépes mérések az $S_c \leq 0{,}15\%$ *túltelítettségénél aktivizálódó felhő-kondenzációs magvak (CCN) tanulmányozására.* Aeroszol részecske (0,09 – 7,5 μm átmérő) és felhő-kondenzációs mag (0,02 – 0,14% túltelítettség) méréseket végeztünk a tenger fölött a határrétegen belül és fölötte, valamint mértük egy stratus felhő cseppspektrumát California partjain kívül, 1980 szeptemberében. A mérések célja az volt, hogy meghatározzuk a CCN koncentráció változását a magassággal a tenger fölött, az oldódó anyag frakciót a CCN-ben, valamint a maximális túltelítettséget a felhőn belül. Azt találtuk, hogy mind a CCN koncentráció, mind az oldódó frakció a CCN-ben csökkent a magassággal a határrétegen belül, ami a CCN óceáni eredetére utal. A maximális túltelítettség a vizsgált felhőben ~0,1% volt, ami azt jelenti, hogy a stratus felhők képződésekor a 0,15%-nál kisebb túltelítettségen aktivizálódó részecskék jelentős szerepet játszanak.

*

Airborne measurements of cloud condensation nuclei active at supersaturations $\leq 0.15\%$. Aerosol particle (0.09 to 7.5 μm diameter) and cloud condensation nucleus (0.02 to 0.14% supersaturation) measurements were obtained within and above the marine boundary layer, and stratus cloud droplet measurements were obtained within the boundary layer offshore of southern California during September 1980. The purpose of the measurements was to determine the vertical variations of the CCN above the sea, the fraction of soluble material in the CCN, and the maximum supersaturations within the clouds. It was found that both the concentrations of the CCN and the fraction of soluble material in the CCN decreased with increasing altitude in the boundary layer indicating an oceanic source for the CCN. The maximum supersaturation in the one cloud investigated was about 0.1% confirming that CCN active at supersaturations $\leq 0.15\%$ are important in stratus cloud formation.

*

Introduction. Airborne measurements of cloud condensation nuclei (CCN) active at critical supersaturations (S_c) greater than about 0.15% using thermal-gradient diffusion cloud chambers (TGDCC) have provided basic meteorological information (e.g., *Twomey* and *Wojciechowski*, 1969 and *Fitzgerald*, 1972). Recently, the isothermal haze chamber (IHC) has been developed to determine the concentrations of CCN that cannot be measured with the TGDCC: CCN active between about 0.01 and 0.15% supersaturation. These nuclei have been shown by *Hoppel* and *Fitzgerald* (1977) and *Hudson* (1980a, b) to be important in the formation of certain fogs and stratus clouds. Isothermal haze chambers also have been developed by *Laktinov* (1972) and *Alofs* (1978). Simultaneous TGDCC and IHC measurements now provide an

* On leave from Dept. Atmospheric Science, Colorado State University, Fort Collins, CO 80523.

accurate representation of the CCN spectrum between 0.01 and about 1% supersaturation as demonstrated in the recent international CCN workshop reported by *Kocmond* et al. (1981).

As a result of these accurate CCN measurement techniques, *Hoppel* (1979) and *Fitzgerald* and *Hoppel* (1981) have shown that the chemical nature of CCN can be estimated from simultaneous CCN spectra and aerosol particle spectra measurements. Further, *Hudson* (1980a, b) has developed a technique using near-simultaneous measurements of haze droplet diameters at 100% relative humidity (d_{100}) from an IHC and fog, and stratus droplet measurements from an optical particle counter in order to estimate the maximum supersaturations in fogs and stratus clouds, a poorly understood property of these meteorological phenomena.

There is little, if any, information about the variations in the vertical of CCN active at $S_c < 0.15\%$, the fraction of soluble material (ε) in the CCN, and the critical supersaturations in coastal stratus clouds. This information will provide realistic initial conditions for numerical simulations of coastal fog and stratus cloud formation. Consequently, an airborne IHC was constructed after *Hudson* (1980a) to obtain the required information.

The IHC was flown along with aerosol particle and cloud droplet measuring equipment as a part of a larger satellite- "air truth" project described by *Hindman, Durkee* and *Sinclair* (1981). Simultaneous CCN and aerosol particle measurements were obtained above and through the depth of the marine boundary layer over the coastal waters offshore of southern California between 19 September and 2 October 1980. From these measurements we show that the CCN originated at the sea surface and, in the one stratus cloud investigated, the maximum supersaturation was about 0.1% which is lower than the supersaturation range of most TGDCC.

1. *Measurement system*

The description and calibration of the airborne IHC has been provided by *Hindman* (1981). Briefly, the size distribution of haze droplets in equilibrium at 100% relative humidity [$N(d_{100})$] is obtained from the chamber. The critical supersaturation of a droplet in equilibrium at 100% relative humidity is given by

$$d_{100}(\mu\text{m}) = 0.082 S_c^{-1}(\%) \qquad (1)$$

after *Laktionov* (1972). *Hoppel* and *Fitzgerald* (1977) have shown that (1) is indepedent of CCN chemical composition and soluble fraction. Consequently, operating on $N(d_{100})$ with (1) produces $N(S_c)$ which is the CCN spectra.

The concentrations of aerosol particles with diameters between 0.09 and 3 μm were measured with an Active Scattering Aerosol Spectrometer Probe (ASASP-X), and the concentrations of particles with diameters between 0.5 and 40 μm were measured with a Forward Scattering Spectrometer Probe (FSSP). Both devices have been described by *Knollenberg* (1976). The submicron size ranges for these instruments were calibrated using known sizes of latex spheres; the supermicron ranges of the FSSP were calibrated using silicon glass spheres. The real portions of the complex index of refraction of the test particles are similar to marine aerosol particles; the imaginary portions are small and probably approximate those of the marine particles.

Consequently, the measurements from the ASASP-X and FSSP should closely approximate the true aerosol particle size distributions.

The IHC and ASASP-X were cross-calibrated in the laboratory using a polydispersion of $(NH_4)_2SO_4$ particles generated with a system described by *Hindman* et al. (1981). The d_{100} spectra obtained from the IHC were converted to CCN spectra using (1). The size spectra of the $(NH_4)_2SO_4$ particles obtained

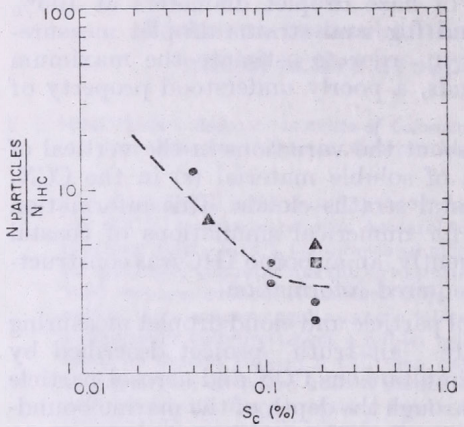

Fig. 1: Number of CCN calculated from ASASP-X measurements (N particles) divided by the number of CCN calculated from simultaneous IHC measurements as a function of critical supersaturation (S_c). The dots are simultaneous ASASP – IHC (non-humidified inlet) measurements of $(NH_4)_2SO_4$ particles, the triangles are simultaneous particle – IHC (humidified inlet) measurements made at the Reno CCN workshop as reported by *Hlndman* (1981) and the square is a simultaneous particle – IHC (non-humidified inlet) measurement also made at Reno

from the ASASP-X were converted to CCN spectra using the following expression from *Fitzgerald* (1973),

$$d(\mu m) = 3.06 \times 10^{-2} \varepsilon^{-0.31} S_c^{-0.66}(\%) \tag{2}$$

where ε is the fraction of the particle which contains $(NH_4)_2SO_4$; in the laboratory studies $\varepsilon = 1$. The CCN spectra obtained from the IHC and ASASP-X

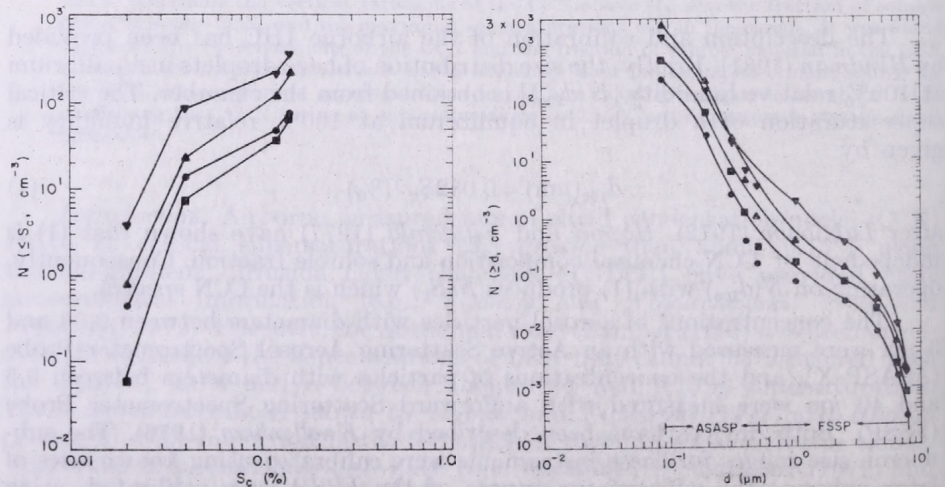

Fig. 2: Simultaneous CCN (left) and aerosol particle (right) measurements on 28 September 1980 in the vicinity of Santa Cruz Island. The symbols represent data collected at the following altitudes and times: ▼ – 500' MSL, 1128–1132 PDT; ▲ – 1700' MSL, 1114–1119 PDT; ■ – 2600' MSL, 1101–1105 PDT; ● – 4800' MSL, 0943–0948 PDT

measurements were compared by dividing the IHC-generated spectra into the ASASP-X generated spectra; the results are presented in *Fig. 1*. It can be seen in Fig. 1 that the CCN concentrations obtained from the ASASP-X measurements were systematically higher than the CCN concentrations obtained from the IHC measurements. This is probably due to slight subsaturations in the IHC as discussed by *Hindman* (1981). Consequently, the airborne CCN concentrations obtained from the IHC (operated with a non-humidified sample inlet) were increased using the values in Fig. 1 (e.g., concentrations measured at 0.14% were increased by a factor of 3, etc.).

The IHC and ASASP-X instruments were mounted inside a Cessna T-207 aircraft and the FSSP was mounted on the wing. The particle losses in the sampling probes for the ASASP-X and IHC were found to be negligible as discussed by *Hindman* (1982). Air-motion (u, v, w, turbulence) and state-variable (T, T_d, P) measurements were obtained from the aircraft. Particles were collected on the high-volume Nuclepore filters and are presently under investigation (sizes, numbers and elemental compositions), consequently results are not available for presentation.

2. *Procedures*

The experimental region was among the Channel Islands offshore o southern California. The region was chosen because of the well-defined marine boundary layer and frequent occurrence of extensive stratus cloud layers. These meteorological phenomena are due to a combination of cool surface water caused by upwelling and subsiding, offshore flow due to the semi-permanent subtropical high-pressure system.

The aircraft took off from the coastal plains and flew offshore above the boundary layer. Once offshore, the aircraft decended to near the surface in a step-wise fashion so a series of 20 to 30 n mi horizontal tracks were flown

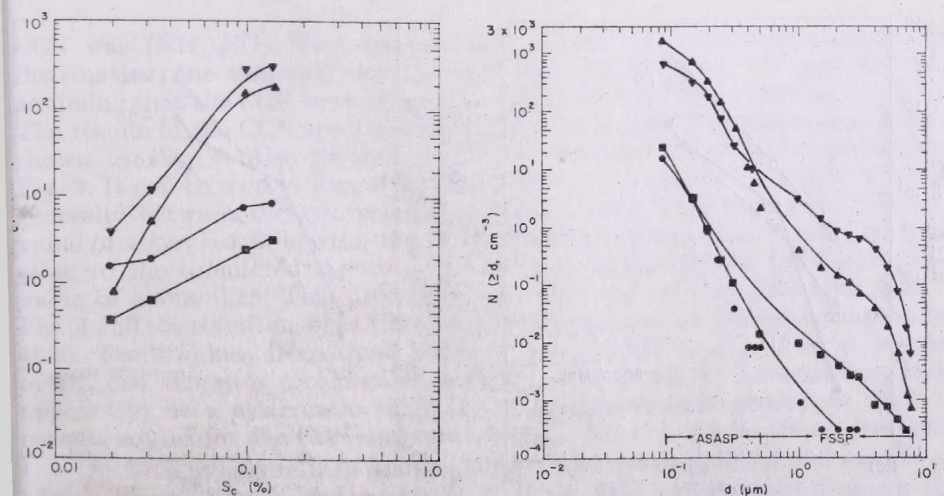

Fig. 3: Simultaneous CCN (left) and aerosol particle (right) measurements on 30 September 1980 offshore of Ventura, CA. The symbols represent data collected at the following altitudes and times: ▼ – 200' MSL, 1244–1249 PDT; ▲ – 700' MSL, 1225–1230 PDT; ■ – 2000' MSL, 1155–1200 PDT; ● – 4500' MSL, 1114–1119 PDT

above and below the marine inversion. The aircraft then climbed from near the surface to higher altitudes for the return trip during which stratus droplet measurements were obtained. The particle, air-motion, state-variable and CCN measurements were obtained continuously throughout the flights. The high-volume samples were collected for 5 min periods along the horizontal flight tracks.

3. Results

Simultaneous IHC and ASASP-X measurements suitable for analysis were obtained on 28 and 30 September 1980. The simultaneous measurements *(Figs 2* and *3)* were obtained at various altitudes in the vicinity of Santa Cruz

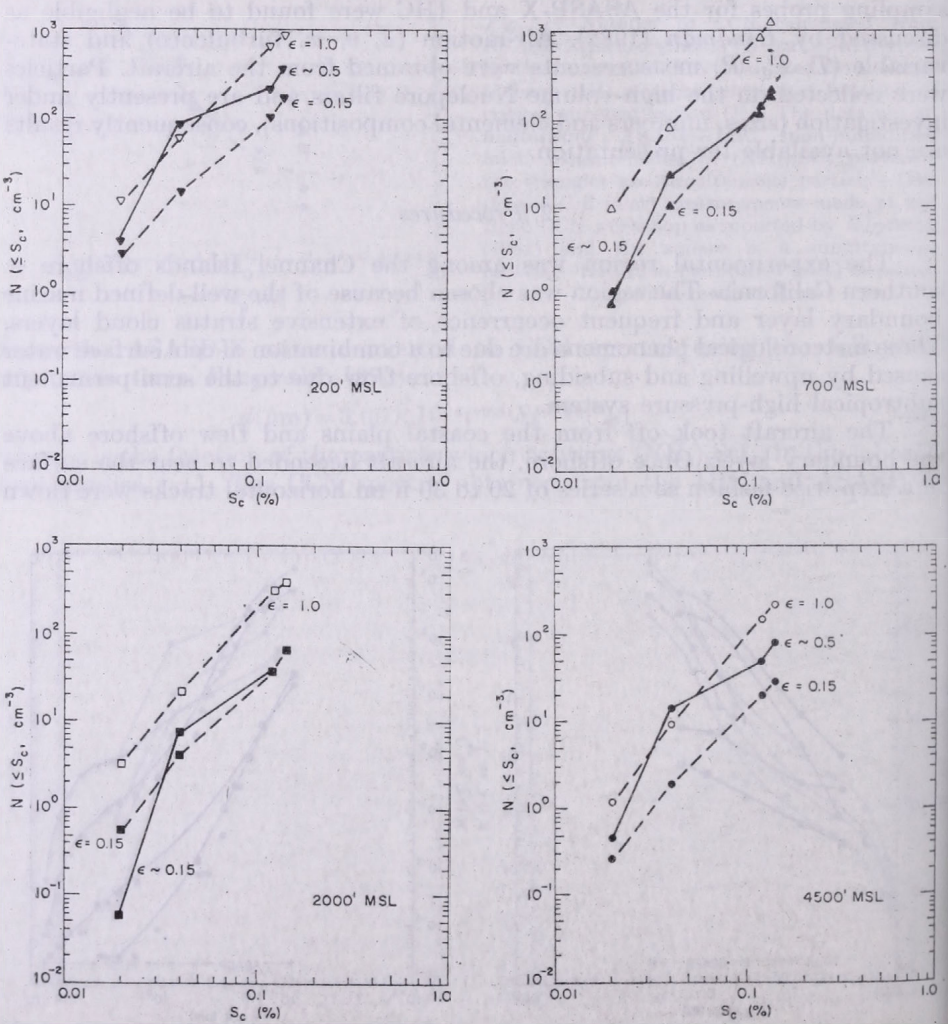

Fig. 4: CCN spectra calculated from the particle measurements made on 30 September 1980, assuming the particles are composed either totally of $(NH_4)_2SO_4$ ($\varepsilon=1.0$) or composed 15% of $(NH_4)_2SO_4$ and 85% insoluble material ($\varepsilon=0.15$). The measured CCN spectra are given by the solid lines and the inferred fraction of soluble material in the CCN are indicated

Island on 28 September 1980 and offshore of the city of Ventura between the city of Santa Barbara and Santa Cruz Island on 30 September 1980. The curves are smoothed to account for the unnatural irregularities where the ASASP and FSSP data merge. These irregularities were caused by loss of sensitivity of the FSSP for particles 0.5 μm in diameter and a slight misalignment of the sample tube within the ASASP-X which caused underestimation of the numbers of the largest particles.

The soluble fraction of the CCN were determined using the following procedure (the procedure is illustrated using the data from 30 September 1980). The particle size distributions in *Fig. 3* were transformed into CCN supersaturation spectra using (2) and assuming that the soluble component of the

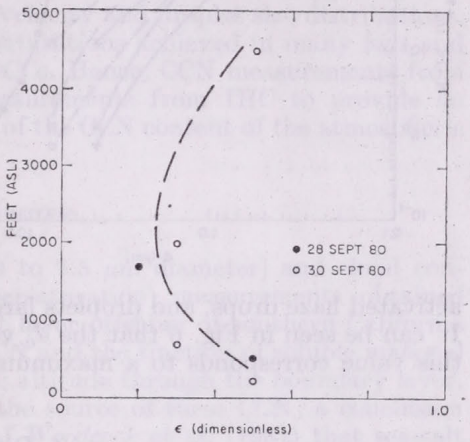

Fig. 5: Variation of the fraction of soluble material (ε) in CCN as a function of altitude above sea level. The measurements on 28 September 1980 were made in the vicinity of Santa Cruz Island

CCN was $(NH_4)_2SO_4$. Two spectra were calculated from each particle size distribution, one assuming that the CCN were all soluble ($\varepsilon = 1$), and the other assuming that the CCN were composed mainly of insoluble material ($\varepsilon = 0.15$). The results of the CCN spectra calculated from the particle measurements are shown in *Fig. 4*. Also plotted in Fig. 4 are the CCN measurements from Fig. 3. It can be seen in Fig. 4 that the spectrum measured at 200 ft MSL lies generally between the two calculated spectra indicating the CCN have an ε value of about 0.5. Likewise, the CCN spectrum measured at 700 ft MSL lies close to the calculated spectra with $\varepsilon \simeq 0.15$ indicating the CCN have an ε value of about 0.15. This procedure was followed for the remaining data in Fig. 4 and the simultaneous CCN and particle measurements from 28 September 1980. The ε values from these analyses are plotted in *Fig. 5* as a function of altitude. There is considerable scatter in the ε values. Nevertheless, there appears to be a systematic variation of ε with altitude consistent with an oceanic source for the CCN measured below about 1,000 ft above sea level.

On 20 September 1980, a stratus layer was investigated a few miles west of San Miguel Island. Measurements with the IHC were obtained above and below the stratus clouds while FSSP measurements were made within the clouds. These measurements are used to estimate the maximum supersaturation in the clouds following a procedure developed by *Hudson* (1980a). The procedure is illustrated in *Fig. 6*. The d_{100} measurements from the IHC are plotted

along with the droplet measurements from the FSSP. The d_{100} values are converted into critical diameter (d_c) values using the following relationship from *Hudson* (1980a)

$$d_c = \sqrt{3}\, d_{100} \tag{3}$$

The intersection of the d_c curves and the droplet curves in *Fig. 6* define the critical diameter for the stratus droplets; droplets smaller than d_c are un-

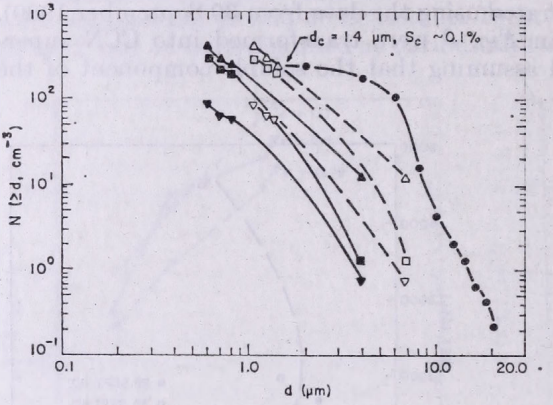

Fig. 6: Measurements of d_{100} beneath (▲ – 650' MSL, 1537 PDT) and above (■ – 3000' MSL, 1522–1525 PDT, ▼ – 5000' MSL, 1432–1437 PDT) a 200' thick stratus layer on 20 September 1980 a few miles west of San Miguel Island. The corresponding d_c values are indicated by the open symbols. The stratus droplet concentrations measured at 1000' MSL at 1538 PDT are denoted by the ● symbols. The critical diameter of the droplet distribution is ~1.4 μm corresponding to a S_c of about 0.1%

activated haze drops, and droplets larger than d_c are activated cloud droplets. It can be seen in Fig. 6 that the d_c value is about 1.4 μm. Using (3) and (1), this value corresponds to a maximum supersaturation of 0.1%.

4. *Discussion*

It can be seen in Figs. 2 and 3 that the highest CCN concentrations were found at the lowest levels and vice versa. This result when combined with the variations of ε in the vertical shown in Fig. 5 leads to the conclusion that the high concentrations of CCN active at $S_c < 0.15\%$ near the sea originated from the sea. The high ε value measured at 4,500 ft MSL is believed due to anthropogenic particles flowing offshore from urban areas.

The conclusion that the CCN active at $S_c < 0.15\%$ originated from the sea is consistent with the following evidence. *Hobbs* (1971) reported from simultaneous airborne measurements over the ocean of sodium-containing particles (SCP) and CCN active at 0.5% that, even at 50 ft above the ocean, the SCP comprised only a small percentage of CCN active at 0.5%. This result indicated that the ocean is not a source of CCN active at 0.5%. Further, *Radke* et al. (1976) from simultaneous measurements near Barrow, Alaska of SCP, and CCN active at 1% concluded the SCP were a small fraction of the CCN. This result extends those of *Hobbs* (1971). However, they concluded, based on extrapolating the CCN measurements to the low supersaturations believed to exist in fogs and stratus, that SCP probably comprise a majority of the fog and stratus droplet nuclei (they stated that the SCP were probably airborne sea salt particles). Finally, *Woodcock* et al. (1981) have shown, through analysis of collected marine fog droplets, that sea-salt particles play an important role in the initiation and growth of marine fogs.

The simultaneous IHC and ASASP-X measurements provided information on the vertical variation of ε above the sea surface, which is consistent with the results of other investigators. This favorable result indicates that simultaneous IHC and ASASP-X measurements made in other regions may be useful in estimating values of ε for CCN.

The estimated maximum supersaturation of 0.1%, in the one stratus investigated, is consistent with the 0.2 to 0.3% maximum supersaturations estimated for coastal stratus by *Hudson* (1980b). The result is substantially less than the maximum instantaneous supersaturations of about 0.4% measured in a forming radiation fog by *Gerber* (1980). The result, however, is greater than the 0.06 to 0.11% maximum supersaturations estimated in coastal fogs by *Hudson* (1980b). Surprisingly, the result compares with *Warner's* (1968) report of a median supersaturation in cumulus clouds of 0.1% based on simultaneous measurements of updraft velocity and droplet size distributions. These results indicate maximum supersaturations achieved in many fogs and clouds are lower than achieved in TGDCCs. Hence, CCN measurements from TGDCC should be combined with measurements from IHC to provide an accurate and meaningful representation of the CCN content of the atmospheric aerosol.

5. *Conclusions*

Simultaneous aerosol particle (0.09 to 7.5 μm diameter) and cloud condensation nucleus (0.02 to 0.14% supersaturation) measurements obtained within and above the marine boundary layer offshore of southern California show that both the concentrations of CCN and the fraction of soluble material (ε) in the CCN decreased with increasing altitude through the boundary layer. This result indicates that the ocean is the source of these CCN; a conclusion which is consistent with the findings of *Woodcock* et al. (1981) that sea-salt particles play an important role in the formation of marine fogs.

Measurements with the IHC were made beneath and above a stratus cloud layer, and cloud droplet measurements were made within the layer in the same region. From these measurements it was estimated that the maximum supersaturation in the cloud layer was about 0.1%. This result indicates that the CCN measured with the IHC are the CCN that are important to the formation of coastal stratus; a result consistent with the findings of *Hoppel* and *Fitzgerald* (1977) and *Hudson* (1980a, b).

Acknowledgements. This research was supported by Office of Naval Research, Contract N00017–79–C–0793. The Geophysics and Range Divisions of the Pacific Missle Test Center, Pt. Mugu, California provided, respectively, meteorological and aircraft support for our flight activities.

REFERENCES

Alofs, D. J., 1978: Performance of a dual-range cloud nucleus counter. *J. Appl. Meteor., 17*, 1286–1297.

Fitzgerald, J. W., 1972: *A study of the initial phase of cloud droplet growth by condensation: comparison between theory and observation.* Ph. D. Dissertation, U. of Chicago, 144 p.

Fitzgerald, J. W., 1973: Dependence of the supersaturation spectrum of CCN on aerosol size distribution and composition. *J. Atmos. Sci., 30*, 628–634.

Fitzgerald, J. W. and *Hoppel, W. A.*, 1981: Measurements of the relationship between the dry size and critical supersaturation of natural aerosol particles. *ICCP Programs and Abstracts IAMAP 3rd Sci. Assembly*, Hamburg, FRG.

Gerber, H. E., 1980: A saturation hygrometer for the measurement of relative humidity between 95% and 105%. *J. Appl. Meteor., 19*, 1196–1208.

Hindman, E. E., 1981: An airborne isothermal haze chamber. *J. Rech. Atmos.*, submitted.

Hindman, E. E., 1982: Experimental determinations of aerosol particle losses in airborne sampling inlets. *In-situ Air Quality Monitoring from Moving Platforms.* Air Poll. Cont. Assn. Specialty Mtg., in preparation.

Hindman, E. E., Durkee, P. A. and *Sinclair, P. C.*, 1981: Meteorological properties of certain anomalous grey-shade regions observed in satellite images. *J. Appl. Meteor.*, in preparation.

Hindman, E. E., Horn, R. D. and *Finnegan, W. G.*, 1981: Particle generation, transport and characterization at the First International Workshop on Light Absorption by Aerosol Particles. *Applied Optics*, submitted.

Hobbs, P. V., 1971: Simultaneous airborne measurements of cloud condensation nuclei and sodium-containing particles over the ocean. *Q.J.R.M.S., 97*, 263–297.

Hoppel, W. A., 1979: Measurement of the size distribution and CCN supersaturation spectrum of submicron aerosols over the ocean. *J. Atmos. Sci., 36*, 2006–2015.

Hoppel, W. A. and *Fitzgerald, J. W.*, 1977: Measurements of CCN spectra at low supersaturations in relation to fog formation off the coast of Nova Scotia. In *Proc. Symp. Rad. in the Atmos.*, H. J. Bolle, editor, Science Press, 171–173.

Hudson, J. G., 1980a: Relationship between fog condensation nuclei and fog microstructure. *J. Atmos. Sci., 37*, 1854–1867.

Hudson, J. G., 1980b: Microphysics of coastal fog and stratus. *Proc. 8th Conf. on Cloud Physics*, Clermont-Ferrand, France, 205–208.

Knollenberg, R. G., 1976: Three new instruments for cloud physics measurements: The 2-D spectrometer, the FSSP and the ASASP. *Preprints Intl. Conf. Cloud Phys.*, AMS, Boston, 554–561.

Kocmond, W. C., C. F. Rogers, U. Katz, J. G. Hudson and *J. E. Jiusto*, 1982: The 1980 International Cloud Condensation Nucleus Workshop. *Időjárás* 86. 160–168.

Laktionov, A. G., 1972: A constant temperature method of determining the concentration of cloud condensation nuclei. *Atmos. Ocean. Physics, 8*, 382–385.

Radke, L. F., P. V. Hobbs and *J. E. Pinnons*, 1976: Observations of cloud condensation nuclei, sodium-containing particles, ice nuclei and the lightscattering coefficient near Barrow, Alaska. *J. Appl. Meteor., 15*, 982–995.

Twomey, S. and *T. A. Wojciechowski*, 1969: Observations of the geographical variations of cloud nuclei. *J. Atmos. Sci., 26*, 684–688.

Warner, J., 1968: The supersaturation in natural clouds. *J. Rech. Atmos., 3*, 233–237.

Woodcock, A. H., D. C. Blanchard and *J. E. Jiusto*, 1981: Marine fog droplets and salt nuclei – Part II, *J. Atmos. Sci., 38*, 129–140.

IDŐJÁRÁS

Az Országos Meteorológiai Szolgálat folyóirata, 86. évf. 2–4. szám, 1982. március–augusztus
Journal of the Hungarian Meteorological Service, Vol. 86. No. 2–4. March–August 1982, Budapes

Measurements with an instantaneous CCN spectrometer

G. HUDSON, C. F. ROGERS and W. C. KOCMOND, *Atmospheric Sciences Center, Desert Research Institute, University of Nevada System P.O.B. 60220 Reno, Nevada 89506, U.S.A.*

Mérések „pillanatnyi" felhő-kondenzációs-mag spektrométerrel. A felhő-kondenzációs magvak (Cloud Condensation Nuclei, CCN) pillanatnyi értékének mérésére szolgáló spektrométer lényegében három folyamatos áramú számlálóból áll. Ez a műszer – megfelelő kalibrálás után – egyidejűleg három vagy több pontot ad a magszám- és a kritikus túltelítettségi CCN spektrum megszerkesztéséhez. Jelen munkában monodiszperz ezüst-jodid és korom részecskékkel végzett mérések eredményeiről számolunk be. Az ezüst-jodid elméleti kritikus túltelítettsége 4% körül volt, ezzel szemben már 0,57%-nál magvasodást tapasztaltunk (más berendezések hasonló eredményt adtak az 1980-ban, Reno-ban (Nevada) végzett összehasonlító mérések során.) A korom részecskék kritikus túltelítettségét 0,15–0,26 μm közötti nagyságú részecskékre határoztuk meg; általában ezek a részecskék csaknem olyan aktívaknak bizonyultak, mint az azonos nagyságú ammóniumszulfát magvak.

*

Measurements with an instantaneous CCN *spectrometer.* The instantaneous cloud condensation nuclei (CCN) spectrometer is essentially three continuous-flow diffusion CCN counters in a series flow arrangement. After appropriate calibrations, this instrument simultaneously yields 3 or more points on a number-*versus*-critical supersaturation CCN spectrum. Application of the device to measurements of the CCN activity of monodisperse silver iodide and coal combustion fly ash aerosols is described. The silver iodide had a theoretical critical supersaturation of about 4%, but was found by this instrument (and others at the 1980 International CCN Workshop) to nucleate at about 0.57%. The fly ash critical supersaturation was measured for a range of particle diameters from 0.15 μm to 0.26 μm; generally this material was found to be nearly as active as ammonium sulfate CCN of the same diameters.

*

Introduction. Measurements of cloud condensation nuclei (CCN) using a new "instantaneous" spectrometer are described in this presentation. The device, essentially three continuous-flow diffusion (CFD) CCN counters in a series flow arrangement, obtains three points on a cumulative number density-*versus*-critical supersaturation spectrum at any one instant in time by generating a trimodal droplet size distribution. The device was used with success during the recent 1980 International CCN Workshop (reported elsewhere in this Journal) on a variety of pure soluble and ambient aerosols. This presen tation will summarize results obtained in measurements of the CCN-activity of two aerosols of practical interest: a sample of coal combustion fly ash, and a sample of silver iodide.

The instantaneous sepctrometer has been described in more detail elsewhere (*Hudson* et al., 1980; *Hudson* et al., 1981). *Figure 1* shows a schematic

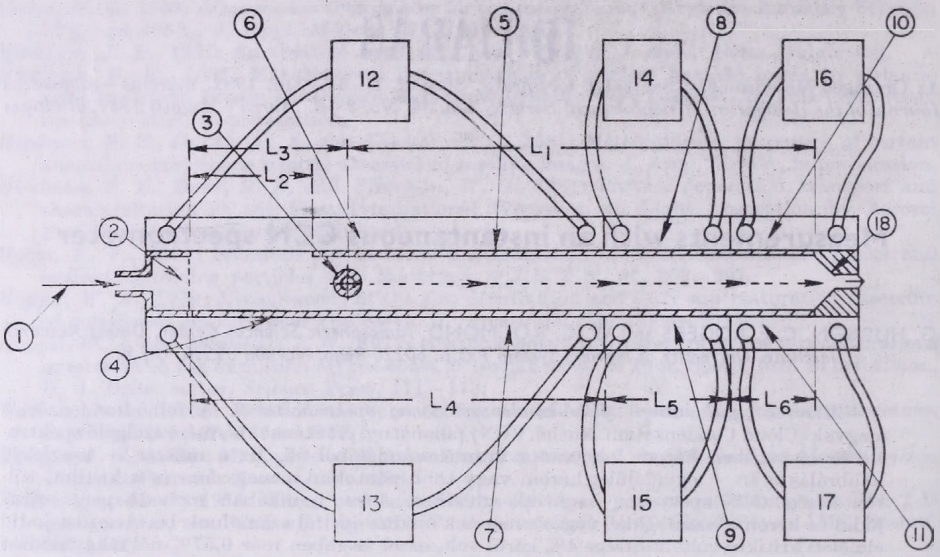

Fig. 1: Schematic of the instantaneous CCN spectrometer: $L_1 = 48$ cm; $L_2 = 8.4$ cm; $L_3 = 10.4$ cm; $L_4 = 38.4$ cm (1st supersaturation zone – S_1, T_3, T_4); $L_5 = 12$ cm (2nd supersaturation zone – S_2, T_2, T_5); $L_6 = 8$ cm (3rd supersaturation zone – S_3, T_1, T_6). *Supersaturation:* $S_1 < S_2 < S_3$. *Plate temp:* $T_1 < T_2 < T_3 < T_4 < T_5$.
1 – Carrier flow entrance; *2* – diffuser screen; *3* – sample injection tube; *4* – cold plate wicking surface; *5* – warm plate wicking surface; *6* – first warm section, T_4; *7* – first cold section, T_3; *8* – second warm section, T_5; *9* – second cold section, T_2; *10* – third warm section, T_6; *11* – third cold section, T_1; *12* – temperature bath at T_4; *13* – temperature bath at T_3; *14* – temperature bath at T_5; *15* – temperature bath at T_2; *16* – temperature bath at T_6; *17* – temperature bath at T_1; *18* – exhaust to OPC

cross-section of the device, where six thermostated circulating water baths are used to maintain three separate regions of temperature differential across the parallel plates. Three regions of supersaturations S_1, S_2, and S_3 are thereby created, with the supersaturation increasing in ascending order along the direction of flow. CCN passing through the spectrometer activate in one of the supersaturation zones if their critical supersaturation S_c is exceeded by S_1, S_2, or S_3. Activated droplets exiting the chamber are then counted and sized by a Royco optical particle counter which is connected to a 512 channel analyzer and to a standard Royco 5 channel analyzer module with printer.

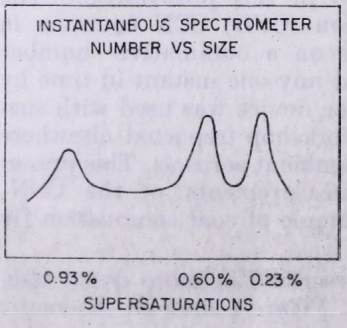

Fig. 2: Trimodal droplet size distribution produced in spectrometer

[In all data, the double-valued region (1.0 to 2.0 μm diameter, approximately) of the Royco response must be avoided.]

In general, then, a polydisperse aerosol will generate a trimodal droplet size distribution, where the least active nuclei have produced the smallest droplets and the most active nuclei, which have been growing the entire length of the spectrometer, have produced the largest droplets (see *Fig. 2*). Expressed as a cumulative distribution, in terms of the number density of droplets of radii greater than, or equal to, the value shown on the abcissa, the general result is as shown for polydisperse NaCl in *Fig. 3*. This Figure is instructive because it illustrates the frequent situation of overlap between the three regions of the trimodal droplet size distribution, an expected phenomenon when the polydisperse aerosol being sampled is not a perfect sum of three monodisperse components, and when there is inevitably some instrumental blurring of the three size components.

The spectrometer is routinely checked and calibrated in two ways to improve the interpretations of these kinds of data. First, the number concentration read out at varying Royco size thresholds in the spectrometer is compared to the concentration read out by a conventional continuous-flow diffusion (CFD) CCN counter operating at one fixed supersaturation setting. That given supersaturation may then be associated with "plateau" regions in data such as Fig. 3. Secondly, nearly monodisperse sodium chloride aerosol (from an electrostatic classifier) passed through the spectrometer allows association of a given output droplet size with a given input critical super-

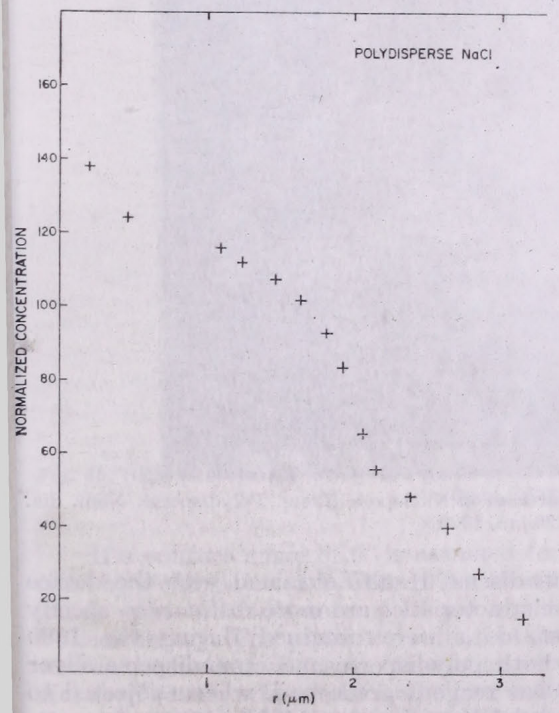

Fig. 3: Cumulative distribution of droplets produced from polydisperse NaCl

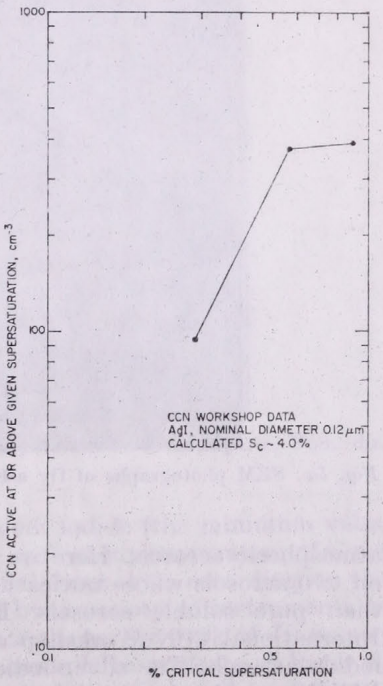

Fig. 4: AgI activated as a function of S_c

saturation. Such calibrations need not to be repeated frequently, but should be performed for each given aerosol carrier flow setting and set of supersaturation settings employed in the spectrometer.

1. Experimental results

The Proceedings of the 1980 International CCN Workshop discuss numerous comparisons of this spectrometer to other CCN counters, on pure soluble aerosols of sodium chloride and ammonium sulfate, and on ambient

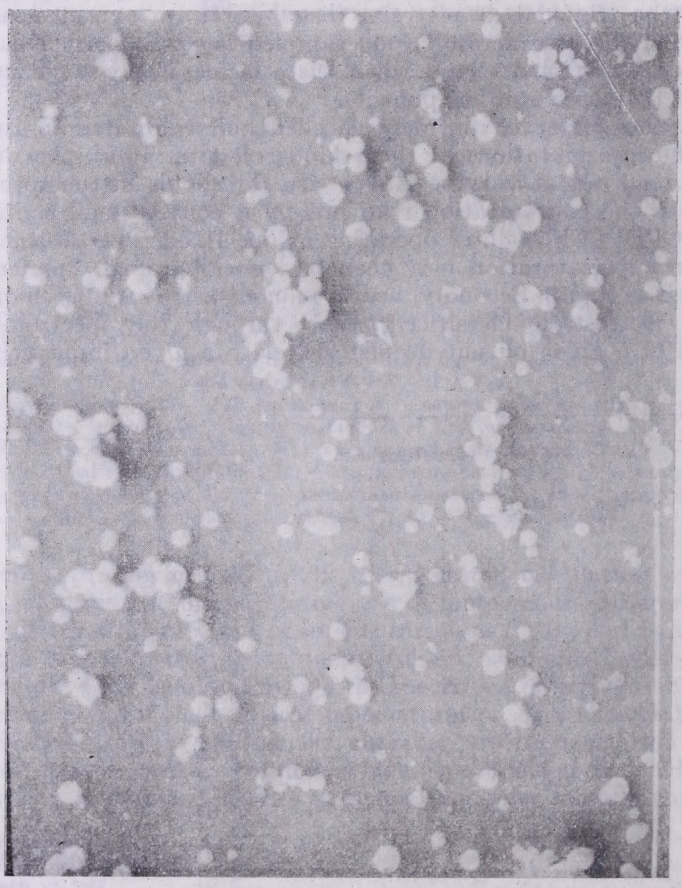

Fig. 5a: SEM photographs of fly ash particles on Nuclepore filters. Polydisperse, Nom. dia. 0.26 μm, 2000×

atmospheric aerosols. Here we will discuss results obtained with the device on two aerosols whose nucleation characteristics are more difficult to specify than pure soluble aerosols. First, data were obtained during the 1980 International CCN Workshop on both polydisperse and monodisperse silver iodide aerosols. The silver iodide was reagent grade and, when subjected to PIXE analysis, appeared to be free of contaminants (*Mach*, 1981). A monodisperse aerosol was prepared by vaporization–recondensation, followed by

passing the polydisperse product through an electrostatic classifier. In *Fig. 4*, the cumulative number concentration of CCN that were activated is displayed as a function of applied supersaturation generated in the instantaneous spectrometer, for nearly-monodisperse silver iodide of nominal diameter 0.12 μm. Above a supersaturation setting of 0.57%, this instantaneously-derived spectrum shows a "plateau" where very few additional CCN are activated as the supersaturation increases; other devices present at the Workshop showed a similar result, usually by sequencing through a number of supersaturation settings, one at a time.

Fig. 5b: SEM photographs of fly ash particles on Nuclepore filters. Monodisperse, Nom. dia. 0.26 μm, 2,000×

If a contact angle of 9° is assumed for silver iodide (the minimum value cited by *Pruppacher* and *Klett*, 1978), then the critical supersaturation of silver iodide spheres of diameter 0.12 μm should be about 4%, according to the Volmer theory. The present results, obtained by a variety of instruments as well as the instantaneous spectrometer, reiterate the earlier work of *Jiusto* and *Kocmond* (1968) who also found silver iodide aerosols to nucleate at lower S_c than theory would indicate. Post-Workshop analysis of the silver iodide is

continuing in an effort to obtain clues leading to an explanation of this anomalous behavior. Whatever the reason for the discrepancy, it appears that generation of an AgI aerosol in this manner lowers the S_c from the theoretical value by a significant amount. This result points to the likelihood that AgI prepared for cloud seeding experiments is active as CCN as well.

The second aerosol that was studied is of distinct atmospheric relevance, but is complex in nature. Bulk samples of coal combustion fly ash were collected from the electrostatic precipitator hoppers of a large electric power generation plant located in the Western USA. Similar material was examined

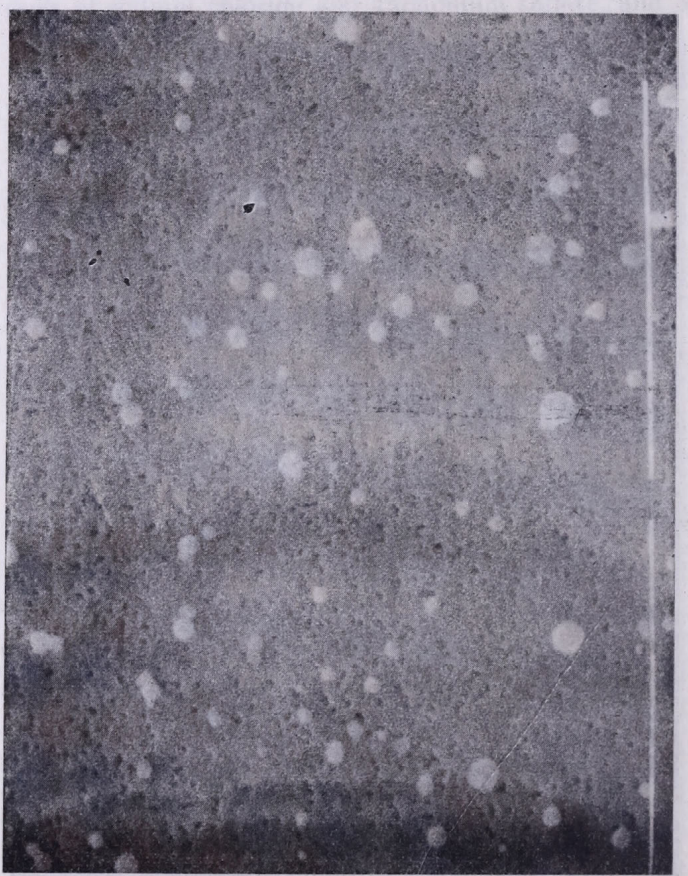

Fig. 6: Fly ash particles on Nuclepore filter. Monodisperse, Nom. dia. 0.26 μm, 10,000×

by *Parungo* et al. (1978), who found that samples collected by aircraft exhibited deliquescence behavior as though most individual particles were surrounded by a layer of soluble material. *Rothenberg* (1980) considered the water vapor adsorption characteristics of small samples of fly ash which were taken from the electrostatic precipitator collection system, or directly from the stack of several Western USA power plants. It was found that adsorption equilibrium was quite slow, suggesting that the fly ash particles were insoluble, porous substrates.

We resuspended the bulk fly ash using a jet of particle-free air; the resulting aerosol was stored in a 200 L conducting plastic bag for aging periods of one to several hours. The bag was then pressurized externally to force its contents in steady flow through an electrostatic classifier, and then to the inlet of the instantaneous spectrometer. It was necessary to confine our studies to the nominal diameter range of about 0.1 μm to 1.0 μm, because the maxima of our resuspended distributions generally occurred in this range, with only very low concentrations to be found at sizes below 0.1 μm. *Figures 5a – b* and 6 are scanning electron micrographs of particles collected on Nuclepore filters;

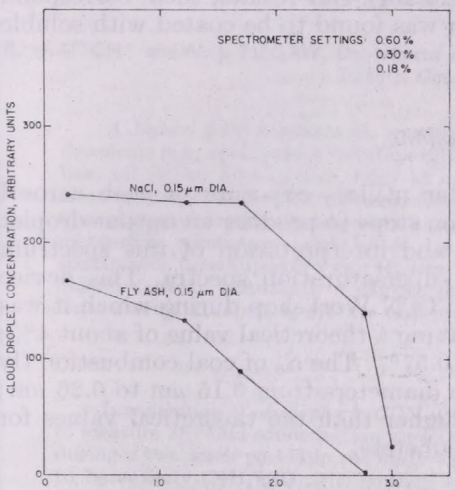

Fig. 7: Size distribution of cloud droplets exiting CCN spectrometer

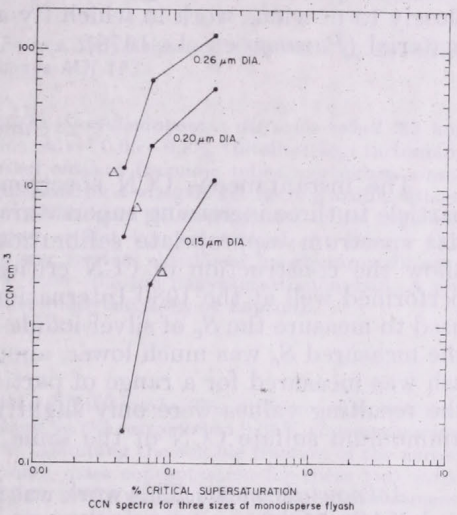

Fig. 8: CCN spectra for three sizes of monodisperse fly ash

monodisperse cases were, of course, collected downstream of the electrostatic classifier.

Figure 7 is a graph of the number of cloud droplets detected by the Royco, as a function of the size threshold settings of the five Royco channels, for both monodisperse fly ash and monodisperse sodium chloride of 0.15 μm diameter. It is evident that the fly ash size distribution, in this cumulative display, does not show the pronounced plateau of the sodium chloride (of theoretical S_c 0.06%); nevertheless, the largest droplets grown on the fly ash CCN approach the size of the largest NaCl. In general, the fly ash exhibited CCN activity almost as pronounced as pure soluble aerosols of the same size, but note that factors other than simple geometrical monodispersity affect the net S_c of the fly ash particles – probably due to variations in the amount of soluble material deposited on the surfaces of individual particles. Very similar results were obtained when the sizes of the aerosols were varied to 0.2 μm and 0.26 μm.

Figure 8 shows three CCN spectra collected with the instantaneous spectrometer for three nominal sizes of monodisperse fly ash. In each case, three data points are shown, but not shown are separate data taken at higher supersaturations, which indicate that only 10% to 20% more nuclei are

activated as the supersaturation is increased from 0.2% to 0.6%. The experiment was repeated several times, with slight variations in the method of preparation of the aerosol, but results were always very similar to Fig .8. (Note that the data at nominal diameter 0.26 μm were taken with electrostatic classifier sheath flow rates reduced below the usual manufacturer's settings.)

In Figure 8 we also show a small triangle adjacent to each curve, to mark the critical supersaturation values for ammonium sulfate particles of the same diameter. It is evident that this sample of fly ash behaved as though composed of mostly soluble material, for the necessary activating supersaturation is almost as low as that of pure ammonium sulfate (and far below the Kelvin wettable-sphere value of around 1% or greater). Our results, then, correspond closely to previous work in which fly ash was found to be coated with soluble material (*Parungo* et al., 1978).

2. *Conclusions*

The instantaneous CCN spectrometer utilizes exposure of each aerosol particle to three increasing supersaturation steps to produce an output droplet size spectrum; appropriate calibrations and interpretation of this spectrum allow the construction of CCN critical supersaturation spectra. This device performed well at the 1980 International CCN Workshop during which it was used to measure the S_c of silver iodide having a theoretical value of about 4%; the measured S_c was much lower, about 0.57%. The S_c of coal combustion fly ash was measured for a range of particle diameters from 0.15 μm to 0.26 μm; the resulting values were only slightly higher than the theoretical values for ammonium sulfate CCN of the same diameters.

Acknowledgements. This work was supported by NASA Grants NAS8-33820 and NAS8-33273.

REFERENCES

Hudson, J. G., Keyser, G. and *Rogers, C. F.*, 1980: Two new CCN spectrometers. *Proc. VIIIth Conf. on Cloud Physics*, Clermont-Ferrand, 15–19 July 1980.

Hudson, J. G., Rogers, C. F. and *Keyser, G.*, 1981: Simultaneous operation of three CCN counters and an isothermal haze chamber at the 1980 International CCN Workshop. Submitted to *J. Rech. Atmos.*

Jiusto, J. E. and *Kocmond, W. C.*, 1968: Condensation on non-hygroscopic particles. *J. Rech. Atmos. 3*, 19–24.

Mach, W. H., 1981: Elemental composition of aerosols in fourteen experiments of the Cloud Condensation Nuclei Workshop. Submitted to *J. Rech. Atmos.*

Parungo, F., Ackerman, E., Proulx, H. and *Pueschel, R.*, 1978: Nucleation properties of fly ash in a coal-fired power plant plume. *Atmos. Environ. 12*, 929–935.

Pruppacher, H. R. and *Klett, J. D.*, 1978: *Microphysics of clouds and percipitation*. D. Reidel Publ. Co., Dordrecht, Holland.

Rothenberg, S. J., 1980: Coal combustion fly ash characterization: Adsorption of nitrogen and water. *Atmos. Environ. 14*, 445–456.

IDŐJÁRÁS

Az Országos Meteorológiai Szolgálat folyóirata, 86. évf. 2–4. szám, 1982. március–augusztus
Journal of the Hungarian Meteorological Service, Vol. 86. No. 2–4. March–August 1982, Budapest

Investigation of atmospheric CCN using the diffusion tube

R. LEAITCH* and W. J. MEGAW, *Department of Physics, York University, 4700 Keele St. Downsview, Toronto, Ont. Canada M3J 1P3*

A légköri felhő-kondenzációs magvak (CCN) tanulmányozása diffúziós csővel. 33 kondenzációs mag spektrumot mértünk diffúziós csővel 0,05–0,3% túltelítettségi tartományban, tél elején. Föltételezve, hogy az aeroszol oldható frakciója teljes mértékben ammónium-szulfátból áll, a CCN mérésekből meghatároztuk a vizsgált két hétre a szulfát átlagos tömegkoncentrációját. A kapott 1,9 μgm^{-3} érték igen jól megegyezett a két regionális monitoring állomáson mért 1,6 és 1,4 μgm^{-3} szulfát koncentrációval. Az átlagos CCN spektrumot összekapcsolva egy tipikus nagyság szerinti eloszlással, meghatároztuk az ε_v oldódó frakció változását a nagysággal a 0,05–0,5 μm nagyságtartományban. A térfogat szerint közepelt ε_v értékre ebben a tartományban 14%-ot kaptunk.

*

Investigation of atmospheric CCN using the diffusion tube. The diffusion tube was used to measure 33 cloud condensation nuclei spectra, in the range 0.3 to 0.05% supersaturation, during a two-week period in the early winter. Assuming the soluble fraction of the aerosol to be entirely $(NH_4)_2SO_4$, the average sulphate mass concentration for these two weeks was derived. A value of 1.9 $\mu g/m^3$ compared favourably with actual sulphate measurements of 1.6 and 1.4 $\mu g/m^3$ taken at two regional air monitoring stations. Coupling the average CCN spectrum with a typical size distribution enabled a derivation of the variation of the volume soluble fraction (ε_v) with sizes in the range 0.05 to 0.5 μm. The volume-averaged ε_v value was determined to be 14% over this size interval.

*

Introduction. There are two parameters of major concern which influence the interaction of a particle with water. One is size, the second is the relative amount of water-soluble material present in the particle. Much effort has been made to measure the size distribution of aerosols and it is a relatively straightforward, if not always easy, task. Still, with the notable exception of *Mészáros* (1978), determinations of the water-soluble components have been primarily chemical analyses of the particle composition of an aerosol fractionated in broad size ranges with little attempt to examine the distribution, with respect to size, on a fine scale. The procedure for such a task is laborious.

Until recent years it has not been possible to make accurate determinations of CCN spectra below 0.2% supersaturation with respect to water (SS). Since chemical identification is mostly undertaken for particles greater than 0.1 μm diameter, it has not been possible to correlate CCN measurements properly with measured concentrations of sulphate and other major ions

* Present address, Atmospheric Environment Service, 4905 Dufferin Street, Downsview, Ont. Canada M3H 5T4.

present in the atmospheric aerosol. In this paper we demonstrate how CCN measurements may be used to extract the soluble (assumed to be ammonium sulphate) mass in the submicron size range in a very rapid manner, and how they may be used as one of the diagnostics to resolve the variation of ε_v with size in the submicron region.

Experimental

During the two weeks from November 24/80 to December 8/80 periodic meaurements were made at the northern edge of Toronto of condensation nuclei (CN), cloud condensation nuclei (CCN) spectra, and ice forming nuclei (IFN) spectra. We deal only with the CN and CCN measurements and primary emphasis is laid on the latter results. CCN active between 0.3% and 0.05% water supersaturation were determined using the diffusion tube (*Leaitch* and *Megaw*, 1981).

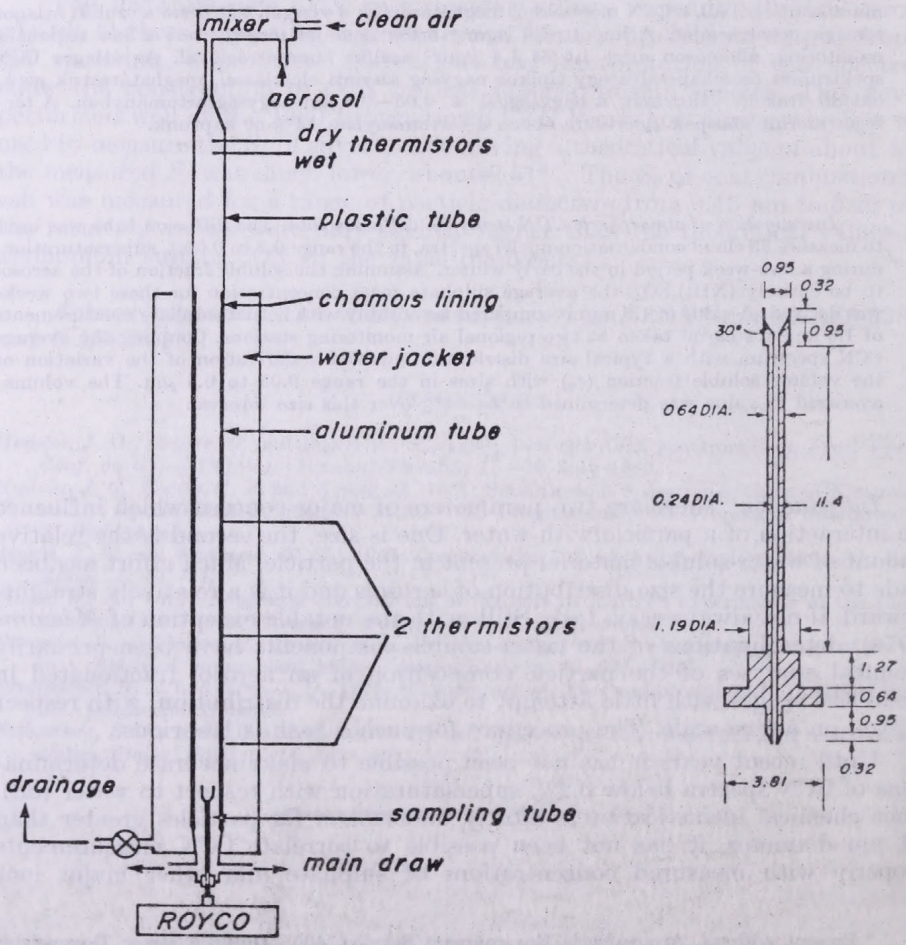

Fig. 1: Schematic of diffusion tube and detail of sampling tube (values are expressed in cm)

Sampling was undertaken on the campus of York University, which sits on the northwestern edge of the metropolitan area of Toronto. The region to the immediate north is used for agriculture, while to the immediate south, buffering the campus from the city core, is a primarily residential area with some light industry. Areas to the east and west are blendings of the above two types with some medium industry. The entire region is heavily interspersed with roadways. One might expect that the campus area is subject to a highly fluctuating air quality dependent of course upon the meteorological situation.

The air to be sampled was pulled down a long tube (7.6 cm diameter) at a flow rate of 60 litres/minute into a laboratory on the upper floor of the physical siences building. The tube extended approximately 6 metres above the roof which put the opening about 19 metres above the ground. Air from the tube was directed isokinetically to a Nolan-Pollak Model 1957 photoelectric counter for determination of the CN concentration and to the diffusion tube for evaluation of the CCN spectra.

The diffusion tube determines the concentration of particles active at water supersaturations ranging from 0.04 to 0.3%. A Royco 25 was used to count and size the droplets. The accuracy of measurement has been estimated at 25%, but tests with monodisperse aerosols have indicated no disparity greater than 11%. A schematic of the diffusion tube is shown in *Fig. 1*. The aerosol-laden air passes down the tube the walls of which are heated isothermally to a few degrees ($\sim 10°C$) above ambient. As it moves down the tube, the air experiences a transient supersaturation which results from the difference in the diffusivities of water and heat and which lasts for about 12 seconds. By the time it reaches the sampling tube the air has returned to very near saturation. Only the central stream of air is sampled which helps to simplify the calculations. Numerical corrections have been made to compensate for the variation in the supersaturation enabling one representative value to be used. Also due to the short growth time, a simple scheme was developed to delineate the CCN.

Efforts were made to take samples three times daily at approximately 0900, 1:400 and 2:000 hours. Each period of actual data collection was about 45 minutes in duration, with one CCN spectrum being measured accompanied by 10 CN values. A total of 33 CCN spectra were obtained.

Results

Details of the CCN data are listed in *Table I*. Included are the number concentrations at 0.05, 0.1, 0.2 and 0.3% supersaturation, the slopes (k) between the indicated supersaturations (derived from CCN $\propto SS^k$) as well as air mass origin and significant weather events (i.e. fog, rain or snow). The CCN concentrations were derived from curves fitted to the measured points. Since CN measurements were taken throughout the compilation of a CCN spectrum, adjustments were made to CCN points when the corresponding CN measurement deviated sharply (≥ 1 standard deviation) from the CN average for an entire sampling period. These adjustments were taken into consideration basically only if they helped to alleviate severe discontinuities in a spectrum.

Two mean spectra were compiled from Table 1, one for all samples and one for those taken when there was no fog, rain or snow present. The mean

curves, shown in *Fig. 2*, were evaluated using the averages of the three slopes combined with the average concentration at 0.3% supersaturation. Shown above the CCN curves are the average CN concentrations for each spectrum. These bear no relation to the supersaturation but are merely extended as such for visual clarity. Both CCN spectra have been extrapolated from 0.3 to 1.0% supersaturation on the basis of the slope between 0.2 and 0.3% and the results of approximately 60 measurement periods using a MEE counter (operated at 1% SS) at the same location in 1976. The average CCN concentration active at 1% measured in 1976 (3600/cm³) agreed reasonably well with the extrapolated values (2900/cm³ for no fog, rain or snow).

TABLE I

CCN data for the period from November 24 to December 8, 1980

Date	Air mass	Notes	CCN (N/cm³)				Slope (k)		
			0.3%	0.2%	0.1%	0.05%	0.3–0.1%	0.1–0.05%	0.2–0.05%
Nov.									
24	MA	Rain	3700	2480	1290	60	0.96	4.1	2.7
24	MA	Rain	2750	1860	950	23	0.97	4.6	3.0
24	MA	Rain	520	405	165	1	1.04	8.8	4.7
25	MA		275	190	102	4.2	1.10	5.0	3.3
25	MA		218	117	47	2.6	1.40	4.1	2.9
25	MA				120	4.1		4.5	
26	MA		2950	1570	340		1.97		
26	MA		1850	750	156	15	2.25	3.8	3.2
26	MA		2750	2050	740	43	1.19	4.1	3.0
27	MA	Snow	855	325	185	1	1.39	8.9	4.2
27	MA		1900	1220	320	5.4	1.36	5.9	3.9
28	MA	Rain	2900	1470	285	11	2.11	4.7	3.8
28	MA	Snow	1480	910	405	18	1.20	4.5	3.0
29	MA	Snow	1030	790	260	13	1.25	4.3	3.2
29	MA		425	325	137	4.0	1.03	5.0	3.4
29	MA		1210	725	234	10	1.50	4.9	3.4
30	MA		485	360	221	4.2	0.72	5.3	3.3
30	MA		3000	1940	143	1.7	2.77	5.7	4.8
Dec.									
2	MA	Rain	3370	2300	900	23	1.20	5.2	3.5
2	MA	Rain	3000	2040	445	6.6	1.74	6.5	4.6
2	MA	Snow	173	110	42	1.7	1.29	4.6	2.6
3	CA				90	2.1		5.0	
3	CA		355	283	87	1.8	1.28	4.8	3.4
3	CA		160	100	39	1.7	1.30	4.2	3.0
4	CA		585	285	83	3.1	1.78	4.1	2.8
4	CA		1070	220	45	1.6	2.88	4.6	3.4
5	CA		2950	1100	148	2.5	2.72	5.7	4.2
5	CA		1630	1170	330	2.2	1.45	6.0	4.2
7	MP	Fog	2550	1780	245	28	0.64	3.0	2.9
7	MP	Fog	3440	2150	950	77	1.16	3.6	2.2
8	MP	Fog		2150	1030	35	1.03	4.6	3.1
8	MP	Rain	1220	580	166	2.5	1.82	5.6	3.4
8	MP		490	410	60	4.0	1.91	3.6	3.2
Average without rain, snow, fog			1200	673	182	6.7	1.60	4.7	3.4
Std. deviation			1050	650	175	7.4	1.00	1.9	0.7

It might be expected that the CCN spectrum which includes precipitation (i.e. scavenging) events should average less than that for drier days; however, preceding and during these events the winds were relatively calm and predominantly southerly, resulting in substantial CCN concentrations. Precipitation experienced during these periods persisted for a day at least and was frequently pushed out by winds from the north to west bringing relatively clean air, although there was a persistent source of Aitken particles (much of it presumably from automobile emissions and other local sources), thus concentrations on dry days were generally much lower than those on wet days.

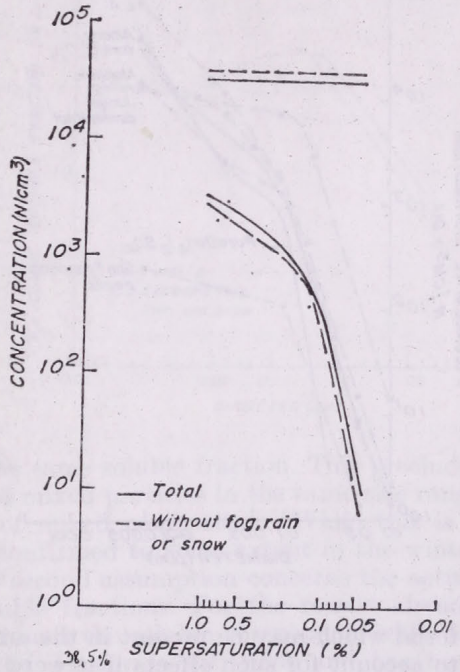

Fig. 2: Average CCN spectra compiled during two-week period from November 24/80 to December 8/80. Shown above the spectra are the average CN values for the same period. The CN values are not related to the supersaturation on the abscissa but merely extended as curves for visual clarity. Total concentration for dashed line 33,000, for solid line 29,000

The relationship between the critical supersaturation (CrSS) of a particle and the quantity of water-soluble material it possesses is unique in the sense that for a given CrSS the absolute amount of the soluble material remains the same regardless of the particle size, although relative amounts (ε_v) in the particles of different size will vary. This means that we can use the CCN spectrum to estimate the quantity of soluble material without reference to the size distribution, simply by converting the CCN spectrum to dry particles of some water-soluble substance, using the relationship between CrSS and dry size for that material. Once the dry particle size distribution is obtained, we may easily determine its mass which will be equivalent to the amount of soluble material in the atmospheric aerosol in a size range specified by the limits of the CCN spectrum. There are, of course, problems associated with this procedure. It is necessary to assume that all the CCN possess some soluble component which is not always true. Still at the low supersaturations dealt with here the concentrations of pure insoluble particles active as CCN will be very much less

than those with some soluble fraction and thus should be of very little consequence. A more difficult assumption is required concerning the molecular constituents of the water-soluble fraction. In the supersaturation range used here (0.05 – 0.3%) most of the particles which are active CCN will be in the submicron range and very likely between 0.06 and 0.6 micron diameter, based on critical supersaturation data. Certainly in this size region ammonium sulphate [$(NH_4)_2SO_4$] is well documented as the principal water-soluble component, thus we use $(NH_4)_2SO_4$ to represent this component. A third assumption is that we can neglect the possible influence of surface-active ma-

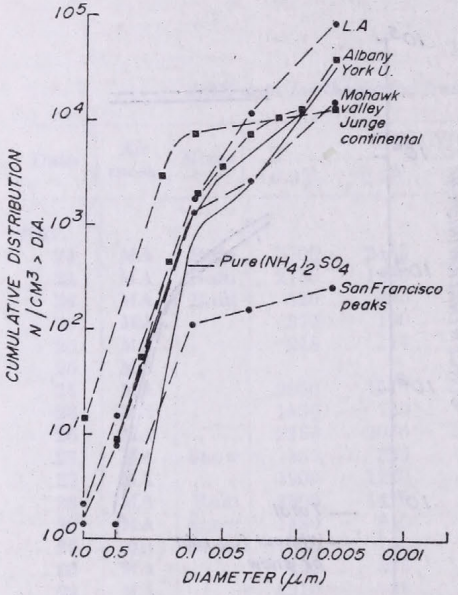

Fig. 3: Cumulative size distributions at indicated locations as determined by *Schaefer* (1976) and *Jiusto and Lala* (1977). Also shown is the Standard Junge Continental Distribution as well as the presumed for this work (York U.). The pure $(NH_4)_2SO_4$ curve results from assuming the dashed curve in Fig. 2 to be composed of pure ammonium sulphate

terial which may be present in the ambient aerosol. It would seem impossible to account for such effects if it were necessary to do so.

The two spectra in Fig. 2 were converted to dry particle size distributions of pure ammonium sulphate. The two distributions were then calculated to have masses of 1.9 $\mu g/m^3$ and 1.6 $\mu g/m^3$ for the total and the no-fog, rain or snow curves, respectively. The medians of the mass distributions were both 0.13 microns diameter.

Generally, for this region one might expect sulphate levels up to 15 $\mu g/m^3$; indeed *Whelpdale* (1978) has shown that during the summer sulphate levels typically may average 5 – 10 $\mu g/m^3$. During the monitoring period of this study two arctic air masses pervaded the region. The more moderate maritime arctic remained for 8 days and provided most of the rain, while a cold dry continental arctic flow occupied the area for 3 or 4 days. Ground wind direction was predominantly northwesterly and at least two stations of the Canadian Air Pollution Network recorded very low sulphate concentrations during the same two-week period. One station located on the northern edge of Lake Superior measured levels at 1.6 $\mu g/m^3$, while a station on Lake Erie, less than 200 km to the southwest of our location, found average concentrations

of 1.0 $\mu g/m^3$ for the period with no-fog, rain or snow, and 1.38 $\mu g/m^3$ for the entire two weeks. These results agree very closely with the values determined using the CCN measurements, suggesting that the CCN spectra are valid, and are useful in estimating sulphate concentrations.

Comparison of the curves in Fig. 2 with the models of *Junge* and *McLaren* (1971) showed these slopes to be steeper than any model results for a constant ε_v. This suggested that there was a significant variation of ε_v through some size range. Before any inferences regarding soluble content can be made, two assumptions are required. One is that within a given size range (presumably

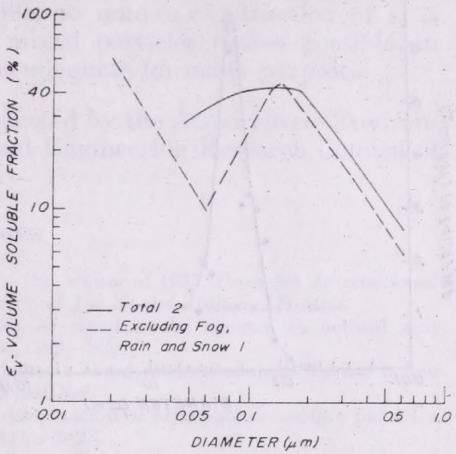

Fig. 4: Volume soluble fraction extracted from the two curves in Fig. 2 and the size distribution in Fig. 3

small) all the particles must possess the same soluble fraction. This precludes having pure soluble, pure insoluble and mixed particles in the same size range and requires all the particles to be of mixed composition. While this is a somewhat sweeping assumption, it is confirmed to some extent in the winter by the results of *Mészáros* (1978). The second assumption concerns the actual composition of the soluble and insoluble fractions. For the reason already discussed we choose $(NH_4)_2SO_4$ to represent the soluble component, while for the insoluble portion knowledge of the density is sufficient and has been assumed here to be 2.65 g/cm^3 (equivalent to SiO_2). A lower value for the density will have a similar effect to increasing the soluble fraction of the aerosol.

Unfortunately, no suitable means was available to measure the size distributions during this sampling episode. Still several "typical" distributions have been measured elsewhere and since the CCN spectra are averaged from several observations, it is felt that a representative distribution might be constructed. General size distributions measured by *Schaefer* (1976) and *Jiusto* and *Lala* (1977) at the indicated locations are shown in *Fig. 3*. Also illustrated is the standard Junge continental distribution. In particular the Albany and Mohawk distributions were felt to be good representatives of our sampling region since the average CN concentration fell in between, they are nearby geographically and the Albany distribution was composed during the winter months as well.

The volume soluble fraction (ε_v) was found by matching CCN concentrations to the size distribution concentrations, hence finding equivalent super-

saturations and diameters. This enabled ε_v to be readily found from critical supersaturation curves. The resulting variations for both CCN spectra are shown in *Fig. 4*. The curve in absence of fog, rain or snow (1) has a volume mean ε_v value of 0.10 for $0.15 \leq d \leq 0.5$ and 0.26 for $0.01 \leq d \leq 0.1$ where d is the diameter in microns. Curve *2* gives for ε_v values of 0.13 and 0.40 respectively. Using the results in Fig. 4, the soluble mass distribution was plotted, in *Fig. 5*, for curve *1*. The median of the distribution is 0.22 microns diameter, while that derived for the total mass was 0.26 microns. Of course, the masses of the

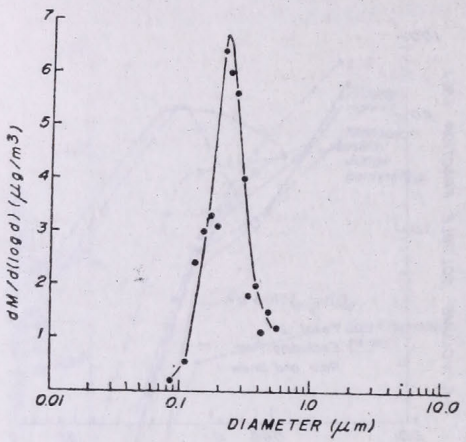

Fig. 5: Mass distribution of soluble material for curve *1* (Fig. 4). Soluble composition was assumed to be $(NH_4)_2SO_4$

distribution were 1.9 and 1.6 $\mu g/m^3$ for curves *2* and *1*, respectively, and the median for *2* was also 0.22 microns. This represents a soluble/insoluble mass ratio of about 14% with respect to the assumed size distribution between 0.05 and 0.5 microns.

The variation of ε_v cannot be validated by comparison of the sulphate mass, since many forms for the variation of ε_v may be used to arrive at the same soluble mass concentration, as already discussed; however, the uniqueness of the interpretation of ε_v may be studied by examining the median diameter of the soluble (or sulphate) mass distribution as well as its spread. Unfortunately, no information is available in this instance concerning the actual distribution of the sulphate.

The variation between the two curves in Fig. 4 would appear easy to explain by the increased coagulation of Aitken particles with submicron particles and enhanced heterogeneous gas-to-particle formation during the periods of high relative humidity. However, conclusions concerning these points are at best tenuous, owing to lack of proper information about the size distributions.

Conclusions

Since for the supersaturation range of operation (i.e. $0.05 - 0.3\%$) virtually all the CCN have some soluble component, then it is reasonable to assume that CCN spectra are a measure of the soluble mass in the submicron region. It has been shown here that CCN spectra may be able to provide good estimates of the sulphate fraction in the submicron range. Indeed this may be a method of validating some CCN counters with natural aerosols.

While it cannot be said that the CCN spectra presented in Fig. 2 are indicative of a continental background aerosol, they do represent a clean continental aerosol modified by local influences, probably the most dominant of which comes from automotive emissions. Some idea of just how clean the air was may be obtained from considering that the arctic aerosol may possess sulphate levels of beyond $1-2$ $\mu g/m^3$ for periods during the winter months (*Rahn* and *Shaw*, 1978).

Several assumptions have been made here in order to extract the variation of the soluble component with size. While assuming a size distribution is avoidable, unless a considerable body of information concerning the mass distribution of soluble material is available, no unique construction of ε_v is possible. Still the assumption of purely mixed particles makes possible an interpretation of ε_v with size, which may be adequate for many purposes.

Acknowledgements. This work was supported by the Atmospheric Environment Service and the National Sciences and Engineering Research Council of Canada.

REFERENCES

Jiusto, J. and *Lala, G. G.*, 1977: Aerosol signature – the winter of 1977. *Proc. 9th International Conference of Atmospheric Aerosols, Condensation and Ice Nuclei, Galway, Ireland.*

Junge, C. E. and *McLaren, E.*, 1971: Relationship of cloud nuclei spectra to aerosol size distribution and composition, *J. Atmos. Sci. 28*, 382 – 390.

Leaitch, R. and *Megaw, W. J.*, 1981: The diffusion tube; a cloud nucleus counter for use below 0.3% supersaturation. Submitted to the *J. Aerosol Sci.*

Mészáros, Á., 1978: On the concentration and size distribution of atmospheric sulfate particles under rural conditions. *Atmos. Environ. 12*, 2425 – 2428.

Rahn, K. and *Shaw, G. E.* 1978: Briefing of Arctic haze and the Arctic aerosol. Paper presented to the *Bureau of Oceans and International Evrinmental and Scientific Affairs*, Department of State, Washington, DC, 20 November.

Schaefer, V. J., 1976: The air quality patterns of aerosols on the global scale. Parts I and II. *Publication No. 406, Atmospheric Sciences Research Centre*, State University of New York, Albany, New York.

Whelpdale, D. M., 1978: Large scale atmospheric sulfur studies in Canada. *Atmos. Environ. 12*, 661 – 670.

IDŐJÁRÁS

Az Országos Meteorológiai Szolgálat folyóirata, 86. évf. 2–4. szám, 1982. március–augusztus
Journal of the Hungarian Meteorological Service, Vol. 86. No. 2–4. March–August 1982, Budapest

Airborne measurements of aerosols and cloud condensation nuclei over Hawaii

F. PARUNGO, C. NAGAMOTO, I. NOLT *and* E. NICKERSON, *Office of Weather Research and Modification ERL/NOAA, Boulder, Colorado 80303, U.S.A.*

Repülőgépes aeroszol- és felhőkondenzációs mag mérések Hawaii fölött. Izokinetikus aeroszol mintavevővel felszerelt kutató repülőgéppel aeroszol mintákat gyűjtöttünk Hawaii fölött 1980 júniusában. A „Nuclepore" szűrőn felfogott részecskéket pásztázó elektronmikroszkóppal (SEM) és röntgenenergia spektrométerrel (XES) tanulmányoztuk. Az eredmények szerint a passzát inverziós felhők szűrőként hatnak az alsóbb légrétegek aeroszol részecskéi – különösen a sórészecskék – szempontjából. Az inverzió alatt az aeroszol koncentráció átlagosan 100 cm^{-3}. A részecskék 50%-a tartalmaz nátriumot és klórt. Az inverzió fölött a részecske koncentráció egy nagyságrenddel alacsonyabb. A nátriumot tartalmazó részecskék az össz-részecskének itt már csak 10%-át teszik ki. Az impaktorral felfogott aeroszol mintákban a szulfát és nitrát részecskéket folt-analízissel azonosítottuk. Amint látható, a szulfát részecskék mindenhol megtalálhatók, míg nitrát részecskék elsősorban a tengerpart mentén mutathatók ki, különösen Hilo közelében. Felhőcseppeket replikátor segítségével gyűjtöttünk, vinilacetáttal bevont filmen. A replikákat SEM-XES rendszerrel vizsgáltuk az individuális kondenzációs magvak (CCN) elemi összetételének meghatározására. Az eredmények szerint a cseppeknek mintegy 60%-a tartalmazott a SEM-mel kimutatható részecskéket (feltehetőleg kondenzációs magvakat). Na-t és Cl-t tartalmazó részecskéket a cseppek 40%-ában, Si, S, K és Ca-t tartalmazó részecskéket a cseppek 20%-ában mutattunk ki. A felhőcsepp nagysága, valamint a kondenzációs mag nagysága és kémiai összetétele közt nem találtunk kapcsolatot.

*

Airborne measurements of aerosols and cloud condensation nuclei over Hawaii. A research aircraft was used to collect aerosol over Hawaii in June 1980 by means of an isokinetic aerosol sampling system. Aerosol samples were collected on Nuclepore filters and analysed with a scanning electron microscope (SEM) and X-ray energy spectrometer (XES). The results show that the trade-wind inversion clouds act as a filter for lower atmospheric aerosols, especially for salt particles. Below the inversion layer the aerosol concentration is approximately 100 cm^{-3}. Na and Cl are present in 50% of the total particles. Above the layer, the particle concentration is one order of magnitude lower. The Na-containing particles reduced to 10% of the aerosol particles. Aerosol particles were also collected with an impactor. Sulfate and nitrate particles were identified with spot tests. It appears that sulfate aerosols are widely distributed whereas nitrate particles are generally found along the seashore, especially close to the city of Hilo. Cloud droplets were collected with a replicator onto a Formvar-coated film. The replicas were examined with SEM–XES system for elemental composition of the individual cloud condensation nuclei (CCN) which were enclosed in the droplet replicas. The results indicated that approximately 60% of the droplets included particles (possibly CCN) visible by SEM. Particles containing Na and Cl were present in 40% of the droplets. Si, S, K, Ca appeared in 20–30%. There seems to be no correlation between cloud droplet size and CCN size, nor any relationship between droplet size and chemical composition of CCN.

*

Introduction. The Hawaiian Islands, located in the Pacific Ocean 4,000 km west of the North American Continent, offer a unique environment for the study of marine aerosols, land-sea-air interactions, local air pollution, and long-range

air pollution transported from industrial America. *Woodcock* (1953) collected aerosol samples over the islands from an aircraft and showed that particle concentration and size varied with altitude, location, and time of sampling. However, he did not use an isokinetic sampling technique; thus the results were limited to giant particles (radius $r > 1$ μm). *Junge* (1957) investigated chemical composition of aerosol particles on the island of Hawaii. However, the results referred to sea level aerosol, and only four kinds of ions were analyzed.

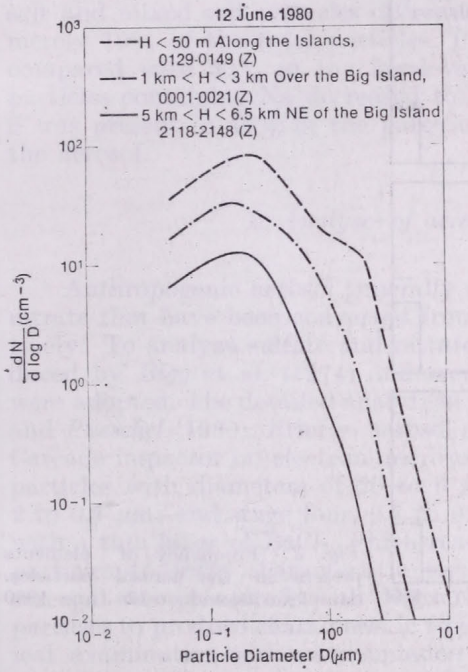

Fig. 1: Aerosol particle size distribution. Samples collected on 12 June 1980

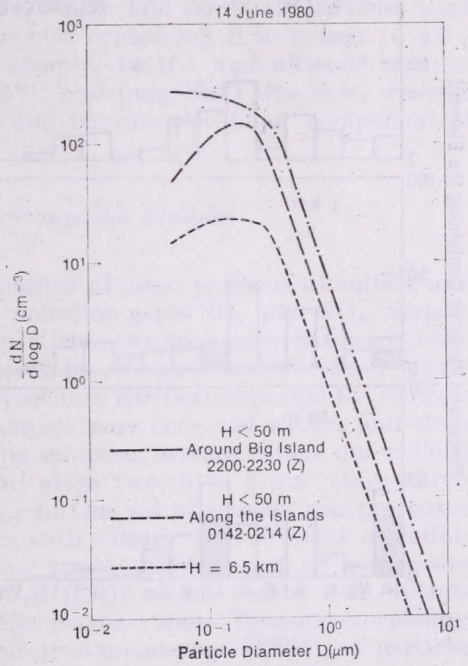

Fig. 2: Aerosol particle size distribution. Samples collected on 14 June 1980

In summer 1980, in conjunction with the NOAA Hawaii Mesoscale Energy and Climate (HAMEC) project, airborne aerosol samples were taken with an isokinetic sampling system from the NOAA research aircraft (P−3). The samples were collected on Nuclepore filters and electron microscope grids and were analyzed for particle concentration and size distribution with scanning and transmission electron microscopes. An X-ray energy spectrometer was used to determine the chemical composition of individual particles. The on-board instrumentation, the flight tracks, and the meteorological conditions during the flight were described by *Nolt* et al. (1980). The in-situ recorded data and sounding systems data sets were compiled by *Dias* et al. (1981). The detailed measurements of aerosols have been documented by *Parungo* et al. (1981). This paper discussed some of the significant results obtained from these aerosol measurements.

1. Analyses of aerosol filter samples

Aerosols were collected from an isokinetic sampling system on Nuclepore filters (pore diameter $d = 0.1$ μm) at ~ 15 L/min, and the filters were brought back to our laboratory for later analyses. A section of the filter was mounted on a carbon block and coated with a thin layer of carbon and then examined with a scanning electron microscope (SEM) with an operational resolution of

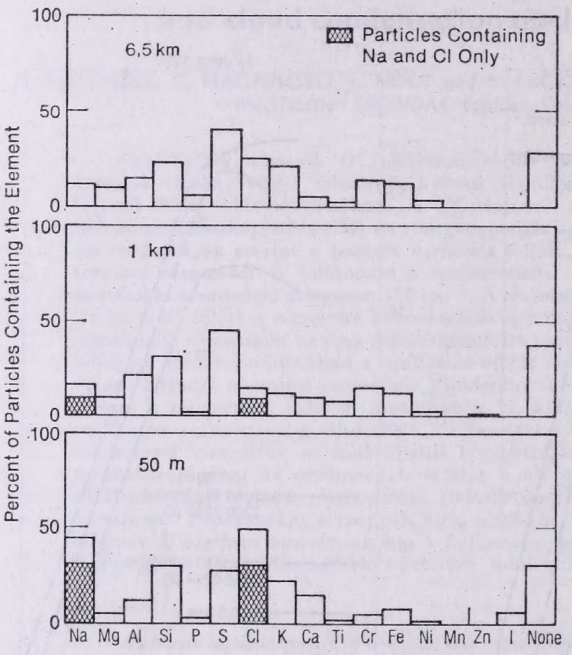

Fig. 3: Frequency of elements present in the aerosol particles. Samples collected on 12 June 1980

0.05 μm. At least 300 particles were measured to obtain particle size distribution for each sample. *Figures 1* and *2* show the results of the samples collected on 12 and 14 June 1980, respectively. Results of other days are similar. At low levels ($H < 50$ m MSL) aerosols were found to be diverse in concentration and size distribution depending on the sampling location and time. Over the open sea the particle concentration was $\simeq 100$ cm^{-3}. Along the coast, the concentration was doubled, and near the city of Hilo, the number of Aitken particles almost tripled. The particle size distribution showed general agreement with Junge's model size distribution of marine aerosol (*Junge*, 1963).

At high altitudes ($5-6$ km MSL) samples were collected upwind (200 km NE), across, and downwind (200 km SE) of the island of Hawaii. The particle concentrations and size distributions of the samples were similar regardless of sampling location, indicating that the air was rather homogeneous and well mixed above the trade-wind inversion. Their concentration was one order of magnitude lower than low-altitude samples.

An X-ray energy spectrometer (XES) which is interfaced with the SEM enables elemental analysis of individual particles. All elements in a particle

whose atomic number is greater than 9 can be detected in one spectrum. From each filter sample, we randomly selected 180 particles including 100 particles with $d \leq 1$ μm and 80 particles with $d > 1$ μm for X-ray analysis. The frequency with which an element appears in the particles, i.e., the percentage of particles containing certain elements, is recorded for comparison. *Figure 3* shows an example of the results. In the samples collected at 50 m over the ocean, approximately 30% of the total particles contained Na and Cl only; they were pure salt. Salt mixed with other elements such as Si, S, K, and Ca contributed another 20%. Twenty percent to 30% were organic particles or soot, which emitted no detectable X-ray, and 30% of the total particles contained S. For the sample collected at the middle level (1 – 3 km), salt and mixed salt particles decreased to 15%, and pure salt particles were merely 10% of the total particles. Particles containing S increased to 45% compared with 30% in the low-level sample. In the high-altitude sample, particles containing Na decreased to 10%, and pure NaCl was rare, whereas S was present in 40% of the particles and became the major component of the aerosol.

2. *Analyses of aerosol impactor samples*

Anthropogenic aerosol generally consists of large portions of sulfate and nitrate that have been converted from pollution gases SO_2 and NO_x, respectively. To analyze sulfate and nitrate particles, two spot tests that were introduced by *Bigg* et al. (1974) and modified by *Mamane* and *De Pena* (1978) were adopted. The detailed analytical procedure has been reported by *Parungo* and *Pueschel* (1980). Briefly, aerosol samples were collected with a four-stage Cascade impactor on electron-microscope sampling screens. Stage one collects particles with diameters of 20 to 6 μm; stage two, 6 to 2 μm; stage three, 2 to 0.7 μm; and stage four, 0.7 to 0.2 μm. One set of screens was precoated with a thin layer of $BaCl_2$, which reacts with sulfuric acid droplets or sulfate particles to form characteristic circular spots. Another set of microscope screens was precoated with Nitron ($C_{20}H_{16}N_4$), which reacts with nitrate particles to produce characteristic fiberlike reaction spots. By using morphological examination with a transmission electron microscope (TEM), all particles containing sulfate or nitrate can be counted in one observation in contrast to X-ray analysis, which is performed on one particle at a time. Furthermore, volatile particles can evaporate in the high vacuum under the intensive electron beam when examined with the SEM-XES system. In spot tests, sulfate or nitrate are fixed to form stable spots, which will remain to be identified. Therefore, the spot test can detect more sulfate particles than the XES analysis. Also, this technique is especially useful in detecting nitrate particles since X-ray analysis fails to do so. (Elements N and O are too light to yield detectable X-rays.)

In 5 days of airborne surveys, we collected 15 samples at various times and locations. The results of the spot tests are listed in *Table I*. All samples showed that $\geq 90\%$ of the 4th-stage particles ($0.2 < d < 0.7$ μm) contained sulfate. This indicates that sulfate was the predominant component of small particles regardless of time, location, or meteorological condition. In general, large particles contained less sulfate; however, large sulfate particles were found in various percentages in all locations.

The nitrate particles were found mostly along the coast, in the early

TABLE I

Analysis of sulfate and nitrate by spot tests

Sample no.	Date and time (Z)[1]	Location[2] and condition	% of sulfate particles on each stage				% of nitrate particles on each stage			
			1	*2*	*3*	*4*	*1*	*2*	*3*	*4*
1	12 June 2108 – 2156	$H = 6.5$ km 200 km NE Sunny	0	15	90	–	0	0	0	0
2	14 June 1352 – 1554	$H = 6.5$ km From 200 km NE to SE Rain	25	25	50	100	0	0	0	0
3	14 June 2217 – 2317	$H < 50$ m Around the island	0	30	10	90	0	0	0	0
4	14 June 2330 – 0030	$H = 6.5$ km from SW to NE	0	20	50	90	0	0	15	0
5	14 June 0142 – 0235	$H < 50$ m Channel	0	20	25	90	0	0	90	0
6	17 June 1441 – 1511	$H = 6.5$ km SW Cloudy	0	0	10	99	0	0	0	0
7	17 June 1540 – 1630	300 – 1000 m Over island to NE Cloudy	0	25	70	100	0	40	20	0
8	17 June 1714 – 1914	$H < 50$ m Channel	15	50	70	95	15	65	95	0
9	19 June 1505 – 1550	$H < 1$ km East coast Clear	0	70	60	90	0	0	50	10
10	19 June 1604 – 1739	$H < 1$ km North coast	0	50	95	90	30	50	90	25
11	19 June 2346 – 0015	$H = 6.5$ km SW	10	10	20	90	10	5	0	0
12	19 June 0020 – 0040	$H = 6.5$ km over land	10	10	30	90	10	5	0	0
13	19 June 0047 – 0140	$H = 6.5$ km NE	0	50	60	99	0	5	0	0
14	19 June 0155 – 0210	$H = 6.5$ km Channel	20	20	30	90	0	5	0	0
15	22 June 2015 – 2121	$H < 50$ m NW	0	50	90	90	0	50	70	10

[1] Z is Greenwich time which is 10 hours later than Hawaii standard time

[2] Location relative to the Island of Hawaii; channel refers to a series of islands between Hawaii and Oahu; H = altitude (MSL)

morning, especially downwind of Hilo (samples 7, 8, 9, 10 and 15 in Table I). They were generally in large sizes ($d > 1$ μm). Similar results concerning nitrate particles elsewhere were reported by *Junge* (1956) and *Parungo* and *Pueschel* (1980). All results indicate that nitrate particles are produced by the interaction of land and marine air masses. Nitrogen oxide gases, which are generated from land either anthropogenically or biologically react with sea spray droplets to form large nitrate particles. Because of their large sizes, they are less mobile and more sedimentary. Therefore they are generally concentrated near the coast.

3. *Analysis of cloud-particle replica samples*

A cloud-particle replicator designed and built by *Hallett* et al. (1978) was installed in the P−3 aircraft. The instrument consists of a roll of 16 mm movie film, Formvar solution, and a long arm extending outside the aircraft. In operation, the film is coated with a layer of the Formvar solution and travels along the arm continuously to pass a slit which exposes the film to the cloud. Particles entering the slit are caught in the wet, soft Formvar coating which dries before reaching the take-up spool. Cloud particles leave permanent replicas on the film and all the non-volatile materials in the cloud particles (cloud condensation nuclei, ice nuclei, solute or scavenged particles, etc.) will be left inside the droplet replicas. The slit is not designed to take air isokinetically; small droplets ($d < 2$ μm) generally escape capture. Because liquid water spreads on impact, the diameter of drop replicas is approximately 1.25 X as large as the real cloud droplets.

Examination of cloud-drop replicas with the SEM-XES system shows that many drops (60%) included solid particles. These particles probably served as cloud condensation nuclei to initiate the growth of cloud drops. During replication, drops evaporated and left CCN behind. Another portion of the drop replicas (40%) did not contain any SEM-visible particles even when examined with the highest magnification (100,000 X). Since homogeneous nucleation is practically impossible, an absence of any residue in the replica may be explained by one of the following reasons: (1) CCN were volatile particles that evaporated during SEM examination; (2) CCN were too small to be detected by SEM; (3) drops split and the secondary drops may not contain the original CCN; or (4) CCN dissolved in the drops which evaporated to leave too thin a layer of CCN material to be detected by SEM. Among the detectable CCN, we used XES to analyze their elemental compositions. *Figure 4* shows cloud-drop replicas, their CCN, and the X-ray spectra of individual CCN. We analyzed 200 CCN for each cloud penetration sample. Two examples of the results are shown in *Fig. 5*. Approximately 40% of the replicas contain no visible CCN; 30 to 40% contain salt, but only 10% are pure NaCl. Si, S, K, and Ca appeared frequently (20%−30%). The results indicate that the elemental compositions of CCN are similar to low-altitude marine aerosols; however, even in the clouds over the ocean, not only NaCl but also other marine substance served as CCN. There seems to be no correlation between droplet size and CCN size, or CCN chemical composition. These observations agree with *Rasool's* (1973) discussion that CCN size and chemical composition may affect a droplet's initial growth rate, but once the droplets reach a critical size (a few micrometers), the growth is no longer dependent on

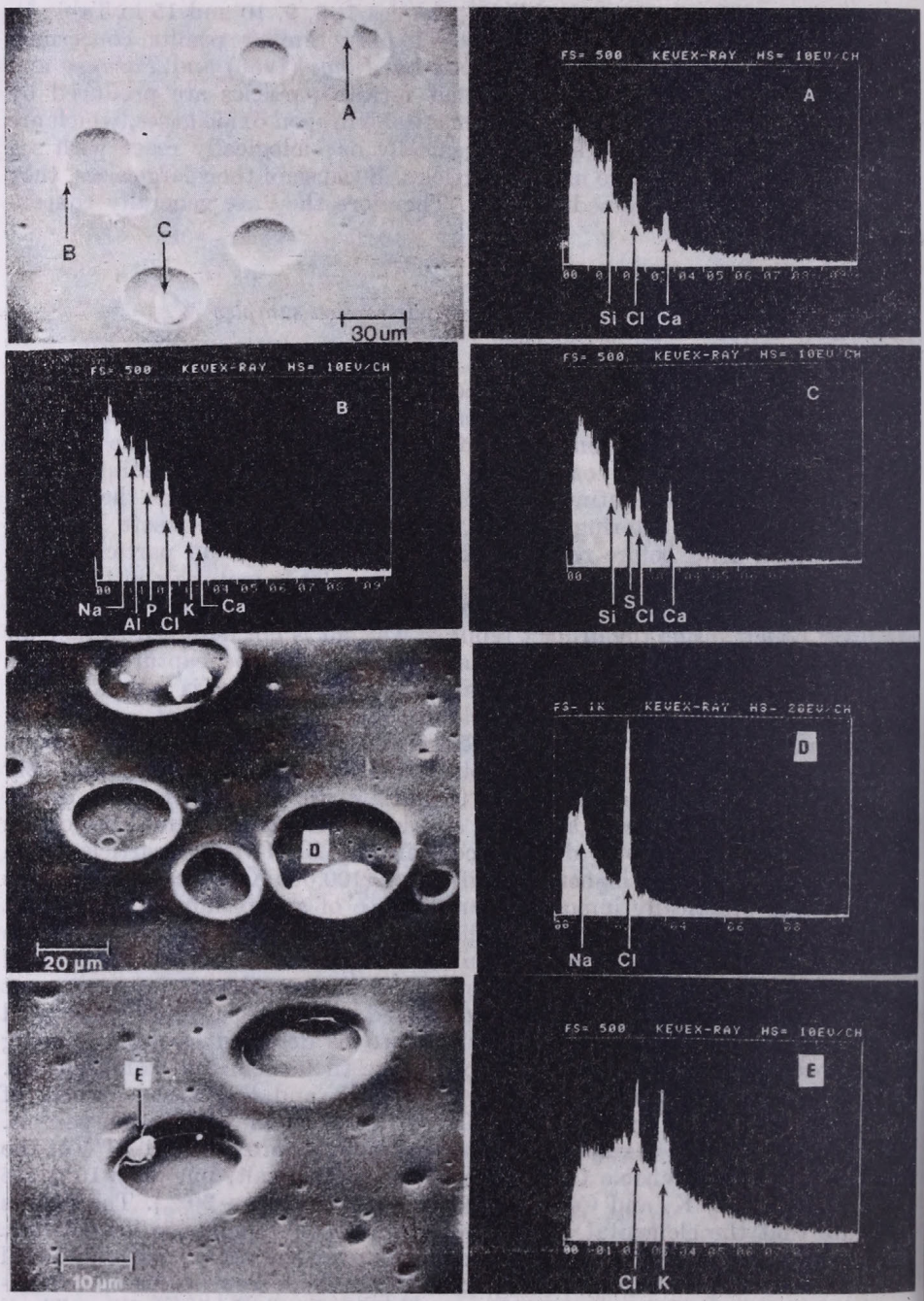

Fig. 4: Electron micrograph of cloud-drop replicas, the CCN inside the drops and their X-ray energy spectra

these factors. Therefore when we examined the matured cloud drops, some large drops (20 to 30 μm) may have contained various sizes of CCN with wide-range chemical compositions, and some small drops (2 to 5 μm) may have included a large salt particle.

4. Conclusion

Airborne measurements of aerosols and cloud condensation nuclei (CCN) were carried out in June 1980 over Hawaii. Throughout this period, the large-scale upper-level westerly flow (at $\sim$600 mbar) was dominated by the tropical

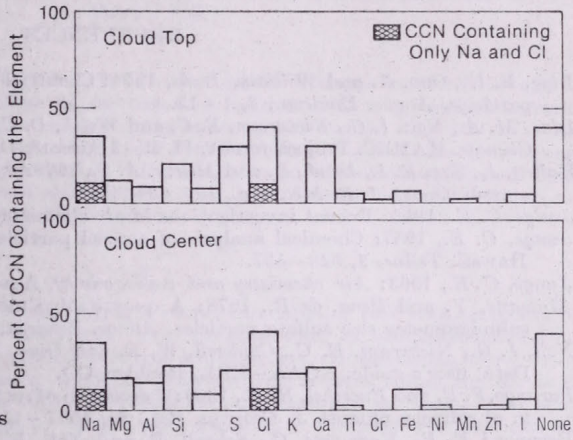

Fig. 5: Frequency of elements present in CCN

upper tropospheric trough and at lower levels the easterly trade winds prevailed. The trade-wind inversions with various depths generally occurred at $\sim$2 km MSL. The trade-wind clouds acted as filters for most marine aerosols. Below the clouds the aerosol concentration was measured at approximately 10^2 cm^{-3}. The elemental analysis by XES showed that Na and Cl were present in 50% of the total particles including 30% containing only Na and Cl as in pure salt, and 20% mixed with other elements. Above the cloud layer, aerosol concentration was one order of magnitude lower and particles containing Na decreased to 10% of the total particles. CCN that remained in cloud-drop replicas were analyzed with XES also .The results showed that Na and Cl were present in 40% of the cloud drops; S, K, or Ca appeared in 20$-$30%, indicating hygroscopic particles served as CCN-forming cloud drops either remaining in the clouds or precipitating out. Therefore, the concentration of marine aerosols, specially Na-containing particles, were distinctively reduced above the trade-wind clouds. However, the relative concentration of S-containing particles did not decrease with increasing altitude; in some cases it even increased slightly. One explanation is that the ocean releases large amounts of S-containing gases such as H_2S and organic sulfide that are oxidized in the atmosphere and converted into sulfate particles as they diffuse to a higher altitude. Another explanation may be the long-range air pollution transported from industrial North America. Spot test result shows that most submicron particles are sulfate, indicating they are most likely formed by gas-to-particles conversion. The nitrate particles are larger ($d > 1$ μm) and present near the

islands; they are probably from local pollution. The reduction of Cl-containing particles with increasing altitude is not proportional to Na. This may be due to Cl in sea salt being replaced by sulfate or nitrate (*Robbins* et al., 1959) to release HCl gas which later recombines with other air components to form different aerosols at higher altitudes.

Acknowledgments. Drs. *R. Schnell*, *A. Delaney*, and Mr. *D. Eyre* developed the isokinetic aerosol sampling system. We thank Dr. *C. Emmanuel* and Mr. *J. Zysko* of NOAA Research Facilities Center and the P–3 crew for their assistance in carrying out this project, and Mr. *W. R. Caldwell* for assistance in the in-flight sampling.

REFERENCES

Bigg, E. K., Ono, A. and *William, J. A.*, 1974: Chemical test for individual submicron aerosol particles. *Atmos. Environ., 8*, 1–13.

Dias, M. A., Nolt, I. G., Nickerson, E. C. and *Welsh, D. C.*, 1981: *Hawaii Mesoscale Energy and Climate*, HAMEC. Project report, II. P–3 Aircraft Data Sets NOAA–ERL, Boulder, CO.

Hallett, J., Sax, R. I., Lamb, D. and *Murty, A. S.*, 1978: Aircraft measurements of ice in Florida cumuli. *Quart. J. R. Met. Soc., 104*, 63–661.

Junge, C. E., 1956: Recent investigations in air chemistry. *Tellus 8*, 127–139.

Junge, C. E., 1957: Chemical analysis of aerosol particles and of gas traces on the island of Hawaii. *Tellus, 9*, 528–537.

Junge, C. E., 1963: *Air chemistry and radioactivity.* Academic Press, New York and London.

Mamane, Y. and *Pena, de R.*, 1978: A quantitative method for the detection of individual submicrometer size sulfate particles. *Atmos. Environ., 12*, 69–82.

Nolt, I. G., Nickerson, E. C., Caldwell, W. R. and *Dias, M.*, 1980: HAMEC project report, I. Data user's guide. NOAA–ERL, Boulder, CO.

Parungo, F. P. and *Pueschel, R. F.*, 1980: Conversion of nitrogen oxide gases to ni trate particles in ol refinery plumes. *J. Geophys. Res., 85*, 4507–4511.

Parungo, i F. P., Nagamoto, C., Schnell, R. and *Nolt, I.*, 1981: HAMEC project report *Atmospheric aerosol and cloud microphysics measurements.* III. NOAA–ERL, Boulder, CO.

Rasool, S. I., 1973: *Chemistry of the lower atmosphere.* Plenum Press. N. Y., 335.

Robbins, R. C., Cadle, R. D. and *Eckhardt, D. L.*, 1959: The conversion of sodium chloride to hydrogen chloride in the atmosphere. *J. Meteorol., 16*, 53–56.

Woodcock, A. H., 1953: Salt nuclei in marine air, a function of altitude and wind force. *J. Meteorol., 10*, 362–371.

IDŐJÁRÁS

Az Országos Meteorológiai Szolgálat folyóirata, 86. évf. 2—4. szám, 1982. március—augusztus
Journal of the Hungarian Meteorological Service, Vol. 86. No. 2—4. March—August 1982, Budapest

Arctic aerosols in surface air

R. JAENICKE and L. SCHÜTZ, *Institute for Meteorology, University of Mainz, Saarstrasse 21, D—6500 Mainz, F.R.G.*

Talajközeli aeroszol az Arktiszon. 1980 nyarán három hónapon keresztül aeroszol méréseket végeztünk a talajközelben az Arktiszon. A kondenzációs mag méréseink szerint az igazi arktikus levegőben a kondenzációs mag koncentráció kisebb, mint 100 cm^{-3}. Az Európai-Arktisz nagy részét az Arktiszon belül lévő források szennyezik. Az aeroszol nagyság szerinti eloszlása a háttér viszonyokra várhatónál alacsonyabb értékeket mutat. Bizonyos feltételek mellett a gázból való részecskeképződés jelentéktelen, míg az 1—10 μm sugarú részecskék hamar kikerülnek a légkörből.

*

Arctic aerosols in surface air. During 3 months in summer 1980 measurements of the arctic surface aerosol were performed. The measurements of the condensation nuclei concentration permit the conclusion that true arctic air has concentrations below 100 cm^{-3}. Large portions of the European Arctic are polluted from sources within the Arctic itself. The aerosol size distribution shows lower values than expected for background aerosols. Under certain conditions, gas-to-particle conversion is not present and particles in the range 1 μm to 10 μm in radius have been removed from the aerosol.

*

Introduction. The study of atmospheric trace substances depends not only on the special interest in one of those substances, but also on

- the availability of sufficiently sensitive measuring devices and
- access to measuring platforms.

In low latitudes, access to measuring platforms usually is available. In polar regions access is limited, and mostly, standard measuring procedures are too insensitive for detecting atmospheric trace substances there.

In summer 1980 it was one of those rare circumstances when

- the Swedish icebreaker YMER was offered as research vessel in the Arctic Ocean to the scientific community and simultaneously,
- a very sensitive Condensation Nuclei Counter became available.

This gave the unique opportunity to study (in connection with other instruments available) the complete size distribution of the natural aerosol in the arctic region.

Usually the polar front is an effective border between air masses. In addition, the pronounced precipitation connected with the polar front effectively removes aerosols from the air. In summer the polar front is moved to the north and thus major anthropogenic aerosol sources remain in the south. Thus, the polar regions during summer should be assumed as areas with minor

anthropogenic influences. It was claimed recently (*Rahn* and *McCaffrey*, 1980) that in the winter season the Arctic is influenced from polluted European air masses after being transported over European Russia and further to the north. In addition, modern oil activities in this region require extensive research on the pre-situation in order to assess possible effects on future developments. Quite surprisingly extensive measurements in summer are lacking.

Instrumentation and measuring platform

During July, August, and September 1980 the Swedish icebreaker YMER operated mostly in permanent ice in the area of Greenland, Svalbard, and Franz-Joseph-Land up to 82.5°N latitude. The air chemistry activities were concentrated on one of the upper decks (16 m above the water surface) in the front of the ship. In order to avoid contamination from the ship itself, scientific activities on the ice, or helicopter flights, the complete air chemistry program was protected by the below-described Condensation Nuclei Counter, which turned off all instruments if a preset condensation nuclei concentration level was exceeded. Condensation nuclei (0.001 μm − 0.1 μm in radius) are produced not only naturally but also in connection with human activities. They are formed by gas-to-particle conversion and are a link betwen trace gases and aerosols. Thus they serve as a very sensitive indicator for anthropogenic pollution.

The condensation nuclei were counted with a continuous Flow Condensation Nuclei Counter[1] (TSI-Counter). For concentrations below 1,000 cm^{-3} the instrument counts individual droplets and thus can be regarded as a direct counter. Its lower detection limit with regard to particle concentration was never reached during the campaign. In contrast to classical condensation nuclei counters, the instrument uses *n*-butyl alcohol as working fluid instead of water. Comparisons with a pocket counter (*Jaenicke*, 1980a) showed a 10% higher concentration readout of the TSI-Counter ($N < 1{,}000$ cm^{-3}). That is acceptable if one keeps in mind the agreement of condensation nuclei counters in general (*Liu* et al., 1979), which is a factor of 2, roughly.

The size distribution of the condensation nuclei was determined in connection with a Diffusion Denuder[2]. This system worked discontinuously and delivered one size distribution every 2 h if not disturbed by local human activities. The evaluation of the penetration dates of the Diffusion Battery requires extensive numerical treatment. The method used has been developed in the authors' institute but has not been yet published.

Further three instruments were used to determine the size distribution of the large particles, namely a Double Stage Impactor (0.1 μm − 1.5 μm in radius), an Impactor (1μm − 30 μm in radius), and a Free Rotating Impactor (20 μm − 200 μm in radius). These instruments are described elsewhere (*Jaenicke* et al., 1971). The collection time for these instruments was up to 12 h and because of frequent interruptions, a complete size distribution could only be measured once every 1 or 2 days. The measurements were analyzed onboard.

[1] No. 3020 of Thermo Systems Inc., St. Paul, Minnesota, USA, based on *Bricard* et al. (1976)
[2] No. 3040 − 1 of Thermo Systems Inc., St. Paul, Minnesota, USA, based on *Sinclair* and *Hoopes* (1976)

Condensation nuclei concentration

The concentration of condensation nuclei varied between 5 cm^{-3} and several thousand per cm^3 in individual measurements, respectively 20 cm^{-3} and several thousand per cm^3 as 12-h averages. To our knowledge, such low concentrations have only been published by *Bullrich* et al. (1968) for locations on the islands of Hawaii. Values similiar to our maximum concentrations have been reported for Greenland on certain occasions by *Flyger* et al. (1980).

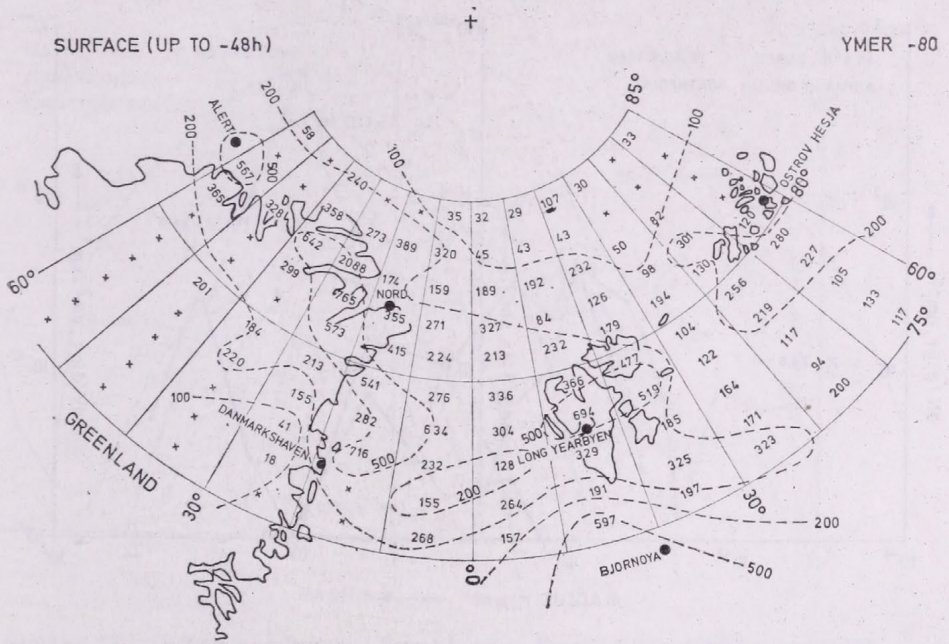

Fig. 1: Average condensation nuclei concentrations (in cm^{-3}) calculated for 12 h positions of surface trajectories over three summer months 1980. The area in the north – east corner obviously has very low nuclei concentrations

In order to organize the results and understand the large variation in condensation nuclei concentration, air mass trajectories have been calculated in steps of 12 h for 48 h backward. Surface level trajectories will be used in this paper because of the stable stratification of arctic air. In addition, the result of this study will justify the use of surface trajectories.

At the 12 h locations determined by the trajectories, the concentration of condensation nuclei was calculated. No source and no mixing was assumed, and the aerosol was permitted to age with a 5-day residence time. A 5-day period is a rather long residence time as compared with the usual 2 days (*Jaenicke*, 1980b), but it is justified because of the reduced removal mechanism in the Arctic. *Figure 1* shows the result. A grid pattern with spacing of 1° N – S and 10° E – W of average concentrations of condensation nuclei has been calculated for the 3 months of observations. Extremely clean air with concentrations below 100 cm^{-3} can be seen on Greenland and north of Svalbard. A region of rather high concentrations ($N > 200$ cm^{-3}) reaches from Northern

Greenland to Svalbard. Concentrations of $N > 500$ cm^{-3} mostly can be located at centers of known human activities, as named in *Fig. 1.* Other human activities are connected with the YMER expedition itself on the Northeast Island of Svalbard (grids 78° – 80° N, 20° – 30° E). In addition, several expeditions travel to the north of Greenland each summer. This explains most of the regions with $N > 500$ cm^{-3}, and encourages even to assume anthropogenic activities (ship surface transport) in the remaining grids with $N > 500$ cm^{-3}. Quite surprising is the rather clean air between Svalbard and Bjornoya (Bear

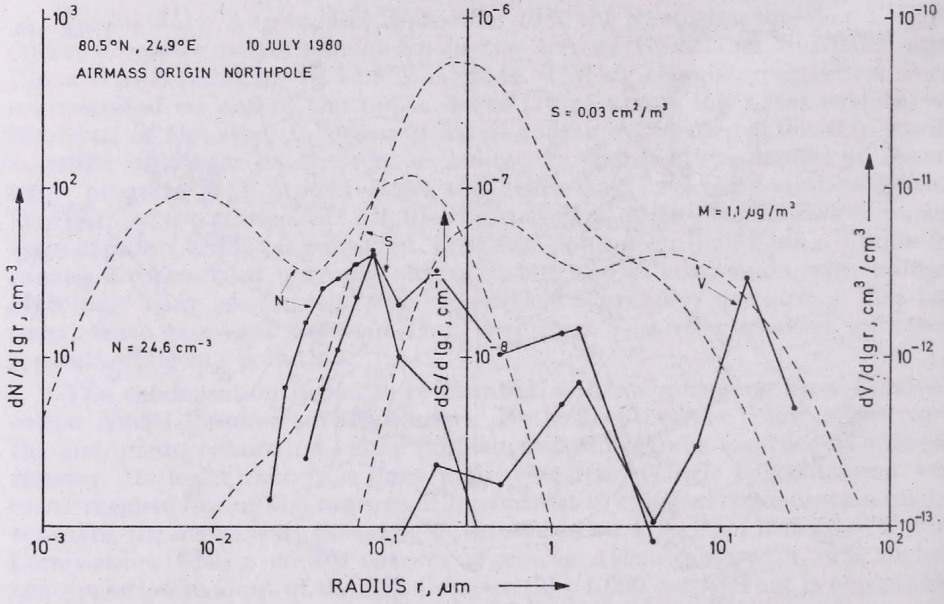

Fig. 2: The aerosol size distribution of very clean arctic air. There are given the number, surface and volume order for a model background distribution (without sea salt) (dashed line) and the actual distribution (solid line) for comparison

Island). These observations were made with air masses coming from the south, from Europe. Obviously, during transport the air was cleansed from condensation nuclei originating in Europe. It seems as if Europe were not the origin of the high condensation nuclei concentrations in the Arctic. This "pollution" seems to originate from human activities in the Arctic itself.

This result for the summer supplements the hypothesis of *Rahn* and *McCaffrey* (1980) about a European genesis of the winter arctic aerosol. In winter, the polar front is moved to the south and thus major centers of anthropogenic pollution are enclosed in the arctic air. This problem is discussed at length by *Rahn* (1981).

Complete size distribution of arctic aerosols

The above-described knowledge about human influence on the arctic aerosol was obtained *after* the expedition. *During* the expedition, the arrival of true arctic aerosol was not foreseeable, hence a complete size distribution was

nly occasionally obtained. *Figure 2* shows the case of 10 July 1980 at 0.5° N, 24.9° E, with air originating from the North Pole.

The size distribution is plotted in its number, surface and volume order. 'or comparison, the model background distribution (without sea salt) (*Jaenicke*, 980b) is given. The number concentration shows a distinct maximum around .1 μm particle radius. The total concentration was $N = 24.6$ cm^{-3}. No particles ave been observed below 0.01 μm and above 30 μm in radius. When comparing iis distribution to the background aerosol, one can see that for all radii lower

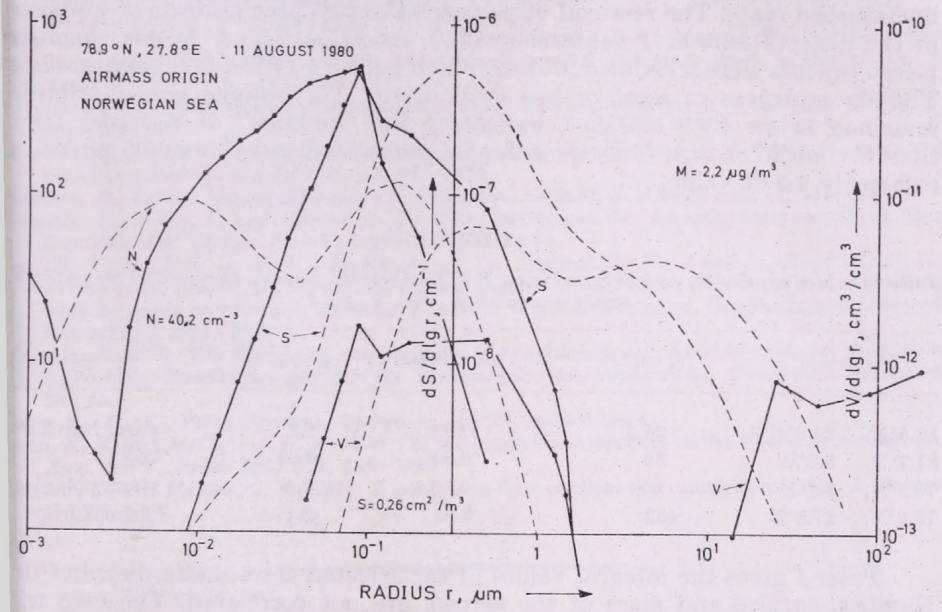

7. 3: Same as *Fig. 2*, but with air from the Norwegian Sea. Practically no particles are present in the range 1 – 10 μm

ncentrations are observed (up to a factor of 10), and the smallest particles e absent. From all we know, this is a well-aged aerosol without gas-to-rticle production.

During parts of the YMER cruise, SO_2 measurements have been performed *Ockelmann*[3] (*Meixner*, 1981). Usually mixing ratios of 10 – 15 pptv have en observed. 10 July 1980 is the only day with SO_2 mixing ratios below the tection limit of 6 pptv. Of similiar shape is a distribution of 23 August 1980 m 78.8° N, 3.2° E with air originating from the permanent ice north of albard.

The situation is different on 11 August 1980 at 78.9° N, 27.8° E, a day ecially selected for air chemistry measurements. The air originated from Norwegian Sea. The distribution, *Fig. 3*, shows a lack of particles in the m – 10 μm range, even if particles up to 200 μm have been counted. This ld be the result of precipitation removal, because the air originated from region of the polar front with its intensive precipitation. Particles around

[3] Private communication

0.1 μm in radius are more abundant than in the model background aeroso and come close to the model remote continental aerosol (*Jaenicke*, 1980b) The existence of particles around 0.001 μm indicates gas-to-particle formation The condensation nuclei concentration was 402 cm^{-3}, indicating anthropogeni influences. The distribution is comparable with observations in Ny-Ålesund Svalbard as published recently (*Heintzenberg*, 1980). Ny-Ålesund, north o Longyearbyen certainly is a remote location, but as Fig. 1 shows, it is locate in an area of increased condensation nuclei concentration. Such measurement indicate how far the aerosol in the Arctic already deviates from its natura undisturbed state. The removal of particles through precipitation is supporte in the observations of 1 September 1980. At 81.7° N, 8.6° W air chemistr measurements were scheduled, during which light fog (VV < 1,000 m) develope The air mass was of more or less local origin. The volume size distributio remained below 10^{-13} cm^3/cm^3, indicating the "absence" of particles large than 0.1 μm in radius. Consequently, the calculated mass was 0.09 μg/m^3, a extremely small value.

TABLE I

Integral values number N, surface S and mass M of four selected aerosols discussed in the paper an partly presented in Figs. 2 and 3

Location	N, cm^{-3}	S, cm^2/m^3	M, μg/m^3	Remarks
80.5°N, 24.9°E	24.6	0.03	1.1	from North Pol
81.7°N, 8.6°W	59	0.01	0.09	fog
78.8°N, 3.2°E	69	0.05	0.5	from polar ice
78.9°N, 27.8°E	402	0.26	2.2	from Europe

Table I gives the integral values of the selected aerosol size distributions Number, surface and mass of the aerosol are not correlated. The case wit typical particle concentrations (400 cm^{-3}) for background air shows a tota mass by a factor of ten lower than expected for background air. Masswise this air is very clean.

Conclusions

Measurements of the arctic aerosol in summer indicates a strong huma influence. The anthropogenic source seems to be located within the Ar tic itself. Obviously, European sources influence this aerosol only to a minor extent True arctic aerosols have condensation nuclei concentrations below 100 cm and can be observed on rare occasions only. These low concentrations mos probably have not been detected in earlier measurements (*Flyger* et al., 1980 because of the insufficient sensitivity of the instrument used. The reported high concentrations of condensation nuclei in that paper – and unexplained so far – could originate from human sources in the Arctic, even 1,000 km away.

The size distribution of arctic aerosols reveals a well-aged aerosol in the range 0.01 μm to 30 μm and concentrations up to a factor of 10 lower than model background distributions.

Acknowledgement. This work was made possible through the invitation and support of the Swedish government and the German Science Foundation through its Sonderforschungsbereich "Atmospheric Trace Substances". We

vould like to thank Prof. Dr. *V. Schytt*, scientific leader of the YMER expe-
lition, and Mr. *V. Johannes* and Dr. *P. Winkler*, participants during part of
he cruise.

REFERENCES

ricard, J., Delatte, P., Madelaine, G. and *Pourprix, M.*, 1976: Detection of ultra-fine particles by means of a continuous flux condensation nuclei counter; in: *Fine particles. B.Y.H. Liu* (Editor), Academic Press, New York.

ullrich, K., Eiden, R., Jaenicke, R. and *Nowak, W.*, 1968: Solar radiation extinction, sky radiation, sky light polarization and aerosol particle total number and size distribution on the Island Maui (Hawaii). *Pageoph 69*, 280–319.

lyger, H., Heidam, N. Z., Hansen, K. A., Rasmussen, L. and *Megaw, W. J.*, 1980: The background levels of the summer tropospheric aerosol and trace gases in Greenland. *J. Aerosol Sci., 11*, 95–110.

leintzenberg, J., 1980: Particle size distribution and optical properties of Arctic haze. *Tellus 32*, 251–260.

aenicke, R., 1980a: The Scholz pocket-counter and its modification – A direct condensation nuclei counter. *J. Aerosol Sci., 11*, 263–265.

aenicke, R., 1980b: Atmospheric aerosols and global climate, *J. Aerosol Sci., 11*, 577–588.

aenicke, R., Junge, C. and *Kanter, H. J.*, 1971: Messungen der Aerosolgrössenverteilung über dem Atlantik. *Meteor Forsch.-Ergebnisse B7*, 1–54.

iu, B. Y. H., Pui, D. Y. H., McKenzie, R. L., Argawal, J. K., Jaenicke, R., Pohl, F. G., Preining, O., Reischl, G., Szymanski, W. and *Wagner, P. E.*, 1979: Recent experiments of the working group on ultrafine aerosols. *The 1979 WUFA Workshop.* Gesellschaft für Aerosolforschung *7*, 245–252.

leixner, F., 1981: Die vertikale Verteilung des atmosphärischen Schwefeldioxids im Tropopausenbereich. *Berichte des Instituts für Meteorologie und Geophysik der Universität Frankfurt*, Nr. 45.

ahn, K. A., ed., 1981: *Atmosph. Environm., 15* (8), special issue.

ahn, K. A. and *McCaffrey, R. J.*, 1980: On the origin and transport of the winter Arctic aerosol. *Ann. N. Y. Acad. Sci., 338*, 486–503.

inclair, D. and *Hoopes, G. S.*, 1976: A continous flow condensation nucleus counter. *J. Aerosol Sci., 6*, 1–7.

IDŐJÁRÁS

Az Országos Meteorológiai Szolgálat folyóirata, 86. évf. 2–4. szám, 1982. március–augusztus
Journal of the Hungarian Meteorological Service, Vol. 86. No. 2–4. March–August 1982, Budapest

Measurements of the relationship between the dry size and critical supersaturation of natural aerosol particles

J. W. FITZGERALD and W. A. HOPPEL, *Naval Research Laboratory, Washington, DC 20375, U.S.A.*

A természetes aeroszol részecskék száraz nagysága és a kritikus túltelítettség közötti kapcsolat mérése. Ismert r_0 sugarú részecskék S_c kritikus túltelítettségét mértük. A kapott adatokat használtuk fel az $S_c = K.r_0^{-3/2}$ összefüggés K konstansának meghatározására. A kísérleti berendezés a következő volt: Egy mozgékonyság-analizátor alacsony relatív nedvesség mellett a kívánt szűk nagyságtartományban részecskéket bocsát be egy termál-gradiens diffúziós felhőkamrába, ahol a részecskék aktiválásához szükséges túltelítettség mérhető. Huszonhat esetben határoztuk meg K értékét a következő helyeken: Washingtonban (DC), Chesapeake-öböl déli részén és New Jersey és Virginia partjain (a tenger fölött). A mozgékonyság-analizátor által átbocsátott részecskék közepes sugara 0,02 és 0,071 μm között volt. K értéke $1{,}82 \times 10^{-11}$ cm$^{3/2}$ és $4{,}07 \times 10^{-11}$ cm$^{3/2}$ tartományban változott, $2{,}44 \times 10^{-11}$ cm$^{3/2}$ közepes értékkel. Ezzel szemben az azonos nagyságú tiszta NaCl és $(NH_4)_2SO_4$ részecskékre K elméleti értéke rendre $1{,}2 \times 10^{-11}$ és $1{,}7 \times 10^{-11}$ cm$^{3/2}$ (20 °C-nál).

*

Measurement of the relationship between the dry size and critical supersaturation of natural aerosol particles. The critical supersaturation (S_c) of atmospheric aerosol particles of known dry size (r_0) was measured. These data were used to evaluate K in the relationship $S_c = Kr_0^{-3/2}$. The experimental method consists of using a mobility analyzer to transmit a narrow size range of particles at low relative humidity to a thermal gradient diffusion cloud chamber, where the supersaturation necessary to activate the particles is measured. Twenty-six determinations of K have been made for aerosols sampled in Washington, DC, in the southern part of Chesapeake Bay and off the coasts of New Jersey and Virginia. The mean radius of the particles transmitted by the mobility analyzer was varied from 0.02 μm to 0.071 μm. K was found to range in value from 1.82×10^{-11} cm$^{3/2}$ to 4.07×10^{-11} cm$^{3/2}$ at 20°C, the average value of K being 2.44×10^{-11} cm$^{3/2}$. By contrast, the theoretical values of K for pure NaCl and $(NH_4)_2SO_4$ particles are approximately 1.2×10^{-11} cm$^{3/2}$ and 1.7×10^{-11} cm$^{3/2}$, respectively, at 20°C.

*

Introduction. The supersaturation spectrum of cloud condensation nuclei (CCN) is one of the factors controlling the number and size of droplets in the lower regions of cumulus clouds. For this reason considerable effort has been spent in measuring CCN spectra over the last twenty years. Most data on the CCN spectrum above 0.2% supersaturation has been obtained with thermal gradient diffusion cloud chambers (TGDCC). However, the CCN spectrum can also be obtained from the dry aerosol size distribution if the relationship between the dry size (r_0) and critical supersaturation (S_c) of aerosol particles is known.

The relationship between S_c and r_0 for partly soluble particles may be written

$$S_c = \left[\frac{4A^3}{27B}\right]^{1/2} r_0^{-3/2} = K r_0^{-3/2} \tag{1}$$

where $A = 4.33 \times 10^{-7} \sigma'/T$ and $B = \overline{\nu}\overline{\Phi}\varepsilon M_w \varrho_0 / \varrho_w \overline{M}_s$. In A and B, ε is the mass fraction of soluble material in the particle; σ' is the surface tension of the droplet at its critical radius; T is temperature; $\overline{\nu}$ is the mean number of moles of ions per mole of salt mixture; $\overline{\Phi}$ is the observed practical osmotic coefficient; M_w is the molecular weight of water; $\overline{M}_s$ is the molecular weight of the soluble material; ϱ_0 is the density of the particle in dry state; and ϱ_w is the density of water. In deriving this equiation, it is assumed that the volume of the particle at its critical radius is large compared to the volume of the particle in dry state so that $(r/r_0)^3 - 1$ can be approximated by $(r/r_0)^3$ in the term describing the effect of the dissolved material on the equilibrium vapor pressure. The validity of this approximation depends on the values of r_0 and ε. In general, Eq. (1) can be applied with acceptable accuracy when $r_0 > 0.02$ μm and $\varepsilon > 0.1$.

For particles having a known, but simple, composition, the value of the coefficient K in Eq. (1) can usually be calculated from available data. However, in the case of atmospheric aerosol particles, which are of unknown composition, the value of K must be determined experimentally.

This paper describes a method of determining K by measuring the critical supersaturation of aerosol particles of known size and presents the results of measurements made in Washington, DC, in the southern part of Chesapeake Bay and in the Atlantic, approximately 150 – 300 km off the coasts of New Jersey and Virginia.

1. Experimental method

An aerosol sample is first brought to charge equilibrium with a ^{210}Po radioactive source and is then passed through the NRL mobility analyzer. The mobility analyzer is designed to measure the size distribution of aerosol particles and is described elsewhere (*Hoppel*, 1978). However, its use in these experiments is, in principle, the same as the electrical aerosol classifier described by *Liu* and *Pui* (1974). The mobility analyzer is set to transmit particles in a narrow size (mobility) range to a static-type TGDCC where the supersaturation necessary to activate the particles is measured. The supersaturation in the TGDCC is gradually increased by slowly increasing the temperature difference between the plates. Typically, from five to ten determinations of the number of activated nuclei are made in the time it takes ΔT to increase by 0.25°C. The average number of particles activated in each 0.25°C interval of ΔT is then plotted as a function of the mean supersaturation for that interval. Next, the number of multiply-charged larger particles, which are transmitted along with the more numerous singly charged particles of the desired size, is estimated from the size distribution and is subtracted from the measured number activated at each supersaturation. The corrected number of particles active at each supersaturation is then normalized to the maximum number activated. The size channel selected for transmission to the TGDCC is chosen to be near the peak in the size distribution so that the number of particles in the larger size channels is much less than in the selected channel.

To illustrate the method, *Fig. 1* shows the normalized number of activated nuclei as a function of supersaturation for two transmitted size ranges. The range of critical supersaturation of the particles in a transmitted size interval is taken to be between the points where 10% and 90% of the particles are activated. These points are identified by the arrows on the curves. The super-

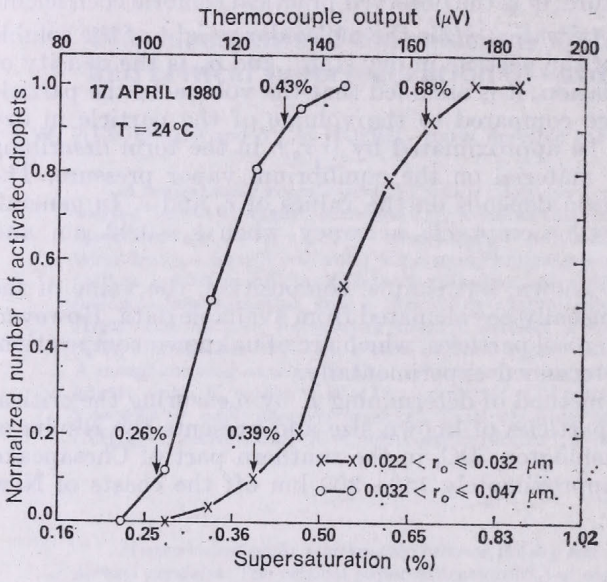

Fig. 1: Normalized number of activated droplets as a function of supersaturation for measurements made off the coast of the U.S.

saturation at which only 90% of the particles are activated is chosen in defining the range of critical supersaturation for the size interval, because statistical fluctuations in the number of droplets in the small viewing volume used in the TGDCC make it impossible to determine the exact supersaturation at which all particles are activated.

The experimental data are plotted as shown in *Fig. 2*. The widths of the boxes are the size intervals transmitted by the mobility analyzer and the heights of the boxes are the measured ranges of critical supersaturation. The S_c *vs.* r_o relationship for $(NH_4)_2SO_4$ is shown for reference. Since a range of particle sizes is transmitted, it is not possible to precisely determine the critical supersaturation of a given particle size within the interval. To compute K, we use the values of S_c and r_o at the center of the box. The maximum uncertainty in K associated with the width of the size interval is estimated to be $\pm 15\%$.

2. *Results and discussion*

A total of twenty-six determinations of K have been made at three general locations over a four-year period. These results are summarized in *Table I* which shows the date and location of the measurements, the particle size range measured, and the computed values of K. Note that except for the data of May 1977, the indicated particle size range encompasses two or three transmitted size ranges. Differences in K due to differences in measurement

temperature were removed by reducing all K values to a temperature of 20 °C. This reduction was based on the temperature dependence of the curvature term A in Eq. (1) for pure water. Table I shows that K ranges from 1.82×10^{-11} $cm^3/^2$ to 4.07×10^{-11} $cm^{3/2}$. The average value of K for all twenty-six measurements is 2.44×10^{-11} $cm^{3/2}$. By contrast, the value of K for $(NH_4)_2SO_4$ and

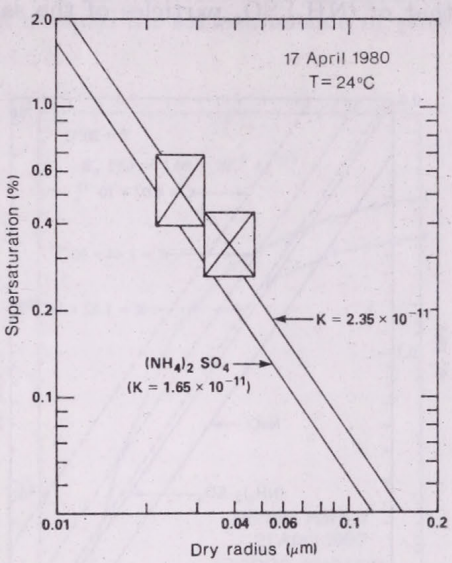

Fig. 2: Critical supersaturation as a function of dry particle radius; the boxes are results for natural aerosol particles collected off the east coast of the U.S.

NaCl particles is approximately 1.7×10^{-11} and 1.2×10^{-11} $cm^{3/2}$, respectively. There is some indication in these data that the values of K increase with increasing particle size. However, we are reluctant to draw any hard conclusions about the variation of K with particle size from such a rather limited set of measurements.

TABLE I

Values of K *for atmospheric aerosol particles.* $T = 20°C$

Location of measurements	Date	Particle size range measured (μm)	K ($cm^{3/2}$)
Washington, DC	29 June 1978	0.020 – 0.052	$2.14-2.82\times10^{-11}$
Washington, DC	26 – 30 July 1979	0.029 – 0.079	$2.16-4.07\times10^{-11}$
Washington, DC	29 Aug. 1980	0.020 – 0.035	$2.19-2.51\times10^{-11}$
Washington, DC	8 Sept. 1980	0.020 – 0.035	$1.99-2.04\times10^{-11}$
Norfolk Harbor	14 May 1977	0.022 – 0.032	2.55×10^{-11}
160 km off coast of New Jersey	16 May 1977	0.032 – 0.047	2.14×10^{-11}
250 km off coast of Virginia	17 – 19 April 1980	0.015 – 0.047	$2.08-2.56\times10^{-11}$
Norfolk Harbor/ Chesapeake Bay	21 – 22 April 1980	0.015 – 0.047	$1.82-2.14\times10^{-11}$

Figure 3 is a plot of critical supersaturation as a function of dry particle radius. The dashed curves show the $S_c - r_0$ relationship computed from Eq. (1) for the average value of K (2.44×10^{-11} cm$^{3/2}$) and extreme values of K calculated from our measurements. The continuous lines are the theoretical curves for pure NaCl and $(NH_4)_2SO_4$ particles. On the average, we found the critical supersaturation of natural aerosol particles to be about 1.45 times that of $(NH_4)_2SO_4$ particles of the same size.

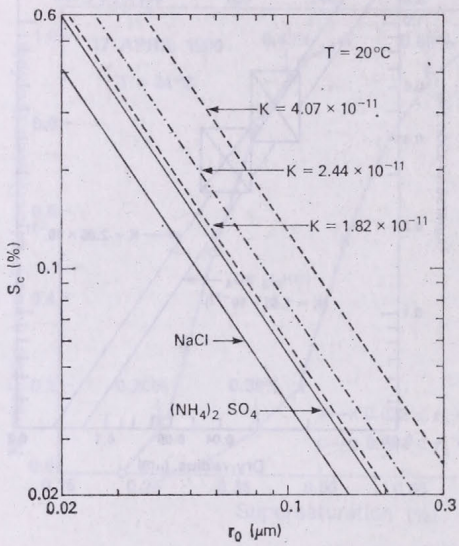

Fig. 3: Critical supersaturation as a function of particle radius; dashed curves are for the average and extreme values of K computed from the measurements of the critical supersaturation of natural particles aerosol of known size; the continuous lines are theoretical curves for puresalt particles

Figure 4 shows a comparison between a CCN spectrum measured with the TGDCC and the one calculated from the particle size distribution and the measured relationship between S_c and r_0. As we frequently find in such comparisons, there is excellent agreement between the shapes of the measured and calculated spectra, but some discrepancy in the number of CCN. Our measured CCN concentrations are often found to be 20 to 60% lower than predicted. For the comparison shown in Fig. 4 the difference is about 55%. Some of this discrepancy may be attributed to errors in CCN concentrations obtained with the TGDCC. First, the measured CCN counts shown in Fig. 4 were obtained with our video camera system. It has been our experience that the count determined from the video recording is about 15% lower than the photographic count. (We normally use the video count in our studies since it can be obtained immediately, unlike the photographic count which requires film processing.) Secondly, the TGDCC can underestimate CCN counts due to the fact that the larger nuclei which are activated first may fall out before the smaller nuclei – which are not activated until the maximum steady-state supersaturation is achieved – can grow to detectable size. As discussed by *Hoppel* and *Wojciechowski* (1976) and *Alofs* and *Carstens* (1976), the error in CCN counts measured with the TGDCC increases as the slope of the CCN spectrum decreases and as the detection limit increases.

The value of K can also be determined if the values of A and B in Eq. (1) are known. The value of B in Eq. (1) is approximately equal (to within 15%)

to $\varrho_o \eta^o / \varrho_w$, where η is the value of the exponential mass increase coefficient at infinite dilution. (The exponential mass increase coefficient is defined as $\overline{\nu}\,\overline{\Phi}\varepsilon M_w / \overline{M}_s$ [*Hänel*, 1976]). *Hänel* (1981) presents data on ϱ_o and η^o for aerosol samples collected at Mainz and Deuselbach, FRG. The particles collected ranged in radius from 0.07 to 10.0 μm. One can compute values of K from *Hänel*'s data if one assumes a value for σ', the surface tension of the particles (droplets) at their critical radius. If we let σ' equal the surface tension of pure

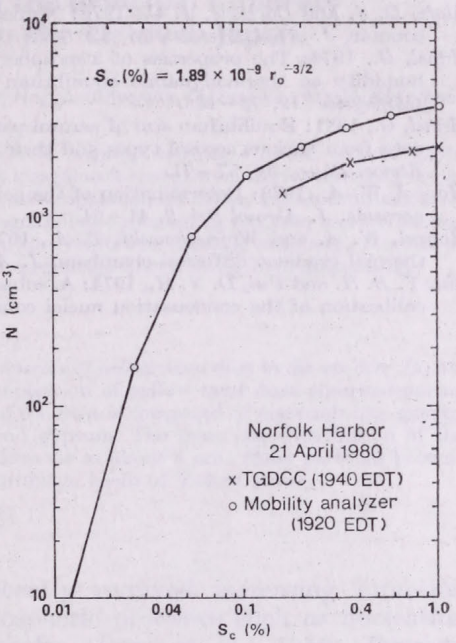

Fig. 4: Comparison of a CCN spectrum measured directly with the TGDCC with that inferred from the particle size distribution and the measured relationship between S_c and r_o

water, then *Hänel*'s data yield values of K ranging from 1.43×10^{-11} to 2.82×10^{-11} cm$^{3/2}$. Five of the seven samples collected at Mainz and Deuselbach had a value of K smaller than the mean value of K calculated from our measurements along the east coast of the U.S.

3. *Summary and conclusions*

The critical supersaturation (S_c) of atmospheric aerosol particles of known dry radius (r_o) was measured. The method involves use of a mobility analyzer to transmit a narrow size range of particles to a thermal gradient diffusion cloud chamber, where the supersaturation necessary to activate the particles is measured.

Twenty-six measurements of S_c and r_o were made in Washington, DC, the southern part of Chesapeake Bay and off the coasts of New Jersey and Virginia. The mean size of the particles transmitted to the thermal diffusion chamber ranged from 0.02 μm to 0.071 μm radius. For each pair of values of S_c and r_o, the value of K in Eq. (1) was calculated. The results are shown in

Table 1. K was found to range from 1.82×10^{-11} $cm^{3/2}$ to 4.07×10^{-11} $c^{3/2}$, the average value being 2.44×10^{-11} $cm^{3/2}$. By contrast, the theoretical values of K for pure NaCl and $(NH_4)_2SO_4$ particles at 20°C are 1.2×10^{-11} $cm^{3/2}$ and 1.7×10^{-11} $cm^{3/2}$, respectively.

Acknowledgements. This work was supported in part by the Naval Air Systems Command.

REFERENCES

Alofs, D. J. and *Carstens, J. C.*, 1976: Numerical simulation of a widely used cloud nucleus counter. *J. Appl. Meteor., 15*, 350–354.

Hänel, G., 1976: The properties of atmospheric aerosol particles as functions of the relative humidity at thermodynamic equilibrium with the surrounding moist air. *Advances in Geophysics 19*, 73–188.

Hänel, G., 1981: Equilibrium size of aerosol particles and relative humidity: New experimental data from various aerosol types and their treatment for cloud physics applications. *Contr. Atmos. Phys., 54*, 57–71.

Hoppel, W. A., 1978: Determination of the aerosol size distribution of the charged fraction of aerosols. *J. Aerosol Sci 9*, 41–54.

Hoppel, W. A. and *Wojciechowski, T. A.*, 1976: Accuracy of CCN measurements made with thermal gradient diffusion chambers. *J. Appl. Meteor. 15*, 107–112.

Liu, Y. B. H. and *Pui, D. Y. H.*, 1974: A. submicron aerosol standard and the primary, absolute calibration of the condensation nuclei counter. *J. Colloid Interface Sci., 47*, 155-171.

IDŐJÁRÁS

Az Országos Meteorológiai Szolgálat folyóirata, 86. évf. 2–4. szám, 1982. március–augusztus
Journal of the Hungarian Meteorological Service, Vol. 86. No. 2–4. March–August 1982, Budapest

Mass size distribution of the principal minerals of yellow sand dust in the air over Japan

Y. ISHIZAKA *and* A. ONO, *Water Research Institute, Nagoya University, Chikusa-ku, Nagoya, 464, Japan*

A sárga homokrészecskék főbb összetevőinek nagyság szerinti eloszlása Japán fölöti levegőben. 1979 áprilisában Japánban végzett vizsgálatok eredményei szerint a sárga homokpor tömegének 30%-a kvarcból, földpátból, csillámpalából, kloritból, kaolinitből, kalcitból és gipszből tevődik össze. A megfigyelt anyagokból álló részecskék nagyság szerinti tömegeloszlásának egyetlen maximuma van 4 μm környezetében. Ezek a részecskék részben az ázsiai sivatagok, részben a Sárga-folyó felső medencéje fölötti levegőből származnak.

*

Mass size distribution of the principal minerals of yellow sand dust in the air over Japan. The results of a study on the chemical composition of yellow sand dust observed during April 1979 in Japan show that about 30% of the dust is composed of materials like quartz, feldspar, illite, chlorite, kaolinite, calcite and gypsum. The mass size distribution of the particles from minerals observed has a single mode at about 4 μm. These particles become airborne over the Asian desert and upper drainage basin of Yellow River.

*

Introduction. Desert dust has recently received increasing attention because of the possible effects on atmospheric processes such as nucleation of ice crystals and radiation energy transfer (*Isono* et al., 1959; *Bertrand* and *Baudet*, 1973; *Carlson* and *Benjamin*, 1980). For a better understanding of the influences of these dust particles on such atmospheric processes, it is essential to know their nature, origin and concentration in the atmosphere. However, relatively little information about the mass size distribution of the minerals of these aerosols is available. This paper presents the results of a study on the material composition of yellow sand dust observed over the period of 12 : 30 JST 14–20 : 30 JST 16 April, 1979, in Japan.

Experimental

Sampling procedures. Dust aerosols were collected by means of two Andersen samplers (Model 21–000, 2000 Inc.) in Nagoya. Each sampler consisted of eight stages followed by a Whatman 41 (cellulose) backup filter. Aerosol particles were fractionated into size classes <0.43, 0.43–0.65, 0.65–1.1, 1.1–2.1, 2.1–3.3, 3.3–4.7, 4.7–7.0, 7.0–11, and >11 μm equivalent aerodynamic diameter. The sampler flow rate was 1 cfm (28.3 L/min). A dust sample was collected over the period of 15 : 00 JST 11–9 : 00 JST 17 April, 1979. In order to examine the aerosol other than yellow sand dust,

a reference sample was collected over the period of 9 : 00 JST 20 – 16 : 00 JST 26. April, 1979.

X-ray analysis. Size-classified dust was treated with ethylene glycol and hydrochloric acid and examined with an X-ray diffractometer to identify mineral species exactly. Furthermore, quantitative analysis of the materials in the dust was carried out by X-ray method. In order to examine the sizes of minerals in the dust particles, aerosol particles on each impactor plate were collected into one group and were also analyzed by X-ray method, after they had been separated into three size classes < 2, $2-4$, > 4 μm equivalent aerodynamic diameter. In order to supplement the result of mass size distribution of yellow sand dust, sizes and concentrations of dust aerosol particles were also measured with a Pollack counter and an optical particle counter.

Results and discussion

Size distribution of yellow sand dust. Figure 1 shows the estimated mass size distribution of yellow sand dust and total suspended particulate matter during Yellow Sand Event. The distribution of yellow sand dust had a single mode, concentrated betwen 1 and 20 μm in diameter and its mass concentration was 182 $\mu g/m^3$. Some of the data obtained by *Patterson* and *Gillette* (1977) and *Levin* et al (1980) were plotted in Fig. 1 as mass distributions. If one uses the *Patterson* and *Gillette* (1977) definitions, one can see that our yellow sand dust can be classified as an event of moderate aerosol loading. Measurement of aerosol size distributions showed a sharp concentration increase between 0,2 and 4 μm in diameter during Yellow Sand Event.

Mineral composition of yellow sand dust. Figure 2a shows the mass size distributions of quartz, feldspar, illite (mica), chlorite, kaolinite, calcite, gypsum and ammonium sulfate during two sampling periods. From the results of Fig. 2a, we estimated the mass size distributions of quartz, feldspar, illite (mica), chlorite, kaolinite, calcite and gypsum originating from yellow sand dust, assuming that each of these minerals has similar distributions during these two sampling periods *(Fig. 2b)*. It is found from Fig. 2b that most

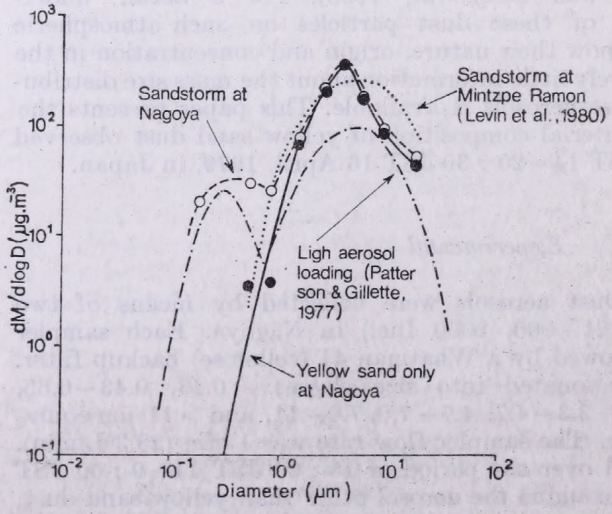

Fig. 1: Mass size distributions of dust aerosols

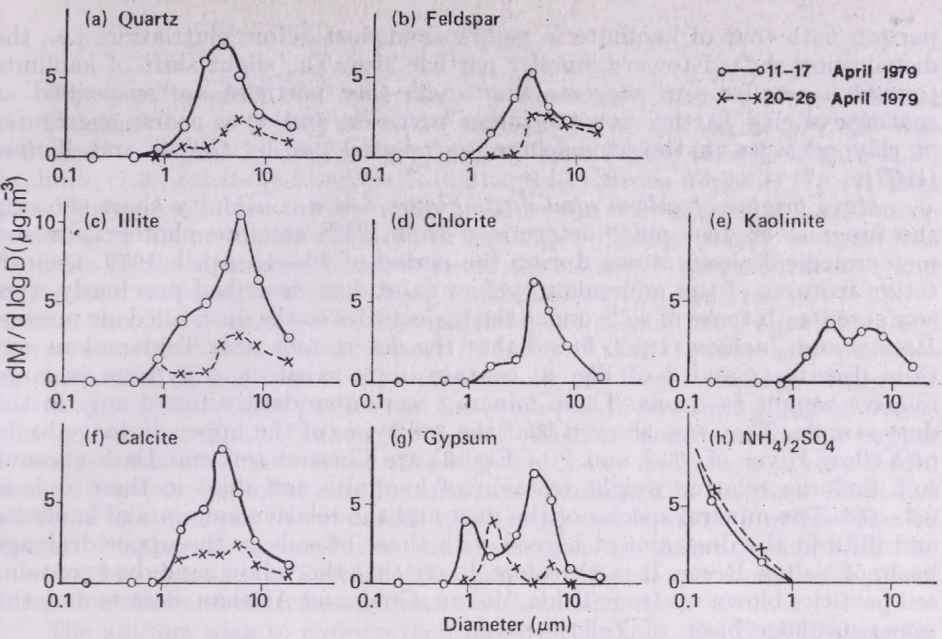

Fig. 2a: Mass size distributions of materials found in the aerosol particles

of the mass of the examinedi mnerals was in the diameter range between 1 and 20 μm and their distributions showed a single mode centered at approximately 4 μm.

Airborne state of dust aerosol particles. The mass size distribution of kaolinite in yellow sand dust changed significantly after elutriation in com-

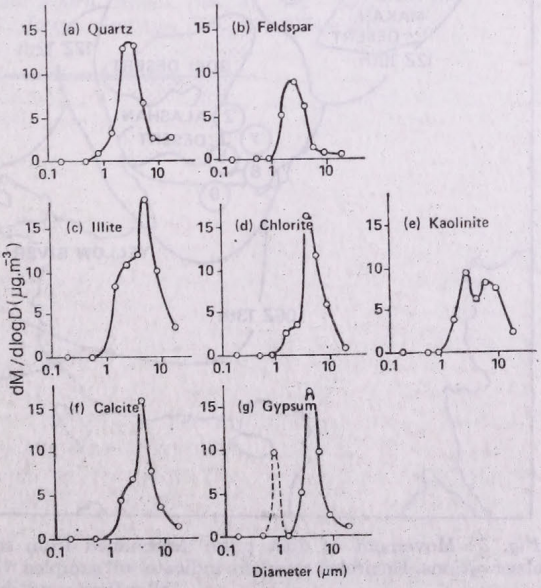

Fig. 2b: Mass size distributions of principal minerals originating from yellow sand dust

parison with that of kaolinite in yellow sand dust before elutriation, i.e., the distribution shifted toward smaller particle size. The slight shift of kaolinite toward a smaller size suggests that some clay particles are suspended as coatings of clay particles on the larger particles, and/or as coarse aggregates of clay particles in the atmosphere, as pointed out by *Gillette* and *Walker* (1977).

Main origins of yellow sand dust. Figure 3 is a continuity chart showing the progress of dust pulse determined from GMS satellite photographs and meteorological observations during the period of 10—15 April, 1979. Quantitative features of the minerals of yellow sand dust described previously were compared with those of soils under the trajectories of the dust-filled air masses. *Hseung* and *Jackson* (1952) found that the desert soils near Taklamakan and Gobi deserts (*1* and *2* of Fig. 3) contain illite, calcite and gypsum in large relative weight fractions. These minerals were abundantly found only in the dust sample. They also showed that the soil types of the upper drainage basin of Yellow River (*5*, *6*, *7* and *9* of Fig. 3) are Chesnut soil and Dark chesnut soil, and the relative weight fraction of kaolinite and illite in these soils is 0.3—0.5. The mineral species of the dust and the relative amounts of kaolinite and illite in the dust almost agreed with those of soils in the upper drainage basin of Yellow River. It is, therefore, likely that the yellow sand dust contains soil particles blown up from Takla Makan, Gobi and Alashan deserts and the upper drainage basin of Yellow River.

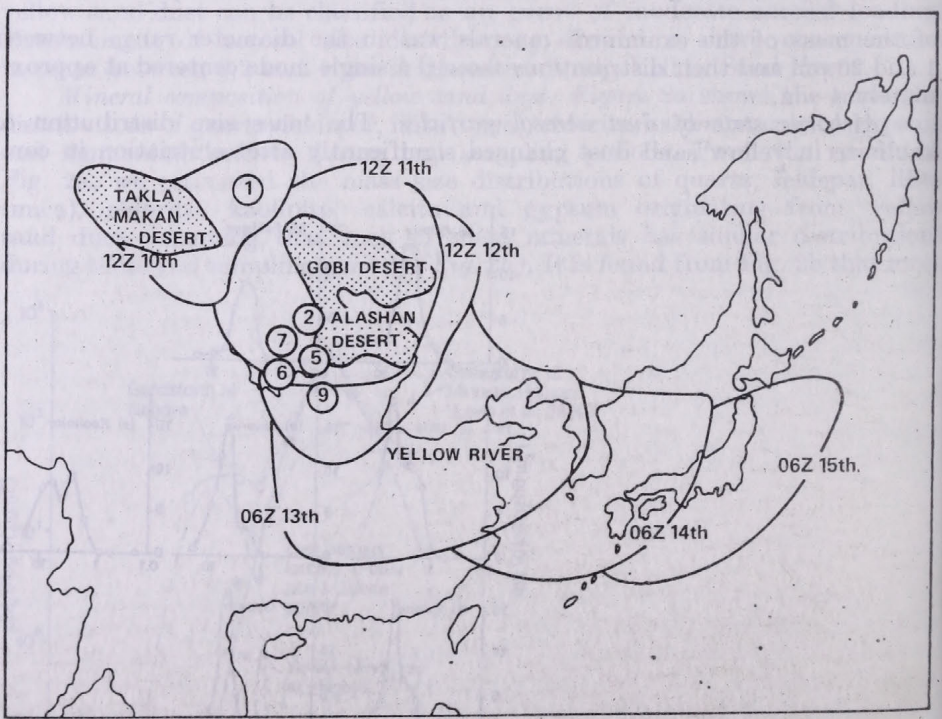

Fig. 3: Movement of dust pulse determined from satellite photographs and meteorological observations. Encircled numbers indicate soil samples which agreed with the mineral composition of yellow sand dust

Conclusion

The results of X-ray analysis of yellow sand dust were as follows: (1) The mass concentration of yellow sand dust was 182 $\mu g/m^3$ and the dust contained quartz (8.1 $\mu g/m^3$), feldspar (6.0), illite (mica) (13.1), chlorite (6.9), kaolinite (7.3), calcite (5.3), gypsum (6.9) and ferriferous minerals (?). (2) Mass size distribution of the minerals contained in the dust showed a single mode centered at about 4 μm. (3) Most of the mass of illite (mica), chlorite and kaolinite in the dust was found to be in the diameter range between 1 and 20 μm, and the same applies to quartz and feldspar. On the basis of the above results, the X-ray analysis of dust particles before and after elutriation and the movement of dust plume, it may be inferred that (1) some clay particles are suspended as coatings of clay particles on the larger particles, and/or as coarse aggregates of clay particles in the atmosphere, and that (2) main origins of the dust are Takla Makan, Gobi and Alashan deserts and the upper drainage basin of Yellow River (Loesslands). X-ray analysis is a very useful method for detection of crystalline substance contained in the dust. However, we could not analyze the materials amounting to about 70% of the dust in weight. Furthermore, ferriferous minerals such as hematite could not be examined in this study. Further extensive investigation is very necessary to determine the material composition of yellow sand dust.

The authors wish to express their sincere thanks to Dr. *S. Kadowaki* for collecting the aerosol samples.

REFERENCES

Bertrand, J. and *Baudet, J.*, 1973: *Journ. Appl. Meteor., 12*, 1191–1195.
Carlson, T. N. and *Benjamin, S. G.*, 1980: *Journ. Atmos. Sci., 37*, 194–213.
Gillette, D. A. and *Walker, T. R.*, 1977: *Soil Sci., 123*, 97–110.
Hseung, Y. and *Jackson, M. L.*, 1952: *Soil Sci. Soc. Amer. Proc., 16*, 294–297.
Isono, K., Komabayasi, M. and *Ono, A.*, 1959: *Journ. Meteor. Soc. Japan, 37*, 211–233.
Levin, Z., Joseph, J. and *Mekler, Y.*, 1980: *Journ. Atmos. Sci., 37*, 882–891.
Patterson, E. M. and *Gillette, D. A.*, 1977: *Journ. Geophys. Res., 82*, 2074–2082.

IDŐJÁRÁS

Az Országos Meteorológiai Szolgálat folyóirata, 86. évf. 2–4. szám, 1982. március–augusztus
Journal of the Hungarian Meteorological Service, Vol. 86. No. 2–4 March–August 1982, Budapest

The response of surface aerosol concentrations to changes in some boundary layer parameters

M. KITCHEN, J. R. LEIGHTON *and* S. J. CAUGHEY, *Meteorological Office, London, Road Bracknell, Berkshire RG12 2SZ, U.K.*

A talajközeli aeroszol koncentrációjának változásai a határréteg paramétereiben bekövetkező változások függvényében. Cardingtonban (Beds, Nagy-Britannia) 1980 márciusában és augusztusában nagyfrekvenciájú kondenzációs mag (CN) számlálóval végzett koncentráció mérések a jól ismert napi menetet eredményezték. A napkelte első 10 percén és a mérhető napsugárzás (<2 Wm^{-2}) első néhány percén belül a CN koncentráció gyors, 100%-t is elérő növekedése következik be, melyet konstans vagy gyengén csökkenő koncentrációjú idő követ, hirtelen csökkenéssel napnyugta után. A határrétegben bekövetkező változásokat nagyteljesítményű akusztikus szondával határoztuk meg. A kondenzációs mag koncentrációnak ezekkel összefüggésbe hozható változásait tárgyaljuk a tanulmányban. A vizsgált esetekben a vertikális kicserélődés csak jelentéktelen mértékben befolyásolta a talajközeli koncentrációt (legalábbis a megfigyelt változások időskáláján).

*

The response of surface aerosol concentrations to changes in some boundary layer parameters. High frequency condensation nucleus (CN) measurements made at Cardington, Beds, UK, during days in March and August 1980 identified the well known diurnal cycle. Within tens of minutes of the sunrise time, and within a few minutes of the appearance of measurable quantities of solar radiation at the surface (<2 Wm^{-2}), a sharp increase of up to 100% occurred in the CN concentration, followed by a time of steady or slowly falling concentrations during the afternoon, with more rapid falls after sunset. A high-power acoustic sounder was used to monitor changes in boundary layer depth and the response of aerosol concentrations to a sudden change is described. The results show that in this particular case the amount of vertical mixing appears to have had little effect on the surface concentrations, at least within the timescale of the observed changes in the layer.

*

Introduction. From observations of diurnal cycles in Aitken nucleus (AN) concentrations, several workers have suggested that the production of AN is related to incoming solar radiation, perhaps through photochemical processes. *Mamane* and *Pueschel* (1980) arrived at this conclusion from the study of mean concentrations for different months at the top of Cedar Mountain, Utah. *Haaf* and *Jaenicke* (1980), from observations of the aerosol size distribution at a height of 1,250 m in the Black Forest, concluded that: "Appearance of small particles was clearly correlated with direct sun irradiation with a response time of $\sim$10 minutes. Measurements during complete cloud cover suggested that diffuse irradiation produced fewer particles". *Mason* (1971), referring to observations of the diurnal AN cycle, reports the occurrence of a minimum around the middle of the day, probably due to enhanced upward transport and mixing as the boundary layer depth increases on convective days. Recently *Desalmand* et al. (1980) attributed daytime minima in cloud condensation

nuclei to this effect of dilution. *Lopez* et al. (1976) also observed such minima and supported *Haaf* and *Jaenicke*'s conclusion that the production of AN was greater on sunny days.

The aim of the work described here was to make observations of the diurnal cycle of CN and, at the same time, to make supporting observations which could enable an estimate of the effects of photochemical production associated with solar radiation and dilution resulting from vertical mixing, albeit for a very limited sample of data at a single location.

Experimental details

The experiments were conducted at the Meteorological Research Unit RAF Cardington during days in March and August 1980. The site is in a rural location, being surrounded by flat agricultural land, but there are possible local sources of aerosol (brickworks) to the west. Condensation nucleus concentrations were measured using a Pollak CN counter, the sample inlet being at a height of 3 m above the surface of a large grass field. Samples were nor-

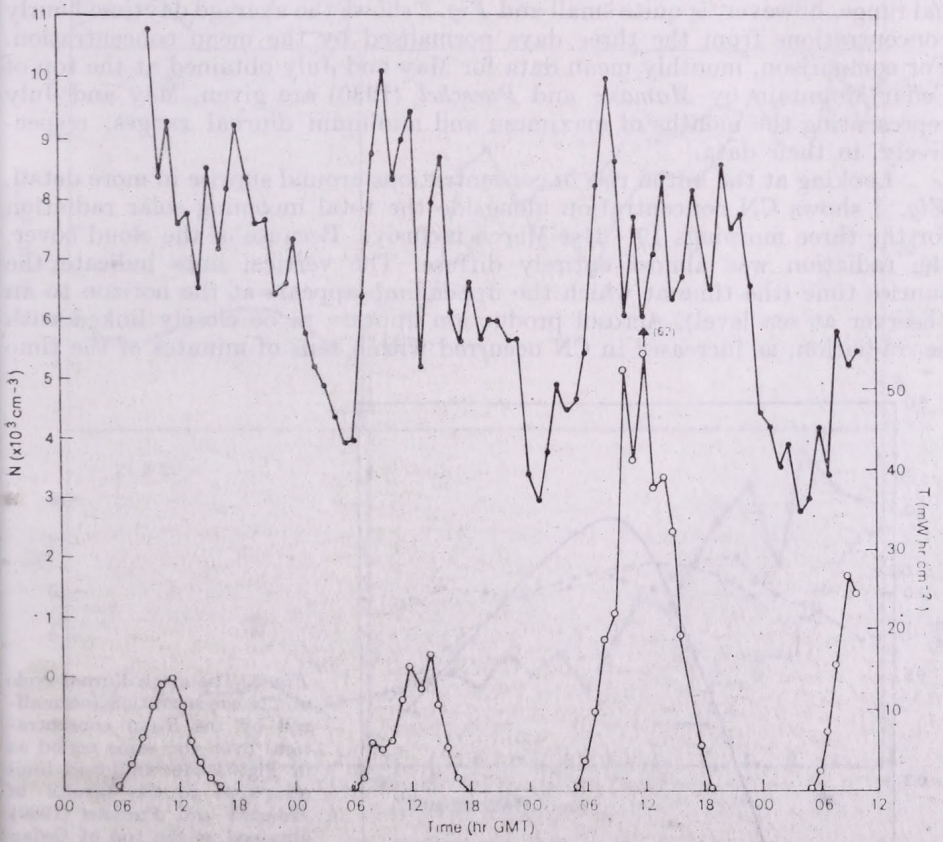

Fig. 1: Hourly means of CN concentrations (full circles) for the period 18–21st March 1980 showing the diurnal cycle. Below are shown the hourly integrated values of the total incoming solar radiation (open circles)

mally taken at 6-minute intervals during the observation periods. In order to monitor changes in the boundary layer structure, a high-power acoustic sounder was used and other supporting observations consisted of the normal synoptic parameters including total and diffuse solar radiation.

Diurnal variations

Figure 1 presents hourly means of CN concentrations for 3 and 1/2 days, 18 – 21st March 1980. Meteorological conditions were very steady throughout this period with an easterly air stream and almost complete layer cloudcover. The data show a strong diurnal cycle with a sharp increase in concentrations after sunrise, followed by a time of steady or slightly falling concentrations during the afternoon. After sunset, concentrations decrease more rapidly with the largest falls occurring around midnight. This form of cycle is very similar to those reported by *Mamane* and *Pueschel* (1980) with the absence of any obvious midday minima. The diurnal range for the three days is remarkably constant with very little change in daily mean concentrations, presumably reflecting the unchanging meteorological conditions. The magnitude of the diurnal range, however, is quite small and *Fig. 2* shows the average daytime hourly concentrations from the three days normalised by the mean concentration. For comparison, monthly mean data for May and July obtained at the top of Cedar Mountain by *Mamane* and *Pueschel* (1980) are given, May and July representing the months of maximum and minimum diurnal ranges, respectively, in their data.

Looking at the initial rise in concentrations around sunrise in more detail, *Fig. 3* shows CN concentration alongside the total incoming solar radiation for the three mornings 19 – 21st March inclusive. Because of the cloud cover, the radiation was almost entirely diffuse. The vertical lines indicate the sunrise time (the time at which the upper limb appears at the horizon to an observer at sea level). Aerosol production appears to be closely linked with he radiation, as increases in CN occurred within tens of minutes of the time

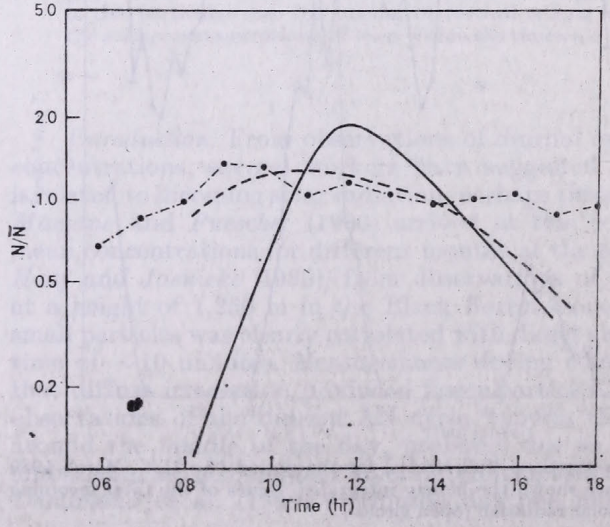

Fig. 2 : The mean diurnal cycle of CN concentration (normalized by the mean concentration) over the same period as in Fig. 1 (dot-and-dash line) compared to the results of *Mamane* and *Pueschel* (1980) obtained at the top of Cedar Mountain during the months of July (solid line) and May (dashed line)

of sunrise and within a few minutes of the lowest detectable level of radiation (< 2 Wm^{-2}) being measured by the solarimeter. Hourly totals of insolation are also plotted in Fig. 1, and it can be seen that incoming radiation levels were considerably higher on the 20th than the two preceding days, although the diurnal range in CN concentrations is similar. Although limited in extent,

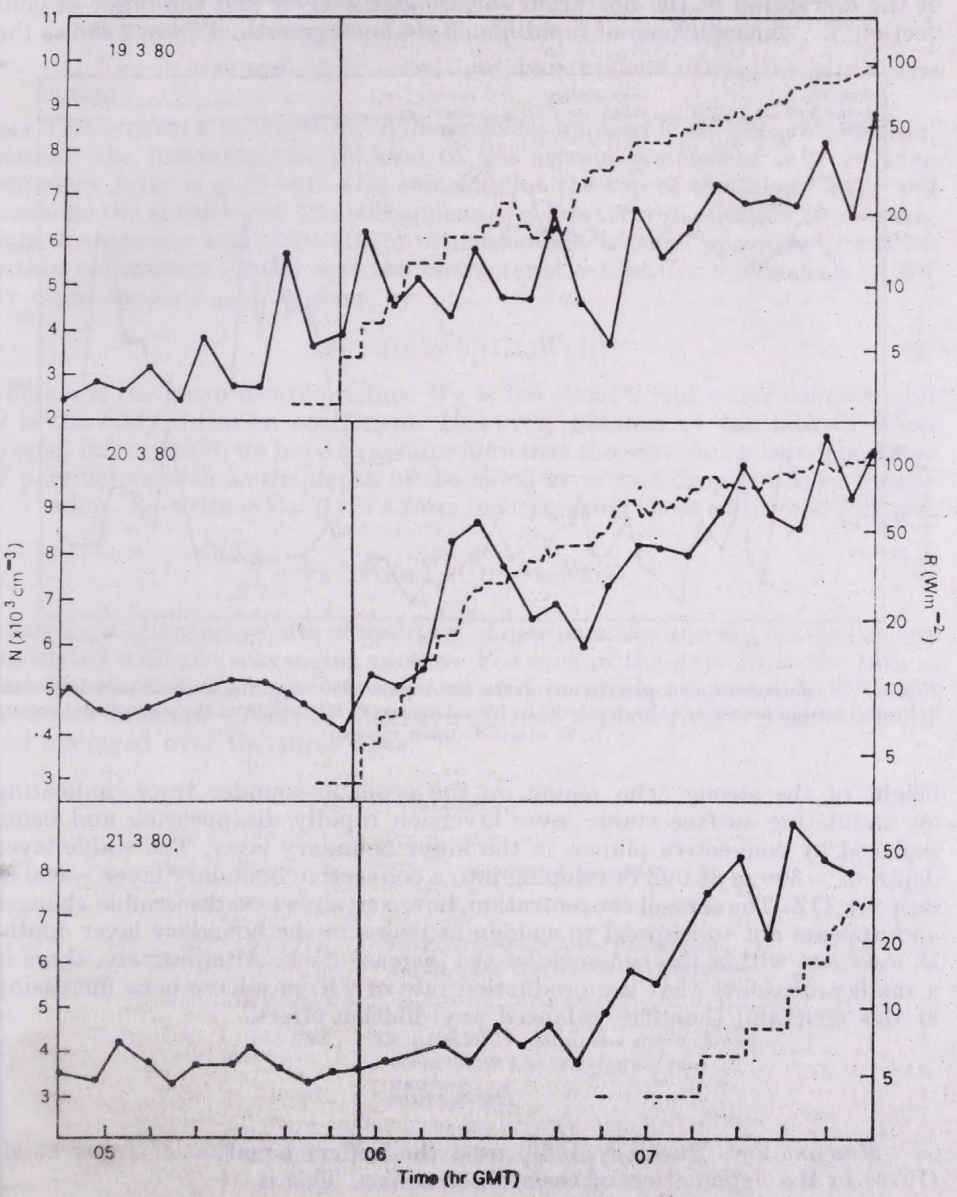

Fig. 3 : The increase in CN concentrations (full circles) after sunrise on the 19, 20, 21st March 1980. The total incident solar radiation R (solid line) is shown and the vertical lines around 0556 GMT are the sunrise times on these days

this data set does not lend support to the suggestion of *Haaf* and *Jaenicke* (1980) that production is higher on sunny days.

As mentioned in the introduction, several workers have reported minima in concentration which have been attributed to dilution of the aerosol population by increased mixing in the vertical. To try and test this idea, a day was selected in August 1980 on which measurements were made around the time of the disruption of the nocturnal surface stable layer and the onset of convection, i.e. during a time of rapid boundary layer growth. *Figure 4* shows the

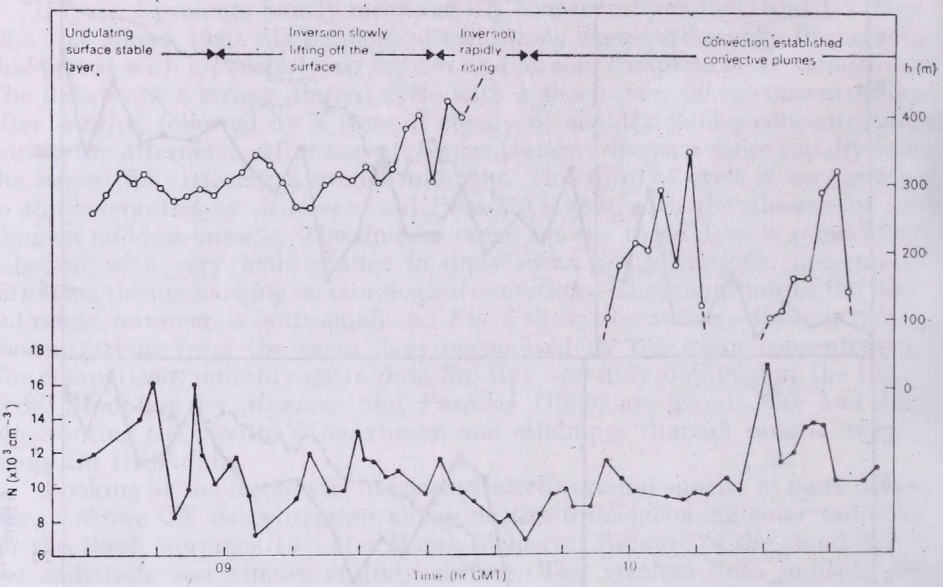

Fig. 4. : CN concentrations (open circles) on the 1st August 1980 when the acoustic sounder record indicated a rapid increase in the depth of the boundary layer. The height of the strong echo region, h, is marked (open circles)

height of the strong echo region on the acoustic sounder trace, indicating an undulating surface stable layer inversion rapidly disappearing and being replaced by convective plumes in the lower boundary layer. The stable layer depth of ~300 m at 09Z developing into a convective boundary layer ~900 m deep by 11Z. The aerosol concentration, however, shows no discernible changes and appears not to respond to sudden increases in the boundary layer depth, at least not within the timescale of the increase itself. Alternatively, there is a small probability that the production rate of CN may have been increasing at this time and therefore balanced any dilution effect.

Discussion

Mamane and *Pueschel* (1980) used the budget equation of *Lopez* et al. (1976) in the explanation of their observations. This is

$$\frac{dN_N}{dt} = \frac{\Phi_N}{h} - K_{NN} N_N^2(t) \qquad (1)$$

where N_N is the AN concentration at time, Φ_N is the nucleus flux, h is the mixing layer depth and K_{NN} is the coagulation constant for AN.

This equation involves the assumptions that

(a) changes in h will result in coincident changes in dN_N/dt ;

(b) advective changes are ignored;

(c) the only removal process in operation is coagulation;

(d) K_{NN} is assumed to be a constant independent of the AN size distribution.

This equation is therefore unlikely to be applicable to the present data, because the instantaneous dilution of the aerosol population in a growing boundary layer is in doubt. Also the cloud at the top of the mixed layer will scavenge the aerosol and this will appear as a loss term in addition to coagulation. *Pruppacher* and *Klett* (1978) estimated the lifetime of aerosol particles within continental clouds and the characteristic time for scavenging of AN by cloud droplets ($\tau_{\frac{1}{2}}$) is given by

$$\tau_{\frac{1}{2}} = (\ln 2a^{-2})/(1.35 W_L D) \tag{2}$$

where a is the mean droplet radius, W_L is the cloud liquid water content, and D is the eddy diffusion coefficient. However, because of the lack of cloud droplet information, we have to assume here that the scavenging is independent of parameters such as the depth of the cloud layer and droplet concentration and radius. Re-writing Eq. (1) in a form incorporating these additional features

$$\frac{dN_N}{dt} = Q_N - K_{NN} N_N^2(t) - K_{Sc} N_N(t) \tag{3}$$

where Q_N is the average rate of insertion of new particles and K_{Sc} is a coefficient associated with the scavenging process. For each of the days from the 18th – 21st March three time periods were selected in which we postulate different processes dominate *(Table I)*. For each of these periods dN_N/dt was calculated and averaged over the three days.

TABLE I

Period	From – To	Dominant process
A	05 – 11Z	Photochemical CN production dominates, rapid rise in CN concentrations
B	11 – 18Z	AN production continues more slowly, coagulation and scavenging rate increased
C	18 – 05Z	Photochemical production ceases, removal processes continue

Starting with period *C*, assuming that the rate of insertion (Q_N) was near zero and taking a value of $K_{NN} \sim 2.4 \times 10^{-9}$ cm^{-3} s^{-1} (*Mamane* and *Pueschel*,

1980), solving Eq. (2) yields $K_{Sc} \sim 8 \times 10^{-6}$ s^{-1}. Using this value to solve Eq. (2) for periods A and B

$$Q_{N_A} \sim 0.26 \pm 0.08 \text{ cm}^{-3} \text{ s}^{-1} \qquad Q_{N_B} \sim 0.13 \pm 0.06 \text{ cm}^{-3} \text{ s}^{-1}$$

If the photochemical production rate of CN was controlled solely by the availability of the particular trace gases, and a build-up in concentrations of these gases occurred during the hours of darkness, then Q_{N_B} could represent a steady production rate of "potential CN" and we can calculate the expected increase in CN after dawn. Assuming that this increase occurs entirely within period A, then during this period we should expect a production rate

$$Q_{N_A} = \frac{Q_{N_B} T_C}{T_A} \sim 0.23 \text{ cm}^{-3} \text{ s}^{-1}$$

where T_C and T_A are the time periods C and A, respectively.,

This agrees closely with Q_{N_A} calculated from the observations of 0.26 ± 0.08 cm^{-3} s^{-1}. A typical residence time τ for these CN in the boundary layer is given by $\tau = N_N/Q_N \sim 4$ h, which suggests that the majority of these CN originated in the agricultural areas upwind.

Conclusions

By making a series of assumptions about the photochemical origin of this aerosol population, and estimates of the relative magnitudes of the two principal removal processes, we have obtained a possible explanation of the observed diurnal variations in CN which is self-consistent. Observations confirm that AN production was indeed closely linked to the presence of solar radiation, and that in an experiment to investigate the effects of vertical mixing no appreciable dilution of surface concentrations was observed during a period of rapidly increasing boundary layer depth.

REFERENCES

Desalmand, F., Baudet, J. and *Serpolay, R.*, 1980: La loi caracteristique des noyaux de condensation nuageuse et son evolution en milieu intertropical humide, *Proc. VIIIth Int. Conf. on Cloud Physics.* Clermont-Ferrand 1980.

Haaf, W. and *Jaenicke, R.*, 1980: Results of improved size distribution measurements in the Aitken range of atmospheric aerosols. *J. Aerosol Sci. 11*, 321–330.

Lopez, A., Fontan, J. and *Servant, J.*, 1976: Mesoscale determination of Aitken nuclei flux near the ground – Use of radioactive tracers (Radon and Pb), *ERDA Symposium, series 38*, pp. 171–191, ERDA Technical Information Center, Oak Ridge, Tennessee.

Mamane, Y. and *Pueschel, R. F.*, 1980: On the properties of the condensation nuclei in rural Utah and New Mexico. *Proc. VIIIth Int. Conf. on Cloud Phys.* Clermont-Ferrand, 1980,

Mason, B. J., 1971: *The physics of clouds.* 2nd edition, Clarendon Press, Oxford.

Pruppacher, H. R. and *Klett, J. D.*, 1978: *Microphysics of clouds and precipitation.* D. Reidel Publ. Co, Dordrecht.

SZERZŐINK FIGYELMÉBE

Az IDŐJÁRÁS célja az elméleti és alkalmazott meteorológia tárgykörébe tartozó tanulmányok publikálása. A tanulmányok új kutatási eredményeket tartalmazó beszámolók, illetve adott szakterület időszerű kérdéseit összefoglaló kritikai szemlecikkek lehetnek. A közlés nyelve: magyar vagy angol. A kettes sortávolsággal gépelt kéziratok két példányban küldendők be a következő címre: **Időjárás Szerkesztősége Budapest, Pf. 38. 1525**

A kéziratokat a szerkesztőbizottság lektoráltatja. A lektor nevét a szerzővel nem közöljük. A kéziratnak a következő formai igényeket kell kielégítenie:

Címrész: Tartalmazza a tanulmány címét, a szerző(k) nevét, munkahelyét és ez utóbbi pontos címét.

Összefoglalás: Külön oldalakon, magyar és angol nyelven, tartalmazza a kutatás célját, módszerét és a kapott eredményeket.

Szövegrész: Alcímekkel értelemszerűen fejezetekre tagolandó.

Irodalmi hivatkozások: Szövegben a hivatkozás tartalmazza a szerző(k) nevét aláhúzva és a publikálás évét. Pl. egyetlen szerző esetén: *Róna* (1909), vagy ha a szerző neve a szövegbe nem illeszthető be: (*Róna*, 1909); két szerző esetén: *Gamow* és *Cleveland* (1973); több szerző esetén: *Bacsó* et al., (1953). Ha adott szerzők ugyanazon évben publikált több cikkére hivatkozunk, akkor az évszámhoz *a*, *b* stb. betűket írunk. Az irodalom felsorolása a **cikk** végén a szerző(k) neve szerinti betűrendben történik. Folyóirat esetén: szerző(k) neve, évszám, a cikk címe, a folyóirat neve, kötetszám, kezdő és befejező oldalszám. Pl.: *Dési, F.*, 1955: A meteorológiai kutatás időszerű kérdései. *Időjárás 57*, 65 – 70. Könyv esetén: Szerző(k) neve, évszám, könyvcím, kiadó, megjelenés helye. Pl. *Junge, C. E.*, 1963: *Air chemistry and radioactivity*. Academic Press, New York and London.

Ábrák: A kézirat első példányához az ábrákat pausz- vagy mm-papíron, a másodikhoz az eredeti ábrák másolatát kell csatolni. Az ábrák aláírásait külön lapon kell mellékelni. Fényképek fekete-fehér színben, fényes, kontrasztos minőségben nyújthatók be.

Táblázatok: A táblázatokat római számozással, szövegükkel együtt, külön lapon kell mellékelni.

Matematikai formulák és jelölések: A nem latin betűket és kézzel írott jeleket a margón ceruzával írt magyarázattal kell ellátni.

A szerzők megjelent tanulmányukért tiszteletdíjat és térítésmentesen 30 db különlenyomatot kapnak. Több különlenyomat a szerző költségére a kézirat elküldésével egyidejűleg rendelhető.

NOTES TO THE AUTHORS

The purpose of IDŐJÁRÁS is to publish papers in the field of theoretical and applied meteorology. These may be reports on new results of scientific investigations or critical review articles summarizing current problems in certain subject. Authors may be of any nationality but papers are published only in Hungarian or English. Two copies of the manuscripts, typed with double space, should be sent to the **Editorial Office of Időjárás. Address: Budapest, P. O. B. 38, H-1525, Hungary.**

Papers will be subjected to constructive criticism by unidentified referees.

The manuscript should meet the following formal requirements:

Title: Should contain the title of the paper, the name(s) of the author(s) with indication of the name and address of employment.

Abstract: Should contain the aim, method and conclusions of the scientific investigation on a separate page.

References: The text citation should contain the name(s) of the author(s) underlined and the year of publication. In case of one author: *Róna* (1909), or if the name of the author cannot be fitted into the text: (*Róna*, 1909); in case of two authors: *Gamow* and *Cleveland* (1973); there are more than two authors: *Bacsó* et al. (1953). When referring to several papers published in the same year by the same author, the year of publication should be followed by letters, *a*, *b* etc. At the end of the paper the list of references should be arranged alphabetically. For an article: the name(s) of author(s), year, title of article, name of journal, volume number, pages. E. g. *Dési, F.* 1955: Current problems of meteorological research. *Időjárás 57*, 65 – 70. For a book: the name(s) of author(s), year, title of book, publisher, place of publication. E. g. *Junge, C. E.*, 1963: *Air chemistry and radioactivity*. Academic Press, New York and London.

Figures: Should be prepared entirely in black India ink upon transparent paper and be attached to the first copy of the manuscript; a copy of the original figures should be attached to the second manuscript copy. The legends of figures should be given on a separate sheet. Photographs of good quality may be provided in black and white.

Tables: Should be marked by Roman numbers and provided on separate sheets together with relevant captions.

Mathematical formulas and symbols: Non Latin letters and hand-written marks should be explained by making marginal notes in pencil.

Authors are receiving 30 **reprints** free of charge. Additional reprints may be ordered at the authors expense when submitting the manuscript.

AZ ORSZÁGOS METEOROLÓGIAI SZOLGÁLAT FOLYÓIRATA

A szerkesztésért felel: dr. Szepesiné Lőrincz Anna

Szerkesztőség: 1024 Budapest, Kitaibel Pál utca 1.
Levélcím: 1525 Budapest, Pf. 38. Tel.: 353-500

Kiadja a Lapkiadó Vállalat, Budapest VII., Lenin körút 9—11. Telefon: 221-285. Levélcím: 1906 Budapest, Pf. 223.
Felelős kiadó: Siklósi Norbert igazgató

82.0149 Athenaeum Nyomda, Budapest — Íves magasnyomás
Felelős vezető: Szlávik András vezérigazgató

INDEX: 26 361

HU ISSN 0324—6329